frontiers | Research Topics

Cutaneous oncology and skin cancer genomics

Edited by
Bahar Dasgeb, Darius Mehregan and Adam Berger

Published in
Frontiers in Medicine

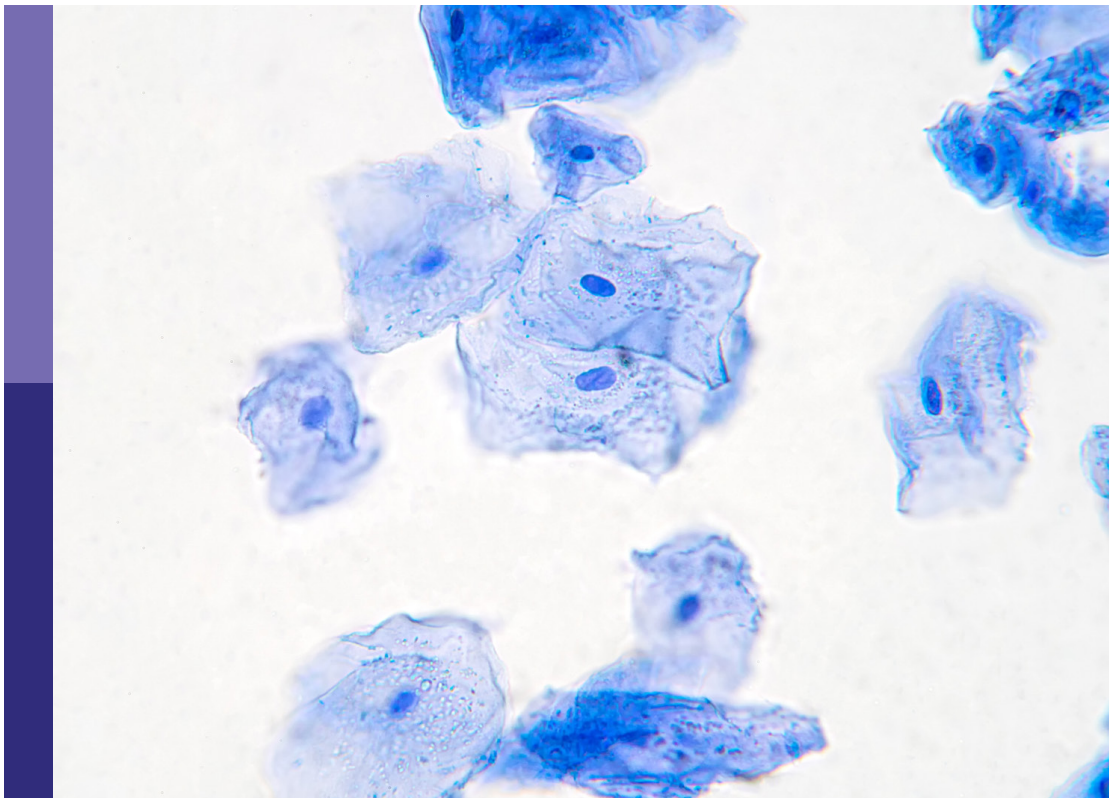

ISSN 1664-8714
ISBN 978-2-8325-5332-9
DOI 10.3389/978-2-8325-5332-9

About Frontiers

Frontiers is more than just an open access publisher of scholarly articles: it is a pioneering approach to the world of academia, radically improving the way scholarly research is managed. The grand vision of Frontiers is a world where all people have an equal opportunity to seek, share and generate knowledge. Frontiers provides immediate and permanent online open access to all its publications, but this alone is not enough to realize our grand goals.

Frontiers journal series

The Frontiers journal series is a multi-tier and interdisciplinary set of open-access, online journals, promising a paradigm shift from the current review, selection and dissemination processes in academic publishing. All Frontiers journals are driven by researchers for researchers; therefore, they constitute a service to the scholarly community. At the same time, the *Frontiers journal series* operates on a revolutionary invention, the tiered publishing system, initially addressing specific communities of scholars, and gradually climbing up to broader public understanding, thus serving the interests of the lay society, too.

Dedication to quality

Each Frontiers article is a landmark of the highest quality, thanks to genuinely collaborative interactions between authors and review editors, who include some of the world's best academicians. Research must be certified by peers before entering a stream of knowledge that may eventually reach the public - and shape society; therefore, Frontiers only applies the most rigorous and unbiased reviews. Frontiers revolutionizes research publishing by freely delivering the most outstanding research, evaluated with no bias from both the academic and social point of view. By applying the most advanced information technologies, Frontiers is catapulting scholarly publishing into a new generation.

What are Frontiers Research Topics?

Frontiers Research Topics are very popular trademarks of the *Frontiers journals series*: they are collections of at least ten articles, all centered on a particular subject. With their unique mix of varied contributions from Original Research to Review Articles, Frontiers Research Topics unify the most influential researchers, the latest key findings and historical advances in a hot research area.

Find out more on how to host your own Frontiers Research Topic or contribute to one as an author by contacting the Frontiers editorial office: frontiersin.org/about/contact

Cutaneous oncology and skin cancer genomics

Topic editors

Bahar Dasgeb — Rutgers, The State University of New Brunswick, United States
Darius Mehregan — Wayne State University, United States
Adam Berger — Rutgers, The State University of New Jersey, Newark, United States

Citation

Dasgeb, B., Mehregan, D., Berger, A., eds. (2024). *Cutaneous oncology and skin cancer genomics*. Lausanne: Frontiers Media SA. doi: 10.3389/978-2-8325-5332-9

It is with deepest sorrow that we share with you the passing of our co-editor Professor Jouni Uitto, to whom we dedicate this collection.

Table of contents

frontiers | Frontiers in Medicine

TYPE Editorial
PUBLISHED 05 August 2024
DOI 10.3389/fmed.2024.1445026

OPEN ACCESS

EDITED AND REVIEWED BY
Robert Gniadecki,
University of Alberta, Canada

*CORRESPONDENCE
Bahar Dasgeb
bahardasgeb@gmail.com

RECEIVED 06 June 2024
ACCEPTED 18 June 2024
PUBLISHED 05 August 2024

CITATION
Dasgeb B (2024) Editorial: Cutaneous oncology and skin cancer genomics. *Front. Med.* 11:1445026. doi: 10.3389/fmed.2024.1445026

Editorial: Cutaneous oncology and skin cancer genomics

Bahar Dasgeb*

Rutgers Cancer Institute of New Jersey, Rutgers, The State University of New Jersey, New Brunswick, NJ, United States

KEYWORDS

cutaneous oncology, skin genomics, complex skin malignancies, complex skin tumors, adverse events, genomics of skin malignancies

Editorial on the Research Topic
Cutaneous oncology and skin cancer genomics

The past 30 years has witnessed an incremental incidence and prevalence of skin malignancies—the most common malignancy in humans globally—with a recent predilection for younger age and a measurable social and economic impact on healthcare systems. This has happened in light of measures taken for sun protection and early detection during this period. Accordingly, further studies are warranted to better understand the additional risk factors underlying the surge in skin malignancies.

In this Research Topic, valuable research and observations of contributing authors shed light on a wide range of aspects of cutaneous malignancies. Included, are two comprehensive review articles on cutaneous angiosarcoma (Guan et al.) and melanoma (Waseh and Lee), both of which do commendably bring the readers up to date with the current knowledge, the cutting-edge developments, and the ongoing progress in the horizon on both subjects. The presented body of work has also made an effort to emphasize the basic importance of clinical risk stratification for prevention and early detection (Banner et al.; Park et al.) along with the emerging role of technology and AI in dermatology (Schreidah et al.).

Beyond prevention and early detection, we have also shed a light on Complex Cutaneous Malignancies (CCM) comprised of numerous, locally advanced, repeatedly recurring, resistant to treatment, which can present in less-sun-exposed or non-sun-exposed skin. These complex skin tumors may present an opportunity for investigating the impact of inherited or acquired oncogenic genes in relation to other risk factors, including sun (Gandarillas, Tang et al.). The contributing prospective of oncogenic genes in increasing incidence of skin malignancies in light of sun protective practices of the past few decades is an important area of investigation, which is reflected in the title of presented Research Topic; "*Cutaneous oncology and skin cancer genomics*" (Warbasse et al.; King et al.). Moreover, understanding of individuals' genomics, including but not limited to HLA system has presented a potential in risk stratification of patients and management of the treatment associated adverse events that warrants attention (Bhatti et al.; Gandarillas, Newland et al.).

I would like to conclude this note in memory of Dr. Jouni Uitto, a co-editor of this Research Topic, whose friendship and mentorship shaped my career. His contagious laugh even in testing times was a gift to all of us around him. I cherish his memories, especially the most impactful moments, when I learned the most from him about life and science, such is this summer afternoon ice cream moment (Figure 1).

On the same note, I would like to express my gratitude for the opportunity of collecting this body of work through which valuable friendships and collaboration was built not only with the contributing authors but also with the outstanding staff of Frontiers in Medicine, especially Josie Wyatt whose professional administrative support was priceless during this process.

FIGURE 1
Summer afternoon ice cream moment, Dr. Jouni Uitto **(Left)** and author BD **(Right)**.

Ethics statement

Written informed consent was obtained from the individual(s) for the publication of any identifiable images or data included in this article.

Author contributions

BD: Conceptualization, Data curation, Formal analysis, Investigation, Methodology, Project administration, Resources, Supervision, Validation, Visualization, Writing – original draft, Writing – review & editing.

Funding

The author(s) declare that no financial support was received for the research, authorship, and/or publication of this article.

Acknowledgments

To the professional administrative support that Josie Wyatt from Frontiers in Medicine provided; to all the outstanding contributing authors that I had the honor to get to know and call friend in the process; to my co-editors Drs. Darius Mehregan and Adam Berger, whose valuable presence in my academic life is shaping the path of my career; and to Jouni Uitto, whom we miss and will remember not only for his impactful contribution to skin genomics but also for his contagious laugh.

Conflict of interest

The author declares that the research was conducted in the absence of any commercial or financial relationships that could be construed as a potential conflict of interest.

Publisher's note

frontiers | Frontiers in Oncology

TYPE Original Research
PUBLISHED 02 August 2022
DOI 10.3389/fonc.2022.943483

OPEN ACCESS

EDITED BY
Nihal Ahmad,
University of Wisconsin-Madison,
United States

REVIEWED BY
Zaki A. Sherif,
Howard University, United States
Xiu-Qiong Fu,
Hong Kong Baptist University,
Hong Kong SAR, China

*CORRESPONDENCE
Carmen Silvia Passos Lima
carmenl@fcm.unicamp.br

SPECIALTY SECTION
This article was submitted to
Skin Cancer,
a section of the journal
Frontiers in Oncology

RECEIVED 13 May 2022
ACCEPTED 01 July 2022
PUBLISHED 02 August 2022

CITATION
Gomez GVB, Lourenço GJ,
Monteiro LMO, Rocha RS,
Fernández KAM, Recio JA, Torricelli C,
Coser LO, Oliveira ALR, Carron J,
Moraes AM and Lima CSP (2022)
Association of JAK/STAT genetic
variants with cutaneous melanoma.
Front. Oncol. 12:943483.
doi: 10.3389/fonc.2022.943483

Association of JAK/STAT genetic variants with cutaneous melanoma

Gabriela Vilas Bôas Gomez[1], Gustavo Jacob Lourenço[1], Lummy Maria Oliveira Monteiro[2], Rafael Silva Rocha[2], Kimberly Anne McGrail Fernández[3], Juan Angel Recio[3], Caroline Torricelli[1], Lilian Oliveira Coser[4], Alexandre Leite Rodrigues Oliveira[4], Juliana Carron[1], Aparecida Machado Moraes[5] and Carmen Silvia Passos Lima[1,5]*

[1]Laboratory of Cancer Genetics, Faculty of Medical Sciences, University of Campinas, Campinas, São Paulo, Brazil, [2]Department of Cellular and Molecular Biology, Faculty of Medicine of Ribeirão Preto, University of São Paulo, São Paulo, Brazil, [3]Animal Models and Cancer Laboratory, Vall d'Hebron Research Institute, Hospital Universitari Vall d'Hebron, Barcelona, Spain, [4]Laboratory of Nerve Regeneration, Department of Structural and Functional Biology, Institute of Biology, University of Campinas, São Paulo, Brazil, [5]Department of Anesthesiology, Oncology and Radiology, Faculty of Medical Sciences, University of Campinas, São Paulo, Brazil

Background: The Janus-activated kinase (JAK)-signal transducer and activator of transcription (STAT) signaling pathway regulates cutaneous melanoma (CM) development and progression. The JAK1, JAK2, and STAT3 proteins are encoded by polymorphic genes. This study aimed to verify whether single-nucleotide variants (SNVs) in *JAK1* (c.1648+1272G>A, c.991-27C>T), *JAK2* (c.-1132G>T, c.-139G>A), and *STAT3* (c.*1671T>C, c.-1937C>G) altered the risk, clinicopathological aspects, and survival of CM patients as well as protein activity.

Methods: CM patients (*N* = 248) and controls (*N* = 274) were enrolled in this study. Genotyping was performed by real-time polymerase chain reaction (PCR), and *JAK1*, *JAK2*, and *STAT3* expression was assessed by quantitative PCR (qPCR). *STAT3* c.-1937C>G SNV was investigated by luciferase, qPCR, western blot, apoptosis, and cell cycle assays in SKMEL-28 cells with CC or GG genotype.

Results: Individuals with *STAT3* c.*1671TT and c.-1937CC genotypes and TC haplotype of both SNVs were under about 2.0-fold increased risk of CM. Specific *JAK1*, *JAK2*, and *STAT3* combined genotypes were associated with up to 4.0-fold increased risk of CM. Higher luciferase activity [4,013.34 vs. 2,463.32 arbitrary units (AU); $p = 0.004$], *STAT3* expression by qPCR (649.20 *vs*. 0.03 AU; $p = 0.003$) and western blot (1.69 *vs*. 1.16 AU; $p = 0.01$), and percentage of cells in the S phase of the cell cycle (57.54 vs. 30.73%; $p = 0.04$) were more frequent in SKMEL-28 with *STAT3* c.-1937CC than with GG genotype. CM cell line with CC genotype

presented higher STAT3 protein levels than the one with GG genotype (1.93 *versus* 1.27 AU, $p = 0.0027$).

Conclusion: Our data present preliminary evidence that inherited abnormalities in the JAK/STAT pathway can be used to identify individuals at a high risk of CM, who deserve additional attention for tumor prevention and early detection.

KEYWORDS

cutaneous melanoma, *JAK1*, *JAK2*, *STAT3*, genetic variant, risk, prognosis

Introduction

Janus-activated kinase (JAK)-signal transducer and activator of transcription (STAT) has been identified as an important signaling pathway involved in cell proliferation, mainly through JAK1, JAK2, and STAT3 proteins, mediating various biological responses induced by cytokines and growth factors (1). In regular melanocytes, the activation of JAK/STAT is rapid and transient, but growth factors and cytokines secreted by abnormal cells as well as in the tumor microenvironment keep this pathway always activated (2, 3). Besides its role in cell proliferation, the JAK/STAT pathway induces angiogenesis, inhibits apoptosis and immune system response, and promotes metastasis, resulting in cutaneous melanoma (CM) development and progression (2–4).

Activation of *STAT3* has been noted as an important event in melanoma progression and metastasis. In addition, JAK1, JAK2, and STAT3 levels have altered the prognosis of CM patients (2, 3). Due to this, targeting STAT3 has been considered a potential therapeutic strategy for CM treatment since several STAT3 inhibitors revealed promising results in early-phase clinical trials (1, 5). It is already well known that JAK1, JAK2, and STAT3 proteins are encoded by polymorphic genes (6). Thus, healthy individuals may present distinct CM risks; CM patients treated equivalently may present diverse outcomes as well.

JAK1 c.1648+1272G>A (rs310211) single-nucleotide variant (SNV) is characterized by a G>A substitution in the intronic region 117268, and *JAK1* c.991-27C>T (rs2256298) SNV consists of the exchange of a C>T in the intronic region 106506, both in the splicing region of the gene (7–9). *JAK2* c.-1132G>T (rs1887429) and c.-139G>A (rs2274472) SNVs are characterized by G>T and G>A modifications in the gene promoter region, respectively, and that gain in the binding site of transcription factors may lead to changes in protein production (10–12). A T>C change in the 3′-UTR region of *STAT3* characterizes the c.*1671T>C (rs1053004) SNV. The gene binding efficiency of microRNAs 423-5p, 31-5p, 21-5p, and 99b-3p is low in carriers of the allele "C", which leads to a decrease in STAT3 mRNA and protein levels (12–14). Lastly, the *STAT3* c.-1937C>G (rs4796793) SNV is characterized by an exchange of a C>G in the gene promoter region (15). The allele "G" was associated with a lower STAT3 expression in B lymphocyte cell lines and better response of renal cell carcinoma patients to interferon alpha (IFNα) than the allele "C" (16). Melanoma cells carrying the allele "G" were the most sensitive to IFNα *in vitro* but did not predict IFNα efficacy in CM patients (15). Thus, the mechanism by which the SNVs interfere in protein function is not well defined.

We analyzed in the present study, for the first time, associations of *JAK1* (c.1648+1272G>A, c.991-27C>T), *JAK2* (c.-1132G>T, c.-139G>A), and *STAT3* (c.*1671T>C, c.-1937C>G) SNVs with CM risk, clinicopathological aspects, and prognosis and conducted functional studies to understand their biological consequences.

Materials and methods

Study population

The study included 248 consecutive patients with a median age of 55 years and primary CM attended at diagnosis at the General Hospital of the University of Campinas between January 2001 and May 2018. Patients with acral or amelanotic tumor were excluded from the analyses because they present distinct histological, phenotypic, and genetic characteristics, suggesting a biological difference when compared to other types of CM. The control group comprised of 274 blood donors with a median age of 50 years seen at the Hematology and Hemotherapy Center of the same university and in the same period. All procedures involving patients and controls were carried out according to the Helsinki Declaration, and the study was approved by the local research ethics committee (process 58186316.1.0000.5404).

Data collection

A standardized questionnaire was applied in patients and controls to obtain clinical information, such as age, gender, presence of nevi, phototype, sun exposure, previous sunburns, and type of sun exposure. Phototype was classified following the classification of Fitzpatrick (17). Six skin phototypes are possible: I—individuals with light white skin, are very sensitive to the sun, and who never tan; II—individuals with white skin who always burn and tan; III—individuals with light brown skin who burn and tan moderately; IV—individuals with dark brown skin who burn little and always tan; V—individuals with brown skin that rarely burn and who always tan; and VI—individuals with black skin who never burn and always tan (17). Sun exposure was defined as intermittent for individuals who were exposed to the sun for more than 2 h a day for more than 10 years and related to recreational activities by less than 50% on the week or vacation. Sun exposure was defined as chronic for those individuals who performed work or home activities more than 50% of the time under exposure. Individuals not exposed to the sun were the ones who did not fit in the previous definitions (18, 19).

The tumor pathologic aspects and survival data of CM patients were obtained from the patients' medical records. CM diagnosis was established by histopathological evaluation of tumor fragments embedded in paraffin and stained with hematoxylin and eosin (20). The tumor was measured by Breslow thickness (21) and Clark levels (22), and clinical stage was defined by the 7th American Joint Committee on Cancer criteria (23). The patients were conventionally treated as described in previous studies with the same population (24). In summary, patients with localized tumor were submitted to excisional surgery, and lymphadenectomy was performed in those with clinically positive lymph nodes or the ones with histological tumor infiltration. Patients with a single operable metastasis or recurrence were treated by surgical resection, whereas those patients with inoperable recurrence or multiple metastases received chemotherapy with dacarbazine. Radiotherapy has been used in patients with hemorrhagic lesions and bone or brain metastases.

SNV selection for study

All steps used for selecting SNVs for the study are presented in **Supplementary Figure S1**. The entire sequences of *JAK1*, *JAK2*, and *STAT3* genes were obtained from dbSNP database (http://www.ncbi.nlm.nih.gov/projects/SNP). First, SNVs that have previously been associated with the risk/survival of cancer patients were selected from public databases (N = 49). Subsequently, the SNVs mostly studied in different types of cancer and that present minor allele frequency ≥0.10 in the HapMap global population were selected (N = 20) (**Supplementary Table S1**). Finally, *in silico* analyses with Variant Effect Predictor (25), Human Splicing Finder (26), Genomatrix (27), SNPinfo (28), MicroSNiPer (29), and MirSNPscore (30) programs were performed. Two SNVs of each gene were selected for the study to analyze the pathway as a whole as well as SNVs with higher biological plausibility of being involved in tumor origin or progression (N = 6) (**Supplementary Table S2**).

JAK1 c.1648+1272G>A (rs310211), *JAK1* c.991-27C>T (rs2256298), *JAK2* c.-1132G>T (rs1887429), *JAK2* c.-139G>A (rs2274472), *STAT3* c.*1671T>C (rs1053004), and *STAT3* c.-1937C>G (rs4796793) were selected for the analyses of CM risk (comparisons of genotype frequencies in patients and controls), clinicopathological aspects (comparisons of genotype frequencies only in groups of patients), patients' survival, and gene expression. Thus, *STAT3* c.-1937C>G was the SNV of greatest interest in the study and the object of additional functional analyses.

Cell line selection for study

Fourteen CM cell lines were analyzed in this study: G361, A375, SKMEL-28, SKMEL-103, MSK8, MMLN9, MMLN10, MMLN14, MMLN23, MMGP3, MMSK22, MMLN24, UACC903, and MEWO. SKMEL-28 was obtained from a Rio de Janeiro cell bank (Rio de Janeiro, Brazil) with short tandem repeat analysis, and the remaining cell lines were acquired from the Animal Models and Cancer Laboratory of Vall d'Hebron Research Institute (Barcelona, Spain). All cell lines were obtained from human melanoma and tested for *BRAF* and *NRAS* drive mutations and *STAT3*c.-1937C>G genotypes.

To obtain melanoma cells with the same characteristics and genetic profile but expressing the wild-type or variant genotypes of *STAT3* c.-1937C>G SNV for the functional studies, the genetic transformation of the SKMEL-28 cells was performed. These cells were chosen for study due to its well-known molecular characterization (*BRAF* mutated), ease of cultivation, and easy genetic transformation. Thus, SKMEL-28 cells with *STAT3* c.-1937CC and GG genotype were used in luciferase, qPCR, apoptosis, cell cycle, and western blot assays. The modified SKMEL-28 and non-modified cell lines, characterized by *RAS* and *BRAF* mutations and *STAT3* c.-1937C>G genotypes, were selected for the analyses of *STAT3* levels; unmodified cell lines were included in the determination of STAT3 levels with the purpose of increasing the cell line sample and verifying, through comparison with modified SKMEL-28 cells, whether STAT3 levels could be altered by the genetic modification of cells.

Cell line culture

Cell lines (2.5×10^6/plate) were cultured in 60-mm-diameter plates containing a specific culture medium for each cell type: Dulbecco's modified Eagle's medium (DMEM) (Gibco, USA)

supplemented with 10% fetal bovine serum (FBS) for G361, A375, SKMEL-28, and SKMEL-103 cell lines; DMEM (Gibco, USA) supplemented with 20% FBS for MSK8, MMLN9, MMLN10, MMLN14, MMLN23, MMGP3, MMSK22, and MMLN24 lines; RPMI medium (Gibco, USA) supplemented with 10% FBS for UACC903 line; and EMEM medium (Gibco, USA) supplemented with 10% FBS for MEWO line. Subsequently, 1% penicillin–streptomycin (100 U/ml) (Gibco, USA), 1% L-glutamine (Gibco, USA), and 100 µl plasmocin (Gibco, USA) were added to each plate. The cells were grown at 37°C in 5% CO_2 condition and tested for mycoplasma contamination. All experiments were performed using mycoplasma-free cells (31).

Genotyping

Genomic DNA was obtained from the leukocytes of peripheral blood samples of patients and controls and from all melanoma cell lines.

Genotyping of individuals and all cell lines was performed by real-time polymerase chain reaction (PCR) method using TaqMan SNV genotyping assay [Applied Biosystems, USA; *JAK1* c.1648+1272G>A (C_176626140), *JAK1* c.991-27C>T (C_176627520), *JAK2* c.-1132G>T (C_1209582910), *JAK2* c.-139G>A (C_1618193310), *STAT3* c.*1671T>C (C_17952851) and *STAT3* c.-1937C>G (C_2797721310)] according to the manufacturer's instructions. Positive and negative controls were used in all reactions. For quality control purposes, 15% of the samples were genotyped twice with a 100% concordance rate.

JAK1, *JAK2*, and *STAT3* expression in peripheral blood

Gene expression was analyzed by quantitative PCR (qPCR). Total RNAs from the leukocytes of the peripheral blood of 40 CM patients and 60 controls with distinct genotypes of *JAK1* (c.1648+1272G>A, c.991-27C>T), *JAK2* (c.-1132G>T, c.-139G>A), and *STAT3* (c.*1671T>C, c.-1937C>G) SNVs were extracted with Trizol reagent (Life Technologies, USA) according to the manufacturer's instructions. RNAs were selected based on integrity and availability to carry out the technique, and all individuals who met these criteria were evaluated by qPCR. cDNA was generated using SuperScript III reagents (Life Technologies, USA), and the experiments were performed with SYBR Green PCR Master Mix reagents (Applied Biosystems, USA). The relative expression level was normalized by β-actin reference gene with the 2^{-DDCt} cycle threshold method. Forward and reverse specific primers in duplicate per sample and a negative control without template were included in each plate (**Supplementary Table S3**). The experiments (15%) were repeated with 100% agreement, and the results were expressed in arbitrary units (AUs).

STAT3 promoter region activity in modified SKMEL-28 cell line

The *STAT3* promoter region activity was analyzed in SKMEL-28 cells with CC or GG genotype of *STAT3* c.-1937C>G SNV by dual luciferase reporter assay. For cell transformation, forward and reverse primers (**Supplementary Table S3**) were designed to amplify 1,940 base pairs of *STAT3* promoter region containing *STAT3* c.-1937C>G SNV by PCR with 2 U of Platinum™ Taq DNA Polymerase, High Fidelity (Thermo Scientific, USA). The PCR products were cloned into pGL-3 basic vector (Promega, USA) using restriction enzymes *Kpn1* and *Nco1* (Thermofisher, USA) according to standard protocols (32, 33). After these procedures, pGL-3luc_C and pGL-3luc_G plasmids were obtained and were transformed into *E. coli* DH5α-competent bacteria (Invitrogen, USA) by electroporation (32, 33). The final construction was verified by restriction enzyme digestion and sequencing by Sanger 3730xL (Applied Biosystems, USA).

SKMEL-28 cells were grown in 12-well cell culture plates (1×10^5 cells/well) for 24 h. Then, they were transiently transfected with a promoterless luciferase vector (empty pGL3luc-basic) or with pGL3luc_C or pGL3luc_G plasmids, and *Renilla* luciferase control reporter (pRL) was used as the normalizing control (Promega, USA). For transfection, Lipofectamine™ 2000 (Invitrogen, USA) and reduced serum medium Opti-MEM (Gibco, USA) were used according to the manufacturer's recommendations. The cells were harvested 24 h after transfection, and luciferase assays were performed with Dual Luciferase Assay Kit (Promega, USA) according to the manufacturer's protocol. Relative firefly luciferase activity was normalized for the pRL vector activity. The assays were performed in triplicate with a negative control in each reaction, and the results were expressed in AUs.

STAT3 expression in modified SKMEL-28 cell line

STAT3 expression was analyzed in SKMEL-28 cells with *STAT3* c.-1937CC or GG genotype by qPCR.

For cell transformation, a complete *STAT3* gene was cloned into pGL-3 basic vector (Promega, USA). For this, pGL3luc_C and pGL3luc_G plasmids were subjected to luciferase region removal by restriction enzymes (*Nco1* and *Xba1*) (Thermofisher, USA) (32, 33). Subsequently, the fragments of interest were amplified from cDNA with forward and reverse primers (**Supplementary Table S3**) and then were ligated to the vector by T4 DNA ligase enzyme (Life Technologies, USA)

(32, 33). In the end, new vectors (pGL3_*STAT3*_C and pGL3_*STAT3*_G) containing the coding region until the gene stop codon were obtained. The SKMEL-28 cells were grown in 60-mm cell culture plates (2.5×10^6 cells/plate) for 24 h. Then, they were transiently transfected with pGL3-basic empty or pGL3_*STAT3*_C or pGL3_*STAT3*_G vectors. For transfection, polyethylenimine (PEI) (Veritas Biotecnologia, USA) and reduced serum medium Opti-MEM (Gibco, USA) were used according to the manufacturer's instructions. The vector with green fluorescent protein (GFP) was used in transfection monitoring. At the end of the experiment, SKMEL-28 cells with *STAT3* c.-1937CC and c.-1937GG genotypes were obtained for the analyses of STAT3 expression, apoptosis and cell cycle.

For the analysis of *STAT3* expression, the cells were harvested 24 h after transfection, and RNA extraction was performed with the Direct-zol RNA MinPrep kit (Zymo Research, USA) according to the manufacturer's protocols. Assays were performed in triplicate using a negative control in each reaction. For each experiment, *STAT3* expression by qPCR was performed, and the results were expressed in AUs.

STAT3 protein levels in modified SKMEL-28 and unmodified cell lines

STAT3 protein levels were analyzed by western blot in SKMEL-28 cells transfected with the empty vector with *STAT3* c.-1937CC or GG genotype. In addition, 14 unmodified melanoma cell lines (G361, A375, SKMEL-28, SKMEL-103, MSK8, MMLN9, MMLN10, MMLN14, MMLN23, MMGP3, MMSK22, MMLN24, UACC903, and MEWO) with different *STAT3* c.-1937C>G genotypes were also used in the determination of STAT3 levels.

The cells were lysed with radioimmunoprecipitation assay buffer containing protease inhibitors. Total protein concentrations were measured by the Bradford method (1976) and bovine serum albumin standard curve. For western blot, total proteins (50 µg) were subjected to 10% sodium dodecyl sulfate polyacrylamide gel electrophoresis, and then they were transferred to nitrocellulose membranes. The membranes were blocked with 5% skimmed milk in phosphate-buffered saline (PBS-Tween) and incubated with specific primary antibodies anti-STAT3 (Santa Cruz, USA) and anti-glyceraldehyde-3-phosphate dehydrogenase (GAPDH) (Santa Cruz, USA) overnight at 4°C. A horseradish peroxidase-conjugated goat anti-mouse IgG was used as the secondary antibody (Santa Cruz, USA). ECL Western Blot Detection Reagents kit (GE Healthcare, USA) was used for protein detection, and the signal intensity was analyzed by ImageJ software (National Institutes of Health, USA). The levels of GAPDH were used as loading control. The protein levels were expressed in AUs.

STAT3 in apoptosis and cell cycle assays in modified SKMEL-28 cell line

For apoptosis assay, 2.5×10^6 SKMEL-28 cells were cultured in 60-mm cell culture plates with DMEM supplemented with 10% FBS. On the next day, the cells were transfected with empty pGL3 or pGL3_*STAT3*_C or pGL3_*STAT3*_G vectors of the *STAT3* c.-1937C>G SNV using PEI watering system (Veritas, USA). GFP vector was used in transfection monitoring. After 6 h of transfection, the cells were subjected to 200 µM of hydrogen peroxide (H_2O_2) (Sigma, USA) in DMEM without FBS and cultured in an atmosphere of 5% CO_2 at 37°C for 22 h to induce apoptosis. A cell culture without H_2O_2 treatment was used as control in the apoptosis assay. The adherent cells were collected by trypsinization after 22 h. The collected cells were washed using PBS and then stained with 195 µl binding buffer (1×), 5 µl Annexin V-FITC, and 5 µl 7-AAD at room temperature for 10 min according to the instruction manual. The samples were analyzed using the NovoCyte flow cytometer (ACEA Bioscience, USA). Early apoptosis was designated as annexin positive/7-AAD negative, and late apoptosis and necrosis were designated as annexin positive/7-AAD positive. All experiments were done in triplicate, and the results (average values of the three experiments) were expressed as a percentage of the cells.

Cell cycle analysis was performed in the SKMEL-28 cell line. Initially, 2.5×10^6 cells were cultured in 60-mm cell culture plates with DMEM supplemented with 10% FBS. On the next day, the cells were transfected with empty pGL3 or pGL3_*STAT3*_C or pGL3_*STAT3*_G vectors of the *STAT3* c.-1937C>G SNV using PEI watering system (Veritas, USA). GFP vector was used to monitor the transfection, and the cell was cultured in an atmosphere of 5% CO_2 at 37°C for 24 h. After 24 h, cells were collected by trypsinization and washed by centrifugation in PBS at 300 g for 10 min 4°C before these were permeabilized in 1 ml cold 70% (v/v) ethanol (1 h, 4°C). Following washes with 0.25% Triton X-100 (PFT), the cells were stained in 300 µl of PFT with 5 µl 7-AAD Viability Stain Solution (Invitrogen, USA). A control tube was prepared without antibody labeling. The samples were analyzed on NovoCyte flow cytometer (ACEA Bioscience, USA). Individual separation of the cells was performed using the Cell Cycle Plot tool of the Novoexpress software, which is an analysis of the intensity of the 7-AAD marking and separation of the G1, S, and G2 cell cycle phases. All experiments were done in triplicate, and the results were expressed as the percentage of cells (average of three experiments) in a particular cycle phase.

Statistical analyses

Hardy–Weinberg equilibrium (HWE) was tested using chi-square (χ^2) for the goodness-to-fit test. Haploview 4.2 software

(www.broad.mit.edu/mpg/haploview) was used to verify if the markers were properly included in the haplotype analysis. Linkage disequilibrium was measured by the disequilibrium coefficient (D'), and significance was considered at $D' \geq 0.80$. Differences between groups were analyzed by χ^2 or Fisher's exact test. Multivariate analysis using the logistic regression model served to obtain age, nevi, and sun exposure status-adjusted crude odds ratios with 95% confidence intervals (CIs) in comparisons involving patients and controls. Bonferroni correction for multiple comparisons was used to adjust the p-values obtained in clinicopathological aspect analyses. Considering continuous variables, data sets were probed for normality using Shapiro–Wilk's test; if the data set assumed normal distribution, t-test and ANOVA were used for analysis, but if it did not assume a normal distribution, Mann–Whitney and Kruskal–Wallis tests were used to compare the groups.

Progression-free survival (PFS) was calculated from the date of surgery until the date of first recurrence, progression of disease, death from any cause, or last follow-up. Melanoma-specific survival (MSS) was calculated from the date of diagnosis until the date of death from the disease or last follow-up. PFS and MSS times were calculated using Kaplan–Meier probabilities, and differences between curves were analyzed by log-rank test. The prognostic impact of age, gender, tumor location, type of growth, Clark level, Breslow thickness, tumor stage, and genotypes of *JAK1*, *JAK2*, and *STAT3* SNVs in the survival of patients was evaluated using Cox proportional hazard ratio regression. In a second step, all variables with $p < 0.15$ were included in a multivariate Cox regression.

For the statistical tests, significance was two-sided and achieved when p-values were <0.05. The intensities of the protein bands were quantitated using ImageJ software (National Institutes of Health, USA), and all tests were performed using SPSS 21.0 software (SPSS Incorporation, IL, USA).

Results

Characteristics of the study population

The clinicopathological aspects of the patients and controls enrolled in the study are presented in Table 1. The controls were younger than the patients (median age: 47 vs. 55 years; $p < 0.0001$), and the patients had more nevi (59.7 vs. 17.2%, $p < 0.0001$), referred more sun exposure (79.0 vs. 44.9%, $p < 0.0001$), sunburn episodes (53.2 vs. 28.8%, $p < 0.0001$), and chronic sun exposure (48.8 vs. 24.8%, $p < 0.0001$) than the controls. Differences in age, number of nevi, sun exposure, and sunburn of individuals of each group were corrected in comparisons of patients and controls by multivariate analysis using the logistic regression model.

Molecular characteristics of cell lines

The MMGP3, MMSK22, MMLN24, and UACC903 cell lines presented the CC genotype, the A375, SKMEL-103, MMLN9, and MMLN10 cell lines presented the CG genotype, and the G361, SKMEL-28, MSK8, MMLN14, MMLN23, and MEWO cell lines presented the GG genotype of the *STAT3* c.-1937C>G SNV.

Mutations of *NRAS* and *BRAF* genes were seen in G361, A375, SKMEL-103, and UACC903 cell lines, *BRAF* gene mutation was seen in SKMEL-28, and *RAS* gene mutation was seen in MMNL9 and MMNL10 cell lines; no mutations of *RAS* and *BRAF* were characterized in the MEWO cell line, and gene mutations were not analyzed in the remaining cell lines (Supplementary Table S4).

SNVs and CM risk

The patients' and controls' samples were in HWE for the loci *JAK1* c.1648+1272G>A ($X^2 = 2.44$, $p = 0.11$; $X^2 = 0.02$, $p = 0.88$), *JAK1* c.991-27C>T ($X^2 = 1.47$, $p = 0.22$; $X^2 = 1.69$, $p = 0.19$), *JAK2* c.-1132G>T ($X^2 = 0.79$, $p = 0.37$; $X^2 = 2.73$, $p = 0.09$), *JAK2* c.-139G>A ($X^2 = 0.01$, $p = 0.92$; $X^2 = 0.001$, $p = 0.97$), *STAT3* c.*1671T>C ($X^2 = 0.24$, $p = 0.62$; $X^2 = 1.59$, $p = 0.20$), and *STAT3* c.-1937C>G ($X^2 = 0.63$, $p = 0.42$; $X^2 = 0.004$, $p = 0.94$), respectively.

The frequencies of *JAK1*, *JAK2*, and *STAT3* genotypes and respective alleles in patients and controls are presented in Table 2. Individuals with *STAT3* c*1671TT and *STAT3* c.-1937CC genotypes were under 1.70 and 1.60-fold increased risks for CM than those with the remaining genotypes.

The frequencies of combined genotypes and significant combined genotypes in patients and controls are shown in Supplementary Table S5 and Table 3, respectively. In combinations of two SNVs, individuals with *JAK1* c.1648+1272GG plus *STAT3* c.*1671TT, *JAK1* c.1648+1272GG plus *STAT3* c.-1937CC, *JAK1* c.991-27CC plus *STAT3* c.*1671TT, *JAK1* c.991-27CC plus *STAT3* c.-1937CC, and *STAT3* c.*1671TT plus *STAT3* c.-1937CC genotypes had 2.54-, 2.15-, 2.32-, 2.10-, and 1.90-fold increased risks of developing CM than those with the remaining genotypes, respectively. Individuals with *JAK1* c.1648+1272GG plus *JAK1* c.991-27CC plus *STAT3* c.*1671TT and *JAK1* c.1648+1272GG plus *JAK1* c.991-27CC plus *STAT3* c.-1937CC genotypes were under 2.66- and 2.35-fold increased risks of CM development than others, respectively, when combinations of three SNVs were considered. In combinations of four SNVs, individuals with *JAK1* c.1648+1272GG plus *JAK1* c.991-27CC plus *JAK2* c.-1132GG plus *STAT3* c.*1671TT, *JAK1* c.1648+1272GG plus *JAK1* c.991-27CC plus *JAK2* c.-1132GG plus *STAT3* c.-1937CC, *JAK1* c.1648+1272GG plus *JAK1* c.991-27CC plus *STAT3* c.*1671TT plus *STAT3* c.-1937CC >G, and *JAK1*

TABLE 1 Distribution of 248 cutaneous melanoma patients and 274 controls stratified by clinicopathological aspects.

Characteristic	Patients, *N* (%)	Controls, *N* (%)	*p*-value
Age (years)			
≤55	125 (50.4)	226 (82.5)	**<0.0001**
>55	123 (49.6)	48 (17.5)	
Gender			
Male	128 (51.6)	140 (51.1)	0.90
Female	120 (48.4)	134 (48.9)	
Nevi[a]			
<20	94 (37.9)	214 (78.1)	**<0.0001**
≥20	148 (59.7)	47 (17.2)	
Phototype[a]			
I or II	157 (63.3)	162 (59.1)	0.07
III to VI	74 (29.8)	107 (39.1)	
Sun exposure[a]			
Yes	196 (79.0)	123 (44.9)	**<0.0001**
No	41 (16.5)	146 (53.3)	
Sunburn episodes[a]			
Yes	132 (53.2)	79 (28.8)	**<0.0001**
No	93 (37.5)	190 (69.3)	
Type of sun exposure[a]			
No/intermittent	97 (39.1)	201 (73.4)	**<0.0001**
Chronic	121 (48.8)	68 (24.8)	
Tumor location			
Limbs	81 (32.7)	NA	
Axial	167 (67.3)		
Ulceration[a]			
Yes	68 (27.4)	NA	
No	107 (43.2)		
Type of growth[a]			
Vertical	111 (44.8)	NA	
Horizontal	33 (13.3)		
Clark level[a]			
I or II	74 (29.8)	NA	
III to V	156 (63.0)		
Breslow thickness (mm)[a]			
≤1.5 mm	118 (47.6)	NA	
>1.5 mm	102 (41.1)		
Clinical stage[a,b]			
0 to II	164 (66.2)	NA	
III or IV	56 (22.6)		
Metastasis[a]			
Yes	18 (7.3)	NA	
No	183 (73.8)		

Significant values are presented in bold.
N, number of individuals; %, percentage; mm, millimeters; NA, not applicable.
[a]The number differed from the total quoted in the study because it was not possible to obtain consistent information in some cases.
[b]Clinical stage was classified by the American Joint Committee on Cancer criteria.

c.991-27CC plus *JAK2* c.-1132GG plus *STAT3* c.*1671TT plus *STAT3* c.-1937CC genotypes had 3.56-, 3.21-, 3.95-, and 3.67-fold increased risks of CM incidence than those with the remaining genotypes, respectively.

Individuals with TC haplotype of *STAT3* c*1671T>C and *STAT3* c.-1937C>G SNVs were under 1.64-fold increased risk for CM than those with the remaining haplotypes of *STAT3* SNVs (Table 4).

10.3389/fonc.2022.943483

TABLE 2 *JAK1*, *JAK2* and *STAT3* genotypes and alleles in 248 cutaneous melanoma patients and 274 controls.

Genotype/allele	Patients *N* (%)	Controls *N* (%)	*p*-value	OR[a] (95% CI)
JAK1 c.1648+1272G>A				
GG	99 (39.9)	100 (36.5)	0.29	Reference
GA or AA	149 (60.1)	174 (63.5)		1.28 (0.81–2.02)
GG or GA	205 (82.7)	230 (83.9)	0.41	Reference
AA	43 (17.3)	44 (16.1)		1.27 (0.70–2.28)
G allele	0.61	0.60	0.76	Reference
A allele	0.39	0.40		1.05 (0.76–1.44)
JAK1 c.991-27C>T				
CC	122 (49.2)	118 (43.1)	0.28	Reference
CT or TT	126 (50.8)	156 (56.9)		1.27 (0.81–1.99)
CC or CT	220 (88.7)	234 (85.4)	0.94	Reference
TT	28 (11.3)	40 (14.6)		1.02 (0.53–1.95)
C allele	0.69	0.64	0.40	Reference
T allele	0.31	0.36		1.15 (0.82–1.60)
JAK2 c.-1132G>T				
GG	109 (44.0)	127 (46.4)	0.33	Reference
GT or TT	139 (56.0)	147 (53.6)		1.24 (0.79–1.95)
GG or GT	215 (86.7)	237 (86.5)	0.78	Reference
TT	33 (13.3)	37 (13.5)		1.09 (0.56–2.11)
G allele	0.65	0.66	0.55	Reference
T allele	0.35	0.34		1.10 (0.79–1.54)
JAK2 c.-139G>A				
GG	244 (98.4)	273 (99.6)	0.25	Reference
GA or AA	04 (1.6)	01 (0.4)		6.09 (0.26–139.20)
GG or GA	248 (100.0)	274 (100.0)	NC	Reference
AA	00 (0.0)	00 (0.0)		NC
G allele	0.99	1.00	0.25	Reference
A allele	0.01	0.00		6.04 (0.26–137.27)
STAT3 c.*1671T>C				
TT	89 (35.9)	83 (30.3)	**0.02**	1.70 (1.05–2.75)
TC or CC	159 (64.1)	191 (69.7)		Reference
TT or TC	205 (82.7)	209 (76.3)	0.43	1.24 (0.71–2.15)
CC	43 (17.3)	65 (23.7)		Reference
T allele	0.59	0.53	0.05	1.36 (1.00–1.87)
C allele	0.41	0.47		Reference
STAT3 c.-1937C>G				
CC	131 (52.8)	120 (43.8)	**0.03**	1.60 (1.02–2.51)
CG or GG	117 (47.2)	154 (56.2)		Reference
CC or CG	226 (91.1)	243 (88.7)	0.77	1.11 (0.54–2.28)
GG	22 (8.9)	31 (11.3)		Reference
C allele	0.72	0.66	0.15	1.28 (0.91–1.79)
G allele	0.28	0.34		Reference

Significant values are presented in bold.
N, number of cases; %, percentage; CI, confidence interval; NC, not calculated.
[a]Odds ratio (OR) was adjusted by age, nevi, and sun exposure by multivariate analysis.

TABLE 3 *JAK1*, *JAK2*, and *STAT3* significant combined genotypes in 248 cutaneous melanoma patients and 274 controls.

Genotype	Patients *N* (%)	Controls *N* (%)	*p*-value	OR[a] (95% CI)
JAK1 c.1648+1272G>A + *STAT3*c.*1671T>C				
GG + TT	38 (27.9)	29 (19.5)	**0.01**	2.54 (1.23–5.25)
GA or AA + TC or CC	98 (72.1)	120 (80.5)		Reference
GG or GA + TT or TC	182 (88.3)	208 (86.7)	0.72	1.13 (0.55–2.32)
AA + CC	24 (11.7)	32 (13.3)		Reference
JAK1 c.1648+1272G>A + *STAT3* c.-1937C>G				
GG + CC	55 (43.0)	44 (31.0)	**0.02**	2.15 (1.12–4.13)
GA or AA + CG or GG	73 (57.0)	98 (69.0)		Reference
GG or GA + CC or CG	188 (97.4)	204 (97.6)	0.12	3.45 (0.71–16.63)
AA + GG	05 (2.6)	05 (2.4)		Reference
JAK1 c.991-27C>T + *STAT3* c.*1671T>C				
CC + TT	46 (35.7)	34 (24.1)	**0.01**	2.32 (1.16–4.64)
CT or TT + TC or CC	83 (64.3)	107 (75.9)		Reference
CC or CT + TT or TC	183 (96.8)	185 (92.0)	0.46	1.49 (0.51–4.35)
TT + CC	06 (3.2)	16 (8.0)		Reference
JAK1 c.991-27C>T + *STAT3* c.-1937C>G				
CC + CC	67 (51.9)	52 (37.1)	**0.02**	2.10 (1.10–4.00)
CT or TT + CG or GG	62 (48.1)	88 (62.9)		Reference
CC or CT + CC or CG	200 (99.0)	208 (97.7)	0.48	1.97 (0.28–13.68)
TT + GG	02 (1.0)	05 (2.3)		Reference
STAT3 c.*1671T>C + *STAT3* c.-1937C>G				
TT + CC	82 (42.7)	74 (33.8)	**0.01**	1.90 (1.13–3.19)
TC or CC + CG or GG	110 (57.3)	145 (66.2)		Reference
TT or TC + CC or CG	201 (91.8)	202 (89.4)	0.70	1.17 (0.51–2.65)
CC + GG	18 (8.2)	24 (10.6)		Reference
JAK1 c.1648+1272G>A + *JAK1* c.991-27C>T + *STAT3* c.*1671T>C				
GG + CC + TT	38 (31.4)	29 (21.3)	**0.01**	2.66 (1.25–5.62)
GA or AA + CT or TT +TC or CC	83 (68.6)	107 (78.7)		Reference
GG or GA + CC or CT + TT or TC	172 (96.6)	183 (92.0)	0.51	1.42 (0.49–4.17)
AA + TT + CC	06 (3.4)	16 (8.0)		Reference
JAK1 c.1648+1272G>A + *JAK1* c.991-27C>T + *STAT3* c.-1937C>G				
GG + CC + CC	55 (47.0)	44 (33.3)	**0.01**	2.35 (1.18–4.67)
GA or AA + CT or TT + CG or GG	62 (53.0)	88 (66.7)		Reference
GG or GA + CC or CT + CC or CG	188 (98.9)	204 (97.6)	0.47	2.02 (0.29–14.12)
AA + TT + GG	02 (1.1)	05 (2.4)		
JAK1 c.1648+1272G>A + *JAK1* c.991-27C>T + *JAK2* c.-1132G>T + *STAT3* c.*1671T>C				
GG + CC + GG + TT	19 (28.8)	11 (14.9)	**0.02**	3.56 (1.22–10.37)
GA or AA + CT or TT + GT or TT + TC or CC	47 (71.2)	63 (85.15)		Reference
JAK1 c.1648+1272G>A + *JAK1* c.991-27C>T + *JAK2* c.-1132G>T + *STAT3* c.-1937C>G				
GG + CC + GG + CC	28 (45.9)	21 (29.2)	**0.01**	3.21 (1.22–8.47)
GA or AA + CT or TT + GT or TT + CG or GG	33 (54.1)	51 (70.8)		Reference
JAK1 c.1648+1272G>A + *JAK1* c.991-27C>T + *STAT3* c.*1671T>C + *STAT3* c.-1937C>G				
GG + CC + TT + CC	34 (36.6)	24 (22.2)	**0.002**	3.95 (1.66–8.95)
GA or AA +CT or TT + TC or CC + CG or GG	59 (63.4)	84 (77.8)		Reference
JAK1 c.991-27C>T + *JAK2* c.-1132G>T + *STAT3* c.*1671T>C + *STAT3* c.-1937C>G				
CC + GG + TT + CC	20 (38.5)	12 (19.0)	**0.01**	3.67 (1.25–10.79)
CT or TT + GT or TT + TC or CC + CG or GG	32 (61.5)	51 (81.0)		Reference

Significant values are presented in bold.
N, number of cases; %, percentage; CI, confidence interval.
[a]Odds ratio (OR) adjusted by age, nevi, and sun exposure by multivariate analysis.

TABLE 4 *JAK1*, *JAK2*, and *STAT3* haplotypes in 248 cutaneous melanoma patients and 274 controls.

Haplotype		Patients' frequency	Controls' frequency	*p*-value	OR[a] (95% CI)
*JAK1*c.1648+1272G>A	*JAK1* c.991-27C>T				
G	C	0.61	0.60	0.76	1.05 (0.76–1.44)
G	T	0.99	1.00	1.00	NC
A	C	0.07	0.04	0.30	1.40 (0.73–2.70)
A	T	0.31	0.36	0.40	1.15 (0.82–1.60)
JAK2 c.-1132G>T	*JAK2* c.-139G>A				
G	G	0.65	0.66	0.52	1.11 (0.79–1.55)
G	A	0.002	0.001	0.55	3.28 (0.06–171.59)
T	G	0.34	0.34	0.63	1.08 (0.77–1.51)
T	A	0.006	0.00	0.99	NC
STAT3 c.*1671T>C	*STAT3* c.-1937C>G				
T	C	0.43	0.35	**0.003**	1.64 (1.19–2.27)
T	G	0.16	0.18	0.16	1.35 (0.88–2.06)
C	C	0.29	0.31	0.07	1.36 (0.96–1.93)
C	G	0.12	0.16	0.67	1.09 (0.70–1.71)

Significant values are presented in bold.
%, percentage; CI, confidence interval; NC, not calculated.
[a]Odds ratio (OR) adjusted by age, nevi, and sun exposure by multivariate analysis.

SNVs and clinicopathological aspects of patients

JAK1 c.991-27CC genotype was more common in male than in female patients (57.8 vs. 40.0%, $p = 0.005$). The frequency of CC genotype was also higher in male patients than in controls (57.8 vs. 37.1%); individuals with CC genotype were under 2.12-fold increased risk for CM than individuals with other genotypes (95% CI: 1.14–3.94,$p = 0.01$). Similar frequencies of *JAK1*, *JAK2*, and *STAT3* genotypes were seen in patients stratified by age, phototype, nevi presence, sun exposure, sunburn episodes, type of sun exposure (Supplementary Table S6), tumor location, ulceration, type of growth, Clark level, Breslow thickness, clinical stage, and metastases (Supplementary Table S7). No associations of *JAK1*, *JAK2*, and *STAT3* combined genotypes, alleles, and haplotypes with the clinicopathological aspects of patients were also seen in the study (data not shown).

Survival analysis

Survival data were obtained from 237 out of 248 CM patients. The median follow-up of patients enrolled in the survival analysis was 101 months (range, 5–249 months). The final status of patients was established in July 2021. At that time, 148 patients were alive without disease, two were alive with disease, 52 died due to CM effects, and 35 died due to unrelated causes.

At 60 months of follow-up, PFS was lower in male patients (61.0 vs. 75.0%, $p = 0.008$), in patients with axial tumor (trunk and head) (63.5 vs. 76.9%, $p = 0.05$), vertical growth tumor (66.7 vs. 87.9%, $p = 0.01$), Clark levels III to V tumors (59.7 vs. 90.3%, $p < 0.0001$), Breslow thickness higher than 1.5 mm (46.4 vs. 89.4%, $p < 0.0001$), and advanced-stage tumors (stage III or IV) (25.6 vs. 79.4%, $p < 0.0001$) (Kaplan Meier estimates) (Supplementary Figure S2). Differences among groups remained the same in the univariate Cox analysis. After multivariate Cox analysis, patients with axial tumor, with Breslow thickness higher than 1.5 mm, and advanced stages had 2.42, 4.26, and 4.08 more chances of presenting disease progression, respectively (Supplementary Table S8).

At 60 months of follow-up, MSS was lower in older patients (78.3 vs. 88.0%, $p = 0.02$), male patients (74.0 vs. 92.8%, $p < 0.0001$), patients with axial tumor (79.2 vs. 91.8%, $p = 0.005$), Clark levels III to V tumors (78.6 vs. 97.2%, $p < 0.0001$), Breslow thickness higher than 1.5 mm (69.1 vs. 99.1%, $p < 0.0001$), and advanced-stage tumors (50.3 vs. 92.5%, $p < 0.0001$) (Kaplan–Meier estimates) (Supplementary Figure S3). Differences among groups remained the same in the univariate Cox analysis. After the multivariate Cox analysis, patients with axial tumor, Breslow thickness higher than 1.5 mm, and advanced stages had 4.52, 7.66, and 3.95 more chances of evolving to death due to CM than others, respectively (Supplementary Table S8).

JAK1 (c.1648+1272G>A, c.991-27C>T), *JAK2* (c.-1132G>T, c.-139G>A) and *STAT3* (c.*1671T>C, c.-1937C>G) did not alter the PFS and MSS of CM patients (Supplementary Table S8). No association of SNV combinations, gene alleles, and haplotypes with PFS or MSS was found in the study (data not shown).

JAK1, *JAK2*, and *STAT3* expression in peripheral blood samples

Similar mean values of *JAK1* (1.02 vs. 1.26 AU, $p = 0.08$) and *JAK2* (1.00 vs. 1.19 AU, $p = 0.32$) expressions were found in the

leukocytes of peripheral blood samples of patients and controls, but the mean value of *STAT3* expression was higher in patients than in controls (1.23 vs. 0.96 AU, $p = 0.03$) (Figure 1A).

The mean value of *JAK1* expression was higher in patients with the CC genotype (1.22 vs. 0.75 AU, $p = 0.01$) and C allele (1.11 vs. 0.75 AU, $p = 0.02$) of *JAK1* c.991-27C>T SNV than in those with the CT or TT genotype and T allele, respectively (Figures 1B, C). The mean value of *STAT3* expression was higher in patients with *STAT3* c.*1671CC genotype than in those with TT or TC genotype (1.76 vs. 1.16 AU, $p = 0.03$) (Figure 1D). Similar mean values of gene expression were seen in the leukocytes of the peripheral blood samples of CM patients with the distinct genotypes of *JAK1* c.1648+1272G>A, *JAK2* c.-1132G>T, *JAK2* c.-139G>A, and *STAT3* c.-1937C>G SNVs (Supplementary Figure S4, Supplementary Table S9).

From the results found in the associations of analyzed SNVs with risk of CM, *JAK1* c.991-27C>T and *STAT3* c.-1937C>G were seen in most of the significant combined genotypes. *STAT3* c.-1937C>G was considered as the SNV of greatest interest in the study; therefore, it was the object of additional functional analyzes.

STAT3 promoter region activity and expression in modified SKMEL-28 cell line

The mean value of luciferase promoter region activity in SKMEL-28 cells with *STAT3* c.-1937CC genotype was higher than that found in cells with *STAT3* c.-1937GG genotype (4,013.34 *vs.* 2,463.32 UA; $p = 0.004$) (Figure 2A).

The mean value of *STAT3* expression in SKMEL-28 cells with *STAT3* c.-1937CC genotype was higher than those found in cells with GG genotype (649.20 vs. 0.03 AU; $p = 0.003$) and in cells with empty vector (649.20 vs. 2.11 AU; $p = 0.001$) (Figure 2B).

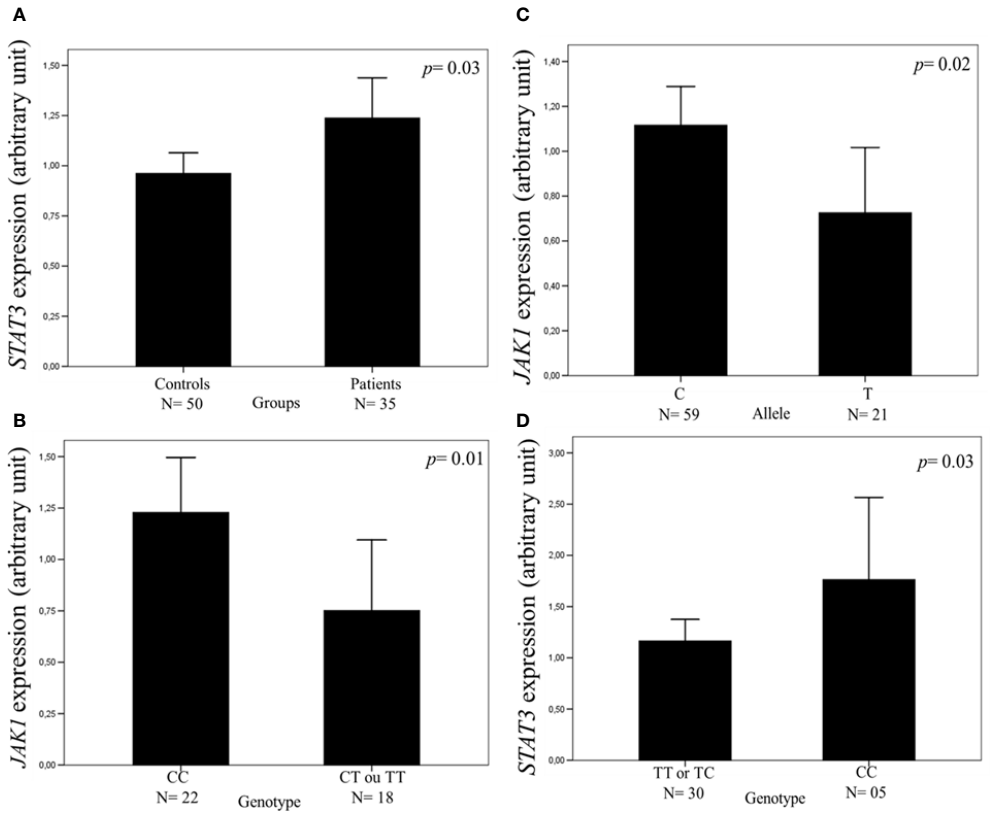

FIGURE 1
Expression of the *JAK1* and *STAT3* genes in the leukocytes of peripheral blood samples measured by real-time polymerase chain reaction. The relative expression level was normalized by β-actin reference gene with the 2^{-DDCt} cycle threshold method. The values of 15% of the samples were repeated in separate experiments with 100% agreement, and the results are expressed in arbitrary units (AUs). The results are shown as means between groups. For the statistical tests, values with p <0.05 were considered significant. The *STAT3* expression was higher in patients with cutaneous melanoma (CM) than in controls (1.23 vs. 0.96 AU) **(A)**. The *JAK1* expression was higher in CM patients with CC genotype **(B)** and with allele C **(C)** than in those with CT or TT genotype and allele T of *JAK1* c.991-27C>T, the single-nucleotide variant (SNV) (1.22 vs. 0.75 and 1.11 vs. 0.75 AU, respectively). The *STAT3* expression was higher in CM patients with CC genotype than in those with TT or TC genotype of c.*1671T>C SNV (1.76 vs. 1.16 AU) **(D)**.

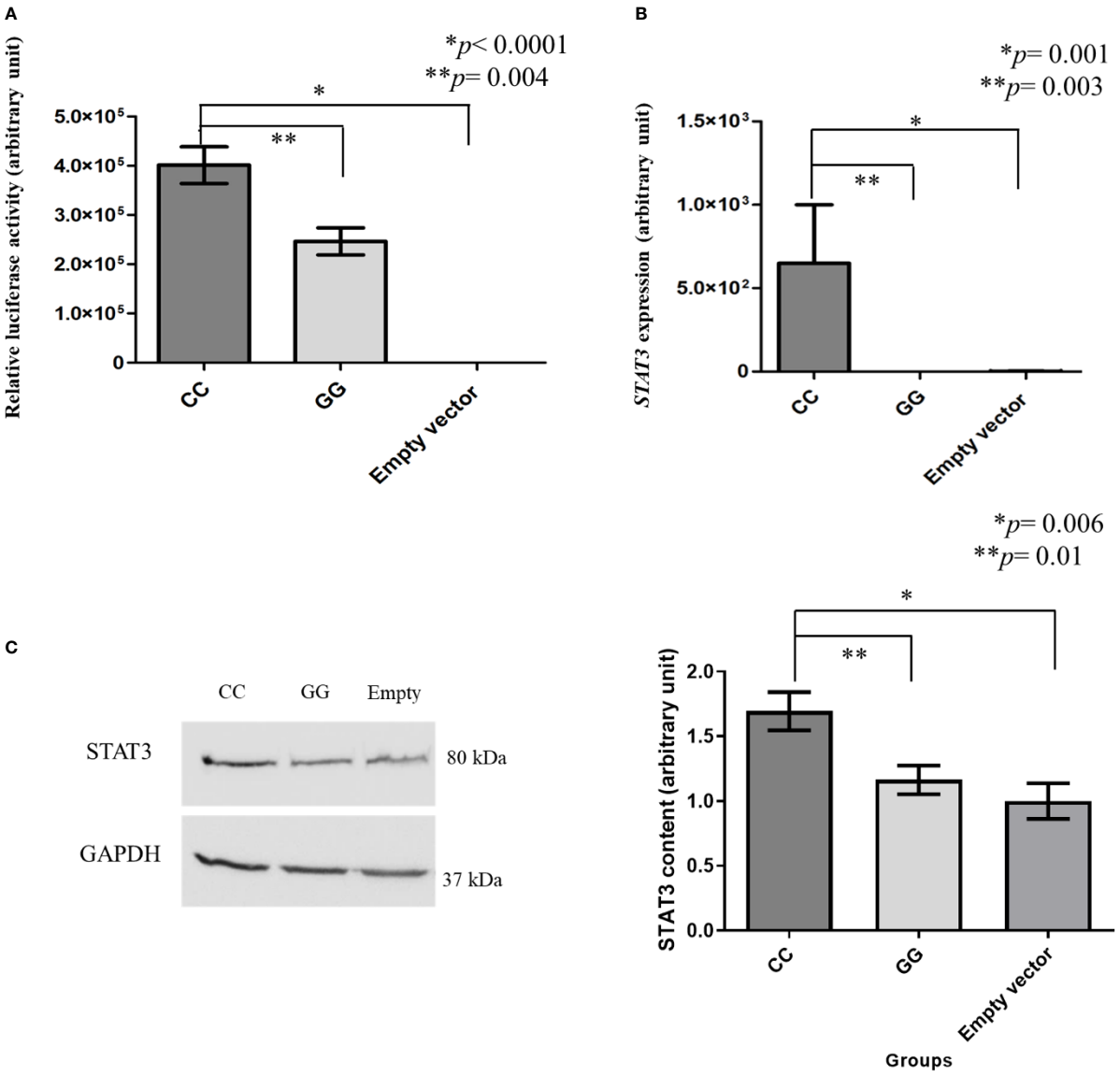

FIGURE 2
Luciferase activity and *STAT3* expression measured by real-time polymerase chain reaction and STAT3 level measured by western blot in modified SKMEL-28 (*STAT3* c.-1937CC or GG genotype). Total proteins (50 µg) were analyzed by 10% sodium dodecyl sulfate polyacrylamide gel electrophoresis, and the separated proteins were transferred to nitrocellulose membranes. The membranes were blocked with 5% skimmed milk in phosphate-buffered saline (PBS-Tween) and incubated with specific primary antibodies anti-STAT3 (Santa Cruz, USA) and anti-GAPDH (Santa Cruz, USA) overnight at 4°C. A horseradish peroxidase-conjugated goat anti-mouse IgG was used as the secondary antibody (Santa Cruz, USA). GAPDH was used as normalizer in the western blot experiments. ECL Western Blot Detection Reagents kit (GE Healthcare, USA) was used, and the intensities of the protein bands were quantitated using ImageJ software (National Institutes of Health, USA). The results are shown as means between groups. For the statistical tests, values with $p < 0.05$ were considered significant. SKMEL-28 cells with CC genotype presented a higher *STAT3* luciferase activity than those with GG genotype [4,013.34 *vs.* 2,463.32 arbitrary units (AU)] and the one with empty vector (4,013.34 vs. 0.0122 AU) **(A)**, a higher *STAT3* gene expression than those with GG genotype (649.20 vs. 0.03 AU) and the one with empty vector (649.20 vs. 2.11 AU) **(B)**, and a higher STAT3 protein level than in those with GG genotype (1.69 *versus* 1.16 AU) and the one with empty vector (1.69 vs. 1.00 AU) **(C)**. * and ** statistically significant result.

STAT3 protein level in modified SKMEL-28 and unmodified cell lines

The STAT3 level was higher in SKMEL-28 cells with *STAT3* c.-1937CC genotype than in those with GG genotype (1.69 *versus* 1.16 AU; $p = 0.01$) and in those with empty vector (1.69 *vs.* 1.00 AU; $p = 0.006$) (Figure 2C).

Unmodified cell lines with *STAT3* c.-1937CC genotype also presented a higher STAT3 level than those with GG genotype (1.93 *versus* 1.27 UA, $p = 0.0027$) (Supplementary Figure S5) despite the status of *RAS* and *BRAF* mutations.

STAT3 in apoptosis and cell cycle assays in modified SKMEL-28 cell line

Initially, cells were identified by size (forward scatter) and granularity (side scatter) as shown in Figure 3A; then, they were evaluated for specific tags. The percentages of live cells (Q2-3) in initial apoptosis (Q2-4), in late apoptosis (Q2-2), and in necrosis (Q2-1) are shown in Figures 3B–E. Similar percentages of apoptotic and necrotic cells were seen in SKMEL-28 with CC and GG genotypes of *STAT3* c.-1937C>G SNV within a 24-h period (Figure 3F).

The cell cycle characteristics of SKMEL-28 line were quantified and evaluated using area (*A*) and height (*H*) for 7-AAD tagging, as shown in Figure 4A, and separation of the G1, S, and G2 phases of the cell cycle is shown in Figures 4B–E. The percentage of cells in S phase was higher than in SKMEL-28 cells with CC genotype than in SKMEL-28 cells with GG genotype of *STAT3* c.-1937C>G SNV (57.54 vs. 30.73%, $p = 0.04$). The percentage of cells in G2 phase was higher in SKMEL-28 cells with *STAT3* c.-1937GG genotype than in cells transfected with the empty vector (10.96 *versus* 4.59%, $p = 0.03$) (Figure 4F).

Discussion

Our group investigated, in the current study, whether *JAK1* (c.1648+1272G>A, c.991-27C>T), *JAK2* (c.-1132G>T, c.-139G>A), and *STAT3* (c.*1671T>C, c.-1937C>G) SNVs alter the risk, clinicopathological aspects, and prognosis of CM as well as the activity of respective proteins.

Firstly, we observed that individuals with TT genotype of *STAT3* c.*1671T>C SNV were under 1.60-fold increased risk for CM than individuals with other genotypes. Previous studies demonstrated that CC genotype conferred protection against gastric cancer (12), pancreatic cancer (13), tongue squamous cell

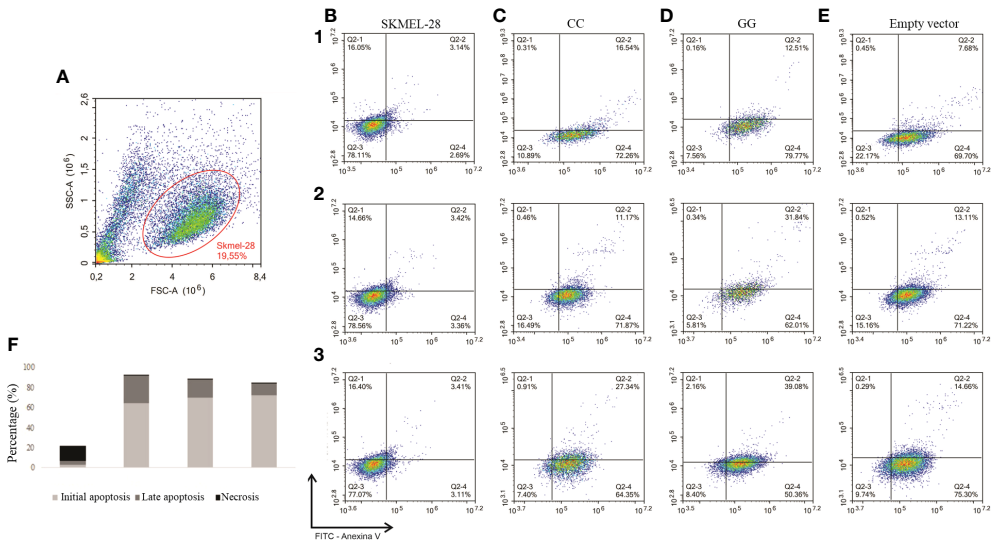

FIGURE 3
Detection of early and late apoptosis by flow cytometry in SKMEL-28 cutaneous melanoma cell line genetically modified to present the different genotypes of *STAT3* c.-1937C> G. The cells were subjected to nutrient deprivation, treated with 200 μM of hydrogen peroxide for 24 h, and marked with the antibodies Annexin V and 7-AAD. Three independent experiments were performed (1, 2, and 3). The identification of cells was performed by separation by size (FSC) and granularity (SSC) **(A)**. Dot plots referring to experiments one to three for the analysis of cell apoptosis, in which viable cells (Q2-3), cells in initial apoptosis (Q2-4), cells in late apoptosis (Q2-2), and necrosis (Q2) were identified in SKMEL-28 **(B)**, cell with CC genotype **(C)**, cell with GG genotype **(D)**, and cell transfection with empty vector **(E)**. For the statistical tests, values with $p < 0.05$ were considered significant. The results are shown as means between groups: CC vs. GG (initial apoptosis: 69.49 vs. 64.05%, $p = 0.57$; late apoptosis: 18.35 vs. 27.81%, $p = 0.36$; necrosis: 0.56 vs. 0.89%, $p = 0.64$), CC vs. empty vector (initial apoptosis: 69.49 vs. 72.07%, $p = 0.44$; late apoptosis: 18.35 vs. 11.82%, $p = 0.27$; necrosis 0.56 vs. 0.42%, $p = 0.50$), and GG vs. empty vector (initial apoptosis: 64.05 vs. 72.07%, $p = 0.40$; late apoptosis: 27.81 vs. 11.82%, $p = 0.12$; necrosis 0.89 vs. 0.42%, $p = 0.54$) **(F)**.

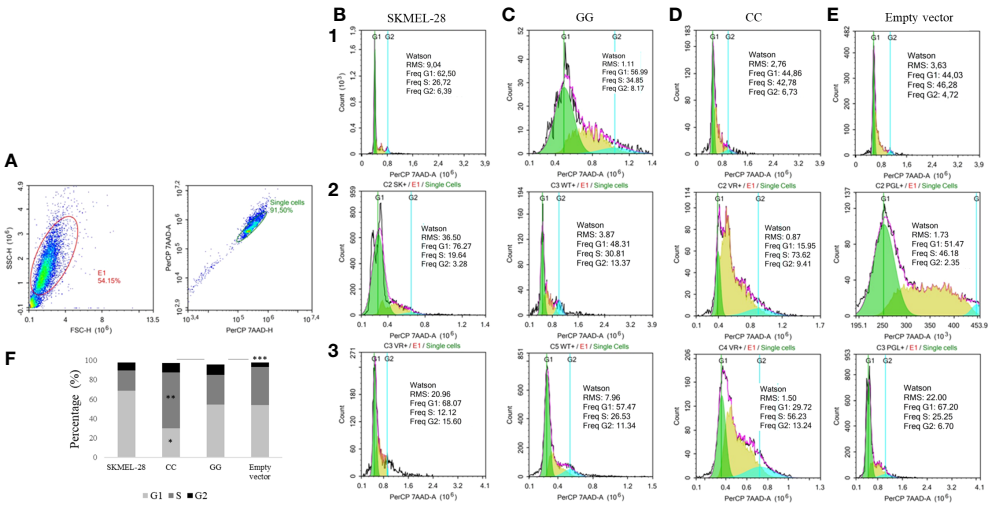

FIGURE 4
Cell cycle detection by flow cytometry in a SKMEL-28 cutaneous melanoma cell genetically modified to present the different genotypes of *STAT3* c.-1937C>G. The cells were stained with the 7-AAD antibody for cell viability. Three independent experiments were performed (1, 2, and 3). The identification of the cells was carried out from the separation by size (FSC) and granularity (SSC). Afterwards, the removal of the doublets was carried out through the area (A) and the height (H) **(A)**. From the individualized cells, the fluorescence intensity of 7-AAD and the separation of phases G1, S, and G2 of the cell cycle of experiments one to three were evaluated using the Watson model in SKMEL-28 **(B)**, cell with GG genotype **(C)**, cell with CC genotype **(D)**, and cell transfection with empty vector **(E)**. For the statistical tests, values with p <0.05 were considered significant. The results are shown as means between groups: CC vs. GG (G1: 30.18 vs. 54.26%, *p = 0.05; S: 57.54 vs. 30.73%, **p = 0.04; G2: 9.79 vs. 10.96%, p = 0.65), CC *vs.* empty vector (G1: 30.18 vs. 54.23%, p = 0.09; S: 57.54 vs. 39.24%, p = 0.18; G2: 9.79 vs. 4.59%, p = 0.08), and GG vs. empty vector (G1: 54.26 vs. 54.23%, p = 0.99; S: 30.73 vs. 39.24%, p = 0.31; G2: 10.96 vs. 4.59%, ***p = 0.03) **(F)**.

carcinoma (14), and hepatocellular carcinoma in women (34). Allele C also protected against tongue squamous cell carcinoma (14). In contrast, the SNV did not alter the risk of non-small cell lung cancer (35), hepatocellular carcinoma (36), and cancer in general (37). The differences between our data and the results obtained in previous studies may be attributed to the heterogeneity of the evaluated tumors and their biological and ethnical differences.

In this study, *STAT3* expression in the leukocytes of peripheral blood samples was higher in patients with *STAT3* c.*1671CC genotype compared to patients with TT or CT genotype; this finding was not expected by us since STAT3 acts on cell proliferation and survival (2), and TT genotype was associated with an increased risk of CM. Lai et al.(14) found a higher *STAT3* gene and microRNA expression in tongue squamous cell carcinoma than in normal tissue; the authors also observed increased STAT3 levels in the tongue squamous cell carcinoma of patients with *STAT3* c.*1671TT genotype than in the ones with other genotypes (14). In addition, an increased expression of *STAT3* gene was seen in lymphoblastoid B cells with TT genotype than in cells with other genotypes (12). We are aware that the *STAT3* expression was evaluated only in peripheral blood samples in this study, and thus further evaluation of gene expression should be conducted in CM fragments or cells of patients with different *STAT3* c.*1671T>C genotypes to obtain consistent conclusions about the role of *STAT3* c.*1671T>C SNV on protein production.

Secondly, we found that individuals with CC genotype of the *STAT3* c.-1937C>G SNV were under 6.70-fold increased risk of CM than individuals with other genotypes. Previous studies demonstrated that GG genotype conferred protection against non-small cell lung cancer (35) and breast cancer (38) development. Other studies showed that carriers of GG genotype were under an increased risk of lung cancer (39) and basal cell carcinoma (40). The allele G was associated with an increased cervical cancer risk (41), and the risks of gastric cancer (12), hepatocellular carcinoma (34), and cancer in general (39, 42) were not altered by the *STAT3* c.-1937C>G SNV. The contrast in the results of the studies may be attributed again to tumor heterogeneity and the populations' ethnical differences.

STAT3 c.-1937C>G SNV is in the 5′ region of the *STAT3* gene, at position 1,633 base pairs ahead of the ATG site (15) and has been associated with increased transcription factor NKX2-5 in the binding site (15) and with unclear functional consequences in the encoded protein. We observed that *STAT3* expression was higher in CM patients than in controls.

In SKMEL-28 cells genetically modified to express different genotypes of the *STAT3* c.-1937C>G SNV, we also observed that cells with CC genotype presented increased luciferase activity, *STAT3* gene expression, and STAT3 levels when compared to cells with the GG genotype. Different CM cell lines with CC genotype also showed higher STAT3 levels than the one with GG genotype in our study despite the differences in *RAS* and *BRAF* mutation status. Ito et al. (16) did not find differences in luciferase activity in metastatic renal carcinoma cells with distinct alleles of *STAT3* c.-1937C>G SNV, and no difference in *STAT3* expression was found in melanoma cells with distinct *STAT3* c.-1937C>G genotypes by Schrama et al. (15). It is possible that the association of the CC genotype of *STAT3* c.-1937C>G SNV with a higher STAT3 expression and levels in different CM cells and experiments in the current study makes our findings more reliable than those described by Schrama et al. Thus, we can infer that the increased risk of CM in patients with the CC genotype of *STAT3* c.-1937C>G SNV is attributed to greater STAT3 protein production.

We also observed that cells with CC genotype presented a higher percentage of cells in the S phase of the cell cycle when compared to cells with the GG genotype in modified SKMELL-28, but similar percentages of apoptotic and necrotic cells were seen in cells with CC and GG genotypes. To the best of our knowledge, there are no studies on the role of *STAT3* c.-1937C>G SNV in apoptosis and cell cycle in CM, and thus it is not possible to compare our results with the others previously described. However, it is already well known that the transition from the G1 phase of the cell cycle to the S phase is crucial for the control of cell proliferation, and its misregulation promotes oncogenesis (43, 44). Since the S phase is responsible for DNA replication, we believe that *STAT3* c.-1937CC genotype possibly increases the JAK/STAT pathway activity, with a greater chance of CM formation and progression, as seen in individuals with *STAT3* c.-1937CC genotype enrolled in our study. It is essential to comment that additional functional studies are required to confirm these hypotheses.

Thirdly, the TC haplotype of *STAT3* c.*1671T>C and *STAT3* c.-1937C>G SNVs was more common in patients than in controls, thus being considered a risk factor for CM. We also observed a progressive increase in the risk of CM (up to 4.0-fold) when combined SNVs were analyzed two by two, three by three, and four by four, demonstrating the importance of evaluating genetic changes together in the signaling pathway instead of them isolated. While the functional impact of a single SNV may be low, the interaction of several SNVs with a slightly increased or reduced functional activity eventually affects cancer risk (45). It is worth commenting that *STAT3* c.-1937C>G and *JAK1* c.991-27C>T SNVs were present in most of all significant genotypic combinations. Once that a high expression of JAK1 has been identified in individuals with *JAK1* c.991-27CC genotype in this study, we believe that *JAK1* c.991-27C>T SNV may have contributed to the STAT3 SNV in maintaining JAK/STAT pathway activation, presenting a greater chance of CM development and progression as a consequence.

Fourthly, we observed that male patients with *JAK1* c.991-27CC genotype were more common than in female patients and that men with this genotype were under 2.12-fold increased risk for CM than the controls. To the best of our knowledge, there are no studies of these SNVs associated with CM risk and clinicopathological aspects.

Finally, we found that age, gender, tumor location, pattern of tumor growth, Clark levels, Breslow thickness, and tumor stage altered the survival of our CM patients as previously reported (46–48). Nevertheless, patients' survival was not altered by the analyzed SNVs. We are again aware that the number of patients with distinct genotypes of SNVs presenting disease progression and/or death may have been insufficient to evidence impacts of the inherited abnormalities in survival.

In conclusion, our data present, for the first time, preliminary evidence that *JAK1* (c.1648+1272G>A, c.991-27C>T), *JAK2* (c.-1132G>T), and *STAT3* (c.*1671T>C, c.-1937C>G) SNVs alter the risk and clinical aspect of CM patients, where *STAT3*c.-1937C>G *JAK1* c.991-27C>T has the most important action. The association of *STAT3* c.-1937C>G SNV with the risk of CM may be attributed to its actions in the promoter region of *STAT3* gene and in the cell cycle, with consequent changes in protein production and cell proliferation. We are aware that the results of the association of genotypes with the clinicopathological aspects and survival of CM patients were obtained from a relatively small number of patients from a single country, a single genetically transformed cell line served for the majority of functional analyses of *STAT3* c.-1937C>G SNV, the mechanisms by which the *STAT3* c.-1937C>G SNV operates in the cell cycle were not totally determined, and functional studies for other SNVs of interest were not performed in the current study. Thus, these results should be validated in a further epidemiological study with CM patients and controls of diverse ethnic populations and clarified in additional functional studies, and if they are, the data can be used to select individuals at a high risk of CM who should receive special attention in tumor prevention and early detection.

Data availability statement

The datasets presented in this study can be found in online repositories. The names of the repository/repositories and accession number(s) can be found in the article/ **Supplementary Material**.

Ethics statement

The studies involving human participants were reviewed and approved by UNICAMP Research Ethics Committee (Process 58186316.1.0000.5404). The patients/participants provided their written informed consent to participate in this study.

Author contributions

GG, RS, JR, and CL were responsible for the study design. GG, LM, KF, LC, JC, and AM were responsible for collecting clinical data and performing the experiment. GG, GL, LM, KF, CT, LC, and AM were responsible for the statistical analysis and interpretation of data. GG was responsible for drafting the manuscript and GL, RS, JR, and CL were responsible for the critical revision of the manuscript for intellectual content. All authors contributed to the article and approved the submitted version.

Funding

This work was supported by grants from the FAPESP (2016/25407-4 and 2019/16776-4) and FAPESP 2019/09168-8.

Conflict of interest

The authors declare that the research was conducted in the absence of any commercial or financial relationships that could be construed as a potential conflict of interest.

Publisher's note

Supplementary material

The Supplementary Material for this article can be found online at: https://www.frontiersin.org/articles/10.3389/fonc.2022.943483/full#supplementary-material

References

1. Arshad S, Navedd M, Ullia M, Javed K, Butt A, Khawar M, et al. Targeting STAT-3 signaling pathway in cancer for development of novel drugs: advancements and challenges. *Genet Mol Biol* (2020) 43:1678–4685. doi: 10.1590/1678-4685-GMB-2018-0160

2. Nicholas C, Lesinski GB. The JAK-STAT signal transduction pathway in melanoma. *Breakthroughs Melanoma Res* (2011) 14:283–307. doi: 10.5772/18876

3. Pan F, Wang Q, Li S, Huang R, Wang X, Liao X, et al. Prognostic value of key genes of the JAK–STAT signaling pathway in patients with cutaneous melanoma. *Oncol Lett* (2020) 9:1928–46. doi: 10.3892/ol.2020.11287

4. Hu X, Yuan L, Ma T. Mechanisms of JAK–STAT signaling pathway mediated by CXCL8 gene silencing on epithelial–mesenchymal transition of human cutaneous melanoma cells. *Oncol Lett* (2020) 1:1973–81. doi: 10.3892/ol.2020.11706

5. Huynh J, Chand A, Gough D, Ernst M. Therapeutically exploiting STAT3 activity in cancer - using tissue repair as a road map. *Nat Rev Cancer* (2019) 19:82–96. doi: 10.1038/s41568-018-0090-8

6. O'Shea JJ, Schwatz DM, Villarino AV, Gadina M, McInnes IB, Laurence A. The JAK-STAT pathway: impact on human disease and therapeutic intervention. *Annu Rev Med* (2015) 66:311–28. doi: 10.1146/annurev-med-051113-024537

7. Sun Q, Mayeda A, Hampson RK, Krainer AR, Rottman FM. General splicing factor SF2/.ASF promotes alternative splicing by binding to an exonic splicing enhancer. *Genes Dev* (1993) 7:2598–608. doi: 10.1101/gad.7.12b.2598

8. Slattery ML, Lundgreen A, Kadlubar SA, Bondurant KL, Wolff RK. JAK/STAT/SOCS-signaling pathway and colon and rectal cancer. *Mol Carcinog* (2013) 52:155–66. doi: 10.1002/mc.21841

9. Slattery ML, Lundgreen A, Hines LM, Torres-Mejia G, Wolff RK, Stern MC, et al. Genetic variation in the JAK/STAT/SOCS signaling pathway influences breast cancer-specific mortality through interaction with cigarette smoking and use of aspirin/NSAIDs: The breast cancer health disparities study. *Breast Cancer Res Treat* (2014) 147:145–58. doi: 10.1007/s10549-014-3071-y

10. Vaclavicek A, Bermejo JL, Schmutzler RK, Sutter C, Wappenschmidt B, Meindl A, et al. Polymorphisms in the janus kinase 2 (JAK)/signal transducer and activator of transcription (STAT) genes: putative association of the STAT gene region with familial breast cancer. *Endocr Relat Cancer* (2007) 14:267–77. doi: 10.1677/ERC-06-0077

11. Wang S, Zhang W. Genetic variants in IL-6/JAK/STAT3 pathway and the risk of CRC. *Tumor Biol* (2015) 37:6561–9. doi: 10.1007/s13277-015-4529-1

12. Zhou F, Cheng L, Qiu L, Wang M, Li J, Sun M, et al. Associations of potentially functional variants in IL-6, JAKs and STAT3 with gastric cancer risk in an eastern Chinese population. *Oncotarget* (2016) 7:28112–23. doi: 10.18632/oncotarget.8492

13. Zhu B, Zhu Y, Lou Z, Ke J, Zhang Y, Li J, et al. A single nucleotide polymorphism in the 3'-UTR of STAT3 regulates its expression and reduces risk of pancreatic cancer in a Chinese population. *Oncotarget* (2016) 7:62306–11. doi: 10.18632/oncotarget.11607

14. Lai H, Xu G, Meng H, Zhu H. Association of SP1 rs1353058818 and STAT3 rs1053004 gene polymorphisms with human tongue squamous cell carcinoma. *Biosci Rep* (2019) 39:1–12. doi: 10.1042/BSR20190955

15. Schrama D, Ugurel S, Sucker A, Ritter C, Zapatka M, Schadendorf S, et al. *STAT3* single nucleotide polymorphism rs4796793 SNP does not correlate with response to adjuvant IFNa therapy in stage III melanoma patients. *Front Med* (2014) 1:47. doi: 10.3389/fmed.2014.00047

16. Ito N, Eto M, Nakamura E, Takahashi A, Tsukamoto T, Toma H, et al. *STAT3* polymorphism predicts interferon-alfa response in patients with metastatic renal cell carcinoma. *J Clin Oncol* (2007) 25:2785–91. doi: 10.1200/JCO.2006.09.8897

17. Fitzpatrick TB. The validity and practicality of sun-reactive skin types I through VI. *Arch Dermatol* (1988) 6:869–71. doi: 10.1001/archderm.124.6.869

18. Rigel DS, Friedman RJ, Levenstein MJ, Greenwald DI. Relationship of fluorescent lights to malignant melanoma: another view. *J Dermatologic Surg Oncol* (1983) 9:836–9. doi: 10.1111/j.1524-4725.1983.tb00741.x

19. Bosserhoff AK. *Melanoma development: Molecular biology, genetics and clinical application* Vol. 447. Springer (2017).

20. Landman G, miller H, fillus N, maceira j, marques M, costa MB, et al. Consenso para laudo anatomopatológico do melanoma cutâneo. grupo multicêntrico e multidisciplinar brasileiro para estudo do melanoma (GBM). *Acta Oncol Bras* (2003) 23:504–10.

21. Breslow A. Tumor thickness, level of invasion and node dissection in stage I cutaneous melanoma. *Ann Surg* (1975) 182:572–5. doi: 10.1097/00000658-197511000-00007

22. Clark WHJr, From L, Bernardino EA, Mihm MC. The histogenesis and biologic behavior of primary human malignant melanomas of the skin. *Cancer Res* (1969) 29:705–27.

23. Balch CM, Gershenwald JE, Soong SJ, Thompson JF, Atkins MB, Byrd DR, et al. Final version of 2009 AJCC melanoma staging and classification. *J Clin Oncol* (2009) 27:6199–206. doi: 10.1200/JCO.2009.23.4799

24. Lourenço GJ, Oliveira C, Carvalho BS, Torricelli C, Silva JK, Gomez GVB, et al. Inherited variations in human pigmentation-related genes modulate cutaneous melanoma risk and clinicopathological features in Brazilian population. *Sci Rep* (2020) 10:12129. doi: 10.1038/s41598-020-68945-9

25. McLaren W, Pritchard B, Rios D. Deriving the consequences of genomic variants with the ensembl API and SNP effect predictor. *Bioinformatics* (2010) 26:2069–70. doi: 10.1093/bioinformática/btq330

26. Desmet FO, Hamroun D, Lalande M, Collod-Béroud G, Claustres M, Béroud C. Human splicing finder: an online bioinformatics tool to predict splicing signals. *Nucleic Acids Res* (2009) 37:e67. doi: 10.1093/nar/gkp215

27. Nazarian A, Gezan AS. GenoMatrix: A software package for pedigree-based and genomic prediction analyses on complex traits. *J Hered* (2016) 107:372–9. doi: 10.1093/jhered/esw020

28. Xu Z, Taylor JA. SNPinfo: Integrating GWAS and candidate gene information into functional SNP selection for genetic association studies. *Nucleic Acids Res* (2009) 37:600–5. doi: 10.1093/nar/gkp290

29. Barenboim M, Zoltick BJ, Guo Y. MicroSNiPer: a web tool for prediction of SNP effects on putative microRNA targets. *Hum Mutat* (2010) 31:1223–32. doi: 10.1002/humu.21349

30. Thomas LF, Saito T, Saetrom P. Inferring causative variants in microRNA target sites. *Nucleic Acids Res* (2011) 39:e109. doi: 10.1093/nar/gkr414

31. Pérez-Alea M, McGrail K, Sánchez-Redondo S, Ferrer B, Fournet G, Cortés J, et al. ALDH1A3 is epigenetically regulated during melanocyte transformation and is a target for melanoma treatment. *Oncogene* (2017) 36:5695–708. doi: 10.1038/onc.2017.160

32. Monteiro LMO, Arruda LM, Silva-Rocha R. Emergent properties in complex synthetic bacterial promoters. *ACS Synthetic Biol* (2018) 7:602–12. doi: 10.1021/acssynbio.7b00344

33. Monteiro LMO, Sanches-Medeiros A, Westmann CA, Silva-Rocha R. Unraveling the complex interplay of Fis and IHF through synthetic promoter engineering. *Front Bioeng Biotechnol* (2020) 8:510. doi: 10.3389/fbioe.2020.00510

34. Xie J, Zhang Y, Zhang Q, Han Y, Yin J, Pu R, et al. Interaction of signal transducer and activator of transcription 3 polymorphisms with hepatitis b virus mutations in hepatocellular carcinoma. *Hepatology* (2013) 5:2369–77. doi: 10.1002/hep.26303

35. Jiang B, Zhu ZZ, Liu F, Yang LJ, Zhang WY, Yuan HH, et al. *STAT3* gene polymorphisms and susceptibility to non-small cell lung cancer. *Genet Mol Res* (2011) 10:1856–65. doi: 10.4238/vol10-3gmr1071

36. Fatemipour M, Zadeh AMA, Molaei H, Geramizadeh B, Fatemipour B. Vahedi SM e malekpourafshar r(2016) Study on the relationship of demographic characteristics of rs1053004 in STAT3 gene in patients with HCC following chronic HBV infection. *Iran J Virol* (2016) 102:40–7. doi: 10.21859/isv.10.2.3.40

37. Moazeni-Roodi A, Hashemi M. Association between *STAT3* rs1053004 polymorphism and cancer risk: a meta-analysis. *Mol Biol Res Commun* (2018) 7:119–24. doi: 10.22099/mbrc.2018.29688.1323

38. Zhao L, Zhang Q, Luan X, Huang X, Zhao S, Zhao H. *STAT3* and *STAT5b* polymorphism contributes to breast cancer risk and clinical outcomes. *Int J Clin Experiment* (2015) 8:2033–8.

39. Gong WJ, Ma LY, Hu L, Lv YN, Huang H, Xu JQ, et al. STAT3 rs4796793 contributes to lung cancer risk and clinical outcomes of platinum-based chemotherapy. *Int J Clin Oncol* (2018) 24:476–84. doi: 10.1007/s10147-018-01386-7

40. Slawinska M, Zablotna M, Glen J, Lakomy J, Nowicki R, Sobjanek M. STAT3 polymorphisms and IL-6 polymorphism are associated with the risk of basal cell carcinoma in patients from northern Poland. *Arch Dermatol Res* (2019) 311:697–704. doi: 10.1007/s00403-019-01952-7

41. Wang K, Zhou B, Zhang J, Xin Y, Lai T, Wang Y, et al. Association of signal transducer and activator of transcription 3 gene polymorphisms with cervical cancer in Chinese women. *DNA Cell Biol* (2011) 30:931-6. doi: 10.1089/dna.2010.1179

42. Yan R, Lin F, Hu C, Tong S. Association between STAT3 polymorphisms and cancer risk: a meta-analysis. *Mol Genet Genomics* (2015) 290:2261–70. doi: 10.1007/s00438-015-1074-y

43. Takeda DY, Dutta A. DNA Replication and progression through s phase. *Oncogene* (2005) 24:2827–43. doi: 10.1038/sj.onc.1208616

44. Bertoli C, Skotheim JM, de Bruin RAM. Control of cell cycle transcription during G1 and s phases. *Nat Rev Mol Cell Biol* (2013) 14(8):518–28. doi: 10.1038/nrm3629

45. Ponder BA. Cancer genetics. *Nature* (2001) 411:336–41. doi: 10.1038/35077207

46. Buettner PG, Leiter U, Eigentler TK, Garbe C. Development of prognostic factors and survival in cutaneous melanoma over 25 years: An analysis of the central malignant melanoma registry of the German dermatological society. *Cancer* (2005) 103:616–24. doi: 10.1002/cncr.20816

47. Mervic L. Prognostic factors in patients with localized primary cutaneous melanoma. *Acta Dermatovenerol Alp Pannonica Adriat* (2012) 21:27–31.

48. Gomez GVB, Rinck-Junior JA, Oliveira C, Silva DHL, Mamoni RL, Lourenço GJ, et al. *PDCD1* gene polymorphisms as regulators of T-lymphocyte activity in cutaneous melanoma risk and prognosis. *Pigment Cell Melanoma Res* (2018) 31:308–17. doi: 10.1111/pcmr.12665

frontiers | Frontiers in Oncology

TYPE Review
PUBLISHED 16 August 2022
DOI 10.3389/fonc.2022.944722

OPEN ACCESS

EDITED BY
Suzie Chen,
The State University of New Jersey,
United States

REVIEWED BY
Kevinn Eddy,
The State University of New Jersey,
United States
Isabelle Caroline Le Poole,
Northwestern University, United States

*CORRESPONDENCE
Jibo Zhou
zhoujibo1000@aliyun.com
Zhaoyang Wang
zhaokekewzy@hotmail.com

SPECIALTY SECTION
This article was submitted to Skin Cancer, a section of the journal Frontiers in Oncology

RECEIVED 15 May 2022
ACCEPTED 25 July 2022
PUBLISHED 16 August 2022

CITATION
Wang C, Wang Z, Yao T, Zhou J and Wang Z (2022) The immune-related role of beta-2-microglobulin in melanoma. *Front. Oncol.* 12:944722. doi: 10.3389/fonc.2022.944722

The immune-related role of beta-2-microglobulin in melanoma

Chuqiao Wang[1,2], Zeqi Wang[1,2], Tengteng Yao[3], Jibo Zhou[1,2]* and Zhaoyang Wang[3]*

[1]Department of Ophthalmology, Shanghai Ninth People's Hospital, Shanghai Jiao Tong University School of Medicine, Shanghai, China, [2]Shanghai Key Laboratory of Orbital Diseases and Ophthalmic Tumor, Shanghai Ninth People's Hospital, Shanghai Jiao Tong University School of Medicine, Shanghai, China, [3]Department of Ophthalmology, Shanghai Tenth People's Hospital Affiliated to Tongji University, Shanghai, China

Despite the remarkable success of immunotherapy in the treatment of melanoma, resistance to these agents still affects patient prognosis and response to therapies. Beta-2-microglobulin (β2M), an important subunit of major histocompatibility complex (MHC) class I, has important biological functions and roles in tumor immunity. In recent years, increasing studies have shown that B2M gene deficiency can inhibit MHC class I antigen presentation and lead to cancer immune evasion by affecting β2M expression. Based on this, B2M gene defect and T cell-based immunotherapy can interact to affect the efficacy of melanoma treatment. Taking into account the many recent advances in B2M-related melanoma immunity, here we discuss the immune function of the B2M gene in tumors, its common genetic alteration in melanoma, and its impact on and related improvements in melanoma immunotherapy. Our comprehensive review of β2M biology and its role in tumor immunotherapy contributes to understanding the potential of B2M gene as a promising melanoma therapeutic target.

KEYWORDS

Beta-2-microglobulin (β2M), major histocompatibility complex (MHC) class I, T cells, melanoma, immunotherapy

1 Introduction

Melanoma is the most aggressive and dangerous form of cancer that develops from transformed melanocytes. Melanoma is widely considered to be one of the most immunogenic cancers due to its high genomic mutational load and expression of cancer-specific or related antigens, so it has a strong potential to elicit recognition by anti-tumor CD8+ T cells and is sensitive to immunotherapy (1). Over the years, a variety of immunotherapies including immune checkpoint blockade (ICB) and adoptive cell

therapy (ACT) have been developed with impressive results in the treatment of melanoma. Although these immunotherapies effectively prolong the median survival of this aggressive cancer and greatly improve the management of the disease, unfortunately, more than half of melanoma patients treated with immunotherapy have some degree of intrinsic resistance or develop acquired resistance to the treatment (2–4). And immune-related adverse events also complicate the treatment. A deeper understanding of effective biomarkers associated with immunotherapy efficacy and mechanisms of immunotherapy resistance is still needed to enable earlier detection of progressive disease and develop novel therapeutics that improve efficacy.

The human beta-2-microglobulin (β2M) gene, B2M, is a small gene located on chromosome 15 (15q21.1), consisting of 4 exons that encode a full-length nonglycosylated protein (12k Da) composed of 119 amino acids. The B2M gene sequence shares a certain homology with genes of the immunoglobulin (Ig) constant region and the α3 domain of the major histocompatibility complex (MHC) class I molecule, so the β2M, which is encoded by B2M, and α3 domain display a similar structure as the Ig fragment c (Ig Fc) CH3 domain seven-stranded β-sheet (Figure 1). The β2M is synthesized by most nucleated cells and exists in two forms, membrane and free soluble β2M. Accumulating data suggests that the free β2M is one of the most important prognostic factors and predictors of survival for various types of cancers. A study in metastatic melanoma reveals that serum levels of β2M are elevated in 24% of patients before treatment, and changes in serum levels of β2M show a good correlation with disease progression (5). The membrane β2M, as a small invariable light chain, is noncovalently associated with the heavy chain of the MHC class I molecule, also known as human leukocyte antigen (HLA), on cell surfaces (6). Because it is not anchored to the cell membrane, the β2M shedding from cell surfaces or released intracellularly can exchange with free β2M present in body fluids. β2M is extensively involved in various physiological and pathological functions in tumor cells, such as cell proliferation, migration, apoptosis, and metastasis (7). However, its best-characterized function is to participate in the formation of MHC class I complexes, which play a fundamental role in tumor immunoregulation by presenting tumor antigens to activate $CD8^+$ cytolytic T lymphocytes (CTLs) and regulating the cytolytic activity of natural killer (NK) cells (8, 9). Recent studies have proposed several genetic drivers of innate or acquired resistance to ICB therapy, some of which confirm that the B2M gene impedes the success of cancer immunotherapy by generating MHC class I-loss tumor variants.

This paper is a literature review focused on the role of B2M gene in tumor immunity in melanoma, in which B2M gene mutations are the common mechanism for the total loss of MHC class I antigen expression. Here we describe how β2M is involved in MHC class I-restricted tumor antigen presentation, different genetic mechanisms of B2M alterations in melanoma tissues and cell lines, and the impact of β2M deficiency on anti-melanoid immune responses and immunotherapy. And We also mention some feasible and promising approaches to improve resistance to immunotherapy caused by B2M defects.

2 β2M as a component of MHC class I participates in tumor antigen presentation

Tumor immune surveillance requires $CD8^+$ T cells to recognize and eliminate tumor cells bearing MHC class I molecules with novel peptides due to accumulated cellular stress and mutations during tumorigenesis. One of the most fundamental and important functions of β2M is to participate in

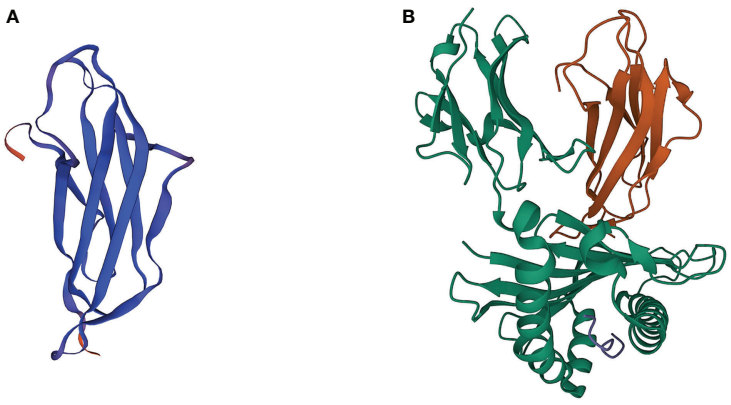

FIGURE 1
3D crystal structures of β2M and MHC class I complex. **(A)** 3D crystal structures of human β2M. **(B)** 3D crystal structures of β2M and HLA-B complex (PDB: 3BP4). Orange ribbons indicate β2M, while green ribbons indicate the HLA proteins.

this MHC class I-restricted tumor antigen presentation machinery (APM), which includes four main steps: 1) protein breakdown; 2) peptide transport and trimming; 3) assembly of MHC class I complex; 4) antigen presentation (Figure 2). Ubiquitinated proteins in the cytoplasm of malignant cells are first transported to the proteasome for deubiquitination and degradation, followed by being released into the cytoplasm again (10). These degradation products are actively transported to the endoplasmic reticulum (ER) by the transporter associated with antigen processing (TAP) and further trimmed into small peptides of 8 to 9 amino acids in length for MHC class I stable binding (11, 12). After cotranslationally inserting into the ER under the coordinated action of multiple chaperone proteins, free MHC class I heavy chain and β2M recognize and bind these modified peptides. Subsequently, the peptide-MHC class I (pMHC-I) complexes translocate from the ER to the Golgi and finally migrate to the plasma membrane where they can be recognized by and interact with the T cell receptors (TCR) on CTLs, which play a crucial role in eradicating tumor cells. The conformational change of the heavy chain due to β2M binding alters its interaction with chaperones such as calreticulin and TAP (13, 14). In addition, the β2M subunit is also necessary for the proper folding of the MHC class I heavy chain. After the cotranslational translocation of MHC class I heavy chains into the ER, two disulfide bonds are formed respectively within its α2 and α3 domains (15). β2M not only provides another disulfide bond for classical Ig folds but also facilitates intrachain disulfide bond formation in MHC class I molecule heavy chains, which promotes conformational changes of heavy chains and enables it to form stable trimolecular complexes with β2M and peptides (15, 16). In contrast, β2M-free MHC class I heavy chains would be retrotranslocated from the ER to the cytosol and eventually degraded by the proteasome due to ER quality control (17).

3 The molecular mechanisms of B2M defects in melanoma

Altered surface expression of MHC class I molecules has been frequently observed in a high proportion of various types of malignancy, among which the proportion is about 67% in melanoma and even higher in metastatic melanoma (18, 19). The heterogeneous molecular mechanisms that cause this defect can be divided into two groups, reversible and irreversible, based on whether MHC class I expression can be recovered or upregulated after cytokine treatment or other immunotherapies (20). Reversible MHC class I alterations result from defective regulation of genes encoding the heavy chain, β2M, and antigen processing machinery components, while B2M mutations often result in irreversible MHC defects. This means that MHC class I levels in MHC class I-deficient tumor cells caused by the B2M gene alteration will not be restored regardless of the type of immunotherapy. Seven major altered MHC class I phenotypes have been defined in different tumor tissues (21, 22), of which phenotype I (total loss of MHC class I antigen expression) is frequently observed in malignant melanoma cell lines and tissue samples. Tumor cells with this phenotype do not express any MHC class I molecule on their surface, so they can escape immunosurveillance and display a higher *in vivo* tumorigenicity, proliferation rate, and migratory and invasive potential (23). Many molecular mechanisms can lead to complete loss of MHC class I antigen expression, while

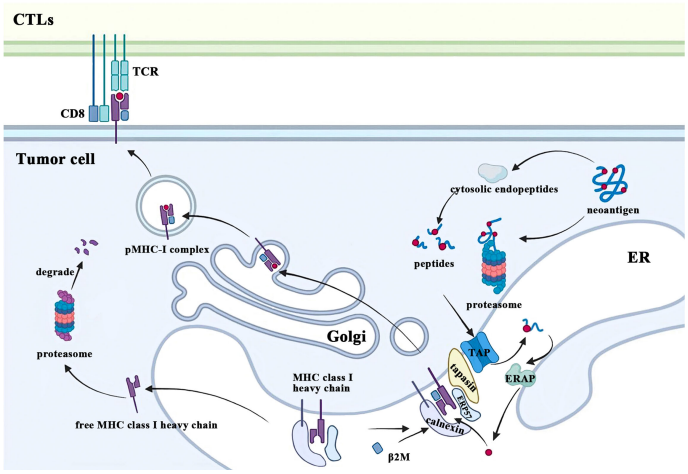

FIGURE 2
β2M is involved in the process of MHC class I antigen presentation. CTLs, cytolytic T lymphocytes; TCR, T cell receptors; ER, endoplasmic reticulum; β2M, beta-2-microglobulin; MHC, major histocompatibility complex; pMHC-I, peptide-MHC class I; TAP, transporter associated with antigen processing; ERAP: endoplasmic reticulum aminopeptidases; ERP57, endoplasmic reticulum resident protein 57.

alterations in the B2M gene have been demonstrated to be the major cause in melanoma (24, 25). In humans, the heavy chains of MHC class I are encoded by MHC class I genes, HLA-A, HLA-B, and HLA-C, which means one HLA mutation will affect a specific MHC class I molecule. Since β2M is present in all MHC class I complexes, B2M defects would broadly impact all variants of MHC class I molecules originating from different HLA alleles. And this may be the reason why the B2M mutation may lead to a decrease in the total amount of MHC class I antigens presenting on the surface of tumor cells (26). A study involving 7630 tumors across 23 major cancer types showed that the incidence of B2M alterations was 2.0% (0.9% gene deletions, 0.6% damaging mutations, and 0.1% putative damaging mutations), including 4.5% in cutaneous melanomas (27). Another study examined β2M expression in 23 primary samples of conjunctival melanoma (CM), a rare type of mucosal melanoma, by immunofluorescence staining and revealed that three cases (14%) showed no staining of β2M while 11 cases (50%) showed weak β2M expression (28). B2M loss is the initial genetic alteration in the development of MHC class I loss, as the structural alteration in the B2M gene can be detected even in HLA-positive melanoma cells (29, 30). The immunogenicity of these HLA-positive B2M gene-altered melanomas is still reduced to varying degrees, which means reduced T cell infiltration and decreased T cell–stimulatory capacity, and this confers an advantage for dissemination and expansion of those melanoma clones with irreversible genetic defects (29). And the accumulation of B2M alterations during metastasis results in a gradual decrease to total loss of HLA class I expression (29). A variety of genetic defects in B2M were observed in tumor biopsies of 29.4% of patients with metastatic melanoma which is higher than primary melanoma (31).

There are a great variety of mechanisms of B2M alterations, and the causative mutations are not only found in various types of tumors but also in systemic amyloidosis, in which misfolded proteins caused by the B2M gene mutations exhibit a strongly enhanced propensity for amyloid aggregation (32). Table 1 summarizes the relevant mechanisms that have been identified in melanoma, including single nucleotide substitutions, small frameshifting deletions/insertions, and loss of a large segment of chromosome 15q21. Analysis of the molecular mechanisms that contributed to the loss of functional β2M in different melanoma cell lines revealed that there is a high frequency of microdeletions/insertions in the repeat region of exon 1 and exon 2 of the B2M gene (Table 1). Although B2M mutations are highly frequent in high-frequency microsatellite instability (MSI-H) tumors, melanoma shows a striking similarity to the mutational patterns found in MSI-H colorectal cancers (CRCs). As in MSI-H CRC, the 8-bp CT repeat region of exon I of the B2M gene has also been described as a mutational hotspot in melanoma (24, 38). Only a small fraction of primary melanomas exhibited an MSI-H pattern and Bernal et al. did not find genomic instability during MSI phenotyping of five melanoma cell lines mutated in this region (44, 45), suggesting that mutations in this hotspot gene in melanoma may not be associated with defects in the DNA mismatch repair (MMR) system. However, Sade-Feldman et al. found somatic mutations in MMR (MSH2) were found in post-Tx and post-Tx-II samples of PatT33 (31). Microdeletion/insertions and single nucleotide substitutions often lead to a frameshift and a premature stop codon, resulting in the production of nonfunctional truncated β2M (Table 1). And a missense mutation causing a Cys to Trp change in the melanoma cell line VMM5b (Me15) blocks the formation of a disulfide bond in the β2M, resulting in its degradation by the proteasome (39). Somatic mutations to B2M also significantly increase the mutation burden of tumor patients (26). Since early mutational events are present in a larger proportion of cancer cells, a better understanding of the timeline of mutational occurrence can be obtained by comparing the percentage of mutated alleles in the same tumor (26). High percentiles of B2M mutations found in the study suggest that B2M mutations may occur early in tumor development (26). It is also worth noting that the coexistence of two different B2M gene mutations has not been detected in all studies involving genetic mechanisms of B2M-deficient melanoma cell lines, suggesting the allelic B2M loss. Detection of chromosome 15 by microsatellite markers or single nucleotide polymorphism (SNP) array analysis found loss of heterozygosity (LOH) in almost all B2M-deficient melanoma samples (45). Therefore, the loss of B2M expression in melanoma is typically caused by the coincidence of mutational events involving both copies of the B2M gene: a mutation in one B2M allele and the loss of the second B2M allele. In fact, the same partial deletion of chromosome 15q as in B2M-deficient tumor cells was also found in some melanoma cell lines without B2M mutations (29). This suggests that the chronological sequence of genetic alterations in B2M defects is as follows: a large deletion encompassing the B2M gene was first acquired on one chromosome 15q, followed by differentiation and independent acquisition of an additional small mutation affecting the second B2M allele. Thus, B2M allele loss owing to chromosome 15 instability is a more frequent form of B2M alteration, and its frequency in melanoma metastases is higher than that of B2M gene mutation. One study showed that LOH in the B2M region on chromosome 15q21 was detected in 16% of metastatic melanoma samples (n = 70) (46). At the same time, since β2M and MHC class I molecules can normally express in melanoma cells with only LOH on chromosome 15q, such chromosomal structural changes may be overlooked. It is also worth highlighting that loss of MHC class I expression was detected in all melanoma cell lines with B2M mutations in current published research (mentioned in Table 1), whereas in other tumor cell lines with B2M mutations, the expression of MHC class I may not necessarily be detected simultaneously. For example, in many colon cancer cell lines, mutations in B2M lead to the synthesis of inefficient β2M variants that only reduce

TABLE 1 Summary of B2M mutations in melanoma.

Cell line/ Tumor tissue	The origin of tumor	B2M gene mutation	B2M mRNA	β2M	Chromosome 15 aberrations	Ref
FO-1		(1) a deletion of Exon I (2)a deletion of a segment of Intron I				(33)
SK-MEL-33	a metastatic melanoma involving regional lymph nodes in the left axilla	a guanosine deletion in codon 76 in Exon II	a frameshift and premature termination	a truncated protein (18 amino acids shorter)		(34)
Me1386	a metastatic lesion	a CT deletion in the 8-bp CT repeat region of Exon I	(1)a shift in the reading frame starting at nucleotide position 45 (2)a premature UGA stop codon at nucleotide position 165		abnormalities in chromosome 15	(24)
Me9923/ Me9923P	a metastatic/primary lesion	(1) a 14-bp deletion in Exon II		a putative COOH-terminal truncated protein of 83 amino acids	abnormalities in chromosome 15	
		(2) a C→G transversion mutation at nucleotide position 258	an in-frame premature stop at codon 86			
Me18105	a metastatic lesion	a point mutation (A→G) at the splice acceptor site of Intron I	a 11-bp deletion creating a frameshift and premature termination		abnormalities in chromosome 15	
LB1622-MEL	a in-transit metastatic lesion	a point mutation (T→A) in the start codon of Exon I			a partial deletion on chromosome 15q (15q21-15q22)	(35)
BB74-MEL	a adrenal gland metastasis	a point mutation (C→G) at codon 31 in Exon II			a partial deletion on chromosome 15q22	
GR34	a primary lesion	a deletion of 4 bases (TTCT) in the 8-bp CT repeat region of codons 15–16 in Exon I	the appearance of a stop codon at position 42	a truncated non-functional 41 amino acid β2M	a partial deletion on chromosome 15q	(36)
UKRV-Mel-2b	a pleural effusion 8 months after diagnosis	a 498-bp deletion including the whole Exon I			an extensive deletion of sequences from one chromosome 15q	(37)
1074MEL	a recurrent metastatic lesion	a point mutation (G→A) at the translation initiation codon	abolish the initiation of translation		LOH in chromosome 15	(38)
1174MEL	a recurrent metastatic lesion	a point mutation (C→G) at codon 31	the introduction of a premature TGA stop codon		LOH in chromosome 15	
1106MEL	a recurrent metastatic lesion	a CT deletion in the 8-bp CT repeat region of codons 13–15 in Exon I			LOH in chromosome 15	
1180MEL	a recurrent metastatic lesion	a CT deletion in the 8-bp CT repeat region of codons 13–15 in Exon I			LOH in chromosome 15	
1259MEL	a recurrent metastatic lesion	a CT deletion in the 8-bp CT repeat region of codons 13–15 in Exon I			LOH in chromosome 15	
VMM5B	a metastatic lesion	a point mutation (C→G) at codon 45 in Exon II		misfolding and degradation of β2M	LOH in chromosome 15	(39)
Mel249	a metastatic lesion	a 2-bp microdeletion in codon 62 in Exon II			broad-range deletions within chromosome 15	(40)
Mel499	a metastatic lesion	a point mutation (T→ A) at position two of the Intron I which destroys the GU donor splice consensus site of Intron I	the insertion of intron I sequences of different lengths, 27 and 407 bp		LOH in chromosome 15	
Mel505	a metastatic lesion				broad-range deletions within chromosome 15	(40)

(Continued)

TABLE 1 Continued

Cell line/ Tumor tissue	The origin of tumor	B2M gene mutation	B2M mRNA	β2M	Chromosome 15 aberrations	Ref
Mel592	a metastatic lesion				broad-range deletions within chromosome 15	
DNR-DC-M010	a right inguinal lymph node metastasis	a point mutation (G→ T) at codon 67 in Exon II	an early stop codon	a short version of β2M	LOH in chromosome 15	(30)
Ma-Mel-48c	lymph node metastases one year after diagnosis of stage IV disease	a 60-bp deletion starting at codon 96 in Exon II			a partial deletion on chromosome 15q (15q13.3-15q21.2)	(29)
Ma-Mel-100b	regional lymph node metastases three years after diagnosis of stage III disease	a 12-bp deletion in Exon II			a partial deletion on chromosome 15q (15q12-15q22.2)	
Ma-Mel-86b	a late recurrent lymph node lesion 1.5 years after diagnosis of stage IV disease	the B2M gene and flanking sequences were lost			a large deletion on chromosome 15q (15q11.2-15q22.31)	(41)
Ma-Mel-86f	a late recurrent lymph node lesion 6 years after diagnosis of stage IV disease	the deletion affected only the B2M gene			a large deletion on chromosome 15q (15q11.2-15q22.31)	(41)
M437	a metastatic lesion	a 4-bp S14 frameshift deletion in Exon I				(42)
Pat208	a metastatic lesion	frameshift mutations in Exon I: p.Leu13fs and p.Ser14fs			LOH in chromosome 15	(31)
PatT33	a metastatic lesion	two B2M frameshift mutations: p.Ser14fs and p.Gly63fs			no LOH in chromosome 15	
	a lymph node metastasis	a 28-bp deletion	a frameshift and truncation starting from codon 3			(43)

the number of MHC class I molecules on the tumor cell surface (47–49). Besides these irreversible defects mentioned above, other mechanisms can also affect B2M expression, e.g., epigenetic regulation of B2M transcription. The data from The Cancer Genome Atlas (TCGA) indicated that the methylation of the NLRC5 promoter was negatively correlated with the expression of β2M in melanoma, resulting in reduced expression of MHC class I and anti-tumor immune evasion (50).

4 Effect of B2M defects on anti-melanoma immune responses

Compelling Evidence shows that β2M deficiency affects tumor immunity by hampering MHC class I-mediated tumor antigen presentation in tumor lesions and contributes to a poor clinical outcome in melanoma. The high intrinsic immunogenicity of melanoma cells makes CTLs recognize multiple peptide epitopes from different types of tumor antigens presented by MHC class I (51, 52), whereas β2M can participate in the presentation of all MHC class I antigens. As a consequence of the poor tissue availability of consecutive melanoma metastases, related melanoma cell lines, and autologous peripheral blood T lymphocytes, only a few studies have kept track of the evolution of melanoma immunogenicity during disease progression (29, 53, 54). However, studies of metastatic cell lines and tissue samples have identified the complete lack of HLA class I antigen expression due to B2M gene deficiency as one of several genetic alterations affecting the tumor cells' immunogenicity. As shown in a study that monitoring three consecutive melanoma metastases from a patient with melanoma, as the tumor progressed, accumulated alterations in the B2M gene acquired by melanoma cells gradually decreased the immunogenicity of tumor cells, which culminated in impaired T-cell recognition caused by the irreversible total lack of HLA class I antigen expression (29). At the same time, the activated CTLs release large amounts of cytokines, such as interferon-γ (IFN-γ) and tumor necrosis factor-α (TNF-α), leading therefore to the formation of the tumor microenvironment and subsequent recruitment of T cells. IFN-γ signaling would upregulate the synthesis and expression of the MHC class I, inducing a positive feedback loop that results in additional T cell recruitment and activation (55). Melanoma cell lines with B2M mutation may lose IFN-γ-mediated MHC class I inducibility, thereby supporting tumor evasion of immune

surveillance (56). After transfection of wild-type B2M gene, melanoma cells with B2M defects restored sensitivity to T cell lysis and ability to induce T cell IFN-γ secretion in an HLA-restricted manner.

In addition, the role of immunity in developing tumors is twofold, not only protecting the host from tumor formation but also shaping tumor immunogenicity by promoting the outgrowth of tumor cells that have developed immune resistance mechanisms (57). During tumor development, rare tumor cells surviving after the elimination phase enter an equilibrium phase, in which the adaptive immune system blocks tumor cells' outgrowth but also exerts selective pressure on them. Among the several immune effector mechanisms in this cancer immunoediting process, the constant immune pressure exerted by tumor antigen-specific T cells is suggested as a potent driver to promote the selection of tumor cell clones. This hypothesis implies that when B2M-defective tumor variants appear, these poorly immunogenic tumor clones become "invisible" to CTLs and thus acquire a growth advantage to take over the other clonal tumor populations (29, 38). These tumor cells that have acquired the ability to circumvent immune recognition develop resistance to the anti-tumor immune response, which leads to tumor immune escape.

MHC class I–negative tumor cells could still be targeted by innate CD56+ NK cells that recognize tumor cells through molecular mechanisms distinct from CTLs and could be another source of IFN-γ. MHC class I molecules, as ligands for inhibitory NK-cell receptors, are involved in the "licensing" or "education" of NK cells (58). The failure of surface MHC class I expression could upregulate the expression of Caspase 3 and KIR2DL1 in tumor cells to recruit NK cells and induce apoptosis. To explore whether B2M-deficient melanomas could be targeted with NK cells, a study transplanted a mixture of parental B2M+/+ and B2M-/- cell lines (in a 1:1 ratio) into mice with or without NK cells (31). The study found that in mice lacking NK cells, the number of B2M-depleted melanoma cells was significantly increased compared with B2M +/+ cells. The expression of activating NK ligands, including MHC class I-related chain A/B (MICA/B) and UL16 binding protein (ULBP), was positive on B2M alteration-induced MHC class I-deficient melanoma cells (30), and the coculture of these cells with NK cells found that they were efficiently killed by NK cells compared with MHC class I-positive melanoma cells (40). Nevertheless, studies detected a low tumor infiltration of CD56+ NK cells in melanoma metastases regardless of the HLA expression (30, 41). Therefore, NK cells could kill these metastatic melanoma cells but rarely migrate into the melanoma lesions due to their potentially impaired migratory function *in vivo* (30). Moreover, the imbalance between activating and inhibitory signals decreases NK cell cytotoxicity against malignant cells, supported by a less robust activity of tissue-infiltrating NK cells in solid tumors and low levels of MICA and ULBP expression in some B2M-deficient melanoma cell lines (59).

5 Association between B2M genetic alterations and immunotherapy

Cancer immunotherapies that enhance the ability of the immune system to eliminate malignant cells and overcome immune escape are now being recognized as the potentially most promising therapies for various cancers. Melanoma is also among the most sensitive malignancies to immune modulation. B2M mutations are closely associated with patient progression on immunotherapy in melanoma. Loss of the B2M gene may lead to innate and acquired resistance to immunotherapy methods on T cell immunity, which means an intrinsic lack of response to the initial therapy, or subsequent progression or new metastases to the site of metastases after the initial response. Here we summarize resistance to different immunotherapeutic approaches caused by B2M disruption in melanoma and promising treatment strategies to overcome it.

5.1 Immune checkpoint blockade therapy

5.1.1 B2M alterations induce ICI resistance while ICIs promote B2M mutations

Immune checkpoint blockade (ICB) therapy is designed to target immune checkpoint receptors on tumors and immune cells, such as programmed cell death-1 (PD-1), programmed death ligand-1 (PD-L1) or cytotoxic associated lymphocyte antigen-4 (CTLA-4), to restore $CD8^+$ T cell-induced anti-tumor immune activity (2, 3, 60). Despite the significant improvements seen in melanoma prognosis with intensive studies on immune checkpoint inhibitors (ICIs), a substantial fraction of patients nevertheless suffers from relapsed disease and eventually die due to treatment resistance. Because the efficiency of ICIs depends on CTLs' recognition of MIHC class I antigens presenting tumor antigen-derived peptides, β2M, as a key factor required for the assembly of MHC class I complexes and the stable presentation of tumor antigens, its deficiency may be a common genetic mechanism of resistance to ICB therapy. Not only that, but strong and persistent T cell selection pressure generated by ICIs also leads to the preferential selection of B2M gene mutations. After an early analysis of molecules involved in functional HLA class I Ag expression in melanoma cell lines originating from recurrent metastases after initial T cell-based immunotherapy, three types of B2M gene mutations resulting in a lack of translation of the β2M were identified (38). Support from correlative clinical samples has been lacking for a long time until Zaretsky et al. identified homozygous B2M truncating

mutations in the baseline and progressive lesions of a patient with pembrolizumab-resistant advanced melanoma (42). A similar alteration in B2M with corresponding LOH was also found in a melanoma patient who had a partial response to nivolumab (61). Rodig et al. assessed the expression of MHC class I and II proteins on tumor cells from 181 patients with melanoma before ICB therapy and correlated the results with clinical outcomes of different ICIs treatments and transcriptomic and genomic profiling in selected cases (62). Loss of MHC class I expression in the majority (>50% of cells) of melanoma cells was observed in 78 of these patients and associated with transcriptional downregulation of HLA and B2M genes. However, they also concluded that this loss of MHC class I expression predicted primary resistance to anti-CTLA-4 therapy, but not anti-PD-1 therapy, which seems inconsistent with the report by Zaretsky et al. Defects in the B2M gene may be an effective predictive marker for ICB therapy in melanoma. In a cohort of metastatic melanoma patients treated with several ICB therapies, Moshe et al. identified B2M aberrations in 29.4% of patients with progressing disease, including point mutations, deletions, or LOH (31). They also found in two independent cohorts of melanoma patients treated with different ICIs that B2M LOH events were significantly enriched in non-responders (about three times as many as responders) and associated with worse overall survival. In contrast, results from a larger cohort of 131 patients with metastatic melanoma showed high levels of β2M expressed either in tumor or stroma are associated with a good response to immunotherapy (63). Uveal melanoma (UM) is a rare subset of melanoma (3%-5% of all melanomas) but also the most common intraocular tumor in adults. UM shares a common origin with cutaneous melanoma, but ICB therapy has had limited success in the clinical treatment of UM due to their different mutational load and antigen expression. Interestingly, there was no difference in B2M expression observed between cutaneous melanoma and UM metastases despite different responses to ICIs (64).

5.1.2 Combination therapy in overcoming ICI resistance with B2M mutation

Talminogene lapherparevec (TVEC) is an FDA-approved genetically-modified herpes simplex virus for the treatment of advanced melanoma (65). Khaddour et al. reported a case of a patient with rapidly progressive immunotherapy refractory intracranial metastatic melanoma who had acquired B2M mutation after initial ICB therapy (66). The patient had a durable complete response to the visceral and intracranial metastatic disease after the therapy of sequential TVEC and pembrolizumab followed by temozolomide. The researchers proposed that local injection of oncolytic viruses may activate the type I IFN pathway, which may explain the reason why TVEC can avoid ICB resistance due to B2M mutations and enhance anticancer immune responses.

In addition, cytokines, as powerful modulators of the immune system, can significantly enhance the immune response to tumors. Bempegaldesleukin, also known as NKTR-214, is a prodrug of conjugated IL2 that provides sustained activation of the IL-2 pathway and leads to a systemic expansion of both CD4+ and CD8+ T cells (67). Combination therapy with bempegaldesleukin and ICI revealed a synergistic antitumor effect, and the systemic administration of bempegaldesleukin attenuated anti-PD-1 resistance in B2M knockout tumors and prolonged survival in B2M knockout melanoma mice (68, 69).

5.2 Cancer vaccines

Cancer vaccines are designed based on specific tumor antigens to induce or enhance anti-tumor immune responses in cancer patients in a preventive or therapeutic way. However, T-cell-based cancer vaccines may develop resistance due to the deficiency of B2M. As early as 1998, Benitez et al. reported B2M mutations identified in two metastatic melanoma patients with tumor progression after immunizations with MAGE peptides (35). In one case report, investigators tracked the chronological sequence of appearance of B2M gene mutation in several successive metastatic melanoma lesions and a lymph node biopsy-derived cell line obtained after immunotherapy with a dendritic cell vaccine (DCV) transfected with autologous tumor mRNA (30). Although this therapy stimulates T cells by the presentation of tumor antigens by DC, helping to eliminate the effects of the loss of MHC class I surface expression in tumor cells, B2M gene defect found in this patient with aggressive clinical course and resistance to DC vaccination might partly explain the failure of the therapy. Subsequently in a study of the application of an RNA-based poly-neoepitope individualized mutanome vaccines in melanoma patients, Sahin et al. reported that one of these patients had a late relapse due to the outgrowth of B2M-deficient melanoma cells after receiving the vaccine (70). In a randomized phase II trial, by analysis of blood samples from melanoma patients treated with two vaccines featuring autologous tumor antigens respectively, researchers found that β2M expression was negatively correlated with immune response and survival in patient-specific autologous DCVs, but positively correlated with those in autologous tumor cell vaccines (TCV) (71).

5.3 B2M gene delivery

Many *in vitro* experiments have shown that using the plasmids or adenoviruses strategy to deliver wild-type human B2M gene into melanoma cells or other tumor cells can restore tumor cell HLA class I antigen expression and peptide-specific T lymphocyte recognition (24, 29, 30, 37, 72). An *in vivo* study using the Ma-Mel-86b tumor xenograft model in nude mice also

showed that the intratumoral injection of B2M-carrying vectors resulted in restoring regular HLA class I expression (72). This mechanism is one of the bases of the Allovectin-7 design. Allovectin-7 consists of a bicistronic plasmid DNA (VCL-1005) encoding two transgene proteins, HLA-B7 and β2M (73, 74). In transfected melanoma cells, β2M can not only combine with HLA-B7 encoded on plasmids but also combine with other endogenous MHC class I heavy chains, thereby enhancing the expression of multiple MHC class I molecules on the cell surface (75). An *in vitro* study indicated that compared with VCL-1004, a plasmid encoding only HLA-B7, cell lines lacking/not lacking endogenous β2M expression transfected with VCL-1005 had significantly increased surface MHC class I expression (75). The phase I clinical trial demonstrated the intratumoral administration of Allovectin-7 delivers these two genes into tumor cells, enabling the synthesis and expression of intact MHC class I complexes on the tumor cell surface and stimulating T cell-based immune responses to transfected cells and foreign antigens (76–78). One Phase II clinical trial evaluated the safety and efficacy of Allovectin-7 among 133 patients (127 evaluable for efficacy) with stage III or IV metastatic melanoma (79). The overall response rate was 11.8%, including 8.7% complete response and 3.1% partial response. The median duration of response, TTP and median overall survival were 13.8, 1.6 and 18.8 months, respectively. While the Phase II results of Allovectin-7 showed a surprising therapeutic effect, the Phase III Allovectin Immunotherapy for Metastatic Melanoma (AIMM) trial found that responders to Allovectin-7 had significantly shorter overall survival (18.8 months versus 24.1 months, $P = 0.491$) despite a longer duration of response compared with controls (intravenous dacarbazine or oral TMZ) (80). Although the Phase III trial of Allovectin-7 failed to meet key endpoints, the success of its Phase I/Phase II trials and related basic studies still demonstrates that B2M gene delivery can address the problems its mutation poses to T-cell-based tumor immunity. We believe that the development of immunotherapy based on this mechanism will bring more treatment options to patients with immunotherapy refractory melanoma caused by mutations. It is expected that gene therapy will have a huge development space and a promising future in tumor immunotherapy.

5.4 Natural killer cell-based therapy

In contrast to T cells, NK cells are essential components of the innate immune system and do not need prior activation to target tumor cells. The activity of NK cells is dependent on a complex interaction of activating and inhibiting receptors on their surfaces. Experiments have shown that malignant melanoma cells express a set of ligands that mediate NK cell-activating receptor recognition, triggering NK cells to become active killers (81). Low or absent HLA class I expression leads to the lack of killer immunoglobulin-like receptors (KIR) engagement, which switches NK cells from a state of equilibrium to activation by decreasing inhibitory signal input (82). Due to the natural activity of NK cells against melanoma cells and their strong killing effect on tumor cells with reduced expression of MCH class I molecules, NK cell-based therapy is promising immunotherapy for ICI-resistant melanoma caused by β2M deficiency (83, 84). However, multiple studies have demonstrated impaired NK cell activity in melanoma patients, and immuno-suppressive tumor microenvironment and inadequate NK cell homing also negatively affect NK cell therapy (85–88). The combination of NK cell-based therapy with other therapies may synergistically improve NK cell recognition and avoid tumor immune evasion (89, 90).

5.5 Chimeric antigen receptor T cell therapy

Currently, adoptive cell therapy (ACT), as a new strategy for improving the treatment of metastatic melanoma, is primarily focused on patients resistant or non-tolerant to the ICIs. The specificity of tumor-associated antigens (TAA) recognition by chimeric antigen receptor (CAR) T cells is defined by the antibody domain, thus freeing antigen recognition from MHC restriction. Therefore, adoptive CAR-T cell therapy is expected to be a potential option for patients with MHC class I antigen presentation deficiency due to B2M defects. Furthermore, disruption of the B2M gene to generate MHC class I-deficient T cells *via* CRISPR/Cas9 can significantly reduce the surveillance of allogeneic T cells and may prevent host rejection driven by HLA differences (91). Although evidence from current clinical studies is very limited in CAR-T cell therapy for melanoma, it may offer new hope for patients with metastatic melanoma.

6 Conclusion

The exploration of potential clinical implications of the B2M gene in melanoma immunity is just starting. Complete loss of MHC class I expression caused by β2M deficiency contributes to immune selection and expansion of melanomas with such genetic defects, while also contributing to immune escape and leading to resistance to T cell-based immunotherapy. Therefore, β2M is gradually becoming a potential biomarker and therapeutic target for melanoma immunotherapy. To a certain extent, the detection of B2M mutations can predict the efficacy of T cell-based immunotherapy in melanoma. B2M gene delivery also provides a new solution to the problem of immune resistance caused by gene mutations. The development and clinical validation of different delivery vehicles such as viruses, plasmids, and nanomaterials are all possible directions for future studies. New technologies and hypotheses in melanoma tumor immunity are

increasingly explored, which may provide additional insights into our understanding of the role of B2M in tumor immunity. Meanwhile, additional studies about new therapeutic strategies for B2M-deficient melanoma are still needed to pave the way for advanced melanoma control and eradication.

Author contributions

CW drafted and revised the manuscript and figures. JZ and ZhW are the corresponding authors who instructed the research. ZeW and TY helped with revising and editing. All authors contributed to the artide and approved the submitted version.

Funding

We acknowledge funding supports from the National Natural Science Foundation of China (81770934); the Program of Science and Technology Innovation Action of Science and Technology Commission of Shanghai Municipality (22Y11910100); the Scientific research project of Shanghai Municipal Health Commission (202140416); and Interdisciplinary research joint fund project of Tongji University(2022-4-ZD-09).

Conflict of interest

The authors declare that the research was conducted in the absence of any commercial or financial relationships that could be construed as a potential conflict of interest.

Publisher's note

References

1. Marzagalli M, Ebelt ND, Manuel ER. Unraveling the crosstalk between melanoma and immune cells in the tumor microenvironment. *Semin Cancer Biol* (2019) 59:236–50. doi: 10.1016/j.semcancer.2019.08.002

2. Robert C, Ribas A, Schachter J, Arance A, Grob JJ, Mortier L, et al. Pembrolizumab versus ipilimumab in advanced melanoma (KEYNOTE-006): post-hoc 5-year results from an open-label, multicentre, randomised, controlled, phase 3 study. *Lancet Oncol* (2019) 20(9):1239–51. doi: 10.1016/S1470-2045(19)30388-2

3. Postow MA, Chesney J, Pavlick AC, Robert C, Grossmann K, McDermott D, et al. Nivolumab and ipilimumab versus ipilimumab in untreated melanoma. *N Engl J Med* (2015) 372(21):2006–17. doi: 10.1056/NEJMoa1414428

4. Gide TN, Wilmott JS, Scolyer RA, Long GV. Primary and acquired resistance to immune checkpoint inhibitors in metastatic melanoma. *Clin Cancer Res Off J Am Assoc Cancer Res* (2018) 24(6):1260–70. doi: 10.1158/1078-0432.CCR-17-2267

5. Hofmann MA, Kiecker F, Küchler I, Kors C, Trefzer U. Serum TNF-α, B2M and sIL-2R levels are biological correlates of outcome in adjuvant IFN-α2b treatment of patients with melanoma. *J Cancer Res Clin Oncol* (2011) 137(3):455–62. doi: 10.1007/s00432-010-0900-1

6. Heegaard NHH. beta(2)-microglobulin: from physiology to amyloidosis. *Amyloid Int J Exp Clin Investig Off J Int Soc Amyloidosis* (2009) 16(3):151–73. doi: 10.1080/13506120903151775

7. Shi C, Zhu Y, Su Y, Chung LWK, Cheng T. β2-microglobulin: emerging as a promising cancer therapeutic target. *Drug Discov Today* (2009) 14(1):25–30. doi: 10.1016/j.drudis.2008.11.001

8. Halle S, Halle O, Förster R. Mechanisms and dynamics of T cell-mediated cytotoxicity *In vivo*. *Trends Immunol* (2017) 38(6):432–43. doi: 10.1016/j.it.2017.04.002

9. Rezvani K, Rouce R, Liu E, Shpall E. Engineering natural killer cells for cancer immunotherapy. *Mol Ther* (2017) 25(8):1769–81. doi: 10.1016/j.ymthe.2017.06.012

10. Leone P, Shin EC, Perosa F, Vacca A, Dammacco F, Racanelli V. MHC class I antigen processing and presenting machinery: organization, function, and defects in tumor cells. *J Natl Cancer Inst* (2013) 105(16):1172–87. doi: 10.1093/jnci/djt184

11. Arora S, Lapinski PE, Raghavan M. Use of chimeric proteins to investigate the role of transporter associated with antigen processing (TAP) structural domains in peptide binding and translocation. *Proc Natl Acad Sci USA* (2001) 98(13):7241–6. doi: 10.1073/pnas.131132198

12. Chang SC, Momburg F, Bhutani N, Goldberg AL. The ER aminopeptidase, ERAP1, trims precursors to lengths of MHC class I peptides by a "molecular ruler" mechanism. *Proc Natl Acad Sci USA* (2005) 102(47):17107–12. doi: 10.1073/pnas.0500721102

13. Ortmann B, Androlewicz MJ, Cresswell P. MHC class i/beta 2-microglobulin complexes associate with TAP transporters before peptide binding. *Nature* (1994) 368(6474):864–7. doi: 10.1038/368864a0

14. Degen E, Cohen-Doyle MF, Williams DB. Efficient dissociation of the p88 chaperone from major histocompatibility complex class I molecules requires both beta 2-microglobulin and peptide. *J Exp Med* (1992) 175(6):1653–61. doi: 10.1084/jem.175.6.1653

15. Dick TB. Assembly of MHC class I peptide complexes from the perspective of disulfide bond formation. *Cell Mol Life Sci CMLS* (2004) 61(5):547–56. doi: 10.1007/s00018-003-3271-9

16. Wang H, Capps GG, Robinson BE, Zúñiga MC. Ab initio association with beta 2-microglobulin during biosynthesis of the h-2Ld class I major histocompatibility complex heavy chain promotes proper disulfide bond formation and stable peptide binding. *J Biol Chem* (1994) 269(35):22276–81. doi: 10.1016/S0021-9258(17)31787-8

17. Hughes EA, Hammond C, Cresswell P. Misfolded major histocompatibility complex class I heavy chains are translocated into the cytoplasm and degraded by the proteasome. *Proc Natl Acad Sci USA* (1997) 94(5):1896–901. doi: 10.1073/pnas.94.5.1896

18. Méndez R, Rodríguez T, Del Campo A, Monge E, Maleno I, Aptsiauri N, et al. Characterization of HLA class I altered phenotypes in a panel of human melanoma cell lines. *Cancer Immunol Immunother CII* (2008) 57(5):719–29. doi: 10.1007/s00262-007-0411-3

19. Kageshita T, Ishihara T, Campoli M, Ferrone S. Selective monomorphic and polymorphic HLA class I antigenic determinant loss in surgically removed melanoma lesions. *Tissue Antigens* (2005) 65(5):419–28. doi: 10.1111/j.1399-0039.2005.00381.x

20. Garrido F, Cabrera T, Aptsiauri N. "Hard" and "soft" lesions underlying the HLA class I alterations in cancer cells: implications for immunotherapy. *Int J Cancer* (2010) 127(2):249–56. doi: 10.1002/ijc.25270

21. Hiraki A, Kaneshige T, Kiura K, Ueoka H, Yamane H, Tanaka M, et al. Loss of HLA haplotype in lung cancer cell lines: implications for immunosurveillance of

altered HLA class I/II phenotypes in lung cancer. *Clin Cancer Res Off J Am Assoc Cancer Res* (1999) 5(4):933–6.

22. Garcia-Lora A, Algarra I, Garrido F. MHC class I antigens, immune surveillance, and tumor immune escape. *J Cell Physiol* (2003) 195(3):346–55. doi: 10.1002/jcp.10290

23. Garrido C, Paco L, Romero I, Berruguilla E, Stefansky J, Collado A, et al. MHC class I molecules act as tumor suppressor genes regulating the cell cycle gene expression, invasion and intrinsic tumorigenicity of melanoma cells. *Carcinogenesis* (2012) 33(3):687–93. doi: 10.1093/carcin/bgr318

24. Hicklin DJ, Wang Z, Arienti F, Rivoltini L, Parmiani G, Ferrone S. beta2-microglobulin mutations, HLA class I antigen loss, and tumor progression in melanoma. *J Clin Invest* (1998) 101(12):2720–9. doi: 10.1172/JCI498

25. Wang H, Liu B, Wei J. Beta2-microglobulin(B2M) in cancer immunotherapies: Biological function, resistance and remedy. *Cancer Lett* (2021) 517:96–104. doi: 10.1016/j.canlet.2021.06.008

26. Castro A, Ozturk K, Pyke RM, Xian S, Zanetti M, Carter H. Elevated neoantigen levels in tumors with somatic mutations in the HLA-a, HLA-b, HLA-c and B2M genes. *BMC Med Genomics* (2019) 12(6):107. doi: 10.1186/s12920-019-0544-1

27. Budczies J, Bockmayr M, Klauschen F, Endris V, Fröhling S, Schirmacher P, et al. Mutation patterns in genes encoding interferon signaling and antigen presentation: A pan-cancer survey with implications for the use of immune checkpoint inhibitors. *Genes Chromosomes Cancer* (2017) 56(8):651–9. doi: 10.1002/gcc.22468

28. Cao J, Brouwer NJ, Jordanova ES, Marinkovic M, van Duinen SG, de Waard NE, et al. HLA class I antigen expression in conjunctival melanoma is not associated with PD-L1/PD-1 status. *Invest Ophthalmol Vis Sci* (2018) 59 (2):1005–15. doi: 10.1167/iovs.17-23209

29. Sucker A, Zhao F, Real B, Heeke C, Bielefeld N, Maβen S, et al. Genetic evolution of T-cell resistance in the course of melanoma progression. *Clin Cancer Res Off J Am Assoc Cancer Res* (2014) 20(24):6593–604. doi: 10.1158/1078-0432.CCR-14-0567

30. del Campo AB, Kyte JA, Carretero J, Zinchencko S, Méndez R, González-Aseguinolaza G, et al. Immune escape of cancer cells with beta2-microglobulin loss over the course of metastatic melanoma. *Int J Cancer* (2014) 134(1):102–13. doi: 10.1002/ijc.28338

31. Sade-Feldman M, Jiao YJ, Chen JH, Rooney MS, Barzily-Rokni M, Eliane JP, et al. Resistance to checkpoint blockade therapy through inactivation of antigen presentation. *Nat Commun* (2017) 8(1):1136. doi: 10.1038/s41467-017-01062-w

32. Valleix S, Gillmore JD, Bridoux F, Mangione PP, Dogan A, Nedelec B, et al. Hereditary systemic amyloidosis due to Asp76Asn variant β2-microglobulin. *N Engl J Med* (2012) 366(24):2276–83. doi: 10.1056/NEJMoa1201356

33. D'Urso CM, Wang ZG, Cao Y, Tatake R, Zeff RA, Ferrone S. Lack of HLA class I antigen expression by cultured melanoma cells FO-1 due to a defect in B2m gene expression. *J Clin Invest* (1991) 87(1):284–92. doi: 10.1172/JCI114984

34. Wang Z, Cao Y, Albino AP, Zeff RA, Houghton A, Ferrone S. Lack of HLA class I antigen expression by melanoma cells SK-MEL-33 caused by a reading frameshift in beta 2-microglobulin messenger RNA. *J Clin Invest* (1993) 91(2):684–92. doi: 10.1172/JCI116249

35. Benitez R, Godelaine D, Lopez-Nevot MA, Brasseur F, Jiménez P, Marchand M, et al. Mutations of the beta2-microglobulin gene result in a lack of HLA class I molecules on melanoma cells of two patients immunized with MAGE peptides. *Tissue Antigens* (1998) 52(6):520–9. doi: 10.1111/j.1399-0039.1998.tb03082.x

36. Pérez B, Benitez R, Fernández MA, Oliva MR, Soto JL, Serrano S, et al. A new beta 2 microglobulin mutation found in a melanoma tumor cell line. *Tissue Antigens* (1999) 53(6):569–72. doi: 10.1034/j.1399-0039.1999.530607.x

37. Paschen A, Méndez RM, Jimenez P, Sucker A, Ruiz-Cabello F, Song M, et al. Complete loss of HLA class I antigen expression on melanoma cells: a result of successive mutational events. *Int J Cancer* (2003) 103(6):759–67. doi: 10.1002/ijc.10906

38. Chang CC, Campoli M, Restifo NP, Wang X, Ferrone S. Immune selection of hot-spot β2-microglobulin gene mutations, HLA-A2 allospecificity loss, and antigen-processing machinery component down-regulation in melanoma cells derived from recurrent metastases following immunotherapy. *J Immunol Baltim Md 1950* (2005) 174(3):1462–71. doi: 10.4049/jimmunol.174.3.1462

39. Chang CC, Ogino T, Mullins DW, Oliver JL, Yamshchikov GV, Bandoh N, et al. Defective human leukocyte antigen class I-associated antigen presentation caused by a novel beta2-microglobulin loss-of-function in melanoma cells. *J Biol Chem* (2006) 281(27):18763–73. doi: 10.1074/jbc.M511525200

40. Paschen A, Arens N, Sucker A, Greulich-Bode KM, Fonsatti E, Gloghini A, et al. The coincidence of chromosome 15 aberrations and beta2-microglobulin gene mutations is causative for the total loss of human leukocyte antigen class I expression in melanoma. *Clin Cancer Res Off J Am Assoc Cancer Res* (2006) 12 (11 Pt 1):3297–305. doi: 10.1158/1078-0432.CCR-05-2174

41. Zhao F, Sucker A, Horn S, Heeke C, Bielefeld N, Schrörs B, et al. Melanoma lesions independently acquire T-cell resistance during metastatic latency. *Cancer Res* (2016) 76(15):4347–58. doi: 10.1158/0008-5472.CAN-16-0008

42. Zaretsky JM, Garcia-Diaz A, Shin DS, Escuin-Ordinas H, Hugo W, Hu-Lieskovan S, et al. Mutations associated with acquired resistance to PD-1 blockade in melanoma. *N Engl J Med* (2016) 375(9):819–29. doi: 10.1056/NEJMoa1604958

43. Richmond CS, Vallatharasu Y, Deviley JA, Vos CR, Parsons BM, Kenny PA. Sequential treatment failures in response to BRAF/MEK and immune checkpoint inhibitors mediated by MAP2K2 and B2M mutations in melanoma. *Exp Mol Pathol* (2019) 110:104260. doi: 10.1016/j.yexmp.2019.104260

44. Hussein MR. Genetic pathways to melanoma tumorigenesis. *J Clin Pathol* (2004) 57(8):797–801. doi: 10.1136/jcp.2003.015800

45. Bernal M, Ruiz-Cabello F, Concha A, Paschen A, Garrido F. Implication of the β2-microglobulin gene in the generation of tumor escape phenotypes. *Cancer Immunol Immunother* (2012) 61(9):1359–71. doi: 10.1007/s00262-012-1321-6

46. Maleno I, Aptsiauri N, Cabrera T, Gallego A, Paschen A, López-Nevot MA, et al. Frequent loss of heterozygosity in the β2-microglobulin region of chromosome 15 in primary human tumors. *Immunogenetics* (2011) 63(2):65–71. doi: 10.1007/s00251-010-0494-4

47. de Miranda NFCC, Nielsen M, Pereira D, van Puijenbroek M, Vasen HF, Hes FJ, et al. MUTYH-associated polyposis carcinomas frequently lose HLA class I expression - a common event amongst DNA-repair-deficient colorectal cancers. *J Pathol* (2009) 219(1):69–76. doi: 10.1002/path.2569

48. Bicknell DC, Kaklamanis L, Hampson R, Bodmer WF, Karran P. Selection for beta 2-microglobulin mutation in mismatch repair-defective colorectal carcinomas. *Curr Biol CB* (1996) 6(12):1695–7. doi: 10.1016/S0960-9822(02)70795-1

49. Bicknell DC, Rowan A, Bodmer WF. Beta 2-microglobulin gene mutations: a study of established colorectal cell lines and fresh tumors. *Proc Natl Acad Sci USA* (1994) 91(11):4751–5. doi: 10.1073/pnas.91.11.4751

50. Yoshihama S, Roszik J, Downs I, Meissner TB, Vijayan S, Chapuy B, et al. NLRC5/MHC class I transactivator is a target for immune evasion in cancer. *Proc Natl Acad Sci USA* (2016) 113(21):5999–6004. doi: 10.1073/pnas.1602069113

51. Coulie PG, Van den Eynde BJ, van der Bruggen P, Boon T. Tumour antigens recognized by T lymphocytes: at the core of cancer immunotherapy. *Nat Rev Cancer* (2014) 14(2):135–46. doi: 10.1038/nrc3670

52. Eyles J, Puaux AL, Wang X, Toh B, Prakash C, Hong M, et al. Tumor cells disseminate early, but immunosurveillance limits metastatic outgrowth, in a mouse model of melanoma. *J Clin Invest* (2010) 120(6):2030–9. doi: 10.1172/JCI42002

53. Ikeda H, Lethé B, Lehmann F, van Baren N, Baurain JF, de Smet C, et al. Characterization of an antigen that is recognized on a melanoma showing partial HLA loss by CTL expressing an NK inhibitory receptor. *Immunity* (1997) 6 (2):199–208. doi: 10.1016/S1074-7613(00)80426-4

54. Yamshchikov GV, Mullins DW, Chang CC, Ogino T, Thompson L, Presley J, et al. Sequential immune escape and shifting of T cell responses in a long-term survivor of melanoma. *J Immunol Baltim Md 1950* (2005) 174(11):6863–71. doi: 10.4049/jimmunol.174.11.6863

55. Thompson JC, Davis C, Deshpande C, Hwang WT, Jeffries S, Huang A, et al. Gene signature of antigen processing and presentation machinery predicts response to checkpoint blockade in non-small cell lung cancer (NSCLC) and melanoma. *J Immunother Cancer* (2020) 8(2):e000974. doi: 10.1136/jitc-2020-000974

56. Rodríguez T, Méndez R, Del Campo A, Jiménez P, Aptsiauri N, Garrido F, et al. Distinct mechanisms of loss of IFN-gamma mediated HLA class I inducibility in two melanoma cell lines. *BMC Cancer* (2007) 7:34. doi: 10.1186/1471-2407-7-34

57. Schreiber RD, Old LJ, Smyth MJ. Cancer immunoediting: integrating immunity's roles in cancer suppression and promotion. *Science* (2011) 331 (6024):1565–70. doi: 10.1126/science.1203486

58. Long EO, Kim HS, Liu D, Peterson ME, Rajagopalan S. Controlling natural killer cell responses: integration of signals for activation and inhibition. *Annu Rev Immunol* (2013) 31:227–58. doi: 10.1146/annurev-immunol-020711-075005

59. Pende D, Rivera P, Marcenaro S, Chang CC, Biassoni R, Conte R, et al. Major histocompatibility complex class I-related chain a and UL16-binding protein expression on tumor cell lines of different histotypes: analysis of tumor susceptibility to NKG2D-dependent natural killer cell cytotoxicity. *Cancer Res* (2002) 62(21):6178–86.

60. Olson DJ, Eroglu Z, Brockstein B, Poklepovic AS, Bajaj M, Babu S, et al. Pembrolizumab plus ipilimumab following anti-PD-1/L1 failure in melanoma. *J Clin Oncol Off J Am Soc Clin Oncol* (2021) 39(24):2647–55. doi: 10.1200/JCO.21.00079

61. Riaz N, Havel JJ, Makarov V, Desrichard A, Urba WJ, Sims JS, et al. Tumor and microenvironment evolution during immunotherapy with nivolumab. *Cell* (2017) 171(4):934–949.e15. doi: 10.1016/j.cell.2017.09.028

62. Rodig SJ, Gusenleitner D, Jackson DG, Gjini E, Giobbie-Hurder A, Jin C, et al. MHC proteins confer differential sensitivity to CTLA-4 and PD-1 blockade in untreated metastatic melanoma. *Sci Transl Med* (2018) 10(450):eaar3342. doi: 10.1126/scitranslmed.aar3342

63. Martinez-Morilla S, Villarroel-Espindola F, Wong PF, Toki MI, Aung TN, Pelekanou V, et al. Biomarker discovery in immunotherapy-treated melanoma patients with imaging mass cytometry. *Clin Cancer Res Off J Am Assoc Cancer Res* (2021) 27(7):1987–96. doi: 10.1158/1078-0432.CCR-20-3340

64. Hoefsmit EP, Rozeman EA, Van TM, Dimitriadis P, Krijgsman O, Conway JW, et al. Comprehensive analysis of cutaneous and uveal melanoma liver metastases. *J Immunother Cancer* (2020) 8(2):e001501. doi: 10.1136/jitc-2020-001501

65. Bommareddy PK, Patel A, Hossain S, Kaufman HL. Talimogene laherparepvec (T-VEC) and other oncolytic viruses for the treatment of melanoma. *Am J Clin Dermatol* (2017) 18(1):1–15. doi: 10.1007/s40257-016-0238-9

66. Khaddour K, Dowling J, Huang J, Council M, Chen D, Cornelius L, et al. Successful administration of sequential TVEC and pembrolizumab followed by temozolomide in immunotherapy refractory intracranial metastatic melanoma with acquired B2M mutation. *Oncotarget* (2020) 11(52):4836–44. doi: 10.18632/oncotarget.27848

67. Charych DH, Hoch U, Langowski JL, Lee SR, Addepalli MK, Kirk PB, et al. NKTR-214, an engineered cytokine with biased IL2 receptor binding, increased tumor exposure, and marked efficacy in mouse tumor models. *Clin Cancer Res Off J Am Assoc Cancer Res* (2016) 22(3):680–90. doi: 10.1158/1078-0432.CCR-15-1631

68. Torrejon DY, Abril-Rodriguez G, Champhekar AS, Tsoi J, Campbell KM, Kalbasi A, et al. Overcoming genetically based resistance mechanisms to PD-1 blockade. *Cancer Discov* (2020) 10(8):1140–57. doi: 10.1158/2159-8290.CD-19-1409

69. Sharma M, Khong H, Fa'ak F, Bentebibel SE, Janssen LME, Chesson BC, et al. Bempegaldesleukin selectively depletes intratumoral tregs and potentiates T cell-mediated cancer therapy. *Nat Commun* (2020) 11:661. doi: 10.1038/s41467-020-14471-1

70. Sahin U, Derhovanessian E, Miller M, Kloke BP, Simon P, Löwer M, et al. Personalized RNA mutanome vaccines mobilize poly-specific therapeutic immunity against cancer. *Nature* (2017) 547(7662):222–6. doi: 10.1038/nature23003

71. Nistor GI, Dillman RO. Cytokine network analysis of immune responses before and after autologous dendritic cell and tumor cell vaccine immunotherapies in a randomized trial. *J Transl Med* (2020) 18(1):176. doi: 10.1186/s12967-020-02328-6

72. Del Campo AB, Aptsiauri N, Méndez R, Zinchenko S, Vales Á, Paschen A, et al. Efficient recovery of HLA class I expression in human tumor cells after Beta2-microglobulin gene transfer using adenoviral vector: Implications for cancer immunotherapy. *Scand J Immunol* (2009) 70(2):125–35. doi: 10.1111/j.1365-3083.2009.02276.x

73. Lew D, Parker SE, Latimer T, Abai AM, Kuwahara-Rundell A, Doh SG, et al. Cancer gene therapy using plasmid DNA: pharmacokinetic study of DNA following injection in mice. *Hum Gene Ther* (1995) 6(5):553–64. doi: 10.1089/hum.1995.6.5-553

74. Bedikian AY, Del Vecchio M. Allovectin-7 therapy in metastatic melanoma. *Expert Opin Biol Ther* (2008) 8(6):839–44. doi: 10.1517/14712598.8.6.839

75. Doukas J, Rolland A. Mechanisms of action underlying the immunotherapeutic activity of allovectin in advanced melanoma. *Cancer Gene Ther* (2012) 19(12):811–7. doi: 10.1038/cgt.2012.69

76. Nabel GJ, Gordon D, Bishop DK, Nickoloff BJ, Yang ZY, Aruga A, et al. Immune response in human melanoma after transfer of an allogeneic class I major histocompatibility complex gene with DNA-liposome complexes. *Proc Natl Acad Sci USA* (1996) 93(26):15388–93. doi: 10.1073/pnas.93.26.15388

77. Nabel GJ, Nabel EG, Yang ZY, Fox BA, Plautz GE, Gao X, et al. Direct gene transfer with DNA-liposome complexes in melanoma: expression, biologic activity, and lack of toxicity in humans. *Proc Natl Acad Sci USA* (1993) 90(23):11307–11. doi: 10.1073/pnas.90.23.11307

78. Stopeck AT, Hersh EM, Hersh EM, Harris DT, Grogan T, Unger E, et al. Phase I study of direct gene transfer of an allogeneic histocompatibility antigen, HLA-B7, in patients with metastatic melanoma. *J Clin Oncol Off J Am Soc Clin Oncol* (1997) 15(1):341–9. doi: 10.1200/JCO.1997.15.1.341

79. Bedikian AY, Richards J, Kharkevitch D, Atkins MB, Whitman E, Gonzalez R. A phase 2 study of high-dose allovectin-7 in patients with advanced metastatic melanoma. *Melanoma Res* (2010) 20(3):218–26. doi: 10.1097/CMR.0b013e3283390711

80. Agarwala SS. Intralesional therapy for advanced melanoma: promise and limitation. *Curr Opin Oncol* (2015) 27(2):151–6. doi: 10.1097/CCO.0000000000000158

81. Lakshmikanth T, Burke S, Ali TH, Kimpfler S, Ursini F, Ruggeri L, et al. NCRs and DNAM-1 mediate NK cell recognition and lysis of human and mouse melanoma cell lines *in vitro* and *in vivo*. *J Clin Invest* (2009) 119(5):1251–63. doi: 10.1172/JCI36022

82. Passweg JR, Huard B, Tiercy JM, Roosnek E. HLA and KIR polymorphisms affect NK-cell anti-tumor activity. *Trends Immunol* (2007) 28(10):437–41. doi: 10.1016/j.it.2007.07.008

83. Casado JG, Pawelec G, Morgado S, Sanchez-Correa B, Delgado E, Gayoso I, et al. Expression of adhesion molecules and ligands for activating and costimulatory receptors involved in cell-mediated cytotoxicity in a large panel of human melanoma cell lines. *Cancer Immunol Immunother CII* (2009) 58(9):1517–26. doi: 10.1007/s00262-009-0682-y

84. Vetter CS, Groh V, thor Straten P, Spies T, Bröcker EB, Becker JC. Expression of stress-induced MHC class I related chain molecules on human melanoma. *J Invest Dermatol* (2002) 118(4):600–5. doi: 10.1046/j.1523-1747.2002.01700.x

85. Paschen A, Sucker A, Hill B, Moll I, Zapatka M, Nguyen XD, et al. Differential clinical significance of individual NKG2D ligands in melanoma: soluble ULBP2 as an indicator of poor prognosis superior to S100B. *Clin Cancer Res Off J Am Assoc Cancer Res* (2009) 15(16):5208–15. doi: 10.1158/1078-0432.CCR-09-0886

86. Balsamo M, Scordamaglia F, Pietra G, Manzini C, Cantoni C, Boitano M, et al. Melanoma-associated fibroblasts modulate NK cell phenotype and antitumor cytotoxicity. *Proc Natl Acad Sci USA* (2009) 106(49):20847–52. doi: 10.1073/pnas.0906481106

87. Hersey P, Edwards A, McCarthy WH. Tumour-related changes in natural killer cell activity in melanoma patients. influence of stage of disease, tumour thickness and age of patients. *Int J Cancer* (1980) 25(2):187–94. doi: 10.1002/ijc.2910250204

88. da Silva IP, Gallois A, Jimenez-Baranda S, Khan S, Anderson AC, Kuchroo VK, et al. Reversal of NK-cell exhaustion in advanced melanoma by Tim-3 blockade. *Cancer Immunol Res* (2014) 2(5):410–22. doi: 10.1158/2326-6066.CIR-13-0171

89. López-Cobo S, Pieper N, Campos-Silva C, García-Cuesta EM, Reyburn HT, Paschen A, et al. Impaired NK cell recognition of vemurafenib-treated melanoma cells is overcome by simultaneous application of histone deacetylase inhibitors. *Oncoimmunology* (2018) 7(2):e1392426. doi: 10.1080/2162402X.2017.1392426

90. Schlecker E, Fiegler N, Arnold A, Altevogt P, Rose-John S, Moldenhauer G, et al. Metalloprotease-mediated tumor cell shedding of B7-H6, the ligand of the natural killer cell-activating receptor NKp30. *Cancer Res* (2014) 74(13):3429–40. doi: 10.1158/0008-5472.CAN-13-3017

91. Ren J, Liu X, Fang C, Jiang S, June CH, Zhao Y. Multiplex genome editing to generate universal CAR T cells resistant to PD1 inhibition. *Clin Cancer Res Off J Am Assoc Cancer Res* (2017) 23(9):2255–66. doi: 10.1158/1078-0432.CCR-16-1300

frontiers | Frontiers in Medicine

TYPE Mini Review
PUBLISHED 09 February 2023
DOI 10.3389/fmed.2023.1096615

OPEN ACCESS

EDITED BY
Bahar Dasgeb,
The State University of New Jersey,
United States

REVIEWED BY
Cedric Ng,
National Cancer Centre Singapore, Singapore
Mohamed Hassan,
Institut National de la Santé et de la Recherche Médicale (INSERM), France

*CORRESPONDENCE
Mahsa Mollapour Sisakht
✉ mmollapour@farabi.tums.ac.ir;
✉ m.molapoursisakht@erasmusmc.nl

SPECIALTY SECTION
This article was submitted to Dermatology, a section of the journal Frontiers in Medicine

RECEIVED 12 November 2022
ACCEPTED 20 January 2023
PUBLISHED 09 February 2023

CITATION
Mollapour Sisakht M, Amirkhani MA and Nilforoushzadeh MA (2023) SWI/SNF complex, promising target in melanoma therapy: Snapshot view. *Front. Med.* 10:1096615. doi: 10.3389/fmed.2023.1096615

SWI/SNF complex, promising target in melanoma therapy: Snapshot view

Mahsa Mollapour Sisakht[1,2]*, Mohammad Amir Amirkhani[3] and Mohammad Ali Nilforoushzadeh[3]

[1]Biotechnology Research Center, Faculty of Pharmacy, Tehran University of Medical Sciences, Tehran, Iran, [2]Department of Biochemistry, Erasmus University Medical Center, Rotterdam, Netherlands, [3]Skin and Stem Cell Research Center, Tehran University of Medical Sciences, Tehran, Iran

Therapeutic strategies based on epigenetic regulators are rapidly increasing in light of recent advances in discovering the role of epigenetic factors in response and sensitivity to therapy. Although loss-of-function mutations in genes encoding the SWItch/Sucrose NonFermentable (SWI/SNF) subunits play an important role in the occurrence of ∼34% of melanomas, the potential of using inhibitors and synthetic lethality interactions between key subunits of the complex that play an important role in melanoma progression must be considered. Here, we discuss the importance of the clinical application of SWI/SNF subunits as a promising potential therapeutic in melanoma.

KEYWORDS

melanoma, SWI/SNF enzymes, epigenetics, chromatin remodeling, synthetic lethality, cancer therapy

1. Introduction

The SWI/SNF complex is a large and evolutionarily conserved chromatin remodeler whose epigenomic changes are characterized in most cancers. This complex consists of 15 subunits encoded by 28 genes, including *SMARCB1* (also known as *SNF5, BAF47*, and *INI1*), *SMARCC1/SMARCC2* (also known as BAF155 and BAF170), and one of the two mutually exclusive ATPase subunits, *SMARCA4* (also known as BRG1) and *SMARCA2* (also known as BRM), which are commonly mutated in 20% of human cancers (1). Although several studies show the function of this complex as a transcriptional regulator, both tumor suppressive and enhancing functions of this complex have been investigated depending on the context. In some patients with hepatocellular carcinoma, ARID1A was strongly expressed in primary tumors but not in metastatic lesions, suggesting that ARID1A may be lost after initiation. Mechanistically, enhancement of ARID1A function promoted initiation by increasing cytochrome P450-mediated oxidative stress, while loss of Arid1a in tumors decreased chromatin accessibility and reduced transcription of genes associated with migration, invasion, and metastasis. At the same time, metastasis was reduced *via* transcriptional regulation of *EMILIN1/MAT1A/LCN2/IL1R1 in vitro*. Conversely, loss of ARID1A may increase the risk of steatohepatitis and cancer progression by altering immunity *in vivo* or tumorigenesis *via* activation of angiopoietin-2 (ANGPT2) transcription *in vitro* and angiogenesis *in vivo* (2). In summary, ARID1A, as a component of the SWI/SNF complex, plays a context-dependent tumor suppressive and oncogenic role in cancer (3). Melanoma results from the malignant transformation of certain cells called melanocytes. These cells are derived from multipotent cells of the neural crest and are responsible for melanin production (4). Metastatic melanoma is a highly aggressive malignancy that responds poorly to chemotherapeutic agents. Although targeted therapy with immune checkpoint inhibitors has resulted in significant improvement in tumor control, many patients do not respond to therapy, making it necessary to identify new therapeutic targets

for patients (5). Despite the improvement in therapies developed for melanoma, the 10-year survival rate for patients with advanced melanoma is ∼10% (6). The SWI/SNF component has been shown to play a critical role that can be targeted to develop a new therapeutic strategy (7). The synthetic lethal effect of the SWI/SNF subunits, demonstrated in several studies, has opened the possibility for new therapies. In light of the previous study, we attempt in this review to simplify and focus on the major subunits of the SWI/SNF complex in melanomagenesis that influence sensitivity to therapeutic agents. This review summarizes recent publications to highlight the most important SWI/SNF components based on statistical analyses related to melanoma progression and resistance and/or response to current therapies associated with this complex.

2. SWI/SNF complex: Structure and function

SWI/SNF is the first identified ATP-dependent chromatin remodeling multicomponent complex (consisting of 4–17 subunits) (8) that regulates the expression of 5% of genes in yeast (9) and plays an important role in transcription, DNA replication, and repair. This complex has a central catalytic subunit which is SMARCA4 (BRG1) or SMARCA2 (BRM) in the BAF complex, and 10–13 associated subunits (4), SMARCA4 or SMARCA2 function as catalytic subunits of other complexes called canonical (c) BAF, polybromo-associated BAF (PBAF) or non-canonical (nc)BAF (Figure 1). The different biological activity of these complexes is not fully understood, several functions of the biological activity of the complex are described by the genetic deletion of its subunits. The polybromo-associated BAF complex (PBAF) can be distinguished from the cBAF (canonical BAF complex) by the inclusion of BAF200 instead of BAF250A/B and BAF180 (10).

The components of the BAF complex can have cell type-specific functions, as evidenced by KD (knock-down) or KO (knock-out) of various subunits that had lethal effects, especially during embryogenesis (11, 12). The function of the BAF complex (esBAF) in pluripotency of embryonic stem cells was demonstrated by HO et al. in 2009 (13), and in 2019, the role of the non-canonical BRD9-containing BAF complex in regulating pluripotency in mouse embryonic stem cells was published (14). In addition, the function of other parts of the BAF complex, such as Baf60c, in the reversion of BAF to heart-specific enhancers during organogenesis (15) and in the differentiation of serotonergic neurons (16) has been published. All SWI/SNF components involve protein-protein or DNA-binding domains that are important for chromatin targeting and remodeling. Based on the biological activity of the complex, this complex contains three functional parts: the actin-related protein (ARP) module as a regulator, Snf2 (ATP-dependent motor that drives the basic DNA translocation reaction), and the substrate recruitment module, SRM. Recently, He and colleagues demonstrated the 12-member SWI/SNF complex *in vitro* by overexpressing the individual subunits in E. coli using the modified EcoExpress system to show the functional modularity of these complexes (9). Recent genomic studies have shown that the BAF and PBAF complexes are the most frequently mutated in various cancers (17). Non-canonical complexes (ncBAF) localize to the transcriptional repressor CTCF (also known as 11-zinc finger protein or CCCTC-binding factor) and can act as synthetic lethal targets specific for synovial sarcoma (SS) and malignant rhabdoid tumor (MRT) (16) or other cBAF-disrupted cancers.

3. SWI/SNF component in melanoma

Loss-of-function mutations in the components of the SWI/SNF complex such as AT-rich interactive domain-containing protein 1A (ARID1A), ARID1B, ARID2, or SMARCA4 are common in melanoma, suggesting that altered chromatin remodeling plays a role in the pathogenesis of this disease (18). A recent comprehensive study published by Dreier et al. using data from the TCGA showed a comparison of the frequency of genetic SWI/SNF alterations in melanoma. Interestingly, the data showed that the ARID2 subunit with missenses and truncating mutations is the most frequently mutated subunit in melanoma and is associated with a UVB mutation signature. Then, ARID1B missense mutations and deep deletions were observed in skin and choroidal melanomas, respectively. SMARCA4 and its paralogue SMARCA2 are almost equally frequently mutated (mostly as missenses) in patients with melanoma (5, 19). Missense mutations in these two tumor suppressors are associated with damage from UV radiation, as the role of SMARCAs is to promote melanin synthesis to protect against damage from solar radiation (20). Based on this study, ARID1A is the third most frequently mutated SWI/SNF, present in 9% of melanoma tumors in the TCGA database and associated with late-stage melanoma and metastasis to the brain (5) (Figure 1). On the other hand, several studies suggest that overexpression of the wild-type of ARID1A in patients with melanoma is more responsive to immune checkpoint inhibitors, while patients with loss of ARID1A may have therapeutic implications by modulating response to immunotherapy (21–23). However, a recent cohort study showed that ARID1A mutations do not have a major impact on survival and particularly on immune checkpoint inhibitors in melanoma. This finding by Griewank et al. (24). showed that ARID1A mutation status in melanoma is not currently relevant to treatment. Recent evidence suggests that ARID2, as a component of the PBAF complex, functions to inhibit invasion *in vitro* and modulate the response to immunotherapy *in vivo* (25). The mechanism of ARID2 as a modulator of tumor immunity is still unclear. The 2021 study by Fukumoto et al. showed that ARID2 knockout sensitizes melanoma to immune checkpoint inhibitors (anti-PD-L1 treatment), which is associated with an increase in the infiltration of $CD8^+$ cytotoxic T cells. These results indicate that ARID2 is an immunomodulator and a potential biomarker indicating the efficacy of immune checkpoint inhibitors in patients with melanoma (25). In addition, mutations (C > T-transitions) in ARID2, PPP6C, SNX31, and TACC1 possibly played a role in UVB-induced melanomagenesis (18).

3.1. Synthetic lethal partners

Synthetic lethality is a concept used as one of the most interesting, effective, and safe strategies in cancer treatment. It aims to target alleles of genes with loss-of-function mutations by drug inhibition, deletion, or reduction of expression to induce cell death. One of the best-known agents targeting inhibition of specific DNA repair pathways, based on the synthetic lethal approach, is the

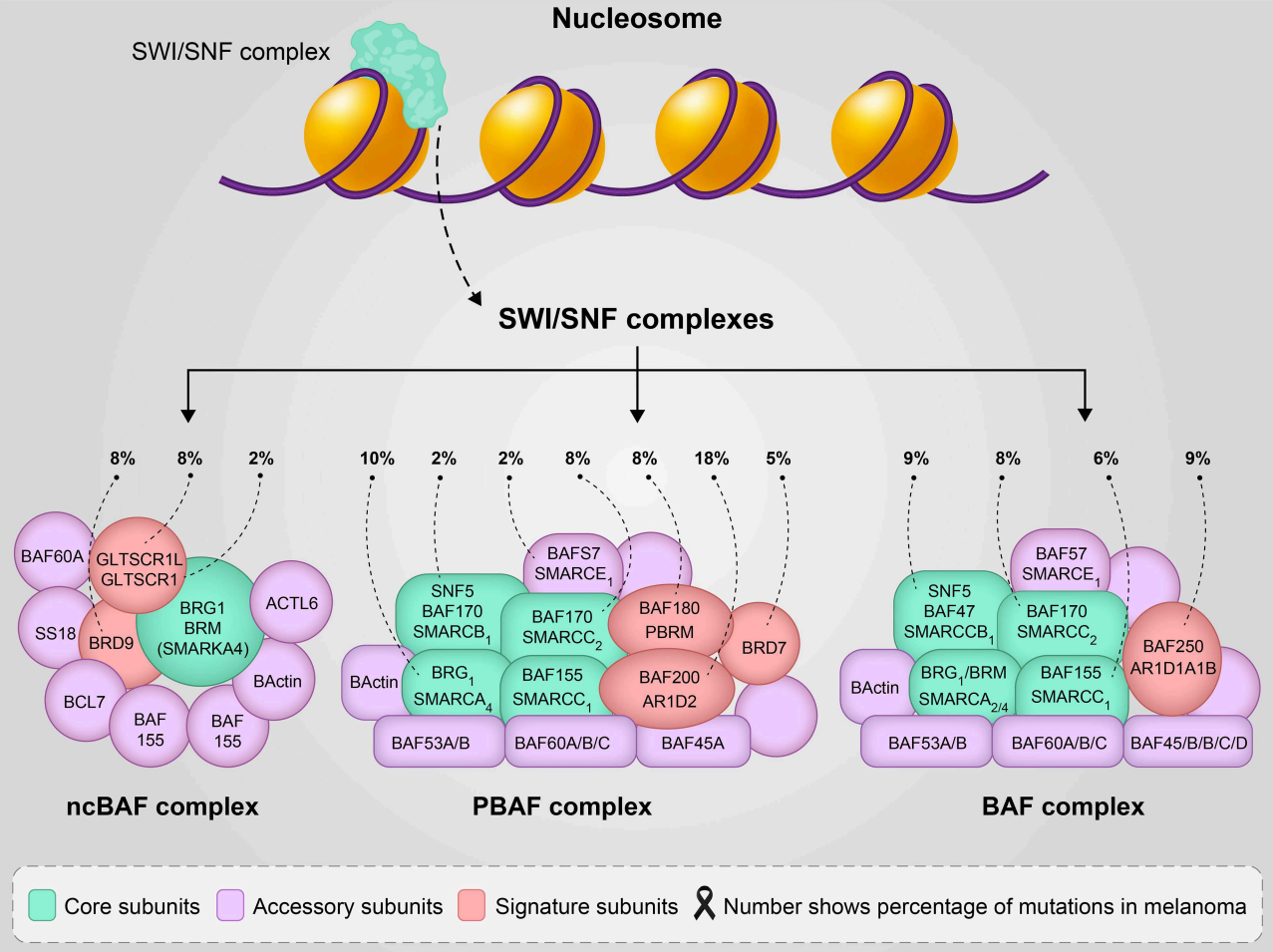

FIGURE 1
The SWI/SNF complexes structure and function, number shows the percentage of mutation involvement in melanoma reported in reference (5).

use of poly(ADP-ribose) polymerase (PARP) inhibitors to target BRCA1/2 mutated tumors (26). A 2019 systematic review by Kubicek et al. demonstrated strong synthetic-lethal interactions between two factors, SMARCA4-ARID2, in subunits of the SWI/SNF chromatin remodeling complex in melanoma. In view of this theory, cancer cells that have a LOF gene mutation lead to cell death when two genes are lost simultaneously, but not when either gene is lost alone, as we have described above. Thus, the relationship between SMARCA4 and ARID2 would be a potential target for synthetic lethal therapy, as SMARCA4 and ARID2 are frequently mutated in melanoma (27). On the other hand, in cancer cells lacking SMARCA4, SMARCB1, ARID1A, and PBRM1 of the SWI/SNF chromatin remodeling complex, inhibition of EZH2 (subunits of Zeste 2 Polycomb Repressive Complex 2; such as tazemetostat[1] or valemetostat) can cause synthetic lethality (19).

ARID1B, as a component of a subset of cBAF complexes, is a homolog of ARID1A that promotes a compensatory pathway in the event of loss of ARID1A in some cancers (28). ARID1A and ARID1B are frequently co-mutated in cancer, but ARID1A-deficient cancers retain at least one functional ARID1B allele. The result suggests that loss of ARID1A and ARID1B alleles (double knockout) together promotes aggressive carcinogenesis, followed by dedifferentiation and hyper-proliferation in the liver and skin (29). Since 10.67% of melanoma patients have altered ARID1A, this may be useful in identifying ARID1B as a potential therapeutic target in patients with ARID1A loss or alteration.

SMARCA4 (BRG1) and SMARCA2 (BRM) are the two critical components of SWI/SNF ATPases that use ATP to generate energy for nucleosome remodeling, which is often mutated or silenced in cancer (30). The first somatic genetic alteration of *SMARC2* was found in human non-melanoma cancer. Both act as tumor suppressors by controlling the cell cycle and regulating adhesion between cells. Several studies have also reported a synthetic lethality relationship between these two (19, 31). A 2018 study by Reyes and Martinez reported that high expression of SMARCA4 correlated with aggressive tumors, while high expression of SMARCA2 was associated with benign differentiated tumors. They showed that the expression of these two factors has a high prognostic value and high expression of SMARCA4 was significantly associated with poor prognosis and survival in uveal melanoma (32, 33), with high expression occurring in later stages of metastatic melanoma (34). Furthermore, one of these subunits is required for melanoma tumorigenesis (33, 35).

1 https://clinicaltrials.gov/ct2/show/NCT02601950

The master regulator of melanocyte differentiation from progenitor cells and survival, *microphthalmia-associated transcription factor (MITF)*, showed several interactions with the SWI/SNF complex. The *MITF* gene plays a cooperative role with the subunits of the complex to promote tumorigenesis, and on the other hand, there is evidence that some SWI/SNF subunits are downregulated (4). SMARCA4 regulates MITF, melanin synthesis, protection against UVR damage, and survival in melanocytes and melanoma cells (36). SMARCA2 does compensate for the function of SMARCA4 in the case of a loss-of-function mutation associated with MITF (37), but SMARCA2 only partially compensates for the loss of SMARCA4 when all MITF targets are expressed (38). In addition to SMARCs, a recent study by Trivedi et al. (39) has shown that inhibition of bromodomain and extra-terminal (BET) by JQ1 can lead to decreased expression of MITF targets.

3.2. Druggable pathway targets

In a recent review article by Guo et al. (40) describing the signaling pathways involved in melanoma, including the mitogen-activated protein kinase (MAPK) pathway, protein kinase B (AKT) pathway, cell cycle regulation pathway, pigmentation-related pathway, and p53 pathway, epigenetic factors were also mentioned as one of the crucial factors in melanoma carcinogenesis. In melanoma, mutations in BRAF (50%−70%), NRAS (15%−30%), NF1, KRAS and HRAS (in 2 and 1% of patients, respectively), and KIT are responsible for MAPK dysregulation. Activation of the MAPK pathway leads to cell proliferation, invasion, metastasis, survival, and angiogenesis (41). BRAF (serine/threonine kinase), which is a member of the Raf family, plays a critical role in MAPK pathway signaling, with a substitution from valine to glutamic acid at codon 600 (V600E) in ∼50% of melanomas (40). The FDA approved vemurafenib (PLX4032) and dabrafenib for the treatment of metastatic melanoma in 2011 and 2013, respectively. The drugs specifically target patients whose tumors have the BRAF V600E gene mutation (Table 1). The phosphatidylinositol 3-kinase (PI3K)/protein kinase B (Akt) pathway, which has more or less the same functions in cells, is another metabolic pathway that is dysregulated in melanoma, although there is no FDA-approved agent that directly inhibits this pathway in melanoma, however, there are several studies showing that synthetic small molecule compounds have an effect on PI3K/AKt and/or PI3K/Akt/mTOR and the associated RAS/RAF/MEK/ERK or MAPK pathway, such as NVP-BEZ235 (53) and Rapalogs (Everolimus, Deforolimus, and Temsirolimus) (54). c-KIT or CD117 is a transmembrane receptor tyrosine kinase (RTK) identified in hematopoietic cells, germ cells, gastrointestinal tract Cajal cells (GI), melanoma cells, B-cell progenitor cells, and mast cells that sends signals to maintain survival, promote cell proliferation, differentiation and regulate growth and development (55). Approximately 70% of KIT mutations in melanoma are missense mutations (well described in reference (55)). Nilotinib, Dasatinib, Sunitinib, and Masitinib are the small molecules that target cKIT and are currently being tested in clinical trials. It should be noted that pathway inhibitors have shown a potential synergistic effect with other antitumor agents in melanoma such as checkpoint inhibitors (56) and anti-cytotoxic T-lymphocyte antigen 4 (CTLA-4) antibodies (57).

3.3. Drugs currently under clinical trials

The results of Martí et al. from 2012 show that the potential target therapies in melanoma can be divided into two categories: first, the strategy may target the tumor cell using molecules that can inhibit growth and/or prevent cell death, or molecules responsible for facilitating invasion and/or metastasis. The second category targets structure rather than cells, such as angiogenesis and immune tolerance. They reported BRAF inhibitors (Sorafenib, PLX4032, GSK2118436, RAF-265, XL281), inhibitors of c-kit tyrosine kinase activity (Imatinib, Sunitinib, Dasatinib, Nilotinib), and anti-cytotoxic T-lymphocyte antigen 4 (CTLA-4) antibodies (Ipilimumab and Tremelimumab), which showed the best test results in patients with melanoma (57). Histone deacetylase inhibitors (HDACI) are the enzyme with anticancer activity, the only agents approved in the clinic for melanoma[2], which inhibit histone deacetylases (HDAC) to inhibit tumor cell proliferation (58). Domatinostat (59), Entinostat[3], Azacytidine[4], ACY-241, and Tinostamustine[5] can be placed in this category, which has been repeatedly demonstrated in preclinical and clinical studies. Garmpis et al. (58) proposed to investigate the synergistic effect of HDACi (Vorinostat (5AIIA, Zalmza), Romidepsin (Istodox, Depsipeptide), Belinostat and Panobinostat (Farydak) with other inhibitors such as BRAF inhibitors and BET inhibitors, which may lead to melanoma treatment. According to this study, the combination of the HDAC inhibitor LBH589 and the BET inhibitor I-BET151 showed apoptosis of melanoma cells but not of melanocytes *via* the mitochondrial pathway in the AKT and Hippo/YAP signaling pathways. This study demonstrated the effect of combination therapy on melanomas, including those resistant to BRAF inhibitors (60). *In vitro* treatment with the histone deacetylase inhibitor Vorinostat (SAHA) resulted in suppression of MITF and cell death in melanocytic nevi (50). A clinical trial of PDR001 and the HDAC inhibitor Panobinostat in patients with metastatic melanoma who have failed prior anti-PD1 or PD-L1 therapy was registered in 2019. The trial was withdrawn by the decision of the sponsor, but another trial evaluating the combination of the HDACi fusion molecule Tinostamustine (EDO-S101) and the anti-PD-1 monoclonal antibody Nivolumab in patients with refractory, locally advanced or metastatic melanoma was initiated in 2019 and is enrolling patients.[6] Since 2010, the FDA has approved a number of therapeutic agents and synergistic approaches against melanoma, including Ipilimumab, Nivolumab, Pembrolizumab and the combination of Ipilimumab and Nivolumab, Vemurafenib, Dabrafenib, the combination of Dabrafenib plus Trametinib, Vemurafenib plus Cobimetinib, and Encorafenib plus Binimetinib (well described in reference (40)). Table 1 shows the information on agents tested or approved for melanoma, categorized by the mechanism of action, most of which have been discussed in this article.

The new strategy of combination therapy, especially in combination with BET inhibitors, showed interesting results in overcoming patient relapse and resistance after treatment with

2 https://clinicaltrials.gov/ct2/show/NCT03022565
3 https://clinicaltrials.gov/ct2/show/NCT03765229
4 https://clinicaltrials.gov/ct2/show/NCT02816021
5 https://clinicaltrials.gov/ct2/show/NCT03903458
6 https://www.clinicaltrials.gov/ct2/show/NCT03903458

TABLE 1 Druggable targets in melanoma-the FDA, clinical trial, or assessment status of different compounds in melanoma.

Mechanism of action	Compound	Status in melanoma	References
Anti–PD-L1	Nivolumab	On 18 March, 2022, the FDA approved nivolumab and relatlimab-rmbw (Opdualag, Bristol-Myers Squibb Company) for adult and pediatric patients 12 years of age or older with unresectable or metastatic melanoma	Sahni et al. (42)
	Pembrolizumab	FDA approves Merck's KEYTRUDA® (pembrolizumab) as adjuvant treatment for adult and pediatric (≥12 years of age) patients with stage IIB or IIC melanoma following complete resection	–
HDAC inhibitor	Domatinostat (*4SC-202*)	FDA approves IND application for Domatinostat (*4SC-202*) in melanoma	–
	Entinostat	Phase II	An exploratory study of pembrolizumab plus entinostat in non-inflamed stage III/IV melanoma: https://clinicaltrials.gov/ct2/show/NCT03765229
	Azacytidine	Phase II	Study of oral azacitidine (CC-486) in combination with pembrolizumab (MK-3475) in patients with metastatic melanoma: https://clinicaltrials.gov/ct2/show/NCT02816021
	Tinostamustine	Phase I	Tinostamustine and nivolumab in advanced melanoma (ENIgMA) https://www.clinicaltrials.gov/ct2/show/NCT03903458
	ACY-241	Phase I	Selective HDAC6 inhibitor ACY-241 in combination with ipilimumab and nivolumab https://clinicaltrials.gov/ct2/show/NCT02935790
EZH2 inhibitors	Tazemetostat	The FDA has approved Tazverik (tazemetostat) on 24 January, 2020, is marketed by Epizyme Inc. to treat adults and children 16 and older with epithelioid sarcoma, Tazverik is only the second targeted therapy (https://www.cancer.org/cancer/soft-tissue-sarcoma/treating/targeted-therapy.html) approved for soft tissue sarcoma and the first treatment option specifically for epithelioid sarcoma (https://www.cancer.org/cancer/soft-tissue-sarcoma/about/soft-tissue-sarcoma.html)	—
	GSK503	*In vitro*	(https://www.ncbi.nlm.nih.gov/pmc/articles/PMC6174981/pdf/PATH-245-433.pdf) and https://pubmed.ncbi.nlm.nih.gov/25609585/
Anti-cytotoxic T lymphocyte antigen 4 (CTLA-4) antibodies	Ipilimumab	FDA approves YERVOY™ (ipilimumab) for the treatment of patients with newly diagnosed or previously-treated unresectable or metastatic melanoma on March 25, 2011	—
	Tremelimumab	Phase III	Ribas et al. (43)
BET (bromodomain and extra-terminal) inhibitors	JQ1	*In vitro*	Trivedi et al. (39)
	NHWD-870	*In vitro*	Deng et al. (44)
	RVX2135 or iBET762	*In vitro*	Muralidharan et al. (45)
BRAF inhibitors (serine/threonine kinase)	Sorafenib	Phase II	Eisen et al. (46)
	Vemurafenib (PLX4032)	FDA approves vemurafenib (PLX4032) on 18 Aug 2011, for treatment of metastatic or unresectable melanoma. The drug specifically targets patients whose tumors express the BRAF V600E gene mutation	–

(Continued)

TABLE 1 (Continued)

Mechanism of action	Compound	Status in melanoma	References
	Dabrafenib or GSK2118436	The FDA approved dabrafenib as a single-agent treatment for patients with BRAF V600E mutation-positive advanced melanoma on May 30, 2013	Ballantyne et al. (47)
	RAF-265 (formerly CHIR-265)	Phase I	Harris (48)
	XL281	Phase I	https://clinicaltrials.gov/ct2/show/NCT00451880
C-kit tyrosine kinase activity inhibitors	Imatinib	Phase III	Wei et al. (49)
	Sunitinib	Phase II	https://www.clinicaltrials.gov/ct2/show/NCT00631618
	Dasatinib	Phase II	https://clinicaltrials.gov/ct2/show/NCT00700882 https://clinicaltrials.gov/ct2/show/NCT00436605
	Nilotinib	Phase I	https://clinicaltrials.gov/ct2/show/NCT04903119
Histone deacetylase inhibitors	SAHA	*In vitro*	Basu et al. (50)
Bromodomain inhibitor	PFI-3 (selective SMARCA2/4 bromodomain inhibitor)	*In vitro*	Yang et al. (51)
	TP-472 (Inhibition of BRD9)	*In vitro*	Mason et al. (52)

approved drugs targeting the MAPK pathway. For example, a recent study (44) showed that secreted phosphoprotein 1 (SPP1) expression can be a melanoma driver, and BET inhibitor NHWD-870 targets the BRD4 subunit and suppresses SPP1 expression and ultimately melanoma progression *via* the non-canonical NF-κB/SPP1 pathway (44). BET inhibitors (RVX2135 or iBET762) in combination with ATRIs [Ataxia-telangiectasia and Rad3-related (ATR) is a kinase belonging to the PI3 kinase-like family; VE821 or AZ20], showed apoptosis effect on melanoma cells as well as the PDX model of melanoma (45). Another study by Paoluzzi et al. (61) showed that the BET inhibitor JQ1 in combination with the BRAF inhibitorV suppressed tumor growth and significantly improved survival compared to either drug alone. Vemurafenib demonstrated safety and efficacy in both treatment-free and pre-treated BRAF-mutated melanoma patients (62).

In this section, we have attempted to provide an update on agents tested or approved for melanoma, most of which target the SWI/SNF complex. However, it should be noted that some *in vitro* or preclinical studies have shown the novel potential of new small molecules, e.g., the study by Zingg et al. (63), showed that EZH2 levels are upregulated in cancer cells after anti-CTLA-4 or IL-2 immunotherapies, leading to loss of tumor control. In this study, combination therapy with EZH2i (i.e., GSK503) may restore tumor immunogenicity. In general, and after reviewing various evidence that showed a contrast in the use of EZH2 inhibitors in cancers, especially mesothelioma, it seems that testing the response to EZH2 should be carefully evaluated before using these molecules as therapy (64). Recent research has shown that a novel bromodomain inhibitor called PFI-3, which targets SWI/SNF, and is responsible for repairing double-strand breaks in cancer, synergistically sensitizes many human cancers cell lines against DNA damage caused by chemotherapeutic agents such as doxorubicin (65). PFI-3 is a selective, potent, and cell-permeable SMARCA2/4 bromodomain inhibitor that has been previously characterized in the setting of various cancers (e.g., lung cancer, synovial sarcoma, leukemia, and rhabdoid tumors) (66). SMARCA2/SMARCA4 ATPases simulate synthetic lethality through multiple inhibitors for cancers containing a BRG1 loss-of-function mutation, as described in the 2018 study by Papillon et al. (67). It should be noted that SMARCA4, SMARCA2, BRD7, BRD9, and PBRM1 contain drug-acting bromodomains that showed interaction with synthetic lethality to serve as therapy. TP-472, a compound with selective function and similarity to the bromodomain of BRD7 and BRD9, has antitumor activity on melanoma (68).

4. SWI/SNF complex as a targeted therapy in other cancers

Mutations in SWI/SNF's subunits are reported in ∼25% of cancers (69). Although this paper is focused on melanoma, this section tries to show the footprint of this complex's mutation in different cancer. A comprehensive review by Centore et al., was published in 2020 based on the large-scale cancer genome-sequencing studies showed targeted therapies in different cancers based on this complex mutation, for example, ARID1A mutation as a hallmark in the bladder, stomach, and endometrial cancers which targeted by ARID1B selective degrader, EZH2 inhibitors and P13K inhibitors. SMARCA4, in nonsmall cell lung carcinoma, was targeted through the synthetic lethal pathway and by targeting SMARCA2 inhibitors (70). In Silico analysis of the SWI/SNF complex shows 70% of mutations with functional impact on lung adenocarcinoma patients (71). SMARCA2 in esophageal, SMARCB1 in malignant rhabdoid tumor and epithelial sarcoma, and PBRM1 in kidney cancer are collectively mutated and reported. These mutations are targeted by SMARCA4-selective inhibitors, BRD9-selective degraders, EZH2 inhibitors, and immune checkpoint inhibitors, respectively (70). On other hand, some of the studies focused on the ATPase part to conduct target therapy, degradation of ATPase subunit of SWI/SNF can disrupt physical chromatin accessibility to disable oncogenic transcription (for instance in prostate cancer) (72), and BRM as a core ATPase subunit is downregulated in hepatocellular carcinoma

(HCC), colorectal and gastric cancer, small cell carcinoma of the ovary (SCCOHT), ovarian clear cell carcinoma (OCCC), non-small cell lung cancer (NSCLC), adenocarcinoma of the lung (AD), large cell carcinoma of the lung (LC), pleomorphic carcinoma of the lung (PL), clear cell renal cell carcinoma (ccRCC), and non-melanoma skin cancer (NMSC) (73). It should be noted that BRM as well as some of the therapeutic agents to target these complex acts context-dependent (as we also mentioned above about liver cancer) (74). Considering context dependency, cancer dependent-specific study is required to validate therapeutic agents targeting SWI/SNF complex subunits.

5. Conclusion and future direction

A theme developed from recent studies showed the crucial role of the SWI/SNF complex in defining the therapeutic efficacy of melanoma. In light of accumulated data, *ARID2, ARID1B, SMARCA4 (BRG1)*, and *SMARCA2 (BRM)* have the most important mutations in melanoma. Considering the important role of epigenetic players in immune therapy resistance in a patient with melanoma. It is crucial to determine how SWI/SNF complex can contribute to melanoma therapy through different subunits. Combinational therapy and synthetic lethality approaches are the well-studied most current findings that show promising clinical responses in melanoma. Of note, further investigations need to be done to elucidate the context-dependent behavior of SWI/SNF subunits, possible off-target inhibition, immunosuppression, and the chance of relapse in target therapy for melanoma. Targeting the druggable SWI/SNF bromodomains (BRD7, BRD9, SMARCA4, SMARCA2), using the BET inhibitors as long as the HDAC inhibitors and identification of synthetic lethal interactions involved in melanoma such as SMARCA4 and ARID2 presents an additional possibility for novel strategies targeting the SWI/SNF subunits toward precise medicine of melanoma. Given the significant role of the SWI/SNF complex in melanoma, future therapeutic approaches must focus on mechanisms of synergic effect and synthetic lethality to enhance the therapeutic benefits of inhibitors, particularly when there is a deficiency in the functional domains mentioned above. We strongly believe an understanding of potential therapeutic vulnerabilities based on SWI/SNF in melanoma is leading to personalized and targeted cures and opening up new areas of clinical investigations.

Author contributions

Conception and design of study: MM and MA. Acquisition of data and revising the manuscript critically for important intellectual content: MA, MN, and MM. Drafting the manuscript: MM. All authors contributed to the article and approved the submitted version.

Acknowledgments

We would like to thank the skin and stem cell research center, Tehran University of Medical Sciences for technical support.

Conflict of interest

The authors declare that the research was conducted in the absence of any commercial or financial relationships that could be construed as a potential conflict of interest.

Publisher's note

References

1. Alver BH, Kim KH, Lu P, Wang X, Manchester HE, Wang W, et al. The SWI/SNF chromatin remodelling complex is required for maintenance of lineage specific enhancers. *Nat Commun.* (2017) 8:14648. doi: 10.1038/ncomms14648

2. Fang J-Z, Li C, Liu X-Y, Hu T-T, Fan Z-S, Han Z-G. Hepatocyte-specific Arid1a deficiency initiates mouse steatohepatitis and hepatocellular carcinoma. *PLoS ONE.* (2015) 10:e0143042. doi: 10.1371/journal.pone.0143042

3. Sun X, Wang SC, Wei Y, Luo X, Jia Y, Li L, et al. Arid1a has context-dependent oncogenic and tumor suppressor functions in liver cancer. *Cancer Cell.* (2017) 32:574-589 e6. doi: 10.1016/j.ccell.2017.10.007

4. Mehrotra A, Mehta G, Aras S, Trivedi A, Serna ILD. SWI/SNF chromatin remodeling enzymes in melanocyte differentiation and melanoma. *Crit Rev Eukaryot Gene Expr.* (2014) 24:151–61. doi: 10.1615/CritRevEukaryotGeneExpr.2014007882

5. Dreier MR, de la Serna IL. SWI/SNF chromatin remodeling enzymes in melanoma. *Epigenomes.* (2022) 6:10. doi: 10.3390/epigenomes6010010

6. Hamid O, Robert C, Daud A, Hodi FS, Hwu WJ, Kefford R, et al. Five-year survival outcomes for patients with advanced melanoma treated with pembrolizumab in KEYNOTE-001. *Ann Oncol.* (2019) 30:582–8. doi: 10.1093/annonc/mdz011

7. Rago F, Elliott G, Li A, Sprouffske K, Kerr G, Desplat A, et al. The discovery of SWI/SNF chromatin remodeling activity as a novel and targetable dependency in uveal melanoma. *Mol Cancer Ther.* (2020) 19:2186–95. doi: 10.1158/1535-7163.MCT-19-1013

8. Tang L, Nogales E, Ciferri C. Structure and function of SWI/SNF chromatin remodeling complexes and mechanistic implications for transcription. *Prog Biophys Mol Biol.* (2010) 102:122–8. doi: 10.1016/j.pbiomolbio.2010.05.001

9. He Z, Chen K, Ye Y, Chen Z. Structure of the SWI/SNF complex bound to the nucleosome and insights into the functional modularity. *Cell Discovery.* (2021) 7:28. doi: 10.1038/s41421-021-00262-5

10. Wang W, Côté J, Xue Y, Zhou S, Khavari PA, Biggar SR, et al. Purification and biochemical heterogeneity of the mammalian SWI-SNF complex. *EMBO J.* (1996) 15:5370–82. doi: 10.1002/j.1460-2075.1996.tb00921.x

11. Menon DU, Shibata Y, Mu W, Magnuson T. Mammalian SWI/SNF collaborates with a polycomb-associated protein to regulate male germline transcription in the mouse. *Development.* (2019) 146:dev174094. doi: 10.1242/dev.174094

12. Bultman S, Gebuhr T, Yee D, Mantia CL, Nicholson J, Gilliam A, et al. A Brg1 null mutation in the mouse reveals functional differences among mammalian SWI/SNF complexes. *Mol Cell.* (2000) 6:1287–95. doi: 10.1016/S1097-2765(00)00127-1

13. Ho L, Ronan JL, Wu J, Staahl BT, Chen L, Kuo A, et al. An embryonic stem cell chromatin remodeling complex, esBAF, is essential for embryonic stem cell self-renewal and pluripotency. *Proc Natl Acad Sci U S A.* (2009) 106:5181–6. doi: 10.1073/pnas.0812889106

14. Gatchalian J, Malik S, Ho J, Lee D-S, Kelso TWR, Shokhirev MN, et al. A non-canonical BRD9-containing BAF chromatin remodeling complex regulates

naive pluripotency in mouse embryonic stem cells. *Nat Commun.* (2018) 9:5139. doi: 10.1038/s41467-018-07528-9

15. Lickert H, Takeuchi JK, Von Both I, Walls JR, McAuliffe F, Adamson SL, et al. Baf60c is essential for function of BAF chromatin remodelling complexes in heart development. *Nature.* (2004) 432:107–12. doi: 10.1038/nature03071

16. Weinberg P, Flames N, Sawa H, Garriga G, Hobert O. The SWI/SNF chromatin remodeling complex selectively affects multiple aspects of serotonergic neuron differentiation. *Genetics.* (2013) 194:189–98. doi: 10.1534/genetics.112.148742

17. Rada-Iglesias ABR, Swigut T, Brugmann SA, Flynn RA, Wysocka J. A unique chromatin signature uncovers early developmental enhancers in humans. *Nature.* (2011) 470:279–83. doi: 10.1038/nature09692

18. Hodis E, Watson IR, Kryukov GV, Arold ST, Imielinski M, Theurillat JP, et al. A landscape of driver mutations in melanoma. *Cell.* (2012) 150:251–63. doi: 10.1016/j.cell.2012.06.024

19. Sasaki M, Ogiwara H. Synthetic lethal therapy based on targeting the vulnerability of SWI/SNF chromatin remodeling complex-deficient cancers. *Cancer Sci.* (2020) 111:774–782 doi: 10.1111/cas.14311

20. Moloney FJ, Lyons JG, Bock VL, Huang XX, Bugeja MJ, Halliday GM. Hotspot mutation of Brahma in non-melanoma skin cancer. *J Invest Dermatol.* (2009) 129:1012–5. doi: 10.1038/jid.2008.319

21. Li J, Wang W, Zhang Y, Cieślik M, Guo J, Tan M, et al. Epigenetic driver mutations in ARID1A shape cancer immune phenotype and immunotherapy. *J Clin Invest.* (2020) 130:2712–26. doi: 10.1172/JCI134402

22. Shen J, Ju Z, Zhao W, Wang L, Peng Y, Ge Z, et al. ARID1A deficiency promotes mutability and potentiates therapeutic antitumor immunity unleashed by immune checkpoint blockade. *Nat Med.* (2018) 24:556–62. doi: 10.1038/s41591-018-0012-z

23. Bitler BG, Aird KM, Garipov A, Li H, Amatangelo M, Kossenkov AV, et al. Synthetic lethality by targeting EZH2 methyltransferase activity in ARID1A-mutated cancers. *Nat Med.* (2015) 21:231–8. doi: 10.1038/nm.3799

24. Thielmann CM, Matull J, Roth S, Placke J-M, Chorti E, Zaremba A, et al. Genetic and clinical characteristics of ARID1A mutated melanoma reveal high tumor mutational load without implications on patient survival. *Cancers.* (2022) 14:2090. doi: 10.3390/cancers14092090

25. Fukumoto T, Lin J, Fatkhutdinov N, Liu P, Somasundaram R, Herlyn M, et al. ARID2 deficiency correlates with the response to immune checkpoint blockade in melanoma. *J Investig Dermatol.* (2021) 141:1564–72.e4. doi: 10.1016/j.jid.2020.11.026

26. Topatana W, Juengpanich S, Li S, Cao J, Hu J, Lee J, et al. Advances in synthetic lethality for cancer therapy: cellular mechanism and clinical translation. *J Hematol Oncol.* (2020) 13:118. doi: 10.1186/s13045-020-00956-5

27. Schick S, Rendeiro AF, Runggatscher K, Ringler A, Boidol B, Hinkel M, et al. Systematic characterization of BAF mutations provides insights into intracomplex synthetic lethalities in human cancers. *Nat Genet.* (2019) 51:1399–410. doi: 10.1038/s41588-019-0477-9

28. Helming KC, Wang X, Wilson BG, Vazquez F, Haswell JR, Manchester HE, et al. ARID1B is a specific vulnerability in ARID1A-mutant cancers. *Nat Med.* (2014) 20:251–4. doi: 10.1038/nm.3480

29. Wang Z, Chen K, Jia Y, Chuang J-C, Sun X, Lin Y-H, et al. Dual ARID1A/ARID1B loss leads to rapid carcinogenesis and disruptive redistribution of BAF complexes. *Nat Cancer.* (2020) 1:909–22. doi: 10.1038/s43018-020-00109-0

30. Caumanns JJ, Wisman GBA, Berns K, van der Zee AGJ, de Jong S. ARID1A mutant ovarian clear cell carcinoma: a clear target for synthetic lethal strategies. *Biochim Biophys Acta Rev Cancer.* (2018) 1870:176–84. doi: 10.1016/j.bbcan.2018.07.005

31. Morel D, Almouzni G, Soria J-C, Postel-Vinay S. Targeting chromatin defects in selected solid tumors based on oncogene addiction, synthetic lethality and epigenetic antagonism. *Ann Oncol.* (2017) 28:254–69. doi: 10.1093/annonc/mdw552

32. Guerrero-Martínez JA, Reyes JC. High expression of SMARCA4 or SMARCA2 is frequently associated with an opposite prognosis in cancer. *Sci Rep.* (2018) 8:2043. doi: 10.1038/s41598-018-20217-3

33. Lin H, Wong RPC, Martinka M, Li G. BRG1 expression is increased in human cutaneous melanoma. *Br J Dermatol.* (2010) 163:502–10. doi: 10.1111/j.1365-2133.2010.09851.x

34. Peng L, Li J, Wu J, Xu B, Wang Z, Giamas G, et al. A pan-cancer analysis of SMARCA4 alterations in human cancers. *Front Immunol.* (2021) 12:762598. doi: 10.3389/fimmu.2021.762598

35. Keenen B, Qi H, Saladi SV, Yeung M, de la Serna IL. Heterogeneous SWI/SNF chromatin remodeling complexes promote expression of microphthalmia-associated transcription factor target genes in melanoma. *Oncogene.* (2010) 29:81–92. doi: 10.1038/onc.2009.304

36. Gelmi MC, Houtzagers LE, Strub T, Krossa I, Jager MJ. MITF in normal melanocytes, cutaneous and uveal melanoma: a delicate balance. *Int J Mol Sci.* (2022) 23:6001. doi: 10.3390/ijms23116001

37. Vachtenheim J, Ondrusová L, Borovanský J. SWI/SNF chromatin remodeling complex is critical for the expression of microphthalmia-associated transcription factor in melanoma cells. *Biochem Biophys Res Commun.* (2010) 392:454–9. doi: 10.1016/j.bbrc.2010.01.048

38. Saladi SV, Wong PG, Trivedi AR, Marathe HG, Keenen B, Aras S, et al. BRG1 promotes survival of UV-irradiated melanoma cells by cooperating with MITF to activate the melanoma inhibitor of apoptosis gene. *Pigment Cell Melanoma Res.* (2013) 26:377–91. doi: 10.1111/pcmr.12088

39. Trivedi A, Mehrotra A, Baum CE, Lewis B, Basuroy T, Blomquist T, et al. Bromodomain and extra-terminal domain (BET) proteins regulate melanocyte differentiation. *Epigenetics Chromatin.* (2020) 13:14. doi: 10.1186/s13072-020-00333-z

40. Guo W, Wang H, Li C. Signal pathways of melanoma and targeted therapy. *Signal Transduct Target Ther.* (2021) 6:424. doi: 10.1038/s41392-021-00827-6

41. Inamdar GS, Madhunapantula SV, Robertson GP. Targeting the MAPK pathway in melanoma: why some approaches succeed and other fail. *Biochem Pharmacol.* (2010) 80:624–37. doi: 10.1016/j.bcp.2010.04.029

42. Sahni S, Valecha G, Sahni A. Role of Anti-PD-1 antibodies in advanced melanoma: the era of immunotherapy. *Cureus.* (2018) 10:e3700. doi: 10.7759/cureus.3700

43. Ribas A, Kefford R, Marshall MA, Punt CJ, Haanen JB, Marmol M, et al. Phase III randomized clinical trial comparing tremelimumab with standard-of-care chemotherapy in patients with advanced melanoma. *J Clin Oncol.* (2013) 31:616–22. doi: 10.1200/JCO.2012.44.6112

44. Deng G, Zeng F, Su J, Zhao S, Hu R, Zhu W, et al. inhibitor suppresses melanoma progression *via* the noncanonical NF-κB/SPP1 pathway. *Theranostics.* (2020) 10:11428–43. doi: 10.7150/thno.47432

45. Muralidharan SV, Einarsdottir BO, Bhadury J, Lindberg MF, Wu J, Campeau E, et al. bromodomain inhibitors synergize with ATR inhibitors in melanoma. *Cell Death Dis.* (2017) 8:e2982. doi: 10.1038/cddis.2017.383

46. Eisen T, Ahmad T, Flaherty KT, Gore M, Kaye S, Marais R, et al. Sorafenib in advanced melanoma: a phase II randomised discontinuation trial analysis. *Br J Cancer.* (2006) 95:581–6. doi: 10.1038/sj.bjc.6603291

47. Ballantyne AD, Garnock-Jones KP. Dabrafenib: first global approval. *Drugs.* (2013) 73:1367–76. doi: 10.1007/s40265-013-0095-2

48. Harris PA. *Cancer Drug Design and Discovery*, 2nd ed. New York, NY: Springer (2014).

49. Wei X, Mao L, Chi Z, Sheng X, Cui C, Kong Y, et al. Efficacy evaluation of imatinib for the treatment of melanoma: evidence from a retrospective study. *Oncol Res.* (2019) 27:495–501. doi: 10.3727/096504018X15331163433914

50. Basu D, Salgado CM, Bauer B, Hoehl RM, Moscinski CN, Schmitt L, et al. Histone deacetylase inhibitor Vorinostat (SAHA) suppresses microphthalmia transcription factor expression and induces cell death in nevocytes from large/giant congenital melanocytic nevi. *Melanoma Res.* (2021) 31:319–27. doi: 10.1097/CMR.0000000000000749

51. Yang C, Wang Y, Sims MM, He Y, Miller DD, Pfeffer LM. Targeting the bromodomain of BRG-1/BRM subunit of the SWI/SNF complex increases the anticancer activity of temozolomide in glioblastoma. *Pharmaceuticals.* (2021) 14:904. doi: 10.3390/ph14090904

52. Mason LD, Chava S, Reddi KK, Gupta R. The BRD9/7 inhibitor TP-472 blocks melanoma tumor growth by suppressing ECM-mediated oncogenic signaling and inducing apoptosis. *Cancers.* (2021) 13:5516. doi: 10.3390/cancers13215516

53. Calero R, Morchon E, Martinez-Argudo I, Serrano R. Synergistic anti-tumor effect of 17AAG with the PI3K/mTOR inhibitor NVP-BEZ235 on human melanoma. *Cancer Lett.* (2017) 406:1–11. doi: 10.1016/j.canlet.2017.07.021

54. Strickland LR, Pal HC, Elmets CA, Afaq F. Targeting drivers of melanoma with synthetic small molecules and phytochemicals. *Cancer Lett.* (2015) 359:20–35. doi: 10.1016/j.canlet.2015.01.016

55. Pham DDM, Guhan S, Tsao H. KIT and melanoma: biological insights and clinical implications. *Yonsei Med J.* (2020) 61:562–71. doi: 10.3349/ymj.2020.61.7.562

56. Seifert AM, Zeng S, Zhang JQ, Kim TS, Cohen NA, Beckman MJ. PD-1/PD-L1 blockade enhances T-cell activity and antitumor efficacy of imatinib in gastrointestinal stromal tumors. *Clin Cancer Res.* (2017) 23:454–65. doi: 10.1158/1078-0432.CCR-16-1163

57. Martí RM, Sorolla A, Yeramian A. New therapeutic targets in melanoma. *Actas Dermo-Sifiliográficas.* (2012) 103:579–90. doi: 10.1016/j.adengl.2012.08.005

58. Garmpis N, Damaskos C, Garmpi A, Dimitroulis D, Spartalis E, Margonis GA, et al. Targeting histone deacetylases in malignant melanoma: a future therapeutic agent or just great expectations? *Anticancer Res.* (2017) 37:5355–62. doi: 10.21873/anticanres.11961

59. Giunta EFA, Curvietto G, Pappalardo M, Bosso A, Rosanova D, Diana M, et al. Epigenetic regulation in melanoma: facts and hopes. *Cells.* (2021) 10:2048. doi: 10.3390/cells10082048

60. Heinemann ACC, De Paoli-Iseppi R, Wilmott JS, Gunatilake D, Madore J, Strbenac D, et al. Combining BET and HDAC inhibitors synergistically induces apoptosis of melanoma and suppresses AKT and YAP signaling. *Oncotarget.* (2015) 6:21507–21. doi: 10.18632/oncotarget.4242

61. Paoluzzi L, Hanniford D, Sokolova E, Osman I, Darvishian F, Wang J, et al. BET and BRAF inhibitors act synergistically against BRAF-mutant melanoma. *Cancer Med.* (2016) 5:1183–93. doi: 10.1002/cam4.667

62. Swaika ACJ, Joseph RW. Vemurafenib: an evidence-based review of its clinical utility in the treatment of metastatic melanoma. *Drug Des Devel Ther.* (2014) 8:775–87. doi: 10.2147/DDDT.S31143

63. Zingg D, Arenas-Ramirez N, Sahin D, Rosalia RA, Antunes AT, Haeusel J, et al. The histone methyltransferase Ezh2 controls mechanisms of adaptive resistance to tumor immunotherapy. *Cell Rep.* (2017) 20:854–67. doi: 10.1016/j.celrep.2017.07.007

64. Schoumacher M, Le Corre S, Houy A, Mulugeta E, Stern MH, Roman-Roman S, et al. Uveal melanoma cells are resistant to EZH2 inhibition regardless of BAP1 status. *Nat Med.* (2016) 22:577–8. doi: 10.1038/nm.4098

65. Lee D, Lee D-Y, Hwang Y-S, Seo H-R, Lee S-A, Kwon J. The bromodomain inhibitor PFI-3 sensitizes cancer cells to DNA damage by targeting SWI/SNF. *Mol Cancer Res.* (2021) 19:900–12. doi: 10.1158/1541-7786.MCR-20-0289

66. Vangamudi B, Paul TA, Shah PK, Kost-Alimova M, Nottebaum L, Shi X, et al. The SMARCA2/4 ATPase domain surpasses the bromodomain as a drug target in SWI/SNF-mutant cancers: insights from cDNA rescue and PFI-3 inhibitor studies. *Cancer Res.* (2015) 75:3865–78. doi: 10.1158/0008-5472.CAN-14-3798

67. Papillon JPN, Nakajima K, Adair CD, Hempel J, Jouk AO, Karki RG, et al. Discovery of orally active inhibitors of brahma homolog (BRM)/SMARCA2 ATPase activity for the treatment of brahma related gene 1 (BRG1)/SMARCA4-mutant cancers. *J Med Chem.* (2018) 61:10155–72. doi: 10.1021/acs.jmedchem.8b01318

68. Zhao RL, Wu Y, Li C, Wei M, Niu Y, Yang W H, et al. BRD7 promotes cell proliferation and tumor growth through stabilization of c-Myc in colorectal cancer. *Front Cell Dev Biol.* (2021) 9:659392. doi: 10.3389/fcell.2021.659392

69. Mittal P, Roberts CWM. The SWI/SNF complex in cancer — biology, biomarkers and therapy. *Nat Rev Clin Oncol.* (2020) 17:435–48. doi: 10.1038/s41571-020-0357-3

70. Centore RC, Sandoval GJ, Soares LMM, Kadoch C, Chan HM. Mammalian SWI/SNF chromatin remodeling complexes: emerging mechanisms and therapeutic strategies. *Trends Genet.* (2020) 36:936–50. doi: 10.1016/j.tig.2020.07.011

71. Peinado P, Andrades A, Cuadros M, Rodriguez MI, Coira IF, Garcia DJ, et al. Multi-omic alterations of the SWI/SNF complex define a clinical subgroup in lung adenocarcinoma. *Clin Epigenetics.* (2022) 14:42. doi: 10.1186/s13148-022-01261-3

72. Xiao L, Parolia A, Qiao Y, Bawa P, Eyunni S, Mannan R, et al. Targeting SWI/SNF ATPases in enhancer-addicted prostate cancer. *Nature.* (2022) 601:434–9. doi: 10.1038/s41586-021-04246-z

73. Jancewicz I, Siedlecki JA, Sarnowski TJ, Sarnowska E, BRM. the core ATPase subunit of SWI/SNF chromatin-remodelling complex—a tumor suppressor or tumor-promoting factor? *Epigenetics Chromatin.* (2019) 12:68. doi: 10.1186/s13072-019-0315-4

74. Tsuda M, Fukuda A, Kawai M, Araki O, Seno H. The role of the SWI/SNF chromatin remodeling complex in pancreatic ductal adenocarcinoma. *Cancer Sci.* (2021) 112:490–7. doi: 10.1111/cas.14768

frontiers | Frontiers in Medicine

TYPE Original Research
PUBLISHED 17 February 2023
DOI 10.3389/fmed.2023.1082402

OPEN ACCESS

EDITED BY
Darius Mehregan,
Wayne State University, United States

REVIEWED BY
Linjun Shi,
Shanghai Jiao Tong University, China
Peizhen Zhao,
Southern Medical University, China

*CORRESPONDENCE
Jun Lyu
✉ lyujun2020@jnu.edu.cn
Liehua Deng
✉ liehuadeng@126.com

†These authors have contributed equally to this work and share first authorship

SPECIALTY SECTION
This article was submitted to Dermatology, a section of the journal Frontiers in Medicine

RECEIVED 28 October 2022
ACCEPTED 12 January 2023
PUBLISHED 17 February 2023

CITATION
Zhang J, Yang W, Lian C, Zhao Q, Ming W-k, Ip CC, Mu H-H, Ching Tom K, Lyu J and Deng L (2023) A nomogram for predicting survival in patients with skin non-keratinizing large cell squamous cell carcinoma: A study based on the Surveillance, Epidemiology, and End Results database.
Front. Med. 10:1082402.
doi: 10.3389/fmed.2023.1082402

A nomogram for predicting survival in patients with skin non-keratinizing large cell squamous cell carcinoma: A study based on the Surveillance, Epidemiology, and End Results database

Jinrong Zhang[1†], Wei Yang[2†], Chengxiang Lian[1], Qiqi Zhao[1,3], Wai-kit Ming[4], Cheong Cheong Ip[1,5], Hsin-Hua Mu[6], Kong Ching Tom[7], Jun Lyu[8*] and Liehua Deng[1,3*]

[1]Department of Dermatology, The First Affiliated Hospital of Jinan University and Jinan University Institute of Dermatology, Guangzhou, China, [2]Office of Drug Clinical Trial Institution, The First Affiliated Hospital of Jinan University, Guangzhou, China, [3]Department of Dermatology, The Fifth Affiliated Hospital of Jinan University, Heyuan, China, [4]Department of Infectious Diseases and Public Health, Jockey Club College of Veterinary Medicine and Life Sciences, City University of Hong Kong, Hong Kong, Hong Kong SAR, China, [5]Department of Dermatology, University Hospital Macau, Macau, Macao SAR, China, [6]General Surgery Breast Medical Center, Taipei Medical University Hospital, Taipei City, China, [7]Primax Biotech Company, Hong Kong, Hong Kong SAR, China, [8]Department of Clinical Research, The First Affiliated Hospital of Jinan University, Guangzhou, China

Introduction: This study aimed to develop and validate a nomogram for predicting cancer-specific survival (CSS) in patients with non-keratinized large cell squamous cell carcinoma (NKLCSCC) at 3, 5, and 8 years after diagnosis.

Methods: Data on SCC patients were collected from the Surveillance, Epidemiology, and End Results database. Training (70%) and validation (30%) cohorts were generated using random selection of patients. Independent prognostic factors were selected using the backward stepwise Cox regression model. To predict the CSS rates in patients with NKLCSCC at 3, 5, and 8 years after diagnosis, all of the factors were incorporated into the nomogram. Indicators such as the concordance index (C-index), area under the time-dependent receiver operating characteristic curve (AUC), net reclassification index (NRI), integrated discrimination improvement (IDI), calibration curve, and decision-curve analysis (DCA) were then used to validate the performance of the nomogram.

Results: This study included 9,811 patients with NKLCSCC. Twelve prognostic factors were identified by Cox regression analysis in the training cohort, which were age, number of regional nodes examined, number of positive regional nodes, sex, race, marital status, American Joint Committee on Cancer (AJCC) stage, surgery status, chemotherapy status, radiotherapy status, summary stage, and income. The constructed nomogram was validated both internally and externally. The nomogram had good discrimination ability, as indicated by the comparatively high C-indices and AUC values. The nomogram was properly calibrated, as indicated by the calibration

curves. Our nomogram was superior to the AJCC model, as illustrated by its superior NRI and IDI values. DCA curves indicated the clinical usability of the nomogram.

Conclusion: The first nomogram for prognosis predictions of patients with NKLCSCC has been developed and verified. Its performance and usability demonstrated that the nomogram could be utilized in clinical settings. However, additional external verification is still required.

KEYWORDS

Surveillance, Epidemiology, and End Results, cancer-specific survival, nomogram, non-keratinizing large cell squamous cell carcinoma, SEER

Introduction

Cutaneous squamous cell carcinoma (cSCC) is the second most common type of non-melanoma skin cancer. It accounts for 20% of skin cancers, with 1 million cases and an estimated 9,000 deaths each year in the United States (1). The reported incidence of cSCC ranges from 5 to 499 per 100,000 patients (2–5). Among the non-Hispanic white population in the United States, the lifetime risk of developing SCC is 14–20% (6, 7). This risk has continued to increase each year, with an estimated increase of between 50 and 200%, and is likely to continue to increase due to the aging population (8). However, the current understanding of non-keratinized large cell squamous cell carcinoma (NKLCSCC) of the skin is inadequate, and its increasing incidence and distinct characteristics from other types of squamous cell carcinoma require it to be independently analyzed.

Some researchers have proposed that the most significant risk factors for cSCC include age, sex, race, and surrounding environment (9), but there is currently no definite prognostic implication for the subtypes of cSCC. The present study addressed the postoperative recurrence of NKLCSCC, which is one of the most common subtypes of squamous cell carcinoma.

A fundamental standard of care for cancer treatment is the standard American Joint Committee on Cancer (AJCC) staging system. But when used to predict the prognosis of NKLCSCC, the AJCC staging system is restricted by the lack of precise demographic and clinical characteristics. Providing clinicians with convenient and thorough guidance requires more detailed and extensive prediction models.

Nomograms are highly accurate and easy-to-use tools that are based on many types of tumor prediction models (10) and make it possible to estimate the survival probability of a specific patient. Many researchers have established nomograms for various cancers, including of the tonsils, parotid gland, and breast (11–13), but no nomogram specifically designed for NKLCSCC has been developed. Therefore we developed and evaluated a nomogram for NKLCSCC using pertinent data from the Surveillance, Epidemiology, and End Results (SEER) database to further investigate the prognosis factors for NKLCSCC and its specific treatment.

We aimed to develop a comprehensive nomogram for patients with NKLCSCC in the SEER database that accounted for key demographics, clinicopathological features, and therapeutic approaches in addition to some fundamental traits. We analyzed the treatments applicable to these patients. Our novel nomogram can provide clinicians with more-thorough and personalized patient survival predictions, which makes it clinically superior to conventional methods.

Patients and methods

Data sources and research factors

Data were filtered and extracted from the SEER database using SEER*Stat software. Part of the SEER database is available to the public, and we requested additional access to the SEER Plus database (14). We collected NKLCSCC cases from the SEER database by adopting the ICD-O-3 (third revision of the International Classification of Diseases for Oncology) histology/behavior code for NKLCSCC ("8072/3: Squamous cell carcinoma, large cell, non-keratinizing, NOS") and the cases where the site was cutaneous were selected.

We selected several factors that may be relevant to disease prognosis, including age, race, sex, marital status, tumor grade, AJCC stage, income, number of regional nodes examined (RNE), number of positive regional nodes (RNP), summary stage, surgery status, radiotherapy status, and chemotherapy status. Tumor extension, lymph node metastasis, and distant metastasis as assessed using the TNM (tumor, node, and metastasis) staging system are all included in the AJCC staging system. Due to substantial multicollinearity caused by including all of these factors in the analysis, this study only used the AJCC staging system. Cancer-specific survival (CSS) was the outcome variable. Since the SEER database used in this study did not contain any personally identifying information, it was not necessary to obtain patient-informed permission.

The data of patients whose baseline and survival data were fully available were selected. The seventh edition of the AJCC staging system was adopted. Using the methods described above, we initially identified 20,839 patients with NKLCSCC between 2000 and 2015. After excluding 178 patients with unknown race, 1,162 with unknown marital status, and 9,678 with unknown AJCC stage, 9,811 NKLCSCC patients were finally included (15). These patients were randomly divided into training (70%) and validation (30%) cohorts to test the model using R software (version 4.2.0[1]). **Figure 1** illustrates the data screening process.

Nomogram and statistical analysis

A log-rank test performed after assigning all subjects to the training and validation cohorts indicated no statistically significant differences between them. The initial baseline characteristics of

1 http://www.r-project.org

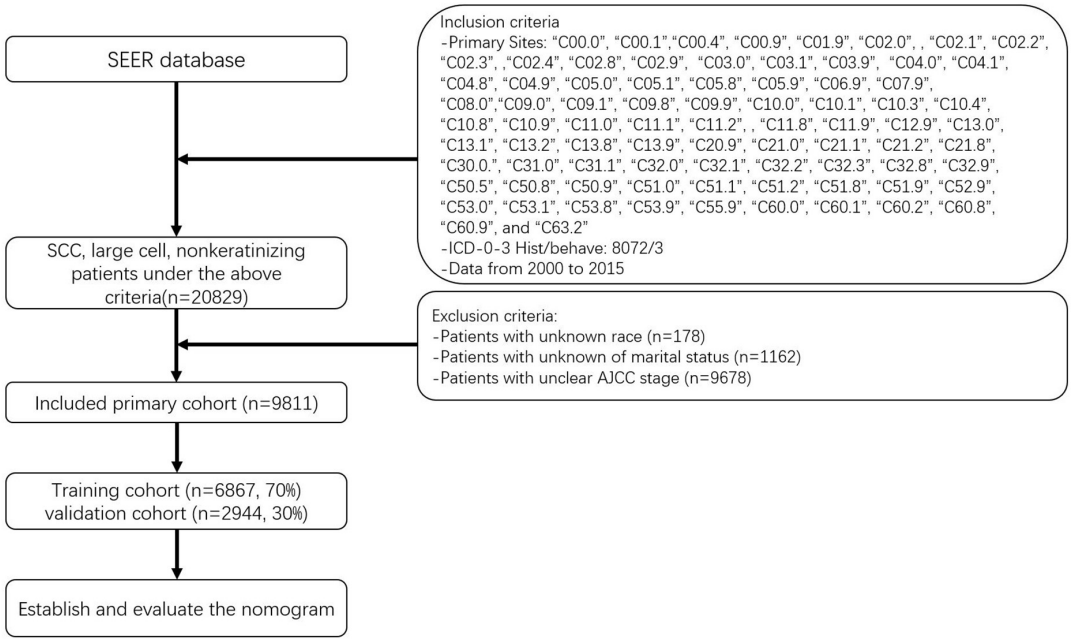

FIGURE 1
Flowchart of sample selection.

each variable in the study cohort were then summarized using SPSS Statistics software (version 27.0, IBM SPSS, Chicago, IL, United States). Other variable data were presented as frequencies and percentages, while age at diagnosis was expressed as median and interquartile range (IQR) values. Nomograms were utilized to estimate the 3-, 5-, and 8-year CSS probabilities for NKLCSCC, and Cox regression was conducted to identify CSS factors related to NKLCSCC, with a significance cut-off of $p = 0.05$. After constructing the nomogram, we evaluated the model using a set of metrics. Two metrics were used to evaluate the discrimination capability of the nomogram: the concordance index (C-index) and the area under the time-dependent receiver operating characteristic (ROC) curve (AUC). Although AUC and C-index are often utilized, their improvements were not significant relative to the existing model. To ascertain if the new model was superior, we additionally used two relatively new metrics: net reclassification index (NRI) and integrated discriminant improvement (IDI). IDI accounts for numerous tangents that can be utilized to assess the overall performance of the model, and NRI is primarily used to evaluate the prediction capacity of old and new models at a certain tangent level (16, 17). These two markers are better understood in actual clinical applications.

A calibration plot was also constructed to graphically display the variation between the two values. The level of model calibration indicates the consistency of predicted and actual values. When the calibration curve is aligned with the 45° standard line, model consistency has advanced. Decision-curve analysis (DCA) curves were employed to evaluate the clinical validity of the model. The abscissa and ordinate of the DCA curve represent the threshold probability and net profit of the model, respectively. The net profit of a model will be higher if the DCA curve is higher (18).

The R software and SPSS Statistics were used to conduct all statistical analyses. SPSS Statistics were used to characterize the fundamental features of the cohort. R software was then used to randomly divide the data into training and validation cohorts, and a log-rank test was conducted. The following R software packages were used: survival, rms, foreign, survival, survivalROC, nricens, and DCA. These analyses included Cox regression analysis, proportional-hazards regression, nomogram establishment, and assessment. Significance was defined as two-sided probability values of $p < 0.05$.

Results

General characteristics

After randomizing 9,811 patients into two cohorts, the log-rank test obtained a probability value ($p = 1$) that indicated no significant differences between them. The fundamental demographic and clinical characteristics of the two cohorts were then described using SPSS (Table 1). The median age at diagnosis was 57 years (IQR = 48–66 years) in the training cohort and 57 years (IQR = 48–65 years) in the validation cohort. The distributions of sex and surgery status were fairly even. Most patients in both the training and validation cohorts were white (78.8 and 79.8%, respectively) and married (56.8 and 55.1%). AJCC stage IV was observed in most cases. Most patients were in the regional cancer summary stage. Most patients were treated with radiotherapy, chemotherapy, and earned US$ 60,000–74,999 per year.

Constructing a nomogram using the training cohort

Age at diagnosis, RNE, RNP, sex, race, marital status, AJCC stage, surgery status, chemotherapy status, radiotherapy status, summary

TABLE 1 Demographic and clinical characteristics of the two cohorts of patients.

Variable	Training cohort (%)	Validation cohort (%)
N	6,867	2,944
Age of diagnosis	57 (48–66)	57 (48–65)
Sex		
Male	3,389 (49.4)	1,483 (50.4)
Female	3,478 (50.6)	1,461 (49.6)
Race		
White	5,413 (78.8)	2,349 (79.8)
Black	647 (9.4)	247 (8.4)
Other	807 (11.8)	348 (11.8)
Marital status		
Single	1,502 (21.9)	655 (22.2)
Married	3,901 (56.8)	1,623 (55.1)
DSW	1,464 (21.3)	666 (22.6)
AJCC stage		
I	1,484 (21.6)	610 (20.7)
II	904 (13.2)	396 (13.5)
III	1,583 (23.1)	697 (23.7)
IV	2,896 (42.2)	1,241 (42.2)
Summary of stage		
Localized	1,727 (25.1)	723 (24.6)
Regional	3,763 (54.8)	1,632 (55.4)
Distant	1,377 (20.1)	589 (20)
Radiation		
Yes	5,318 (77.4)	2,257 (76.7)
No/unknown	1,549 (22.6)	687 (23.3)
Chemotherapy		
Yes	4,381 (63.8)	1,868 (63.5)
No/unknown	2,486 (36.2)	1,076 (26.5)
Income		
<$35,000, $35,000–$44,999	542 (7.9)	237 (8.1)
$45,000–$59,999	1,456 (21.2)	615 (20.9)
$60,000–$74,999	2,888 (42.1)	1,283 (43.6)
$75,000+	1,981 (28.8)	809 (27.5)
Surgery		
Yes	3,166 (46.1)	1,367 (46.4)
No/unknown	3,701 (53.1)	1,577 (53.6)

stage, and income were the 12 variables that were included after performing multivariate Cox stepwise regression ($p < 0.05$). Table 2 lists the factors that were found to be significant following the multivariate Cox regression analysis, which were age at diagnosis (hazard ratio [HR] = 1.031, $p < 0.0001$), RNE (HR = 0.997, $p < 0.0001$), RNP (HR = 1.003, $p < 0.0001$), sex (HR = 1.237, $p < 0.0001$), black race (versus white: HR = 1.243, $p < 0.0001$), married (versus single: HR = 0.697, $p < 0.0001$), AJCC stage II (versus stage I: HR = 1.429, $p < 0.0001$), AJCC stage III (versus stage I: HR = 1.937, $p < 0.0001$), AJCC stage IV (versus stage I: HR = 2.095, $p < 0.0001$), distant summary stage (versus localized: HR = 2.343, $p < 0.0001$), no/unknown radiotherapy status (versus radiotherapy: HR = 1.702, $p < 0.0001$), no/unknown chemotherapy status (versus chemotherapy: HR = 1.268, $p < 0.0001$), no/unknown surgery status (versus surgery: HR = 1.428, $p < 0.0001$), and income of $75,000+

TABLE 2 Selected variables by multivariate Cox stepwise regression analysis.

	Multivariate analysis		
Variable	HR	95% CI	*p*-Value
Age of diagnosis	1.031	1.028–1.033	<0.0001
RNE	0.997	0.995–0.998	<0.0001
RNP	1.003	1.002–1.004	<0.0001
Sex			
Male	Reference		
Female	1.237	1.154–1.326	<0.0001
Race			
White	Reference		
Black	1.243	1.127–1.371	<0.0001
Other	0.977	0.884–1.08	0.6478
Marital status			
Single	Reference		
Married	0.697	0.644–0.755	<0.0001
DSW	0.998	0.912–1.092	0.9641
AJCC stage			
I	Reference		
II	1.429	1.22–1.674	<0.0001
III	1.937	1.616–2.321	<0.0001
IV	2.095	1.734–2.532	<0.0001
Summary of stage			
Localized	Reference		
Regional	1.163	0.995–1.359	0.0572
Distant	2.343	1.968–2.79	<0.0001
Radiation			
Yes	Reference		
No/unknown	1.702	1.554–1.865	<0.0001
Chemotherapy			
Yes	Reference		
No/unknown	1.268	1.167–1.379	<0.0001
Income			
<$35,000, $35,000–$44,999	Reference		
$45,000–$59,999	0.891	0.791–1.004	0.0573
$60,000–$74,999	0.823	0.736–0.919	0.0006
$75,000+	0.738	0.655–0.831	<0.0001
Surgery			
Yes	Reference		
No/unknown	1.428	1.317–1.547	<0.0001

per year (versus <US$ 35,000 and US$ 35,000–44,999: HR = 0.738, $p < 0.0001$).

The finally constructed nomogram is shown in Figure 2. Based on the relevant factors stated above, the multiple regression model of the nomogram may be utilized to predict CSS probabilities. According to Figure 2, the summary stage had the greatest effect on survival rate, followed by AJCC stage, radiotherapy status, surgery status, chemotherapy status, race, sex, age at diagnosis, RNP, marital status, and income. Each component is represented as a line segment on the nomogram, and the numerical scale of the line defines the risk level presented by that factor. The sum of the scores for all of the criteria for each patient produces a total score that corresponds to their 3-, 5-, and 8-year CSS probabilities.

Evaluating the nomogram using the validation cohort

The C-index in the nomogram model was 0.710 for the training cohort and 0.725 for the validation cohort. The C-index for AJCC training cohort is 0.595, and validation cohort is 0.599. The new model's C-index outranks the AJCC for training cohort by 0.115, and for validation cohort by 0.126. The AUCs at years 3, 5, and 8 were 0.739, 0.732, and 0.745, respectively, for the training cohort, and 0.766, 0.751, and 0.759 for the validation cohort (Figure 3).

The discrimination ability of the nomogram was evaluated using the NRI and IDI. The NRI values for the 3-, 5-, and 8-year CSS probabilities were 0.568 (95% confidence interval [CI] = 0.514–0.625), 0.581 (95% CI = 0.542–0.630), and 0.625 (95% CI = 0.587–0.682), respectively, for the training cohort, and 0.708 (95% CI = 0.623–0.796), 0.689 (95% CI = 0.612–0.762), and 0.748 (95% CI = 0.666–0.817) for the validation cohort. The IDI values for the 3-, 5-, and 8-year CSS probabilities were 0.125, 0.142, and 0.151, respectively, for the training cohort ($p = 0.001$), and 0.152, 0.158, and 0.168 for the validation cohort ($p = 0.001$).

In order to test between the real and ideal values of the model, the calibration plot was first utilized to confirm the discrimination ability of the model. The calibration plots of 3-, 5-, and 8-year CSS probabilities in the model were very close to the standard line (Figure 4), demonstrating that it had a high level of calibration.

Finally, a DCA curve was drawn to demonstrate the clinical validity of the nomogram. The survival probability curves for the new model were all higher than those for the AJCC model (Figure 5), indicating that using the new method to predict 3-, 5-, and 8-year CSS probabilities is superior overall.

Discussion

The newest guideline by the American Academy of Dermatology in 2018 paid more attention to individual factors in assessing NKLCSCC (19). Other classifications focus on molecular and immunohistochemical information, and biopsy techniques (20, 21). However, these current guidelines do not provide definite prognostic predictions for NKLCSCC. This study was therefore designed to analyze the combined prognostic factors for NKLCSCC in detail for

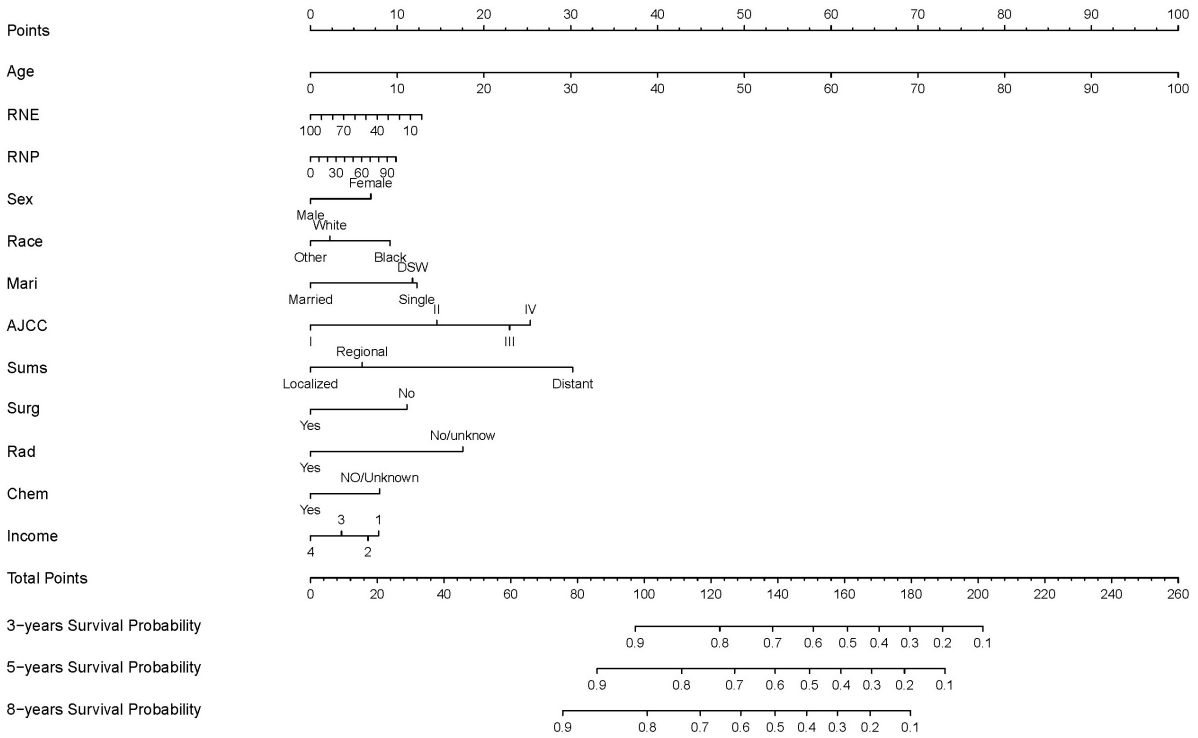

FIGURE 2
Nomogram predicting 3-, 5-, and 8-years CSS probability. Mari, marital status; Sums, summary of stage; Surg, surgery status; Rad, radiotherapy status; Chem, chemotherapy status; DSW, divorced, spereated, or widowed; income 1: <$35,000, $35,000–$44,999; income 2, $45,000–$59,999; income 3, $60,000–$74,999; income 4, $75,000+.

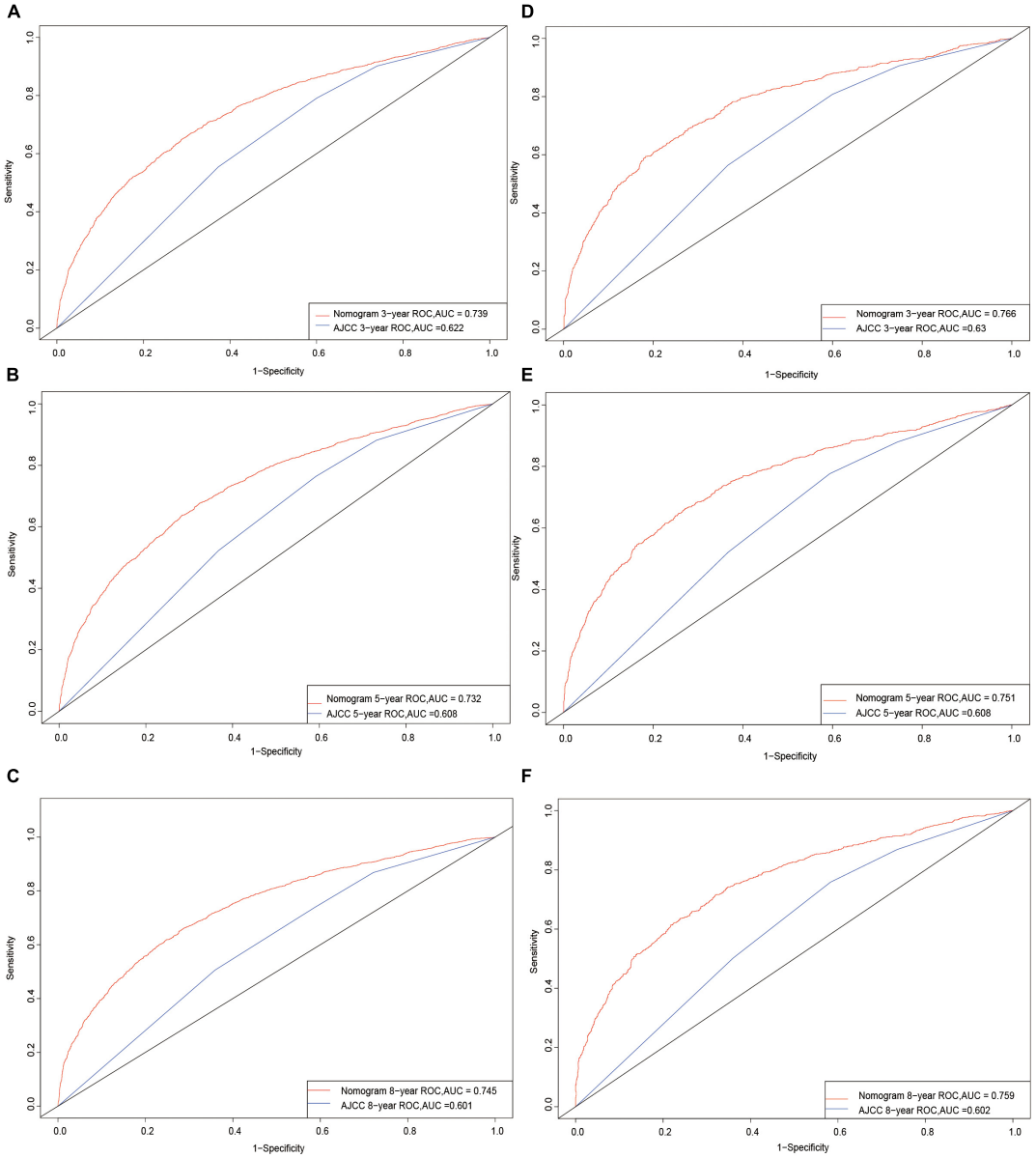

FIGURE 3
Receiver operating characteristic curves. The area under the ROC curve (AUC) for 3-, 5-, and 8-year CSS probability of the training cohort **(A–C)** and validation cohort **(D–F)**.

the first time. Most of the published research studies have considered prognosis factors as an independent item (19, 21). Although most cSCCs can be successfully eradicated by surgical resection, cSCCs are somewhat characterized by high probabilities of recurrence, metastasis, and death. cSCC is most common in Caucasians and is more common in males than in females (with a 3:1 ratio) (22). Incidence increases with age, with an average age at diagnosis in the mid-60s (23), which differs from our results. All of these attributes indicate the need to develop a clinical prediction nomogram specific to NKLCSCC to assist doctors in making informed decisions. We were successful in creating a predictive nomogram that utilized the SEER database based on an integrated examination of demographic and clinicopathological factors. We then ascertained if the new model was superior to the AJCC staging system by comparing them.

The Cox regression results included in the nomogram indicate that besides summary stage, AJCC stage was the factor with the strongest effect on CSS probability. This was mostly due to the AJCC staging system including information on regional lymph node and distant metastases, which are very important prognostic factors in NKLCSCC (24). Summary stage as a factor only represents the metastasis of the patient, which had the highest HR. Among demographic characteristics, age has always been an important prognostic factor for tumors, and the present results were no exception. Black race also presented a worse prognosis than white or other race, and being married had a better prognosis than being single or divorced, separated, or widowed (DSW), which was consistent with the findings of other studies (25, 26).

While the incidence of NKLCSCC was previously found to be higher in males than in females (27), the sex distribution in the present study was relatively even. A particularly interesting aspect of this study was that previous studies have not investigated the impact of marital status on NKLCSCC prognosis; this study found

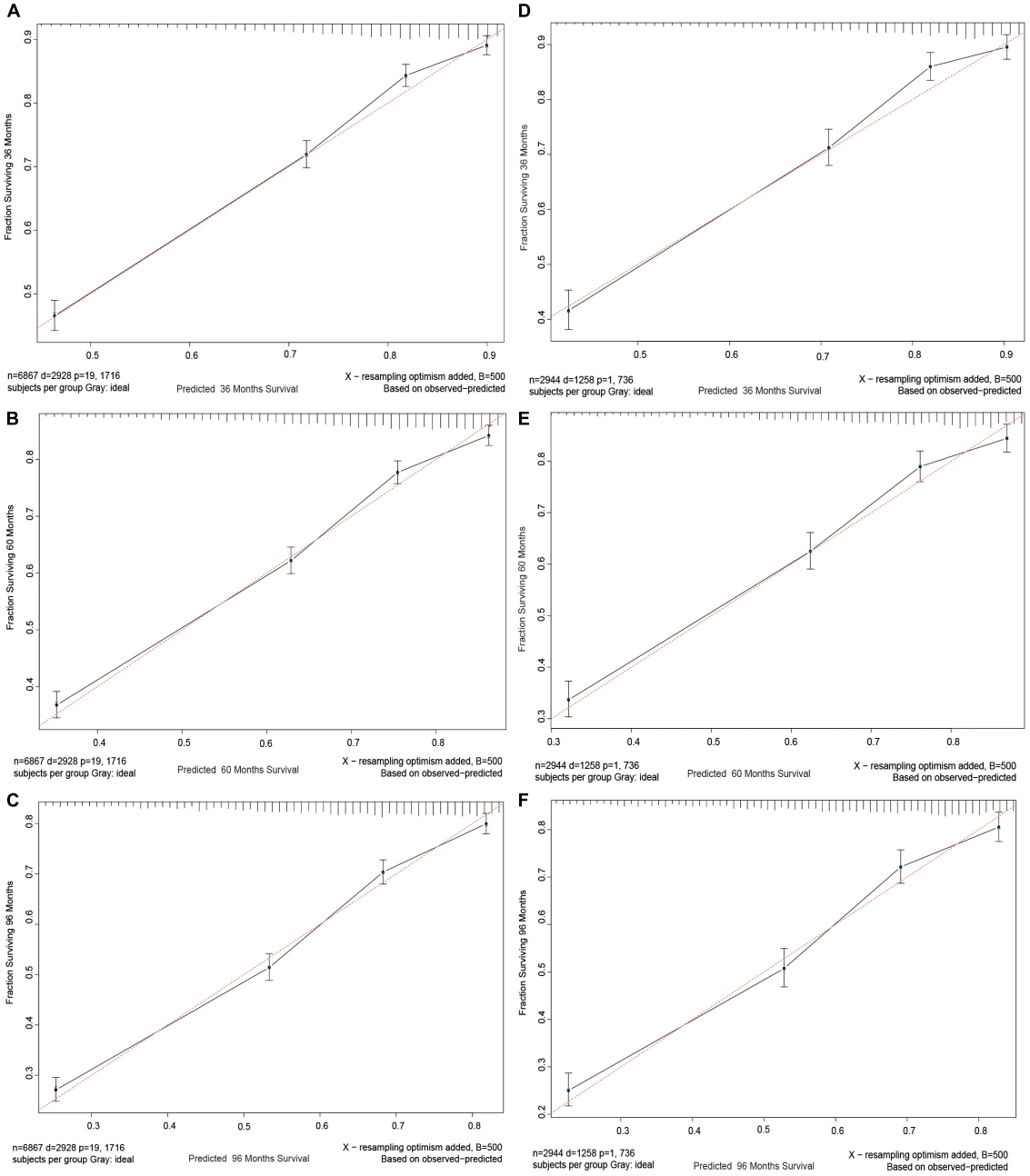

FIGURE 4
Calibration curves. Calibration curves for 3-, 5-, and 8-years CSS probability depict the calibration of each model in terms of the agreement between the predicted probabilities and observed outcomes of the training cohort **(A–C)** and validation cohort **(D–F)**.

that being single or DSW were risk factors for the prognosis. Regarding clinicopathological features, AJCC staging is known to influence treatment selection, outcome, and prognosis. We found that summary stage significantly affected the NKLCSCC CSS probability in a similar way to RNP, and a larger RNP increased the effect on the prognosis. As can be seen from Figure 2, surgery, radiotherapy, and chemotherapy treatments were also significant prognostic factors.

Prior to actually applying the model, we performed a number of assessments that are essential for clinical prediction models after constructing the nomogram and accounting for the indicated prognostic factors. First, we verified the discrimination ability of the model. The conventional ROC curve is a simple approach (28), and Figure 3 displays a nomogram with an AUC of >0.7. This illustrates the good overall discrimination capability of the nomogram. Comparing the ROC of the new model with that of the AJCC model also revealed that the new model outperformed it. Second, the C-index is a more generalized measure of the discrimination ability of prediction models between different outcomes for survival data (29). The current findings further demonstrate the outstanding discrimination ability of our new model. NRI is frequently used to compare the accuracy of the predictive capability of two models, and in contrast to AUC and the C-index, it quantifies the number of subjects correctly

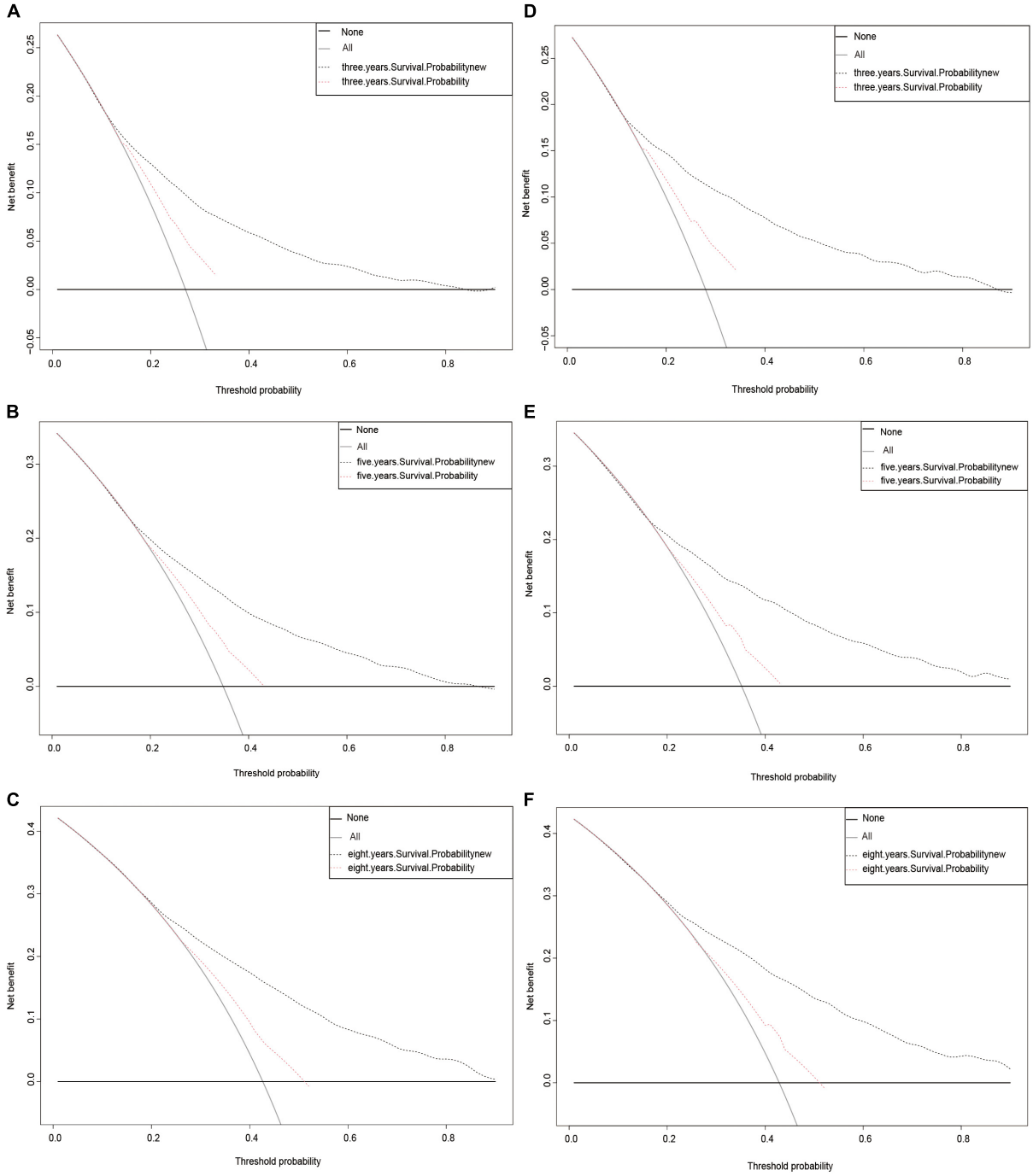

FIGURE 5
Decision curve analysis curves. Decision curve analysis of the training cohort **(A–C)** and validation cohort **(D–F)** for 3-, 5-, and 8-years CSS probability.

characterized by two models at a given set of cut-off points (30). In the training cohort, NRI values indicated increases in the proportion of correctly classifying CSS probabilities at 3, 5, and 8 years of 56.8, 58.1, and 62.4%, respectively, while those for the validation cohort were 70.8, 68.9, and 74.8% (p = 0.001). IDI is another metric that accounts for different cut-off points and can be used to reflect the overall improvement of a model, complementing NRI to a certain extent (31). The present IDI values demonstrated that, when compared with the AJCC model, the new model had better predictive power for 3-, 5-, and 8-year CSS probabilities by 12.5, 14.2, and 15.1% in the training cohort, respectively, and by 15.2, 15.8, and 16.8% in the validation cohort (p = 0.001).

The aforementioned four indicators unmistakably demonstrate the strong discrimination ability of the nomogram and that the model is capable of accurately predicting the survival rate of patients with NKLCSCC. We also drew calibration plots to assess the calibration accuracy of the model. In Figure 4, the calibration curve of the model demonstrates a uniform distribution and is fairly near to the standard line. This suggested that the model-predicted incidence was very close to the actual incidence, indicating that the model has good conformity. The model demonstrated a good performance level

for estimating 3-, 5-, and 8-year CSS probabilities in patients with NKLCSCC when combined with the examination of discrimination and calibration abilities.

Finally, we assessed how effectively the model performed in healthcare situations. DCA is increasingly being used by researchers to evaluate the overall value of medical treatments for patients (17, 32). Our new approach had a better overall net benefit than the AJCC staging system and greater tolerance of survival probability, as seen in **Figure 5**. This indicates that the new model will provide patients with a greater overall benefit and assist physicians in making more informed treatment decisions.

Naturally, there were certain limitations to this study. First, we used the SEER database to collect analytic data in a retrospective manner, which could have induced some information bias. Second, several genetic markers, biomarkers, behavioral patterns, and other characteristics were not included in the study. Future cohort studies should more precisely pinpoint key prognostic markers and concentrate on including more prognostic factors and evaluating the model in external cohorts to provide more accurate findings.

Conclusion

Based on a reasonably large retrospective population, we have developed the first nomogram for predicting 3-, 5-, and 8-year CSS probabilities in patients with NKLCSCC. This nomogram incorporates demographic and clinicopathological characteristics, and thorough validation and assessment make this model helpful and simple for doctors to utilize when making clinical decisions for specific patients. It was also demonstrated to provide beneficial recommendations. In the future, we hope to construct more-thorough nomograms based on a larger variety of data sources.

Data availability statement

Publicly available datasets were analyzed in this study. This data can be found here: SEER database.

Ethics statement

Approximately 34.6% of the U.S. population is represented in the population-based cancer registries used by SEER to gather data on cancer incidence. Each spring, based on information provided by the registry in November of the previous year, SEER releases a standardized set of research data. The database utilized for this study did not contain any personal identities and only comprised publically available data, therefore institutional review board permission was not necessary. These were acquired *via* the SEER*Stat software after receiving further clearances.

Author contributions

All authors listed have made a substantial, direct, and intellectual contribution to the work, and approved it for publication.

Conflict of interest

KC was employed by the Biotech Company.

The remaining authors declare that the research was conducted in the absence of any commercial or financial relationships that could be construed as a potential conflict of interest.

Publisher's note

References

1. Waldman A, Schmults C. Cutaneous squamous cell carcinoma. *Hematol Oncol Clin North Am.* (2019) 33:1–12. doi: 10.1016/j.hoc.2018.08.001

2. Staples M, Elwood M, Burton R, Williams J, Marks R, Giles G. Non-melanoma skin cancer in Australia: the 2002 national survey and trends since 1985. *Med J Austr.* (2006) 184:6–10. doi: 10.5694/j.1326-5377.2006.tb00086.x

3. Nguyen K, Han J, Li T, Qureshi A. Invasive cutaneous squamous cell carcinoma incidence in US health care workers. *Arch Dermatol Res.* (2014) 306:555–60. doi: 10.1007/s00403-014-1469-3

4. Brewster D, Bhatti L, Inglis J, Nairn E, Doherty V. Recent trends in incidence of nonmelanoma skin cancers in the East of Scotland, 1992-2003. *Br J Dermatol.* (2007) 156:1295–300. doi: 10.1111/j.1365-2133.2007.07892.x

5. Andersson E, Paoli J, Wastensson G. Incidence of cutaneous squamous cell carcinoma in coastal and inland areas of Western Sweden. *Cancer Epidemiol.* (2011) 35:e69–74. doi: 10.1016/j.canep.2011.05.006

6. Miller D, Weinstock M. Nonmelanoma skin cancer in the United States: incidence. *J Am Acad Dermatol.* (1994) 30:774–8. doi: 10.1016/S0190-9622(08)81509-5

7. Stern R. Prevalence of a history of skin cancer in 2007: results of an incidence-based model. *Arch Dermatol.* (2010) 146:279–82. doi: 10.1001/archdermatol.2010.4

8. Muzic J, Schmitt A, Wright A, Alniemi D, Zubair A, Olazagasti Lourido J, et al. incidence and trends of basal cell carcinoma and cutaneous squamous cell carcinoma: a population-based study in Olmsted County, Minnesota, 2000 to 2010. *Mayo Clin Proc.* (2017) 92:890–8. doi: 10.1016/j.mayocp.2017.02.015

9. Ildstad S, Tollerud D, Bigelow M, Remensnyder JP. A multivariate analysis of determinants of survival for patients with squamous cell carcinoma of the head and neck. *Ann Surg.* (1989) 209:237–41. doi: 10.1097/00000658-198902000-00016

10. Balachandran V, Gonen M, Smith J, DeMatteo R. Nomograms in oncology: more than meets the eye. *Lancet Oncol.* (2015) 16:e173–80. doi: 10.1016/S1470-2045(14)71116-7

11. Li C, Yang J, Zheng S, Xu F, Han D, Bai L, et al. Establishment and validation of a nomogram for tonsil squamous cell carcinoma: a retrospective study based on the SEER database. *Cancer Control.* (2020) 27:1073274820960481. doi: 10.1177/1073274820960481

12. Xu F, Feng X, Zhao F, Huang Q, Han D, Li C, et al. Competing-risks nomograms for predicting cause-specific mortality in parotid-gland carcinoma: a population-based analysis. *Cancer Med.* (2021) 10:3756–69. doi: 10.1002/cam4.3919

13. Xu F, Yang J, Han D, Huang Q, Li C, Zheng S, et al. Nomograms for estimating cause-specific death rates of patients with inflammatory breast cancer: a competing-risks analysis. *Technol Cancer Res Treat.* (2021) 20:15330338211016371. doi: 10.1177/15330338211016371

14. Yang J, Li Y, Liu Q, Li L, Feng A, Wang T, et al. Brief introduction of medical database and data mining technology in big data era. *J Evid Based Med.* (2020) 13:57–69. doi: 10.1111/jebm.12373

15. Wu W, Li Y, Feng A, Li L, Huang T, Xu A, et al. Data mining in clinical big data: the frequently used databases, steps, and methodological models. *Milit Med Res.* (2021) 8:44. doi: 10.1186/s40779-021-00338-z

16. Parikh C, Coca S, Thiessen-Philbrook H, Shlipak M, Koyner J, Wang Z, et al. Postoperative biomarkers predict acute kidney injury and poor outcomes after adult cardiac surgery. *J Am Soc Nephrol.* (2011) 22: 1748–57.

17. Steyerberg E, Vickers A, Cook N, Gerds T, Gonen M, Obuchowski N, et al. Assessing the performance of prediction models: a framework for traditional and novel measures. *Epidemiology.* (2010) 21:128–38.

18. Vickers A, Cronin A, Elkin E, Gonen M. Extensions to decision curve analysis, a novel method for evaluating diagnostic tests, prediction models and molecular markers. *BMC Med Inform Decis Mak.* (2008) 8:53. doi: 10.1186/1472-6947-8-53

19. Kim J, Kozlow J, Mittal B, Moyer J, Olenecki T, Rodgers P. Guidelines of care for the management of cutaneous squamous cell carcinoma. *J Am Acad Dermatol.* (2018) 78:560–78.

20. Farberg A, Goldenberg G. New guidelines of care for the management of nonmelanoma skin cancer. *Cutis.* (2018) 101:319–21.

21. Newlands C, Currie R, Memon A, Whitaker S, Woolford T. Non-melanoma skin cancer: United Kingdom national multidisciplinary guidelines. *J Laryngol Otol.* (2016) 130:S125–32. doi: 10.1017/S0022215116000554

22. Que S, Zwald F, Schmults C. Cutaneous squamous cell carcinoma: incidence, risk factors, diagnosis, and staging. *J Am Acad Dermatol.* (2018) 78: 237–47.

23. Xiang F, Lucas R, Hales S, Neale R. Incidence of nonmelanoma skin cancer in relation to ambient UV radiation in white populations, 1978-2012: empirical relationships. *JAMA Dermatol.* (2014) 150:1063–71. doi: 10.1001/jamadermatol.2014.762

24. Karia P, Morgan F, Califano J, Schmults C. Comparison of tumor classifications for cutaneous squamous cell carcinoma of the head and neck in the 7th vs 8th edition of the AJCC cancer staging manual. *JAMA Dermatol.* (2018) 154:175–81. doi: 10.1001/jamadermatol.2017.3960

25. Yang J, Pan Z, Zhao F, Feng X, Liu Q, Li Y, et al. A nomogram for predicting survival in patients with nodular melanoma: a population-based study. *Medicine.* (2019) 98:e16059. doi: 10.1097/MD.0000000000016059

26. Yin T, Zhao Y, Yang Y, Xu H, Zheng D, Lyu J, et al. Nomogram for predicting overall survival in acral lentiginous melanoma: a population-based study. *Int J Gen Med.* (2021) 14:9841–51. doi: 10.2147/IJGM.S336443

27. Vazquez A, Khan M, Govindaraj S, Baredes S, Eloy J. Nasopharyngeal squamous cell carcinoma: a comparative analysis of keratinizing and nonkeratinizing subtypes. *Int Forum Allergy Rhinol.* (2014) 4:675–83.

28. Hanley J, McNeil BJ. A method of comparing the areas under receiver operating characteristic curves derived from the same cases. *Radiology.* (1983) 148:839–43.

29. Wang Y, Li J, Xia Y, Gong R, Wang K, Yan Z, et al. Prognostic nomogram for intrahepatic cholangiocarcinoma after partial hepatectomy. *J Clin Oncol.* (2013) 31: 1188–95.

30. Iki M, Fujita Y, Tamaki J, Kouda K, Yura A, Sato Y, et al. Trabecular bone score may improve FRAX® prediction accuracy for major osteoporotic fractures in elderly Japanese men: the fujiwara-kyo osteoporosis risk in men (FORMEN) cohort study. *Osteoporos Int.* (2015) 26:1841–8. doi: 10.1007/s00198-015-3092-3

31. Chambless L, Cummiskey C, Cui G. Several methods to assess improvement in risk prediction models: extension to survival analysis. *Stat Med.* (2011) 30:22–38.

32. Vickers A, van Calster B, Steyerberg EW. A simple, step-by-step guide to interpreting decision curve analysis. *Diagn Progn Res.* (2019) 3:18. doi: 10.1186/s41512-019-0064-7

frontiers | Frontiers in Medicine

TYPE Review
PUBLISHED 13 March 2023
DOI 10.3389/fmed.2023.1090168

OPEN ACCESS

EDITED BY
Darius Mehregan,
Wayne State University,
United States

REVIEWED BY
Christoffer Gebhardt,
University Medical Center Hamburg-Eppendorf,
Germany
Motoki Nakamura,
Nagoya City University,
Japan

*CORRESPONDENCE
Roman Groisberg
✉ roman.groisberg@rutgers.edu

†These authors have contributed equally to this work and share first authorship

SPECIALTY SECTION
This article was submitted to Dermatology, a section of the journal Frontiers in Medicine

RECEIVED 05 November 2022
ACCEPTED 21 February 2023
PUBLISHED 13 March 2023

CITATION
Guan L, Palmeri M and Groisberg R (2023) Cutaneous angiosarcoma: A review of current evidence for treatment with checkpoint inhibitors.
Front. Med. 10:1090168.
doi: 10.3389/fmed.2023.1090168

Cutaneous angiosarcoma: A review of current evidence for treatment with checkpoint inhibitors

Lucy Guan†, Marisa Palmeri† and Roman Groisberg*

Department of Medicine, Rutgers Cancer Institute of New Jersey, Robert Wood Johnson Medical School, Rutgers University, New Brunswick, NJ, United States

Cutaneous angiosarcoma (cAS) is a rare and aggressive subtype of soft tissue sarcoma with poor prognosis and suboptimal treatment options. Clinical presentation is variable, but cAS often arises from the head and neck. The most widely accepted current approach, surgical excision with adjuvant radiotherapy, is associated with high recurrence rates and can leave patients with profound disfigurement. Chemotherapy and targeted therapy alternatives have had limited success. Thus, there is a significant unmet need to address the absence of durable treatments for advanced and metastatic cAS. Like melanoma and cutaneous squamous cell carcinoma, tumor types with known response to immunotherapy, cAS harbors immune biomarkers, such as tumor mutational burden high (TMB-H), PD-L1 positivity, ultraviolet signature expression, and tertiary lymphoid structures. While data on the use and efficacy of immunotherapy in cAS is limited, the biomarkers suggest a promising advancement in future treatment options. This review aims to summarize and discuss current data from case reports, case series, retrospective studies and clinical trials regarding immunotherapy treatment and outcomes for cAS.

KEYWORDS

cutaneous angiosarcoma, immunotherapy, checkpoint inhibition/blockade, anti-PD-1 immunotherapy, anti-PD-L1

Introduction

Soft tissue sarcomas (STS), are rare tumors of mesenchymal origin that are made up of over 70 subtypes that vary by tissue of origin, location, histology, immunogenic phenotype, and genomic landscape (1). Angiosarcomas, representing 1 to 2% of all STS, are a heterogeneous and aggressive group of tumors of vascular and lymphatic origin that have the tendency to metastasize to distant visceral sites (2, 3). Cutaneous angiosarcoma (cAS) is the most common form, with the majority of lesions arising from the head and neck (4). Head and neck cAS are associated with advanced age, with a median age of diagnosis of 77, as well as ultraviolet radiation exposure. Overall, the prognosis of patients with cAS is poor, with one analysis indicating a mean 5-year survival rate of 33.5% (3).

For localized cutaneous disease, a combined-modality approach of surgical resection and adjuvant radiotherapy has been the mainstay of treatment despite high recurrence rates. Surgery, however, is contraindicated in many older patients due to age-related comorbidities. Curative radiotherapy has also been reported for local control as local control rates are poor even with resection with wide surgical excision (5). However, due to high distant failure rates and high

radiation doses suggested for improved local control (6), this remains a suboptimal treatment modality. For locally advanced or metastatic disease, the first-line standard of care regimen includes cytotoxic chemotherapy, most commonly taxane or anthracycline-based. Radiotherapy can be used as an adjunct. Efficacy of single agent paclitaxel was confirmed in the Phase II ANGIOTAX study of weekly paclitaxel in metastatic or unresectable AS in which 6 of 30 (20.0%) patients had skin or scalp AS. However, median progression free survival (PFS) and median overall survival (OS) were only 4 months and 8 months, respectively (7). More recent studies such as *Roy et al*, which evaluated non-metastatic cAS patients specifically, have shown an overall survival (OS) benefit for concurrent paclitaxel-based chemotherapy and radiotherapy (8). Additionally, radiotherapy with rIL-1 immunotherapy has also been shown to provide improved distant metastasis-free survival rates in patients with angiosarcoma of the scalp (9).

Targeted therapies have also been used in the management of angiosarcomas. Vascular endothelial growth factor (VEGF), which is upregulated in angiosarcoma, can be targeted by tyrosine kinase inhibitors such as pazopanib, regorafenib, sorafenib, and anlotinib as well as monoclonal antibodies such as bevacizumab. Pazopanib which is approved as a second-line agent for the treatment of STS appeared to show a signal of activity (10), but a retrospective study by *Kollar et al* reported limited efficacy. Of the 40 AS patients, which included 15 (37.%) patients with cAS, there was a response rate of 20%, median PFS of 3 months, and median OS of 9.9 months (11). In a phase II trial of anlotinib, a multi-kinase inhibitor, 4 patients had cAS and none of them had objective responses (12). Similarly underwhelming results were seen for regorafenib (13), sorafenib (14), and bevacizumab (15). Alternatives are needed to attain more significant and durable treatment responses.

There has been increased interest in immune regulation as a potential therapeutic avenue in sarcoma treatment, prompting investigation of whether anti-programmed cell death protein 1 (PD-1) or ligand (PD-L1) immune checkpoint inhibitors may have a role in treatment. Suggested biomarkers of response to immunotherapy include tumor infiltrating lymphocytes (TILs), PD-L1 expression, microsatellite instability, immunogenic genomic profile, UV signature, inflamed hypermutated tumors, and tertiary lymphoid structures (16). Tumor mutational burden (TMB) high (≥10 mutations/Megabase (Muts/Mb)) and microsatellite instability high (MSI-H) are biomarkers for which pembrolizumab (17), an anti-PD-1 agent, is approved in the tumor-agnostic setting (18, 19). Furthermore, a study by *Honda et al* investigated the association between PD-1/PD-L1 expression and cAS prognosis. Among 106 immunohistochemically studied cAS cases, 30.2% of patients' samples were positive for PD-L1, and 17.9% showed high infiltration of PD-1 positive cells. Univariate analyses revealed a significant relationship between high infiltration of PD-1 positive cells with tumor site PD-L1 expression and favorable survival in stage 1 patients ($p = 0.014$). Regression analyses also revealed that patients with high infiltration of PD-1-positive cells with tumor site PD-L1 expression had an increased likelihood of favorable survival, after adjustment with possible confounders (hazard ratio = 0.38, $p = 0.01$, 95%CI: 0.16–0.86).

Certain biomarkers known to be positive in cAS suggest potential for response to immunotherapy. For instance, in head and neck cAS the median TMB is 20 Muts/Mb (20) and in an analysis of 143 angiosarcomas by *Espejio et al* PD-L1 positivity was seen in 33% of head and neck cAS. Head and neck cAS also harbors similarities to known immune checkpoint inhibitor (ICI) responsive tumor types, such as melanoma and cutaneous squamous cell carcinoma (21). One similarity includes the presence of ultraviolet (UV) mutational signatures, defined as a high number of genomic variations caused by demethylation of cPG islands, which is associated with response to anti-PD-1 agents (22). In an evaluation by *Chan et al*, 9 of 18 head and neck cAS patients had UV mutational signatures (23, 24). Another similarity to melanoma and cSCC includes the predominant immune rich microenvironment of cAS, specifically of the head and neck region, with the presence of high levels of CD8+ TILs (24–28).

Given the lack of durable treatment options for advanced or metastatic cAS, further treatments beyond chemotherapy and targeted therapy are necessary to address this significant unmet need. Data, albeit promising, on the use and efficacy of immunotherapy in cAS is limited. The present review aims to summarize and discuss current data from case reports, case series, retrospective studies and clinical trials regarding immunotherapy treatment and outcomes for cAS.

Clinical studies supporting use of immunotherapy in cAS

There are numerous case reports, case series, retrospective studies and clinical trials that report promising responses to immune checkpoint inhibition in patients with cAS (Table 1). The results are summarized as follows:

Case reports

A case report published by *Sindhu et al* describes a 63-year-old Caucasian man with refractory cAS of the nose who was treated with pembrolizumab after surgical resection and adjuvant chemotherapy with nab-paclitaxel and evofosfamide was insufficient to control his disease (29). Significant disease progression led to development of multiple new hepatic lesions, a jaw mass, and a right tongue mass. Tumor tissue staining revealed positive PD-L1 expression, as measured by >5% of tumor cells staining positive. Off-label treatment with pembrolizumab dosed at 2 mg/kg every 21 days was initiated with concurrent radical excision of jaw soft tissue angiosarcoma. Restaging CT scans during treatment revealed a significant response of the liver lesion. Additional body scans after 1 year revealed further reduction and no new disease.

Hamacher et al. describe a 74-year-old man with left retroauricular cAS who underwent primary resection, radiotherapy to localized disease, and surgical re-resection after locoregional recurrence, including lymph node metastases (30). After complete disappearance of local lesions following 10 cycles of liposomal pegylated doxorubicin (30 to 35 mg/m^2 once every 28 days), he developed multifocal progression in the left submandibular and right temporoparietal region. He then started on second-line chemotherapy of paclitaxel 80 mg/m^2 once per week resulting in partial response of the cutaneous lesions lasting for 4 months. Due to peripheral neuropathy induced by

TABLE 1 Summary of case reports, case series, and completed clinical trials.

Report	Type	#cAS (%)	ORR	Duration of response	PFS	OS	Notes
Sindu et al. (29)	Case report	1 (100)	n/a	Ongoing	n/a	n/a	
Hamacher et al. (30)	Case report	1 (100)	n/a	Ongoing	n/a	n/a	
Florou et al. (31)	Case series	5 (100)	80%	Ongoing in 4 patients, 14 weeks in 1 patient	n/a	n/a	
Rosenbaum et al. (32)	Retrospective study	15 (42.9)	n/a	n/a	cAS, median: 17.9 weeks	cAS: Not reached	
Phase II SWOG S1609 (DART) trial (33)	Study	Head and neck cAS: 5 (31.3)	Head and neck cAS: 60% Overall: 25%	n/a	6 m PFS rate: 38% (95% Cl 20 to 70%)	Overall: Not reached	3 of 5 head and neck cAS patients had a confirmed objective response to treatment. 2 radiation induced breast cAS patients were excluded from this table.
Phase II study of durvalumab plus tremelimumab (NCT02815995) (34)	Study	1 (1.8)	Overall: 12%	n/a	Overall, median: 12.2 weeks	Overall, median: 93.9 weeks	The 1 cAS patient had a partial response and was the only responder of 5 AS patients.
Phase II study of TVEC and pembrolizumab (NCT03069378) (35)	Study	3 (15)	Overall: 35%	Overall: 56.1 weeks	Overall, median: 17.1 weeks	Overall, disease specific survival: 74.6 weeks	Partial response in 2 cAS patients. Both completed 52 weeks of study therapy.

chemotherapy, he then switched to trabectedin 1.5 mg/m^2, which was discontinued due to poor tolerance. During this time, the patient's cutaneous lesions progressed significantly leading to ulcerations with constant bleeding and requiring analgesics. Fourth-line therapy with pazopanib 800 mg/day was initiated; however, there was continued progression and need for weekly red blood cell transfusions. A histopathological examination of the biopsy taken at recurrence revealed expression of PD-L1 on sarcoma cells of 10% of the sections, prompting the patient's care team to initiate treatment with pembrolizumab 2 mg/kg once every 21 days. Within 3 weeks, the patient's lesions had improved significantly; ulcerations had stopped bleeding and as they continued to heal, blood transfusions and analgesic use were discontinued. A good clinical response of all sarcoma lesions was noted after 5 cycles of pembrolizumab, and after an additional 5 cycles, ulcerations had healed completely. The patient had also tolerated pembrolizumab well without clinically relevant toxicities.

Case series and retrospective study

A case series by Florou et al. describes seven total patients, including five patients with chemotherapy-refractory cAS of the head and neck (31). All patients had received prior systemic chemotherapy and, following progression, received 5 to 14 doses of ICI. After 12 weeks of treatment with AGEN1884, an experimental monoclonal IgG1 antibody targeting CTLA-4, one patient with locally advanced cAS of the face had an ongoing complete response, marking the first reported complete response in cAS to anti-CTLA-4 monotherapy. TMB was surprisingly low at only 0.09 muts/mb, which further highlights the need to explore additional biomarkers. A second patient with cAS of the nose progressed through anti-CTLA-4 monotherapy. Another patient with metastatic cAS with lymph node and bone involvement was treated with pembrolizumab with a partial response for 14 weeks followed by ipilimumab/nivolumab with ongoing partial response. This patient had TMB-H of 15 muts/mb. The remaining two patients had multifocal cAS with scalp involvement and were treated with pembrolizumab, resulting in ongoing partial response. One of these patients had TMB of 12 muts/mb, while the other lacked sufficient archived tumor tissue for analysis.

A retrospective analysis of 35 patients with AS, of whom 15 (42.9%) had cAS, treated with ICI-based therapy aimed to clarify patterns of response and identify prognostic or predictive biomarkers (32). The study performed a retrospective analysis of patients treated with various ICI regimens and investigated correlations between clinical benefit, defined as PFS ≥16 weeks, and various clinical characteristics, results of exome and transcriptome sequencing, and immunohistochemical analyses. ICI regimens were categorized as follows: ICI monotherapy (anti-PD-1 or anti-PD-1 therapy alone), ICI combination therapy (anti-CTLA-4 with anti-PD-1 therapy), and ICI plus other (anti-PD-1 or anti-PD-L1 agent plus a novel immunomodulatory therapy). The median PFS was 11.9 (95%CI 7.4 to 31.9) weeks, and about 40% of all patients had PFS of ≥16 weeks. The study found that patients who received ICI in combination with another novel immune modulator had longer survival rates than patients who received either ipilimumab plus nivolumab or ICI monotherapy. This finding further suggests that novel combinatorial

therapies may be more effective in improving outcomes, compared to ICI monotherapy.

Combination immunotherapy

Building upon these cases, series, and retrospective studies, the following trials provide further insight on the utility of combination therapy.

Anti-PD-L1 and anti-CTLA-4 combination therapy

The following two trials have explored the efficacy of combining anti-PD-L1 and anti-CTLA-4 therapies:

An angiosarcoma cohort (cohort 51) was added to the multicenter phase II SWOG S1609 (DART) trial. This was the first prospective trial of immunotherapy in AS, examining dual anti-CTLA-4 and anti-PD-1 blockade with ipilimumab and nivolumab in metastatic or unresectable AS (33). Sixteen AS patients, who had a median age of 68 years, were enrolled. Genomic characterization as part of routine medical care was only available for eight patients, which revealed that all eight patients had at least 2 deleterious genomic alterations, with no two patients having the same set of alterations. One of seven patients whose TMB was analyzed showed high TMB of 24 muts/mb; all others ranged from 0 to 8.4 muts/mb. Of the three patients with available PDL-1 immunohistochemistry, PDL-1 tumor proportion score (TPS) was 0% (arm), 30% (skin of face), and 50% (scalp). Nine patients had cutaneous primary tumors, among which five had primary tumors arising from the face or scalp and four had primary tumors of other sites, including two with radiation-associated cutaneous breast tumors. The remaining seven had non-cutaneous primary tumors. Patients received intravenously nivolumab 240 mg every 2 weeks and ipilimumab 1 mg/kg every 6 weeks. Overall, the objective response rate (ORR) was 25% (95% CI: 9 to 45%), 6-month PFS was 38% (95% CI: 20 to 71%), and 12.5% (2 of 16) experienced grade 3 to 4 serious adverse events. The most common adverse events were ALT/AST elevation, diarrhea, hypothyroidism, pneumonitis, pruritis, and rash. Three of the five patients (60%) with cAS of the head and neck had partial responses to therapy. One of these patients had a high TMB of 24 muts/mb (PD-L1 status was unavailable), while another had strong PD-L1 expression at 30% and a TMB of 8.4 muts/mb.

A single center, phase II multi-arm study evaluated the combination of anti-PD-L1 durvalumab and anti-CTLA-4 tremelimumab in 57 patients with various advanced or metastatic sarcoma subtypes (34). The cohort had a median (range) age of 48 (22–77) and a median (range) of 2 (0–6) prior lines of therapy. The study yielded mOS of 21.6 months (95%CI: 12.3–30.9), and mPFS of 2.8 months (95%CI: 1.8–6.4). Fourteen (24.6%) patients experienced grade > 3 related adverse events. Five patients in the study cohort had AS, including one cAS patient who achieved partial response. The study also found higher TIL immune scores to be associated with clinical benefit.

Anti-PD-L1 and T-VEC combination therapy

Combination pembrolizumab and oncolytic virus therapy Talimogen Laherparapvec (T-VEC) was assessed in an ongoing single center, open-label phase II study that enrolled 20 patients with metastatic and advanced sarcoma (35). The safety and efficacy of this combination therapy was previously demonstrated in patients with melanoma, thus supporting potential similar outcomes in cAS patients (36, 37). Overall, ORR was 35% (7 of 20) with all objective responders achieving partial responses. Of patients with recurrent locally advanced disease, the ORR was 75%. Where tissue samples were available for analysis, positive PD-L1 expression was detected in 83% of responders and 38% of non-responders. There were three cAS patients enrolled on study. Among the responders, two patients had recurrent locally advanced cAS and completed 52 weeks of treatment on study. One patient received 3 prior lines of chemotherapy as well as prior immunotherapy (TIGIT ab and atezolizumab) while the other received one prior line of chemotherapy but no prior immunotherapy. The ongoing trial plans to report further evaluation of T-VEC in combination with pembrolizumab.

Ongoing trials

Several ongoing efforts may further elucidate the utility of immunotherapy in patients with cutaneous angiosarcoma. Ongoing clinical trials in the U.S. are detailed in Table 2. Additionally, an ongoing phase II study in Japan is assessing response rates to nivolumab for patients with unresectable or metastatic cAS refractory to first-line paclitaxel (38).

Discussion

Current evidence of immune checkpoint blockade treatment in patients with cAS highlights the exciting future of cAS treatment. The overall positive results in cAS, particularly head and neck, are consistent with its known biomarkers of response to ICI such as TMB-High, PD-L1 positivity, UV mutational signature, and presence of TILs in the tumor microenvironment. A number of these immune biomarkers are predictive of respond to immunotherapy, notably those also found in patients with melanoma and squamous cell carcinoma, suggesting promising future directions for cAS treatment. Large phase II and phase III trials of ICIs in cAS are warranted, especially those with longer follow-up times to better evaluate recurrence and overall survival. Continued challenges include the rarity of AS as well as the heterogeneity within the subtypes; this makes it difficult to attain sufficient cAS patients within larger AS and sarcoma trials. To further evaluate AS and other sarcomas that may respond to ICIs, biomarker-based criteria should be considered for clinical trials. Challenges regarding this technique, however, include the wide variety of biomarkers to select from, and that there are multiple interacting factors that influence response. Additionally, precision biomarker-restricted therapy will inevitably encounter practical challenges associated with the high cost of research and development of companion diagnostics.

TABLE 2 Ongoing clinical trials.

NCT	Trial name	Angiosarcoma	Enrollment status	Preliminary data
NCT04784247	Lenvatinib and Pembrolizumab in People with advanced soft tissue Sarcoma	Includes experimental arm for vascular sarcomas (including angiosarcoma and epithelioid hemangioendothelioma)	Recruiting	Ongoing
NCT04668300	Oleclumab and Durvalumab for the treatment of recurrent, refractory, or metastatic sarcoma (DOSa)	Includes patients with metastatic angiosarcoma, recurrent angiosarcoma	Recruiting (estimated enrollment of 75 participants)	Ongoing
NCT03069378	A study of Talimogene Laherparepvec (T-VEC) in Combination with Pembrolizumab in Patients with metastatic and/or locally advanced Sarcoma	Includes patients with sarcoma, epithelioid sarcoma, and cutaneous angiosarcoma	Recruiting (estimated enrollment of 50 patients)	See above
NCT04339738	Testing the addition of Nivolumab to Chemotherapy in Treatment of Soft Tissue Sarcoma	Skin angiosarcoma, skin radiation-related angiosarcoma, visceral angiosarcoma	Recruiting (estimated enrollment of 90 participants)	Ongoing

Author contributions

LG and MP performed literature review, wrote original draft and all edits, created tables and were involved in manuscript from conception. RG provided guidance and direction, literature review, and review of manuscript as well as formulation of background and discussion. All authors contributed to the article and approved the submitted version.

Conflict of interest

RG is an employee of Merck, Sharp & Dohme LLC, Rahway, NJ, United States.

The remaining authors declare that the research was conducted in the absence of any commercial or financial relationships that could be construed as a potential conflict of interest.

Publisher's note

References

1. Ardakani AHG, Woollard A, Ware H, Gikas P. Soft tissue sarcoma: recognizing a rare disease. *Cleve Clin J Med*. (2022) 89:73–80. doi: 10.3949/ccjm.89a.21078

2. Dossett LA, Harrington M, Cruse CW, Gonzalez RJ. Cutaneous angiosarcoma. *Curr Probl Cancer*. (2015) 39:258–3. doi: 10.1016/j.currproblcancer.2015.07.007

3. Shin JY, Roh SG, Lee NH, Yang KM. Predisposing factors for poor prognosis of angiosarcoma of the scalp and face: systematic review and meta-analysis. *Head Neck*. (2017) 39:380–6. doi: 10.1002/hed.24554

4. Espejo-Freire AP, Elliott A, Rosenberg A, Costa PA, Barreto-Coelho P, Jonczak E, et al. Genomic landscape of angiosarcoma: a targeted and immunotherapy biomarker analysis. *Cancers (Basel)*. (2021) 13:4816. doi: 10.3390/cancers13194816

5. Hata M. Radiation therapy for angiosarcoma of the scalp: Total scalp irradiation and local irradiation. *Anticancer Res*. (2018) 38:1247–53. doi: 10.21873/anticanres.12346

6. Suzuki G, Yamazaki H, Takenaka H, Aibe N, Masui K, Kimoto T, et al. Definitive radiation therapy for angiosarcoma of the face and scalp. *In Vivo*. (2016) 30:921–6. doi: 10.21873/invivo.11014

7. Penel N, Bui BN, Bay JO, Cupissol D, Ray-Coquard I, Piperno-Neumann S, et al. Phase II trial of weekly paclitaxel for unresectable angiosarcoma: the ANGIOTAX study. *J Clin Oncol*. (2008) 26:5269–74. doi: 10.1200/JCO.2008.17.3146

8. Roy A, Gabani P, Davis EJ, Oppelt P, Merfeld E, Keedy VL, et al. Concurrent paclitaxel and radiation therapy for the treatment of cutaneous angiosarcoma. *Clin Transl Radiat Oncol*. (2021) 27:114–0. doi: 10.1016/j.ctro.2021.01.009

9. Ohguri T, Imada H, Nomoto S, Yahara K, Hisaoka M, Hashimoto H, et al. Angiosarcoma of the scalp treated with curative radiotherapy plus recombinant interleukin-2 immunotherapy. *Int J Radiat Oncol Biol Phys*. (2005) 61:1446–53. doi: 10.1016/j.ijrobp.2004.08.008

10. Lee ATJ, Jones RL, Huang PH. Pazopanib in advanced soft tissue sarcomas. *Signal Trans Target Ther*. (2019) 4:16. doi: 10.1038/s41392-019-0049-6

11. Kollár A, Jones RL, Stacchiotti S, Gelderblom H, Guida M, Grignani G, et al. Pazopanib in advanced vascular sarcomas: an EORTC soft tissue and bone sarcoma group (STBSG) retrospective analysis. *Acta Oncol*. (2017) 56:88–92. doi: 10.1080/0284186X.2016.1234068

12. Chi Y, Fang Z, Hong X, Yao Y, Sun P, Wang G, et al. Safety and efficacy of Anlotinib, a multikinase angiogenesis inhibitor, in patients with refractory metastatic soft-tissue sarcoma. *Clin Cancer Res*. (2018) 24:5233–8. doi: 10.1158/1078-0432.CCR-17-3766

13. Agulnik M, Schulte B, Robinson S, Hirbe AC, Kozak K, Chawla SP, et al. An open-label single-arm phase II study of regorafenib for the treatment of angiosarcoma. *Eur J Cancer*. (2021) 154:201–8. doi: 10.1016/j.ejca.2021.06.027

14. Ray-Coquard I, Italiano A, Bompas E, le Cesne A, Robin YM, Chevreau C, et al. Sorafenib for patients with advanced angiosarcoma: a phase II trial from the French sarcoma group (GSF/GETO). *Oncologist*. (2012) 17:260–6. doi: 10.1634/theoncologist.2011-0237

15. Agulnik M, Yarber JL, Okuno SH, von Mehren M, Jovanovic BD, Brockstein BE, et al. An open-label, multicenter, phase II study of bevacizumab for the treatment of angiosarcoma and epithelioid hemangioendotheliomas. *Ann Oncol*. (2013) 24:257–3. doi: 10.1093/annonc/mds237

16. Magara T, Nakamura M, Nojiri Y, Yoshimitsu M, Kano S, Matsubara A, et al. Tertiary lymphoid structures correlate with better prognosis in cutaneous angiosarcoma. *J Dermatol Sci*. (2021) 103:57–9. doi: 10.1016/j.jdermsci.2021.05.006

17. Palmeri M, Mehnert J, Silk AW, Jabbour SK, Ganesan S, Popli P, et al. Real-world application of tumor mutational burden-high (TMB-high) and microsatellite instability (MSI) confirms their utility as immunotherapy biomarkers. *ESMO Open*. (2022) 7:100336. doi: 10.1016/j.esmoop.2021.100336

18. Marabelle A, Fakih M, Lopez J, Shah M, Shapira-Frommer R, Nakagawa K, et al. Association of tumour mutational burden with outcomes in patients with advanced solid tumours treated with pembrolizumab: prospective biomarker analysis of the multicohort, open-label, phase 2 KEYNOTE-158 study. *Lancet Oncol*. (2020) 21:1353–65. doi: 10.1016/S1470-2045(20)30445-9

19. Cristescu R, Aurora-Garg D, Albright A, Xu L, Liu XQ, Loboda A, et al. Tumor mutational burden predicts the efficacy of pembrolizumab monotherapy: a pan-tumor retrospective analysis of participants with advanced solid tumors. *J Immunother Cancer*. (2022) 10:e003091. doi: 10.1136/jitc-2021-003091

20. Tawbi HA, Burgess M, Bolejack V, van Tine BA, Schuetze SM, Hu J, et al. Pembrolizumab in advanced soft-tissue sarcoma and bone sarcoma (SARC028): a multicentre, two-cohort, single-arm, open-label, phase 2 trial. *Lancet Oncol*. (2017) 18:1493–01. doi: 10.1016/S1470-2045(17)30624-1

21. Mata DA, Williams EA, Sokol E, Oxnard GR, Fleischmann Z, Tse JY, et al. Prevalence of UV mutational signatures among cutaneous primary Tumors. *JAMA Netw Open*. (2022) 5:e223833. doi: 10.1001/jamanetworkopen.2022.3833

22. Painter CA, Jain E, Tomson BN, Dunphy M, Stoddard RE, Thomas BS, et al. The angiosarcoma project: enabling genomic and clinical discoveries in a rare cancer through patient-partnered research. *Nat Med*. (2020) 26:181–7. doi: 10.1038/s41591-019-0749-z

23. Boichard A, Wagner MJ, Kurzrock R. Angiosarcoma heterogeneity and potential therapeutic vulnerability to immune checkpoint blockade: insights from genomic sequencing. *Genome Med*. (2020) 12:61. doi: 10.1186/s13073-020-00753-2

24. Chan JY, Lim JQ, Yeong J, Ravi V, Guan P, Boot A, et al. Multiomic analysis and immunoprofiling reveal distinct subtypes of human angiosarcoma. *J Clin Invest*. (2020) 130:5833–46. doi: 10.1172/JCI139080

25. Fujii H, Arakawa A, Utsumi D, Sumiyoshi S, Yamamoto Y, Kitoh A, et al. CD8+tumor-infiltrating lymphocytes at primary sites as a possible prognostic factor of cutaneous angiosarcoma. *Int J Cancer*. (2014) 134:2393–02. doi: 10.1002/ijc.28581

26. Chen SMY, Krinsky AL, Woolaver RA, Wang X, Chen Z, Wang JH. Tumor immune microenvironment in head and neck cancers. *Mol Carcinog*. (2020) 59:766–4. doi: 10.1002/mc.23162

27. Chan JY, Tan GF, Yeong J, Ong CW, Ng DYX, Lee E, et al. Clinical implications of systemic and local immune responses in human angiosarcoma. *NPJ Precis Oncol*. (2021) 5:1–13. doi: 10.1038/s41698-021-00150-x

28. Tan GF, Chan JY. Towards precision oncology in angiosarcomas using next generation "omic" technologies. *Oncotarget*. (2021) 12:1953–5. doi: 10.18632/oncotarget.27996

29. Sindhu S, Gimber LH, Cranmer L, McBride A, Kraft AS. Angiosarcoma treated successfully with anti-PD-1 therapy - a case report. *J Immunother Cancer*. (2017) 5:58. doi: 10.1186/s40425-017-0263-0

30. Hamacher R, Kämpfe D, Reuter-Jessen K, Pöttgen C, Podleska LE, Farzaliyev F, et al. Dramatic response of a PD-L1-positive advanced angiosarcoma of the scalp to pembrolizumab. *JCO Precis Oncol*. (2018) 2:1–7. doi: 10.1200/PO.17.00107

31. Florou V, Rosenberg AE, Wieder E, Komanduri KV, Kolonias D, Uduman M, et al. Angiosarcoma patients treated with immune checkpoint inhibitors: a case series of seven patients from a single institution. *J Immunother Cancer*. (2019) 7:213. doi: 10.1186/s40425-019-0689-7

32. Rosenbaum E, Antonescu CR, Smith S, Bradic M, Kashani D, Richards AL, et al. Clinical, genomic, and transcriptomic correlates of response to immune checkpoint blockade-based therapy in a cohort of patients with angiosarcoma treated at a single center. *J Immunother Cancer*. (2022) 10:e004149. doi: 10.1136/jitc-2021-004149

33. Wagner MJ, Othus M, Patel SP, Ryan C, Sangal A, Powers B, et al. Multicenter phase II trial (SWOG S1609, cohort 51) of ipilimumab and nivolumab in metastatic or unresectable angiosarcoma: a substudy of dual anti-CTLA-4 and anti-PD-1 blockade in rare tumors (DART). *J Immunother Cancer*. (2021) 9:e002990. doi: 10.1136/jitc-2021-002990

34. Somaiah N, Conley AP, Parra ER, Lin H, Amini B, Solis Soto L, et al. Durvalumab plus tremelimumab in advanced or metastatic soft tissue and bone sarcomas: a single-Centre phase 2 trial. *Lancet Oncol*. (2022) 23:1156–66. doi: 10.1016/S1470-2045(22)00392-8

35. Kelly CM, Antonescu CR, Bowler T, Munhoz R, Chi P, Dickson MA, et al. Objective response rate among patients with locally advanced or metastatic sarcoma treated with Talimogene Laherparepvec in combination with pembrolizumab: a phase 2 clinical trial. *JAMA Oncol*. (2020) 6:402–8. doi: 10.1001/jamaoncol.2019.6152

36. Andtbacka RH, Kaufman HL, Collichio F, Amatruda T, Senzer N, Chesney J, et al. Talimogene Laherparepvec improves durable response rate in patients with advanced melanoma. *J Clin Oncol*. (2015) 33:2780–8. doi: 10.1200/JCO.2014.58.3377

37. Long GV, Dummer R, Ribas A, Puzanov I, Michielin O, VanderWalde A, et al. A phase I/III, multicenter, open-label trial of talimogene laherparepvec (T-VEC) in combination with pembrolizumab for the treatment of unresected, stage IIIb-IV melanoma (MASTERKEY-265). *J Immunother Cancer*. (2015) 3:P181. doi: 10.1186/2051-1426-3-S2-P181

38. Fujisawa Y, Yoshino K, Isei T, Namikawa K, Fujimura T, Yasuda M, et al. A multicenter, open-label, uncontrolled phase II study of ONO-4538 for cutaneous angiosarcoma (Angio check study). *J Clin Oncol*. (2021) 39:TPS11579. doi: 10.1200/JCO.2021.39.15_suppl.TPS11579

frontiers | Frontiers in Medicine

TYPE Original Research
PUBLISHED 06 April 2023
DOI 10.3389/fmed.2023.1110511

OPEN ACCESS

EDITED BY
Bahar Dasgeb,
Rutgers, The State University of New Jersey, United States

REVIEWED BY
Nicola Pimpinelli,
University of Florence, Italy
Darius Mehregan,
Wayne State University, United States

*CORRESPONDENCE
Neda Nikbakht
✉ neda.nikbakht@jefferson.edu

SPECIALTY SECTION
This article was submitted to Dermatology, a section of the journal Frontiers in Medicine

RECEIVED 28 November 2022
ACCEPTED 14 March 2023
PUBLISHED 06 April 2023

CITATION
Banner L, Joffe D, Lee E, Porcu P and Nikbakht N (2023) Incidence of cutaneous melanoma and Merkel cell carcinoma in patients with primary cutaneous B-cell lymphomas: A population study of the SEER registry.
Front. Med. 10:1110511.
doi: 10.3389/fmed.2023.1110511

Incidence of cutaneous melanoma and Merkel cell carcinoma in patients with primary cutaneous B-cell lymphomas: A population study of the SEER registry

Lauren Banner[1], Daniel Joffe[1], Emily Lee[1], Pierluigi Porcu[2] and Neda Nikbakht[1]*

[1]Department of Dermatology and Cutaneous Biology, Thomas Jefferson University, Philadelphia, PA, United States, [2]Division of Hematologic Malignancies and Hematopoietic Stem Cell Transplantation, Department of Medical Oncology, Thomas Jefferson University, Philadelphia, PA, United States

Introduction: The increased incidence of cutaneous melanoma (CM) and Merkel cell carcinoma (MCC) in patients with hematologic malignancies (HM) is well established. While the risk of CM has been assessed in some subtypes of HM including cutaneous T-cell lymphoma, the incidence in patients with primary cutaneous B-cell lymphoma (PCBCL) has not been interrogated.

Methods: Here we evaluated the standardized incidence ratio (SIR) of CM and MCC in 5,179 PCBCL patients compared to approximately 1.5 billion individuals in the general population using the Surveillance, Epidemiology and End Results (SEER) database. Among patients with PCBCL, we identified subgroups that were at increased risk for CM or MCC as a second primary cancer.

Results: We found 36 cases of CM in the PCBCL cohort (SIR, 1.35; 95% CI, 0.94–1.86), among which SIR was significantly elevated for non-Hispanic White patients compared to the general population (SIR, 1.48; 95% CI, 1.03–2.06). Males had a significantly increased risk of developing CM after a diagnosis of PCBCL (SIR, 1.60; 95% CI, 1.10–2.26). We found that males in the age group of 50–59 were at increased risk for CM development (SIR, 3.02; 95% CI, 1.11–6.58). Males were at increased risk of CM 1–5 years after PCBCL diagnosis (SIR, 2.06; 95% CI, 1.18–3.34). Patients were at greater risk of developing MCC within 1 year of diagnosis of PCBCL (SIR, 23.60; 95% CI, 2.86–85.27), particularly in patients who were over the age of 80 (SIR, 46.50; 95% CI, 5.63–167.96). Males aged 60–69 with PCBCL, subtype marginal zone, were also at increased risk for MCC (SIR, 42.71; 95% CI, 1.08–237.99).

Conclusion: There is an increased incidence of CM in White, middle-aged males within 5 years of diagnosis of PCBCL and an increased risk of MCC in elderly patients within 1 year of PCBCL diagnosis. These data suggest that certain subgroups of patients with PCBCL may require more rigid surveillance for CM and MCC.

KEYWORDS

primary cutaneous B-cell lymphoma (PCBCL), primary cutaneous follicle center lymphoma (PCFCL), cutaneous melanoma (CM), Surveillance, Epidemiology, and End Results (SEER), Merkel cell carcinoma (MCC), primary cutaneous marginal zone lymphoma (PCMZL)

Introduction

Cutaneous melanoma (CM) is the fifth most common type of cancer and represents 5.2% of the cancers diagnosed in the United States. CM is responsible for 1.3% of all cancer deaths and is most prevalent in non-Hispanic White males between the ages 65–74 (1). The age-adjusted rate of CM is 22.2 per 100,000 as calculated by SEER*Stat software package 8.4.0.1 (National Cancer Institute, Bethesda, MD). Merkel cell carcinoma (MCC) is a rare aggressive cutaneous neuroendocrine tumor that is common in older white males with an age-adjusted rate of 0.6 per 100,000. An increased association of CM in patients with hematologic malignancies (HM) has been reported (**Table 1**) (2–28). MCC incidence has not been as widely studied in patients with HM, but it has been consistently reported to develop at an increased incidence in patients with HM (**Table 1**) (5, 24–33). When examining all subtypes of HM, over two thirds of cohorts exhibited a significantly increased risk of CM occurring after an HM diagnosis (**Table 1**) (2, 3, 5, 6, 8, 9, 11, 12, 14–19, 21, 34). Three studies examined the development of second primary solid malignancies in cutaneous T-cell lymphomas (CTCL), two of which found up to a 9-fold increase in the risk of second primary CMs (9, 10, 35).

Primary cutaneous B-cell lymphomas (PCBCL) are subtypes of HM that represent one quarter of all cutaneous lymphomas. The incidence of PCBCL is <1/100,000 person years and increases with age. The two most common types of PCBCL are primary cutaneous marginal zone lymphoma (PCMZL) and primary cutaneous follicle center lymphoma (PCFCL) which are typically indolent. Primary cutaneous diffuse large B-cell lymphoma, leg type (PC-DLBCL, LT) tends to be the most aggressive (36, 37). No previous studies have examined the incidence of CM or MCC in PCBCL. We endeavored to analyze the incidence of CM and MCC in the PCBCL population compared the general population using the Surveillance, Epidemiology and End Results Projects (SEER) database.

Materials and methods

SEER patient cohort selection

The SEER cohort selection of patients with PCBCL was adapted from Bomze et al. (38). Patients were diagnosed between January 2000 and December 2019 in 17 cancer registries that included San Francisco, Connecticut, Hawaii, Iowa, New Mexico, Seattle (Puget Sound), Utah, Atlanta (Metropolitan), San Jose-Monterey, Los Angeles, Alaska Natives, Rural Georgia, California excluding SF/SJM/LA, Kentucky, Louisiana, New Jersey and Greater Georgia [SEER 17 Regs excluding AK Research Data, November 2021 Sub (2000–2019)]. Patients with PCBCL were identified according to the World Health Organization's International Classification of Diseases for Oncology, third edition (ICD-O-3) by the following histological codes: diffuse large B-cell lymphoma (ICD-O-3 9680); follicular lymphoma (ICD-O-3 9690), follicular lymphoma grades 1–3 (ICD-O-3 9691, 9695, 9698), extranodal marginal zone lymphoma of mucosal associated lymphoid tissue-MALT (ICD-O-3 9699), Non-Hodgkin Lymphoma, NOS (ICD-O-3 9591), B-cell lymphoma, between diffuse large B and HL (ICD-O-3 9596), Primary cutaneous follicle center lymphoma (ICD-O-3 9597), large B, diffuse, immunoblastic (ICD-O-3 9684). We included cases with the topography code for skin (C44) as the primary site. PCBCL was selected as the first primary cancer. The outcome event variables were selected using the Site recode ICD-O-3/WHO 2008 (for SIRs) codes for CM and MCC. The timing of the first primary diagnosis of PCBCL was used as the initial date from which CM and MCC latency were calculated. Patients were excluded if the report was obtained solely from a death certificate or autopsy report with no confirmation of diagnosis. Study of this SEER cohort was exempt from institutional review board approval.

Statistical analysis

The measure of relative risk was estimated as the standardized incidence ratio (SIR), the ratio of observed cases to expected cases of CM or MCC (O/E) in the SEER cohort. An SIR of 1 indicated no difference in incidence compared to the general population. The statistical significance of SIR was assessed using a 95% confidence interval (CI).

To calculate the number of expected CMs and MCCs, a reference rate file of CM per 100,000 was calculated using SEER*Stat software package 8.4.0.1 (National Cancer Institute, Bethesda, MD) and applied to the number of patients in the SEER-17 registry of 1,628,926,957 persons. In the SEER cohort, the number of person-years at risk among patients from diagnosis of PCBCL to a second diagnosis of CM or MCC was calculated by SEER*Stat software package 8.4.0.1 (National Cancer Institute, Bethesda, MD, USA).

Results

Patients from SEER cohort

The SEER PCBCL cohort consisted of 5,179 patients of whom 36 (0.70%) received a diagnosis of CM (SIR, 1.35; 95% CI, 0.94–1.86) and three (0.06%) received a diagnosis of MCC (SIR, 3.74 95% CI 0.77–10.92). The median age range of developing the subsequent CM was 70–79. Two patients who developed MCC were over 85 years old, and the other patient was 69. There were no cases of subsequent CM or MCC diagnosed before the age of 40. CM occurred most frequently in PCBCL patients over age 80. The most frequent latency period for CM to appear was between 1 and 5 years after PCBCL diagnosis. Two second primary MCCs occurred within a year and one MCC occurred 1–5 years after PCBCL diagnosis. Eleven CMs were reported as stage I and the remaining cases did not have a stage reported. All the second primary MCCs were localized.

Thirty-five of the thirty-six CMs in patients with PCBCL occurred in non-Hispanic White persons (97%). The SIR showed a significant elevation at 1.48; 95% CI, 1.03–2.06. Only one CM occurred in the non-White group (3%). This patient's race was reported as Asian or Pacific Islander. All patients who developed second primary MCC after PCBCL diagnosis were white.

TABLE 1 Epidemiologic studies for CM and MCC as subsequent primary malignancy after HM (2, 3, 5, 6, 8, 9, 11, 12, 14, 15, 17–19, 21, 30, 31, 33–35).

Reference	Location	Type of lymphoma	Number of patients	Number of CMs after lymphoma diagnosis	Relative risk or standardized incidence ratio	95% confidence interval or *p*-value
CM occurring after diagnosis of HM						
Travis et al. (17)	United States	NHL	29,153	44	***2.44****	1.78–3.28
Travis et al. (18)	United States	CLL	9,456	28	***2.79****	1.85–4.03
Adami et al. (2)	Denmark, Sweden	NHL	34,641	52	***2.4****	1.8–3.2
		CLL	17,400	34	***3.1****	2.1–4.4
Dong and Hemminki (21)	Sweden	NHL	18,960	33	1.14	0.78–1.60
Goggins et al. (8)	United States	NHL	62,597	139	**1.75***	1.48–2.07
McKenna et al. (14)	Scotland	NHL	13,857	18	***2.1****	1.2–3.6
		CLL	4,016	6	2.3	0.0–2.4
Hisada et al. (11)	United States	CLL	16,367	90	***3.18****	$p < 0.05$
Brennan et al. (34)	International	NHL	109,451	258	***1.92****	1.69–2.16
Huang et al. (12)	United States	CTCL	1,798	10	***2.60****	1.25–4.79
Brownell et al. (35)	United States	CTCL	672	2	2.82	0.34–10.18
Tsimberidou et al. (19)	United States	CLL/SLL	2,028	19	***6.17****	3.97–9.24
Brewer et al. (5)	United States	CLL	28,964	268	***2.0****	1.8–2.2
		NHL	94,967	441	***1.5****	1.4–1.6
Chang et al. (6)	United States	MM	31,622	63	1.27	0.97–1.62
Archibald et al. (3)	United States	CLL	470	22	***6.32****	3.45–10.60
Goyal et al. (9)	United States	CTCL < 1 year	6,742	4	***9.61****	2.62–24.62
		CTCL > 1 year		20	***9.0****	5.5–13.90
Singh et al. (15)	United States	MM	79,174	280	***1.26****	$p < 0.001$
MCC occurring after diagnosis of HM						
Howard et al. (33)	United States	CLL	17,315	14	***6.89****	3.77–11.57
		NHL	81,743	16	***3.37****	1.93–5.47
		MM	23,949	4	***3.70****	1.01–9.47
Koljonen et al. (30)	United States	CLL	4,164	4	***15.7****	3.2–46.0
Koljonen et al. (31)	Nordic Countries	NHL	109,838	18	***4.34****	2.57–6.85
Brewer et al. (5)	United States	CLL	28,964	31	***8.2****	5.6–11.6
		NHL	94,967	23	***5.9****	3.8–8.9

CM, cutaneous melanoma; MCC, Merkel cell carcinoma; HM, hematologic malignancy; PCBCL, primary cutaneous B-cell lymphoma. Asterisk (*), bold, italics indicates $p < 0.05$.

Risk of second primary CM and MCC as a function of sex, attained age and latency

Males with PCBCL comprised 57% of the cohort (n = 2,973) and females comprised 43% (n = 2,206). Thirty-two males (1.1%) and four females (0.18%) developed CM. Two males (0.06%) and 1 female (0.04%) developed MCC. When comparing gender, males had a significantly increased risk of developing CM after a diagnosis of PCBCL (SIR, 1.60; 95% CI, 1.10–2.26). Whereas females were not at an increased risk of developing CM (SIR, 0.59; 95% CI, 0.16–1.51). Males in the age groups 50–59 were the most at risk of CM (SIR, 3.02; 95% CI, 1.11–6.58) (Table 2). Males were also at an increased risk of CM between 1 and 5 years after diagnosis of PCBCL (SIR, 2.06; 95% CI, 1.18–3.34) (Table 3). For males, the age group 60–69 was most at risk for CM when accounting for the 1–5-year latency period (SIR, 3.07; 95% CI, 1.13–6.68). Patients with PCBCL were more at risk for developing MCC within a year of their lymphoma diagnosis (SIR, 23.60; 95% CI, 2.86–85.27) (Table 3). Patients who were 80 or older were at an increased risk of developing MCC with a year of diagnosis of PCBCL (SIR, 46.50; 95% CI, 5.63–167.96). Females over 80 years old were at an increased risk for MCC within 1 year of PCBCL diagnosis (SIR, 66.06; 95% CI, 1.67–368.06).

The risk of second primary CM and MCC by type of PCBCL

Of the three most common types of PCBCL, there were 13 cases of CM in 1,844 PCFCL patients (0.70%) with an SIR of 1.25 (95%

TABLE 2 Age and gender specific instances of CM and MCC.

Age	Gender					
	CM			MCC		
	All SIR (95% CI)	Male SIR (95% CI)	Female SIR (95% CI)	All SIR (95% CI)	Male SIR (95% CI)	Female SIR (95% CI)
40–49	2.32 (0.28–8.39)	3.53 (0.43–12.74)	0 (0–12.56)	0 (0–1,065.17)	0 (0–1,409.08)	0 (0–4,364.30)
50–59	2.15 (0.79–4.68)	***3.02* (1.11–6.58)***	0 (0–4.59)	0 (0–127.41)	0 (0–167.97)	0 (0–527.60)
60–69	1.38 (0.63–2.61)	1.44 (0.58–2.96)	1.20 (0.15–4.33)	8.78 (0.22–48.93)	11.67 (0.30–65.04)	0 (0–130.76)
70–79	0.93 (0.40–1.84)	1.20 (0.52–2.36)	0 (0–1.95)	0 (0–14.90)	0 (0–20.14)	0 (0–57.27)
80+	1.42 (0.71–2.54)	1.58 (0.72–3.00)	0.98 (0.12–3.55)	4.90 (0.59–17.69)	3.59 (0.09–19.99)	7.70 (0.19–42.91)
Total	1.35 (0.94–1.86)	***1.60* (1.10–2.26)***	0.59 (0.16–1.51)	3.74 (0.77–10.92)	3.49 (0.42–12.62)	4.34 (0.11–24.19)

CM, cutaneous melanoma; MCC, Merkel cell carcinoma; PCBCL, primary cutaneous B-cell lymphoma; SIR, standardized incidence ratio; CI, confidence interval. Asterisk (*), bold, italics indicates $p < 0.05$.

TABLE 3 Patient latency to diagnosis of CM and MCC from PCBCL stratified by gender.

Latency (months)	Gender					
	CM			MCC		
	All SIR (95% CI)	Male SIR (95% CI)	Female SIR (95% CI)	All SIR (95% CI)	Male SIR (95% CI)	Female SIR (95% CI)
<12	0.73 (0.09–2.64)	0.51 (0.01–2.82)	1.31 (0.03–7.30)	***23.60* (2.86–85.27)***	17.15 (0.43–95.56)	37.85 (0.96–210.87)
12–59	1.60 (0.93–2.57)	***2.06* (1.18–3.34)***	0.35 (0.01–1.97)	3.11 (0.08–17.32)	4.43 (0.11–24.70)	0 (0–38.38)
60–119	1.10 (0.50–2.08)	1.30 (1.18–3.34)	0.49 (0.01–2.72)	0 (0–15.19)	0 (0–21.24)	0 (0–53.33)
120–179	1.71 (0.69–3.52)	1.90 (0.70–4.13)	1.08 (0.03–5.99)	0 (0–30.61)	0 (0–41.22)	0 (0–118.91)
180+	0.89 (0.02–4.97)	1.13 (0.03–6.27)	0 (0–15.91)	0 (0–112.20)	0 (0–146.16)	0 (0–482.91)
Total	1.35 (0.94–1.86)	***1.60* (1.10–2.26)***	0.59 (0.16–1.51)	3.74 (0.77–10.92)	3.49 (0.42–12.62)	4.34 (0.11–24.19)

CM, cutaneous melanoma; MCC, Merkel cell carcinoma; PCBCL, primary cutaneous B-cell lymphoma; SIR, standardized incidence ratio; CI, confidence interval. Asterisk (*), bold, italics indicates $p < 0.05$.

CI, 0.67–2.14). All patients were male (Table 4). There was 1 MCC case found in a male PCFCL patient (SIR, 3.31; 95% CI 0.08–18.42) (Table 4). Eleven CMs were in 1,641 PCMZL patients (0.67%) with an SIR of 1.49 (95% CI, 0.74–2.66) (Table 4). One MCC occurred in a male patient after diagnosis of PCMZL (SIR, 5.03; 95% CI 0.13–28.03) (Table 4). There were four patients with CM occurring after diagnosis of PC-DLBCL (n = 1,235; 0.32%) with an SIR of 0.66 (95% CI, 0.18–1.69) (Table 4). These patients were all male. There was one female patient who developed MCC after diagnosis of PC-DLBCL (SIR, 4.83; CI 95% 0.12–26.89) (Table 4). The remaining second primary CMs occurred in patients with other rare PCBCLs and in patients with PCBCL not specified. When accounting for age, gender, and subtype, the SIR was significantly increased for males 50–54 with PCFCL to develop CM (SIR, 8.31; 95% CI, 1.01–30.03). Males in the age group 60–69 with the subtype of PCMZL were at an increased risk for MCC (SIR, 42.71; 95% CI 1.08–237.99).

Discussion

This study is the first to define the relationship between PCBCL and the incidence of CM and MCC. In the SEER cohort, we were able to identify at-risk populations among PCBCL patients. The incidence ratio for developing CM after diagnosis of PCBCL was significantly increased in males but not in females. The risk of acquiring CM was higher between 1 and 5 years of a diagnosis of PCBCL. Females over the age of 80 with a diagnosis of PCBCL were at an increased risk of developing MCC within 1 year of diagnosis. Males in the age groups 50–54 were at particularly increased risk for CM, especially with the subtype PCFCL. Subtype PCMZL carried the highest risk of MCC for males aged 60–69. These observations highlight the importance of vigilant monitoring of these populations for a second primary skin cancer.

When CM is caught early, it is highly treatable with a 99% 5-year survival for localized disease compared to a 32–52% 5-year survival for distant stage CM (1, 39, 40). MCC is also treatable with an 81% 5-year survival for stage 1 disease compared to an 11% 2-year survival rate for stage 4 disease (4). There is a lack of national consensus on the screening guidelines for CM and non-melanoma skin cancers. The United States Prevention Services Task Force (USPSTF) cites insufficient evidence to recommend screenings for asymptomatic persons. However, both the USPSTF and the American Academy of Dermatology (AAD) recommend that dermatologists examine high-risk individuals more frequently. It is therefore crucial to define risk factors for CM and MCC, so that surveillance opportunities are not missed. Based on our findings, patients with PCBCL, specifically PCFCL or PCMZL, who are middle-aged to elderly can benefit from annual total body skin exams (TBSEs) within 5 years of diagnosis of cutaneous B-cell lymphoma.

TABLE 4 Incidence of CM and MCC in PCBCL stratified by type, age and gender.

		Gender					
Subtype	Age	CM			MCC		
		All SIR (95% CI)	Male SIR (95% CI)	Female SIR (95% CI)	All SIR (95% CI)	Male SIR (95% CI)	Female SIR (95% CI)
PCFCL	40–49	0 (0–13.38)	0 (0–21.33)	0 (0–35.88)	0 (0–3,377.67)	0 (0–4,514.28)	0 (0–13,415.15)
	50–59	2.99 (0.62–8.74)	4.11 (0.85–12.01)	0 (0–13.48)	0 (0–349.61)	0 (0–450.59)	0 (0–1,560.01)
	60–69	1.13 (0.23–3.30)	1.46 (0.30–4.26)	0 (0–6.13)	0 (0–80.03)	0 (0–102.35)	0 (0–366.90)
	70–79	0.84 (0.17–2.46)	1.04 (0.21–3.03)	0 (0–5.51)	0 (0–36.79)	0 (0–47.28)	0 (0–165.81)
	80+	1.42 (0.39–3.65)	1.92 (0.52–4.90)	0 (0–5.13)	6.90 (0.17–38.45)	10.14 (0.26–56.49)	0 (0–79.71)
	Total	1.25 (0.67–2.14)	1.63 (0.87–2.78)	0 (0–1.54)	3.30 (0.08–18.39)	4.51 (0.11–25.13)	0 (0–45.41)
PCMZL	40–49	2.51 (0.06–13.98)	3.91 (0.10–21.76)	0 (0–25.87)	0 (0–2,414.04)	0 (0–3,334.02)	0 (0–8,748.48)
	50–59	1.04 (0.03–5.77)	1.61 (0.04–8.97)	0 (0–10.69)	0 (0–383.75)	0 (0–550.41)	0 (0–1,267.38)
	60–69	1.54 (0.32–4.50)	1.50 (0.18–5.41)	1.63 (0.04–9.07)	29.78 (0.75–165.92)	***42.71**** ***(1.08–237.99)***	0 (0–362.80)
	70–79	0.93 (0.11–3.36)	1.23 (0.15–4.43)	0 (0–7.13)	0 (0–60.18)	0 (0–83.82)	0 (0–213.44)
	80+	2.24 (0.61–5.74)	1.52 (0.18–5.50)	4.23 (0.51–15.29)	0 (0–39.85)	0 (0–57.49)	0 (0–129.85)
	Total	1.49 (0.74–2.66)	1.52 (0.66–3.00)	1.39 (0.29–4.06)	5.03 (0.13–28.03)	7.17 (0.18–39.93)	0 (0–62.27)
DLBCL	40–49	0 (0–30.85)	0 (0–43.70)	0 (0–104.87)	0 (0–6,757.31)	0 (0–8,441.33)	0 (0–33,871.90)
	50–59	1.81 (0.05–10.10)	2.31 (0.06–12.88)	0 (0–30.99)	0 (0–622.03)	0 (0–763.79)	0 (0–3,351.45)
	60–69	0.76 (0.02–4.22)	0.98 (0.02–5.49)	0 (0–12.08)	0 (0–156.67)	0 (0–204.56)	0 (0–669.20)
	70–79	0 (0–1.96)	0 (0–2.74)	0 (0–6.84)	0 (0–63.54)	0 (0–94.77)	0 (0–192.80)
	80+	0.93 (0.11–3.35)	1.32 (0.16–4.76)	0 (0–5.78)	8.40 (0.21–46.79)	0 (0–47.76)	23.90 (0.61–133.17)
	Total	0.66 (0.18–1.69)	0.91 (0.25–2.32)	0 (0–2.23)	4.83 (0.12–26.89)	0 (0–26.45)	14.77 (0.37–82.30)

CM, cutaneous melanoma; MCC, Merkel cell carcinoma; PCBCL, primary cutaneous B-cell lymphoma; SIR, standardized incidence ratio; CI, confidence interval; PCFCL, primary cutaneous follicle center lymphoma; PCMZL, primary cutaneous marginal zone lymphoma; DLBCL, diffuse large B-cell lymphoma. Asterisk (*), bold, italics indicates $p < 0.05$.

Most prior studies found a highly increased risk for CM and MCC development in hematologic malignancy (Table 1). Several mechanisms may contribute to the increased risk of CM and MCC in patients with hematologic malignancies, including their immunocompromised status (4, 13, 41). A bidirectional relationship has been noted in prior studies between HM and CM or MCC (2, 7, 20, 30, 31, 33). Another factor that may be contributing to the development of MCC and CM in patients with hematologic malignancy is receiving immunosuppressive treatments such as radiation (a commonly used treatment modality in PCFCL and PCMZL) and chemotherapy (13, 23). Unfortunately, using data available in SEER, we were not able to determine if the sites of MCC and CM were the same sites previously radiated.

The two most common subtypes of PCBCL are PCMZL and PCFCL. They are more indolent than their nodal counterparts, with 5-year disease specific survival rates of 99 and 95%, respectively (37). PC-DLBCL, LT is a less common but more aggressive subtype of PCBCL with a disease specific survival rate of 40–60% (37, 41). Interestingly, only indolent PCFCL and PCMZL had increased SIRs for CM and MCC, respectively, implying that aggressive molecular features in PCBCL may not drive pre-disposition to CM or MCC. Ultimately, mechanisms that lead to the development of CM and MCC after cutaneous B-cell lymphomas remain to be elucidated. Overall, indolent PCBCLs require monitoring for both recurrence of cutaneous lymphoma as well as CM and MCC.

There were several limitations to our study. Firstly, the cohorts were reviewed retrospectively instead of prospectively, and given the rarity of PCBCL, the cohort in SEER was small. Coding for primary cutaneous B-cell lymphoma is a multi-step process which may lead to cases being missed in the registry. Additionally, patients with PCBCL may be seen more frequently at dermatology offices rather than oncology practices, where SEER data entry is commonly performed. Another limitation was that we were unable to account for family history as a risk factor for these malignancies using the SEER data. As the occurrences of MCC and PCBCL are very rare, it is likely that larger sample sizes may be needed to assess correlations. We recommend future large, multi-institutional prospective studies on the risk of CM and MCC in patients with PCBCL.

Data availability statement

The raw data supporting the conclusions of this article will be made available by the authors, without undue reservation.

Ethics statement

Ethical review and approval was not required for the current study in accordance with the local legislation and institutional requirements. Written informed consent for participation was not required for this study in accordance with the national legislation and the institutional requirements.

Author contributions

LB participated in the data analysis and wrote the manuscript. DJ contributed to the data collection and edited the manuscript. EL contributed to the statistical analysis and wrote the manuscript. PP and DJ edited the manuscript. NN participated in the research design, editing, and supervised the production of the manuscript. All authors contributed to the article and approved the submitted version.

Acknowledgments

We thank Krupa Gandhi for her guidance on the use of SEER*Stat.

Conflict of interest

The authors declare that the research was conducted in the absence of any commercial or financial relationships that could be construed as a potential conflict of interest.

Publisher's note

References

1. National Cancer Institute. *SEER cancer stat facts: melanoma of the skin*. Frederick, MD: National Cancer Institute (2022).

2. Adami J, Frisch M, Yuen J, Glimelius B, Melbye M. Evidence of an association between non-Hodgkin's lymphoma and skin cancer. *BMJ.* (1995) 310:1491–5. doi: 10.1136/bmj.310.6993.1491

3. Archibald W, Meacham P, Williams A, Baran A, Victor A, Barr P, et al. Management of melanoma in patients with chronic lymphocytic leukemia. *Leuk Res.* (2018) 71:43–6. doi: 10.1016/j.leukres.2018.07.003

4. Bichakjian C, Lowe L, Lao C, Sandler H, Bradford C, Johnson T, et al. Merkel cell carcinoma: critical review with guidelines for multidisciplinary management. *Cancer.* (2007) 110:1–12. doi: 10.1002/cncr.22765

5. Brewer J, Shanafelt T, Call T, Cerhan J, Roenigk R, Weaver A, et al. Increased incidence of malignant melanoma and other rare cutaneous cancers in the setting of chronic lymphocytic leukemia. *Int J Dermatol.* (2015) 54:e287–93. doi: 10.1111/ijd.12564

6. Chang T, Weaver A, Brewer J, Kyle R, Baum C. Risk of melanoma in patients with multiple myeloma: A Surveillance, Epidemiology, and End Results population-based study. *J Am Acad Dermatol.* (2018) 78:621–3. doi: 10.1016/j.jaad.2017.10.014

7. Famenini S, Martires K, Zhou H, Xavier M, Wu J. Melanoma in patients with chronic lymphocytic leukemia and non-Hodgkin lymphoma. *J Am Acad Dermatol.* (2015) 72:78–84. doi: 10.1016/j.jaad.2014.09.030

8. Goggins W, Finkelstein D, Tsao H. Evidence for an association between cutaneous melanoma and non-Hodgkin lymphoma. *Cancer.* (2001) 91:874–80. doi: 10.1002/1097-0142(20010215)91:4<874::AID-CNCR1076>3.0.CO;2-O

9. Goyal A, O'Leary D, Goyal K, Rubin N, Bohjanen K, Hordinsky M, et al. Increased risk of second primary hematologic and solid malignancies in patients with mycosis fungoides: A Surveillance, Epidemiology, and End Results analysis. *J Am Acad Dermatol.* (2020) 83:404–11. doi: 10.1016/j.jaad.2019.07.075

10. Goyal AO, Goyal K, Patel K, Pearson D, Janakiram M. Cutaneous T-cell lymphoma is associated with increased risk of lymphoma, melanoma, lung cancer, and bladder cancer. *J Am Acad Dermatol.* (2021) 85:1418–28. doi: 10.1016/j.jaad.2020.06.1033

11. Hisada M, Biggar R, Greene M, Fraumeni J Jr, Travis L. Solid tumors after chronic lymphocytic leukemia. *Blood.* (2001) 98:1979–81. doi: 10.1182/blood.V98.6.1979

12. Huang K, Weinstock M, Clarke C, McMillan A, Hoppe R, Kim Y. Second lymphomas and other malignant neoplasms in patients with mycosis fungoides and Sezary syndrome: evidence from population-based and clinical cohorts. *Arch Dermatol.* (2007) 143:45–50. doi: 10.1001/archderm.143.1.45

13. Kubica A, Brewer J. Melanoma in immunosuppressed patients. *Mayo Clin Proc.* (2012) 87:991–1003. doi: 10.1016/j.mayocp.2012.04.018

14. McKenna DB, Stockton D, Brewster DH, Doherty VR. Evidence for an association between cutaneous malignant melanoma and lymphoid malignancy: a population-based retrospective cohort study in Scotland. *Br J Cancer.* (2003) 88:74–8. doi: 10.1038/sj.bjc.6600692

15. Singh P, Tomtschik J, Ibrahim S. Increased Incidence of Melanoma in Patients With Multiple Myeloma: A Cross-Sectional Analysis of the Surveillance, Epidemiology, and End Results Database. *Dermatol Surg.* (2022) 48:783–4. doi: 10.1097/DSS.0000000000003478

16. Tashima C. Association of malignant melanoma and malignant lymphoma. *Lancet.* (1973) 2:266. doi: 10.1016/S0140-6736(73)93174-7

17. Travis L, Curtis R, Boice J Jr, Hankey B, Fraumeni J Jr. Second cancers following non-Hodgkin's lymphoma. *Cancer.* (1991) 67:2002–9. doi: 10.1002/1097-0142(19910401)67:7<2002::AID-CNCR2820670729>3.0.CO;2-E

18. Travis L, Curtis R, Hankey B, Fraumeni J Jr. Second cancers in patients with chronic lymphocytic leukemia. *J Natl Cancer Inst.* (1992) 84:1422–7. doi: 10.1093/jnci/84.18.1422

19. Tsimberidou A, Wen S, McLaughlin P, O'Brien S, Wierda W, Lerner S, et al. Other malignancies in chronic lymphocytic leukemia/small lymphocytic lymphoma. *J Clin Oncol.* (2009) 27:904–10. doi: 10.1200/JCO.2008.17.5398

20. Verwer N, Murali R, Winstanley J, Cooper W, Stretch J, Thompson J, et al. Lymphoma occurring in patients with cutaneous melanoma. *J Clin Pathol.* (2010) 63:777–81. doi: 10.1136/jcp.2010.077768

21. Dong C, Hemminki K. Second primary neoplasms among 53 159 haematolymphoproliferative malignancy patients in Sweden, 1958-1996: a search for common mechanisms. *Br J Cancer.* (2001) 85:997–1005. doi: 10.1054/bjoc.2001.1998

22. Khezri F, Brewer J, Weaver A. Merkel cell carcinoma in the setting of chronic lymphocytic leukemia. *Dermatol Surg.* (2011) 37:1100–5. doi: 10.1111/j.1524-4725.2011.02045.x

23. Medina-Franco H, Urist M, Fiveash J, Heslin M, Bland K, Beenken S. Multimodality treatment of Merkel cell carcinoma: case series and literature review of 1024 cases. *Ann Surg Oncol.* (2001) 8:204–8. doi: 10.1007/s10434-001-0204-4

24. Quaglino D, Di Leonardo G, Lalli G, Pasqualoni E, Di Simone S, Vecchio L, et al. Association between chronic lymphocytic leukaemia and secondary tumours: unusual occurrence of a neuroendocrine (Merkell cell) carcinoma. *Eur Rev Med Pharmacol Sci.* (1997) 1:11–6.

25. Safadi R, Pappo O, Okon E, Sviri S, Eldor A. Merkel cell tumor in a woman with chronic lymphocytic leukemia. *Leuk Lymphoma.* (1996) 20:509–11. doi: 10.3109/10428199609052438

26. Vlad R, Woodlock T. Merkel cell carcinoma after chronic lymphocytic leukemia: case report and literature review. *Am J Clin Oncol.* (2003) 26:531–4. doi: 10.1097/01.coc.0000037108.86294.5E

27. Warakaulle D, Rytina E, Burrows N. Merkel cell tumour associated with chronic lymphocytic leukaemia. *Br J Dermatol.* (2001) 144:216–7. doi: 10.1046/j.1365-2133.2001.03996.x

28. Ziprin P, Smith S, Salerno G, Rosin R. Two cases of merkel cell tumour arising in patients with chronic lymphocytic leukaemia. *Br J Dermatol.* (2000) 142:525–8. doi: 10.1046/j.1365-2133.2000.03370.x

29. Ben-David A, Lazarov A, Lev S, Nussbaum B. Merkel cell tumor and chronic lymphocytic leukemia–coincidence or a possible association? *Dermatol Online J.* (2005) 11:16. doi: 10.5070/D31NQ1874G

30. Koljonen V, Kukko H, Pukkala E, Sankila R, Bohling T, Tukiainen E, et al. Chronic lymphocytic leukaemia patients have a high risk of Merkel-cell polyomavirus

DNA-positive Merkel-cell carcinoma. *Br J Cancer.* (2009) 101:1444–7. doi: 10.1038/sj.bjc.6605306

31. Koljonen V, Rantanen M, Sahi H, Mellemkjaer L, Hansen B, Chen T, et al. Joint occurrence of Merkel cell carcinoma and non-Hodgkin lymphomas in four Nordic countries. *Leuk Lymphoma.* (2015) 56:3315–9. doi: 10.3109/10428194.2015.1040010

32. Youlden D, Youl P, Peter Soyer H, Fritschi L, Baade P. Multiple primary cancers associated with Merkel cell carcinoma in Queensland, Australia, 1982-2011. *J Invest Dermatol.* (2014) 134:2883–9. doi: 10.1038/jid.2014.266

33. Howard R, Dores G, Curtis R, Anderson W, Travis L. Merkel cell carcinoma and multiple primary cancers. *Cancer Epidemiol Biomarkers Prev.* (2006) 15:1545–9. doi: 10.1158/1055-9965.EPI-05-0895

34. Brennan P, Scelo G, Hemminki K, Mellemkjaer L, Tracey E, Andersen A, et al. Second primary cancers among 109 000 cases of non-Hodgkin's lymphoma. *Br J Cancer.* (2005) 93:159–66. doi: 10.1038/sj.bjc.6602654

35. Brownell I, Etzel C, Yang D, Taylor S, Duvic M. Increased malignancy risk in the cutaneous T-cell lymphoma patient population. *Clin Lymphoma Myeloma.* (2008) 8:100–5. doi: 10.3816/CLM.2008.n.011

36. Vitiello P, Sica A, Ronchi A, Caccavale S, Franco R, Argenziano G. Primary Cutaneous B-Cell Lymphomas: An Update. *Front Oncol.* (2020) 10:651. doi: 10.3389/fonc.2020.00651

37. Willemze R, Cerroni L, Kempf W, Berti E, Facchetti F, Swerdlow S, et al. The 2018 update of the WHO-EORTC classification for primary cutaneous lymphomas. *Blood.* (2019) 133:1703–14. doi: 10.1182/blood-2018-11-881268

38. Bomze D, Sprecher E, Goldberg I, Samuelov L, Geller S. Primary cutaneous B-cell lymphomas in children and adolescents: A SEER population-based study. *Clin Lymphoma Myeloma Leuk.* (2021) 21:e1000–e5. doi: 10.1016/j.clml.2021.07.021

39. Larkin J, Chiarion-Sileni V, Gonzalez R, Grob J, Rutkowski P, Lao C, et al. Five-Year Survival with Combined Nivolumab and Ipilimumab in Advanced Melanoma. *N Engl J Med.* (2019) 381:1535–46. doi: 10.1056/NEJMoa1910836

40. Robert C, Grob J, Stroyakovskiy D, Karaszewska B, Hauschild A, Levchenko E, et al. Five-Year Outcomes with Dabrafenib plus Trametinib in Metastatic Melanoma. *N Engl J Med.* (2019) 381:626–36. doi: 10.1056/NEJMoa1904059

41. Jaffe E. Navigating the cutaneous B-cell lymphomas: avoiding the rocky shoals. *Mod Pathol.* (2020) 33(Suppl. 1):96–106. doi: 10.1038/s41379-019-0385-7

frontiers | Frontiers in Medicine

TYPE Review
PUBLISHED 29 September 2023
DOI 10.3389/fmed.2023.1218404

OPEN ACCESS

EDITED BY
Mitchell Stark,
The University of Queensland, Australia

REVIEWED BY
Vanessa F. Bonazzi,
The University of Queensland, Australia
Márta Medvecz,
Semmelweis University, Hungary
Harald Oey,
The University of Queensland, Australia

*CORRESPONDENCE
Andrew D. King
✉ andrewking@wayne.edu

RECEIVED 07 May 2023
ACCEPTED 04 September 2023
PUBLISHED 29 September 2023

CITATION
King AD, Deirawan H, Klein PA, Dasgeb B, Dumur CI and Mehregan DR (2023) Next-generation sequencing in dermatology. *Front. Med.* 10:1218404. doi: 10.3389/fmed.2023.1218404

Next-generation sequencing in dermatology

Andrew D. King[1]*, Hany Deirawan[1], Paytra A. Klein[2], Bahar Dasgeb[3], Catherine I. Dumur[4] and Darius R. Mehregan[1]

[1]Department of Dermatology, Wayne State University School of Medicine, Detroit, MI, United States, [2]Albany Medical College, Albany, NY, United States, [3]Department of Surgical Oncology, Rutgers Cancer Institute of New Jersey, New Brunswick, NJ, United States, [4]Bernhardt Laboratories, Sonic Healthcare Anatomic Pathology Division, Jacksonville, FL, United States

Over the past decade, Next-Generation Sequencing (NGS) has advanced our understanding, diagnosis, and management of several areas within dermatology. NGS has emerged as a powerful tool for diagnosing genetic diseases of the skin, improving upon traditional PCR-based techniques limited by significant genetic heterogeneity associated with these disorders. Epidermolysis bullosa and ichthyosis are two of the most extensively studied genetic diseases of the skin, with a well-characterized spectrum of genetic changes occurring in these conditions. NGS has also played a critical role in expanding the mutational landscape of cutaneous squamous cell carcinoma, enhancing our understanding of its molecular pathogenesis. Similarly, genetic testing has greatly benefited melanoma diagnosis and treatment, primarily due to the high prevalence of BRAF hot spot mutations and other well-characterized genetic alterations. Additionally, NGS provides a valuable tool for measuring tumor mutational burden, which can aid in management of melanoma. Lastly, NGS demonstrates promise in improving the sensitivity of diagnosing cutaneous T-cell lymphoma. This article provides a comprehensive summary of NGS applications in the diagnosis and management of genodermatoses, cutaneous squamous cell carcinoma, melanoma, and cutaneous T-cell lymphoma, highlighting the impact of NGS on the field of dermatology.

KEYWORDS

next-generation sequencing, skin cancer, melanoma, squamous cell carcinoma, cutaneous lymphoma, genodermatoses

Introduction

Next,-generation sequencing (NGS) is a high-throughput nucleotide sequencing method that allows simultaneous sequencing of massive amounts of DNA reads in parallel. Since its introduction, NGS has revolutionized the field of genomics as it allows for fast and scalable sequencing of human genomes at a lower cost. The technical capabilities allowed by NGS heralds improvement in clinical diagnostics and is especially exciting in the field of dermatology.

The chain termination method of determining the sequence of nucleotides in a DNA fragment, developed in 1977, was the first DNA sequencing method. Sanger sequencing has over 99.9% accuracy and is considered the gold standard for nucleic acid sequencing (1). However, this method is time-consuming and expensive as it can only sequence small genomic regions (approximately 300 to 1,000 base pairs) at a time (2). This costs approximately $500 USD per megabase amounting to $1.5 million to sequence an entire human genome. These time and cost limitations sparked an increased demand for novel DNA sequencing methods that were faster and

cheaper, which led to the advent of NGS. NGS can sequence an entire human genome for less than $0.50 per megabase (3). Ongoing efforts to drive down the cost have achieved costs as low as $1 per gigabase, resulting in genomes costing $100 to sequence (4). This reduction in time and cost has led to increased access to sequencing technologies and a subsequent explosion in research and clinical diagnostics (5).

With regards to DNA sequencing, techniques can be broadly categorized into three main scales: whole-genome sequencing (WGS), whole-exome sequencing (WES), and targeted sequencing. WGS spans the entire genome and can detect mutations in both protein-coding and non-protein-coding DNA regions (6). WES restricts sequencing to the exome, which targets protein-coding regions, splice junctions, neighboring gene regulatory regions (e.g., promoter, untranslated regions), as well as non-coding RNAs. Exomes comprise approximately 1 % of the genome (5). Since exonic mutations represent most known disease-causing mutations, WES is considered a cost-effective and preferred alternative to WGS (5, 7). Lastly, targeted sequencing involves limiting sequencing to specifically selected sets of genes or genomic regions and is thus cheaper and more commonly used when a specific disease is suspected.

NGS platforms mostly share similar steps, starting with generation of nucleic acid libraries that consist of small fragments of DNA with ligated adapters. The libraries are then amplified and bound to a substrate (e.g., patterned flow cells that contain billions of nanowells), where individual unique DNA fragments form clusters. In the most common method, sequencing by synthesis, the nucleotide sequence is detected through visualization of fluorescence brought on by the addition of a modified nucleotide to a growing DNA strand. This is cyclically repeated for the length of the short DNA fragments spanning 50 to 150 base pairs. Digital sequences collected from sequencing devices are then sent through quality control and mapped to a reference genome. Further analysis can be performed and varies based on the specific application.

In this review, we will review the application of NGS in different areas of dermatology with a focus on clinical studies in genodermatoses, melanoma, keratinocyte carcinoma, and cutaneous lymphoma. Other applications such as use in inflammatory conditions, infectious diseases, and microbiome studies are not included in the scope of this review. Similarly, our discussion is limited to DNA sequencing.

Genodermatoses

The ability of next generation sequencing to resequence the human genome at a massive scale has made a tremendous impact in the area of genetic skin diseases, both in terms of discovery and diagnosis. There has been a plethora of discoveries made with NGS, including identification of underlying somatic mosaic mutations in *IDH1* and *IDH2* in Maffucci syndrome and germline *CHST8* mutations in autosomal recessive peeling skin syndrome (8, 9). NGS has also been used to identify novel genes in genodermatoses with well-established causes, such as the discovery of novel germline *EXPH5* mutations in epidermolysis bullosa (EB) (10). The topic of discovery has been recently reviewed by Chiu and colleagues who show 166 new disease-gene associations, 35 of which were novel uncharacterized diseases between 2009 and 2019 since NGS technology has entered clinical use (11).

The utility of NGS in dermatology clinics for use in diagnosis of genodermatoses has not yet reached its full potential due to limited understanding of the complete genetic basis of hundreds of diverse disorders. One key challenge in the use of NGS in clinical diagnosis is its poor diagnostic yield. Of the first 250 patients referred for whole exome sequencing in a single center in 2011, only 25% yielded a molecular diagnosis (12). This was considered higher than other genetic tests, such as karyotype (5-15%), chromosomal microarray (15-20%), and Sanger sequencing. A recent meta-analysis reported mean rate of diagnosis among 37 studies of genetic disease to be 31% (13).

NGS is increasingly being utilized in dermatology clinics for diagnosing classic Mendelian genodermatoses with well-defined genetic underpinnings, particularly in diseases with skin fragility and disorders of cornification exemplified by epidermolysis bullosa and ichthyosis, respectively. These two categories will be the focus of this section.

Disorders with skin fragility – epidermolysis bullosa

Disorders with skin fragility are a group of genetic skin conditions characterized by peeling or blistering of the skin due to decreased mechanical resilience. Epidermolysis bullosa is the prototypical disease of this group, which is itself a heterogeneous disease divided into four main types and over 30 clinical subtypes. Underlying this disease are up to 21 different genes and up to 47 for the broader group of disorders with skin fragility (14, 15).

Traditionally, the diagnosis of EB has relied on the identification of candidate genes with immunofluorescence antigen mapping (IFM) and transmission electron microscopy (TEM), followed by confirmation using Sanger sequencing. Given the large number of possible genes and difficulty distinguishing between clinical subtypes early in the disease course, diagnosis has required these former steps prior to identification of genetic mutations. However, NGS is an ideal tool enabling parallel sequencing of many genes, which is not feasible with Sanger sequencing. For example, the sequencing of *COL7A1* alone requires more than 70 primer pairs to cover its 118 exons and flaking introns using Sanger sequencing (16). Guidelines for diagnosis of EB have already incorporated NGS in molecular testing of EB (17, 18). Furthermore, retrospective analysis of EB patients in North America has shown increasing use of genetic testing over the past 30 years, with the highest rates since the introduction of NGS (19).

Several studies over the past decade have explored use of NGS in the clinical diagnosis of EB (Table 1). Outside of individual case reports used for discovery of gene mutations, clinical NGS with both WES and targeted sequencing panels were used for diagnosis of EB patients starting in 2015. In one study from the United Kingdom, WES was able to identify pathogenic mutations in all 9 patients for

Abbreviations: NGS, Next-generation sequencing; WGS, Whole-genome sequencing; WES, Whole-exome sequencing; EB, Epidermolysis bullosa; IFM, Immunofluorescence antigen mapping; TEM, Transmission electron microscopy; ARCI, Autosomal recessive congenital ichthyosis; KPI, Keratinopathic ichthyosis; PPKs, Palmoplantar keratodermas; cSCC, Cutaneous Squamous Cell Carcinoma; UV, Ultraviolet; CSD, Cumulative solar damage; TMB, Tumor mutational burden; TCR, T-cell receptor; IHC, Immunohistochemistry; FISH, Fluorescence *in-situ* hybridization; CL, Cutaneous lymphoma; CTCL, Cutaneous T-cell lymphomas; MF, Mycosis Fungoides; SS, Sezary Syndrome; CE, Capillary electrophoresis.

TABLE 1 Epidermolysis bullosa cohorts with clinical NGS testing.

# of patients	Yield	Platform	Panel size (genes)	Region	Reference
138	100%	Targeted	19 *COL17A1, COL7A1, DSP, DST, EXPH5, FERMT1, ITGA3, ITGA6, ITGB4, KLHL24, KRT14, KRT5, LAMA3, LAMB3, LAMC2, PKP1, PLEC, TGM5*	China	(20)
91	84%	Targeted	21 *CD151, CDSN, CHST8, COL17A1, COL7A1, DSP, DST, EXPH5, FERMT1, ITGA3, ITGA6, ITGB4, JUP, KRT14, KRT5, LAMA3, LAMB3, LAMC2, PKP1, PLEC, TGM5*	Iran	(21)
87	94%	Targeted	11 *COL7A1, COL17A1, FERMT1, ITGB4, KRT14, KRT5, LAMA3, LAMB3, LAMC2, PLEC, TGM5*	Brazil	(22)
57	100%	WES	--	China	(23)
43	98%	Targeted	21 *CD151, CDSN, CHST8, COL7A1, COL17A1, DSP, DST, EXPH5, FERMT1, ITGA3, ITGA6, ITGB4, JUP, KRT14, KRT5, LAMA3, LAMB3, LAMC2, PKP1, PLEC1, TGM5*	United States	(24)
40	90%	Targeted	49 *ARHGAP31, CD151, CDSN, CHST8, COL16A1, COL17A1, COL23A1, COL7A1, CSTA, CTGF, DCN, DSC3, DSG1, DSG2, DSG3, DSG4, DSP, DST, EXPH5, FERMT1, FLII, GRIP1, ILK, ITGA2, ITGA3, ITGA5, ITGA6, ITGB1, ITGB4, JUP, KLHL24, KRT14, KRT5, KRT6A, KRT6C, LAMA3, LAMA5, LAMB1, LAMB3, LAMC1, LAMC2, MMP1, NID1, NID2, PKP1, PLEC, SOX18, SOX7, TGM5*	Germany	(25)
21	95%	WES	--	India	(26)
9	100%	WES	--	United Kingdom	(16)
8	100%	Targeted	34 *ATP2A2, CD151, COL17A1, COL1A1, COL7A1, CSTA, DSP, EXPH5, FERMT1, FREM1, GRIP1, ITGA2, ITGA2B, ITGA3, ITGA5, ITGA6, ITGB4, ITGB6, KRT1, KRT10, KRT14, KRT2, KRT5, KRT9, LAMA3, LAMB2, LAMB3, LAMC1, LAMC2, MMP1, PKP1, PLCG2, PLEC, TGM5*	Italy	(27)

10.3389/fmed.2023.1218404

whom biopsy analysis and Sanger sequencing failed (16). Similarly, a group from Italy developed a 34 gene targeted sequencing panel that successfully identified predominately pathogenic germline mutations in all 8 trios with previously unknown genetic diagnoses (27). Of note, the targeted sequencing pipeline allowed identification of mutations in a 72-h procedure by utilizing the low throughput Ion PGM platform.

These early studies paved the way for subsequent studies, including the largest one to date, which utilized a targeted panel of 19 genes and demonstrated a high diagnostic yield with all its 138 patients having pathogenic mutations identified (20). The clinical utility of NGS targeted panel was compared with IFM alone, showing that IFM established EB subtypes in 76% (19 of 25) of cases, while 90% (36 of 40) were diagnosed by NGS (25). This is consistent with a recent retrospective analysis of 771 EB patients showing frequent equivocal findings with IFM compared to NGS (19). Overall, diagnostic yield ranged from 84 to 100% with three WES-based cohorts yielding genetic diagnoses in 95-100% of patients and six targeted sequencing cohorts yielding 84-100% (Table 1). Diagnostic yield for EB is among the highest for NGS among genetic conditions as seen in a study from the University of Minnesota assessing yield of gene panel testing of genetic disease across multiple specialties (28).

Disorders of cornification – ichthyosis and PPK

Disorders of cornification are a category of genetic skin diseases characterized by xerosis, scaling, and/or hyperkeratosis due to abnormal keratinization. Inherited ichthyosis is the prototypical disease with 36 forms divided into syndromic and nonsyndromic forms (29). Nonsyndromic inherited ichthyoses are further subdivided into common ichthyoses, autosomal recessive congenital ichthyosis (ARCI), keratinopathic ichthyosis (KPI), and other. Up to 67 genes have been associated with ichthyosis and 28 genes with palmoplantar keratoderma (30–32).

Inherited ichthyosis and related disorders of cornification represent a diagnostic challenge due to heterogeneity and complex genotype–phenotype relationships. Mutations in different genes may produce similar phenotypes. This is exemplified by mutation screening in ARCI group patients for which 6 genes have been implicated, yet clinically are difficult to distinguish from one another due to overlap between subtypes. Meanwhile, mutations in one gene can also cause different subtypes of ichthyosis. Given the heterogeneity within ichthyoses, genetic testing has been particularly challenging due to the large number of associated genes. Various tests have been used to narrow candidate genes for genetic testing with Sanger sequencing. Traditionally, these include a combination of histopathology, transmission electron microscopy, and biochemical assays.

NGS has been applied in several large clinical cohorts (Table 2). The earliest targeted gene panel utilized microarray capture of probes across 24 genes in 14 patients (36). Of the 14 patients, 10 (71%) yielded pathogenic mutations, the majority of which were not previously reported. The largest study to date includes 1,000 genotyped ichthyosis patients from an international registry (30). In this large cohort, mutations were found in a total of 59 genes with description of 266 novel variants. When targeted sequencing failed to identify pathogenic variants, exome sequencing was performed, yielding a mutation in 87% of patients. The majority of patients were in the ARCI spectrum, among which severity of disease was associated with whether mutations were missense or nonsense.

Several other groups have utilized targeted sequencing panels specially for cohorts of ARCI group patients in United Kingdom, Denmark, Sweden, Iran, Czech Republic, and India (37–41). The diagnostic yield within these cohorts ranged from 79 to 91% with a mean yield of 84%. In the cases where mutations were not identified, one concern was the possibility of missed mutations being in genes outside of those included in the panels. Evidence of this was shown in a study of patients from Iran where the initial 38 gene panel yielded pathogenic mutations in 79% of patients, however when homozygosity mapping and Sanger sequencing of three additional genes more recently associated with ARCI were included, yield was further increased to 83% (39).

Panel sizes varied between studies ranging from 13 genes to 541 genes. Larger panels included genes associated with other genodermatoses not directly related to ichthyoses. Diagnostic yields generally were higher with larger panels, with cohorts showing the highest diagnostic yields being larger than 50 genes (30, 35, 38, 40). Compared to EB, yields were lower with larger panels indicating the greater heterogeneity in ichthyosis.

Palmoplantar keratodermas (PPKs) are a related group of conditions under disorders of cornification, characterized by hyperkeratosis of the palms and soles. One cohort of 64 patients with clinically diagnosed hereditary PPK were tested with either an in-house 35-gene NGS panel, a commercial NGS panel, or WES (42). Only 31 (48%) had a pathogenic mutation identified, with 21 (33%) having variants of unknown significance, and 12 (18%) with no suggestive variants identified.

Squamous cell carcinoma

Cutaneous squamous cell carcinoma (cSCC) is the second most common cutaneous malignancy, comprising about 20% of all skin cancers (43). This results in roughly 1 million cases per year in the United States (44). Two to 5 % of cSCCs metastasize to lymph nodes or distant sites, and those that do have a worse prognosis (43, 45). In the US, cSCC is estimated to be responsible for 9,000 deaths per year (46). The mortality rate is estimated at 1-3 per 100,000 (47). The recent advances in deciphering the molecular biology of cSCC using NGS permits greater insight into pathogenesis and sets the stage for new diagnostic and therapeutic approaches (46, 48). For example, NGS has shown that cSCC is largely driven by mutations in tumor suppressor genes similar to other squamous cell carcinomas (49).

Mutational landscape

The role of UV radiation has been shown to be central to the pathogenesis of cutaneous SCC, both in human and in animal models. Whole exome sequencing of cutaneous SCC and matched normal skin has shown that UV signature C-to-T transition base substitutions to be the most common mutational change in the tumors (50). In cases of squamous differentiation and more importantly in cases of undifferentiated histopathology, detection of the UV damage signature using NGS allows the identification of the source of Carcinoma of unknown primary (51). This has important clinical applications since

TABLE 2 Ichthyosis cohorts with clinical NGS testing.

# of patients	Yield	Platform	Panel size (genes)	Region	Reference
1,000	87%	Targeted & WES	52 *AAGAB, ABCA12, ABHD5, ALDH3A2, ALOX12B, ALOXE3, AQP5, ATP2A2, ATP2C1, CARD14, CDSN, CERS3, CLDN1, CSTA, CYP4F22, DKC1, DSC2, DSG1, DSP, EBP, EDA, FLG, GJA1, GJB2, GJB3, GJB4, GJB6, KANK2, KRT1, KRT10, KRT16, KRT17, KRT2, KRT6C, KRT9, LOR, MBTPS2, NIPAL4, NSDHL, PNPLA1, POGLUT1, RHBDF2, RSPO1, SERPINB7, SLC27A4, SLURP1, SNAP29, SPINK5, SREBF1, STS, TGM1, TRPV3*	USA, Latin Am	(30)
64	83%	Targeted	37 *ABCA12, ABHD5, ALDH3A2, ALOX12B, ALOXE3, AP1S1, C7ORF11, CLDN1, CYP4F22, EBP, ERCC2, ERCC3, GBA, GJB2, GJB3, GJB4, GTF2H5, KRT1, KRT10, KRT2, LIPN, LOR, MBTPS2, NIPAL4, NSDHL, PEX7, PHYH, PNPLA1, POMP, SLC27A4, SNAP29, SPINK5, ST14, STS, SUMF1, TGM1, VPS33B*	Italy	(33)
45	79%	WES	40* *ABCA12, ABHD5, ALOX12B, ALOXE3, AP1S1, CDSN, CERS3, CLDN1, CSTA, CYP4F22, DSG1, EBP, ELOVL4, ERCC2, ERCC3, FLG, GJB2, GJB3, GJB4, GJB6, GTF2H5, KRT1, KRT10, KRT2, KRT9, LIPN, LOR, MBTPS2, NIPAL4, PNPLA1, POMP, SLC27A4, SLURP1, SNAP29, SPINK5, ST14, STS, TGM1, TGM5, TRPV3*	Norway	(34)
35	91%	Targeted	541 Includes following genes: *AAGAB, ABCA12, ABHD5, ALOX12B, ALOXE3, AP1S1, AQP5, ATP2A2, CDSN, CERS3, CLDN1, CSTA, CTSC, CYP4F22, DSG1, DSP, EBP, ELOVL4, ERCC2, ERCC3, FLG, GJB2, GJB3, GJB4, GJB6, GTF2H5, JUP, KRT1, KRT10, KRT14, KRT16, KRT17, KRT2, KRT6A, KRT6B, KRT9, LIPN, LOR, MBTPS2, NIPAL4, PKP1, PNPLA1, POMP, PTEN, RHBDF2, SDR9C7, SERPINB7, SLC27A4, SLURP1, SNAP29, SPINK5, ST14, STS, SULT2B1, TGM1, TGM5, TRPV, TRPV3, WNT10A*	China	(35)
14	71%	Targeted	24 *ABCA12, ABHD5, AP1S1, ALOXE3, ALOX12B, CDSN, CSTA, CYP4F22, DSG1, DSP, GJB2, GJB3, GJB4, KRT1, KRT2, LOR, NIPAL4, POMP, SLC27A4, SLURP1, SPINK5, STS, TGM1, TGM5*	United Kingdom	(36)
146 (ARCI)	83%	Targeted	38 *ABCA12, ABHD5, AGPS, ALDH3A2, ALOX12B, ALOXE3, AP1S1, ARSE, CERS3, CLDN1, CYP4F22, EBP, ELOVL4, GJB2, GJB3, GJB4, GJB6, KRT1, KRT10, KRT2, KRT9, LIPN, LOR, NIPAL4, PEX7, PHYH, PNPLA1, PNPLA2, POMP, SLC27A4, SNAP29, SPINK5, ST14, STS, TGM1, TGM5, VPS33B, ZMPSTE24*	United Kingdom	(37)
132 (ARCI)	85%	Targeted	79 Includes: *ABCA12, ABHD5, ALOX12B, ALOXE3, CERS3, CYP4F22, LIPN, NIPAL4, PNPLA1, SLC27A4, TGM1*	Denmark, Sweden	(38)
125 (ARCI)	79%	Targeted	38 *ABCA12, ABHD5, AGPS, ALDH3A2, ALOX12B, ALOXE3, AP1S1, ARSE, CERS3, CLDN1, CYP4F22, EBP, ELOVL4, GJB2, GJB3, GJB4, GJB6, KRT1, KRT10, KRT2, KRT9, LIPN, LOR, NIPAL4, PEX7, PHYH, PNPLA1, PNPLA2, POMP, SLC27A4, SNAP29, SPINK5, ST14, STS, TGM1, TGM5, VPS33B, ZMPSTE24*	Iran	(39)
34 (ARCI)	91%	Targeted	81 *ABCA12, ABHD5, ALDH3A2, ALOX12B, ALOXE3, AQP5, ATP2A2, BMP1, CALCR, CERS3, COL1A1, COL1A2, COL3A1, COL5A1, COL5A2, COL7A1, COL17A1, CRTAP, CTSC, CYP4F22, DSG1, DSP, DST, EDA, EDAR, EDARADD, EDN3, EDNRB, EXPH5, FBN1, FERMT1, FKBP10, GJB2, IKBKG, ITGA3, ITGA6, ITGB4, JUP, KRT1, KRT2, KRT5, KRT6A, KRT6B, KRT6C, KRT9, KRT10, KRT14, LAMA3, LAMB3, LAMC2, LEMD3, LEPRE1, LIPN, LOR, LRP5, MITF, NIPAL4, OCA2, PAX3, PDLIM4, PKP1, PLEC, PLOD1, PLOD2, PLS3, PNPLA1, PPIB, SERPINF1, SLC45A2, SNAI2, SOX10, SPINK5, STS, TGM1, TGM5, TNXB, TP63, TYR, TYRP1, VDR, WNT1*	Czech Republic	(40)
28 (ARCI)	79%	Targeted	13 *ABCA12, ALOX12B, ALOXE3, CASP14, CERS3, CYP4F22, LIPN, NIPAL4, PNPLA1, SDR9C7, SLC27A4, SULT2B1, TGM1*	India	(41)

*Only 40 ichthyosis-related genes were analyzed for variants of the WES data. ARCI, Autosomal recessive congenital ichthyosis.

10.3389/fmed.2023.1218404

cancer of unknown primaries account for 3-5% of all newly diagnosed advanced cancers (52).

TP53 mutation is one of the first described and most established mutations in the pathogenesis of cSCC. Computational modeling using WES data showed that the loss of the second allele of *TP53* precedes other simple oncogenic mutations (50). Another study employing WES also found that acquisition of TP53 mutation promotes SCC *in-situ* (53). These findings further establish that early loss of *TP53* is an essential step of carcinogenesis in cSCC, similar to many other cancers such ovarian cancer, whether ensued from UV-induced DNA damage or other modes, confirming its driver role. *TP53* is the most frequently reported mutations in metastatic disease and is seen in ranges of 80-100% of patients (54–56).

Schwaederle et al. employed NGS to analyze over 200 genes in a large sample of SCC from different organ systems including the skin and found a common "squamousness gene signatures" consisting of *TP53*, *PIK3CA*, *CCND1*, *CDKN2A*, *SOX2*, *NOTCH1*, and *FBXW7* aberrations (57). They also made the interesting observation that *KRAS* alterations were absent in all types of SCC and that in cutaneous SCC specifically, p53 and Cyclin pathways and PIK3CA/SOX alterations were mutually exclusive. However, cSCC appears to partially differ in the presence of other driver mutations from that of other SCCs. Mutations in the oxidative stress gene *NFE2L2* and *PIK3CA* reported in lung and head and neck squamous cell carcinomas were rarely reported in cSCC (58). The anatomic location of cSCC is also associated with differences in genomic drivers. *KMT2C*, *KMTCD* and *PTCH1* are more common in periocular and eyelid cSCC (59). Human papillomavirus (HPV) infection has been linked to a large proportion of head and neck SCC and to the majority of genital and cervical SCC (60–62). cSCC has been shown to only rarely harbor HPV (63).

CDKN2A has been reported to be an early event in ocular surface and cutaneous SCC (63). It has also been reported in cSCC of the head and neck at a high frequency (64). *MYC* has been reported in precursor lesions along with *CCND1* and *EGFR* gains. NGS has shown that many DNA repair pathways are altered in cSCC. *PIK3C2B* mutations occur at a similar frequency in primary, recurrent and metastatic sSCC suggesting that these mutations are early events that may promote metastatic potential (65). *PIK3CA* have also been reported to be more common in locally advanced sSCC. *PIK3CG* mutation is common in metastatic cSCC (63).

The NOTCH family of receptors constitutes a conserved signaling pathway that has an essential role in epithelial cell fate determination such as proliferation and apoptosis (66). Mutations affecting the *NOTCH1* gene have been found to have differential roles in different human cancers. Activation of *NOTCH1*, whether through direct mutations or pathway activating mutations, are well established in the pathogenesis of lymphoblastic and lymphocytic leukemias (67, 68). On the other hand, *NOTCH1* and *NOTCH2* are genes that have been shown to have tumor suppression functions in human keratinocytes (69). *NOTCH1* and *NOTCH2* mutations have been reported to occur at high frequency in cSCC, shown in studies applying both WES and NGS panels among more than 200 patients combined (50, 54, 64, 70). WGS was used to discover a high frequency of *NOTCH1* and *NOTCH2* mutations in a cohort of 20 patients with advanced cSCC (71). Targeted deep sequencing was used to validate NOTCH mutations in 150 cases of cutaneous squamous neoplasia and confirmed NOTCH mutations in 82% of samples. South, et al. in this study also made the remarkable observation that *NOTCH1* mutations were present in precursor lesions as well. Through sequencing of adjacent and distant normal looking skin and correlation with western blotting and immunohistochemistry, they provided convincing evidence that *NOTCH1* is a main driver mutation occurring early in cSCC carcinogenesis, independent of *TP53* mutations. Zheng et al. confirmed these observations and showed that NOTCH mutations may precede *TP53* mutations in SCC *in-situ* by using WES. They also found that NOTCH loss-of-function mutations enriched in SCC *in-situ* differ from those in the adjacent epidermis. NOTCH mutations are also seen frequently in recurrent and metastatic cSCC and in immunocompromised hosts (49, 56, 65). Zilberg et al. also observed NOTCH1 mutations in non-metastatic cSCC but at a comparatively lower incidence than reported in metastatic cSCC in the literature (64), although their sample size was 10 patients.

Tumor mutational burden (TMB) is another consequence of UV-radiation unique to cutaneous SCC. The mutational burden in non-UV exposed squamous cell carcinoma of the penis is much lower, similar to head and neck and visceral squamous carcinomas (51). Despite the high mutational burden in cSCC, mutations leading to microsatellite instability such as *MLH1* are rare and exclusively seen in younger patients (72).

Epigenetic alterations

Beyond dipyrimidine base substitutions mutations, UV radiation exerts epigenetic changes that directly promote carcinogenesis. Whole transcriptome and targeted RNA sequencing of clinical cSCC showed that *ID4*, a tumor suppressor gene, is downregulated by DNA methylation induced by UVB. The role of *ID4* methylation in promoting development of SCC was then elegantly confirmed using both animal models and *in-vitro* assays (73).

Precursor lesions to cSCC (actinic keratosis and SCC *in-situ*) have been shown to harbor recurrent somatic mutations and copy number changes almost identical to invasive cSCC. A key difference found using whole transcriptome sequencing was significant upregulation of genes promoting invasion including *MMP1*, *MMP3*, *MMP9*, *LAMC2*, *LGALS1*, and *TNFRSF12A* (63). These findings implicate alterations in epigenetic structure and machinery in promoting aggressive and metastatic behavior. Chromatin remodeling and histone modification seem to be shared among squamous cell carcinomas of different tissues of origin (74, 75). WES of primary cSCC and their corresponding metastasis allowed the discovery of *KMT2D* (MLL2) as a preferentially mutated gene in metastatic cSCC (56). *KMT2D* encodes a histone methyltransferase involved in chromatin remodeling and when mutated, it leads to genomic instability (76). In the same cohort, it was shown that other genes involved in epigenetic regulation including *KMT2C* (MLL3), *KMT2A*, *SETD2*, *EP300*, *KDM6A* and *CREBBP*, all previously reported in other visceral malignancies, were mutated in metastatic cSCC at higher rates. *KMT2D* (MLL2) and *KMT2C* (MLL3) have also been reported in primary cSCC (54).

Predicting biologic behavior

Although the majority of cSCC are locally controlled by curative surgery, a subset presents as advanced disease or display aggressive

biologic behavior with distant spread causing significant morbidity and mortality. Although clinical and pathological staging is used to stratify patients' risk and guide therapy, it may not fully capture the risk of aggressive behavior in some early-stage tumors while overestimating the risk of other advanced tumors, as is the case with other cancer (77). For example, tumor thickness has been shown to be the single most significant predictor of metastasis (78). On the other hand, differentiation has often failed to correlate with disease outcome (65).

PI3K/AKT signaling pathway correlates with E-cadherin to N-cadherin expression, a step in epithelial-to-mesenchymal transition that may facilitate metastasis (79). Oncogenic alterations activating the RAS/RTK/PI3K pathway have been reported to be prevalent in approximately half of cSCCs from the head and neck region with lymph nodes metastasis and correlate with a worse progression-free survival (64). Genes implicated in epigenetic regulation such as the KMT2 family have been observed in metastatic disease more frequently. *MSH6* mutation in periocular and eyelid cSCC carries a higher risk of nodal and distant metastasis in periocular and eyelid cSCC (59). DNA repair genes may also serve as a marker for aggressive disease. A systematic review by Lobl et al. found that *P53*, *TERT*, *SPEN*, *MLL3*, and *NOTCH2* mutations were significantly more likely to be found in metastatic versus localized SCCs (46). Lobl et al. noted less mutation concordance between primary and metastatic tumors in immunosuppressed patients supporting that the loss of the anti-tumor immune response promoted metastasis by the loss of immune editing (48). CD274 (PD-L1) amplification was rare in metastatic penile SCC and cSCC (51). Copy number alterations in the 3q chromosome may predict response to immune checkpoint inhibition (65).

Despite the significant insight into the biology of cSCC and potential future applications for prognosis and therapies, current studies have displayed several limitations. Most studies only have 30-40 patients, few studies conducted WES or WGS analyzes, and the source of tissue was also almost always formalin-fixed paraffin-embedded tissue. Almost all studies only sampled the cancer once to obtain genetic materials, which increases the risk of bias given presence of intertumoral heterogeneity. Future studies should focus on amending these limitations and include larger numbers of participants to improve the generalizability and clinical relevance of findings.

Melanoma

Melanoma is a malignant tumor of pigment-forming melanocytes. It is an aggressive cutaneous malignancy, making up 1% of all skin cancers yet accounting for the majority of skin cancer deaths (80). The genetic underpinning of melanoma was established by identification of somatic *BRAF* and germline *CDKN2A* mutations in cutaneous melanoma and familial melanoma, respectively (81–83). *BRAF* is one of the most frequently mutated genes in melanoma, with rates ranging from 20 to 80%, and the hotspot V600E mutation accounting for 60-80% of BRAF mutations (81, 84). Other somatic mutations have also since been identified in melanomas including *TERT*, *NRAS*, *NF1*, and *KIT* in approximately 70-85%, 20-30%, 10-15, and 10% of melanomas, respectively (84–87). Melanomas have traditionally been classified based on histologic type and anatomic location, including superficial spreading melanoma, nodular melanoma, lentigo maligna melanoma, acral lentiginous melanoma, and uveal melanoma. Genomic analysis has demonstrated variation in frequency of somatic mutations differing based on subtype. More recently, classification into nine distinct melanoma evolutionary pathways have been developed based on histologic, clinical, and epidemiological features (88, 89). Somatic *BRAF* mutations are found most frequently in skin with low cumulative solar damage (CSD), which predominately present as superficial spreading melanomas. Meanwhile, melanomas arising in high CSD skin, which present as lentigo maligna melanomas, contain more *NRAS* and *KIT* mutations. Acral melanomas harbor *KIT*, *NRAS*, and *BRAF* mutations, mucosal melanomas *KIT* and *NRAS* mutations, and uveal and melanomas arising in blue nevi uniquely have *GNA11* and *GNAQ* mutations.

Identification of these mutations have resulted in the use of targeted therapies, such as the BRAF inhibitor vemurafenib in melanomas with V600E mutation, which was approved in 2011 (90). Sequencing has been used to detect these mutations, traditionally by real-time PCR-based techniques such as the FDA approved cobas 4,800 BRAF V600 mutation test, which is approved as a companion diagnostic for vemurafenib and cobimetinib. Next-generation sequencing represents a powerful tool that can take advantage of the broadening mutational landscape and is increasingly used in the clinic in the management of melanomas.

While large-scale whole-genome and whole-exome sequencing were used in identifying and cataloging mutations in melanoma, these techniques are impractical for routine use given cost and excessive data requiring customized bioinformatic analysis. Targeted sequencing panels utilize DNA capture technology to select particular genes and genomic loci to resequence. Compared to traditional PCR-based tests, which are designed to test small portions of single genes, sequencing panels can cover the entire span of a gene as well as many genomic loci in parallel. Targeted sequencing represents a middle ground between PCR-based testing of individual loci and whole genome and exome-based comprehensive testing. This allows for efficient testing focused on genes known to be important in disease and actionable targets for therapeutics and has become the preferred molecular test for melanoma.

Next-generation sequencing panels for somatic mutations in melanoma

Many NGS gene panels with various designs have been developed and tested in the past decade. The utility of these panels is exhibited by the high yields, with 70 to 92% of tested melanomas identifying one or more pathogenic mutations (Table 3) (94, 96). Among identified mutations, a large number are actionable with management implications. One study utilizing a panel of 248 genes found that 16 of among 18 patient-derived tumors samples (89%) had actionable mutations including those in *BRAF*, *ALK*, *ERBB4*, *KIT*, and *PIK3CA* (98). Similarly, in a cohort of 36 melanomas from Korea, 92% had an alteration detected and 70% of patients had actionable alterations, which were amenable to treatment with standard or investigational drugs (96). Real-world assessment of actionability showed that melanomas had the highest frequency of actionable alterations among 49 cancer types with 28 of 37 (76%) melanomas harboring actionable alterations based on the OncoKB database (103). Many of these

TABLE 3 Melanoma cohorts with clinical NGS testing.

# of samples	Population	Yield	Panel size (genes)	Reference
699	Cutaneous melanoma (including acral), mucosal melanoma, uveal melanoma; United States (somatic)	556/699 (80%)	46 *ABL1, AKT1, ALK, APC, ATM,* **BRAF**, *CDH1, CDKN2A, CSF1R, CTNNB1, EGFR, ERBB2, ERBB4, FBXW7, FGFR1, FGFR2, FGFR3, FLT3, GNAS, HNF1A, HRAS, IDH1, JAK2, JAK3, KDR, KIT, KRAS, MET, MLH1, MPL, NOTCH1, NPM1,* **NRAS**, *PDGFRA, PIK3CA, PTEN, PTPN11, RB1, RET, SMAD4, SMARCB1, SMO, SRC, STK11,* **TP53**, *VHL*	(91)
132 patients	Cutaneous (including acral lentiginous melanoma, melanoma in blue nevus), uveal melanoma, mucosal melanoma; United Kingdom (somatic)	93/132 (70%)	7 **BRAF**, *GNA11,* **GNAQ**, *KIT, KRAS, MAP2K1,* **NRAS**	(92)
121	Cutaneous melanoma; United States (somatic)	104/121 (86%)	50 *ABL1, AKT1, ALK, APC, ATM,* **BRAF**, *CDH1,* **CDKN2A**, *CSF1R, CTNNB1, EGFR, ERBB2, ERBB4, EZH2, FBXW7, FGFR1, FGFR2, FGFR3, FLT3, GNA11, GNAQ, GNAS, HNF1A, HRAS, IDH1, IDH2, JAK2, JAK3, KDR, KIT, KRAS, MET, MLH1, MPL, NOTCH1, NPM1,* **NRAS**, *PDGFRA, PIK3CA, PTEN, PTPN11, RB1, RET, SMAD4, SMARCB1, SMO, SRC, STK11, TP53, VHL*	(93)
100	Cutaneous melanomas; Spain (somatic)	85/100 (85%)	35 *ADAMST18, ALK, BPA1,* **BRAF**, *CDK4, CDKN2A, EPHA7, ERBB4, GNA11, GNAQ, GRIN2A, GRM3, HOXD8, HRAS, IRS4, KIT, KRAS, MAP2K1, MAP2K2, MC1R, MET, MITF, NF1,* **NRAS**, *PIK3CA, PPP6C,* **PREX2**, *PTEN, RAC1, STK11, STK19, STK31, TAF1L, TERT, TRRRAP*	(94)
71	Mucosal melanomas; Germany (somatic)	50/71 (70%)	29 *ARID1A, ARID2, BAP1,* **BRAF**, *CDK4, CDKN2A, CTNNB1, EZH2, FBXW7, GNA11, GNAQ, HRAS, IDH1, KIT, KRAS, MAP2K1, MAP2K2, MITF,* **NF1**, **NRAS**, *PIK3CA, PIK3R1, PTEN, RAC1, SF3B1, SMARCA4, TERT, TP53, WT1*	(95)
36	*BRAF* wild-type recurred or metastatic melanoma (acral); Korea (somatic)	33/36 (92%)	225 *ABL1, ABL2, AKT1, AKT2, AKT3, ALK, APC, AR, ARAF, ARID1A, ATM, ATR, AURKA, AURKB, AURKC, AXL, BAP1, BARD1, BCL2, BRAF, BRCA1, BRCA2, BRIP1, BTK, CBFB, CBL, CCND1, CCND2, CCND3, CCNE1, CDH1, CDK1, CDK4, CDK6, CDK11B, CDK12, CDKN1A, CDKN1B,* **CDKN2A**, *CDKN2B, CDKN2C, CEBPA, CHEK1, CHEK2, CREBBP, CSF1R, CTNNB1, DDR1, DDR2, DICER1, DNMT3A, DOT1L, DPYD, EGFR, EIF1AX, EMSY, EP300, EPCAM, EPHA3, ERBB2, ERBB3, ERBB4, ERCC2, ERG, ESR1, ETV1, EWSR1, EZH2, FAM175A, FANCA, FANCC, FANCD2, FANCG, FANCI, FANCL, FANCM, FBXW7, FGF3, FGF4, FGF6, FGF10, FGF14, FGF19, FGF23, FGFR1, FGFR2, FGFR3, FGFR4, FLT1, FLT3, FLT4, FOXA1, FOXL2, GNA11, GNAQ, GNAS, GNB2L1, HDAC1, HDAC9, HGF, HRAS, IDH1, IDH2, IGF1R, IGF2, IGFBP3, INPP4B, IRF1, JAK1, JAK2, JAK3, JUN, KDM5C, KDM6A, KDR, KEAP1,* **KIT**, *KMT2D, KRAS, LATS1, LATS2, MAP2K1, MAP2K2, MAP2K4, MAP3K1, MAP3K4, MAPK1, MAPK8, MCL1, MDM2, MDM4, MET, MLH1, MPL, MRE11A, MSH2, MSH6, MTOR, MUTYH, MYC, MYCN, NEK2, NF1, NF2, NFE2L2, NOTCH1, NOTCH2, NOTCH3, NOTCH4, NPM1,* **NRAS**, *NRG1, NTRK1, NTRK2, NTRK3, NUTM1, PAK2, PALB2, PARP1, PARP2, PBRM1, PDGFB, PDGFRA, PDGFRB, PIK3CA, PIK3CB, PIK3CD, PIK3R1, PIK3R2, PMS2, POLD1, POLE, POLQ, PPARG, PPP2R2A, PRKCB, PTEN, RAD21, RAD50, RAD51, RAD51B, RAD51C, RAD51D, RAD54L, RB1, RBM10, RELA, RET, RHEB, RICTOR, RIT1, RNF43, ROS1, RPTOR, RSPO1, SDHB, SDK1, SETD2, SMAD4, SMARCA4, SMARCB1, SMG1, SOX2, SPOP, SQSTM1, SRC, SS18, STAT1, STAT6, STK11, SUMO1, SYK, TERT, TFE3, TOP2A, TP53, TP63, TPMT, TSC1, TSC2, TSHR, UGT1A1, VHL, XRCC2, ZBTB16*	(96)

(Continued)

10.3389/fmed.2023.1218404

TABLE 3 (Continued)

# of samples	Population	Yield	Panel size (genes)	Reference
30	Melanoma metastases; United States (somatic)	30/30 (100%)	182 *ABL1, ABL2, AKT1, AKT2, AKT3, ALK, APC, AR, ARAF, ARFRP1, ARID1A, ATM, ATR, AURKA, AURKB, BAP1, BCL2, BCL2A1, BCL2L1, BCL2L2, BCL6,* **BRAF**, *BRCA1, BRCA2, CARD11, CBL, CCND1, CCND2, CCND3, CCNE1, CD79A, CD79B, CDH1, CDH2, CDH5, CDH20, CDK4, CDK6, CDK8, CDKN2A, CDKN2B, CDKN2C, CEBPA, CHEK1, CHEK2, CRKL, CRLF2, CTNNB1, DDR2, DNMT3A, DOT1L, EGFR, EPHA3, EPHA5, EPHA6, EPHA7, EPHB1, EPHB4, EPHB6, ERBB2, ERBB3, ERBB4, ERCC2, ERG, ESR1, EZH2, FANCA, FBXW7, FGFR1, FGFR2, FGFR3, FGFR4, FLT1, FLT3, FLT4, FOXP4, GATA1, GNA11, GNAQ, GNAS, GPR124, GUCY1A2, HOXA3, HRAS, HSP90AA1, IDH1, IDH2, IGF1R, IGF2R, IKBKE, IKZF1, INHBA, INSR, IRS2, JAK1, JAK2, JAK3, JUN, KDM6A, KDR, KIT, KRAS, LRP1B, LRP6, LTK, MAP2K1, MAP2K2, MAP2K4, MCL1, MDM2, MDM4, MEN1, MET, MITF, MLH1, MLL, MPL, MRE11A, MSH2, MSH6, MTOR, MUTYH, MYC, MYCL1, MYCN,* **NF1**, *NF2, NKX2-1, NOTCH1, NPM1, NRAS, NTRK1, NTRK2, NTRK3, PAK3, PAX5, PDGFRA, PDGFRB, PHLPP2, PIK3CA, PIK3CG, PIK3R1, PKHD1, PLCG1, PRKDC, PTCH1, PTCH2, PTEN, PTPN11, PTPRD, RAF1, RARA, RB1, RET, RICTOR, RPTOR, RUNX1, SMAD2, SMAD3, SMAD4, SMARCA4, SMARCB1, SMO, SOX2, SOX10, SRC, STAT3, STK11, SUFU, TBX22, TET2, TGFBR2, TNFAIP3, TNKS, TNKS2, TOP1,* **TP53**, *TSC1, TSC2, USP9X, VHL, WT1*	(97)
18	Cutaneous melanoma (metastatic); United States (somatic)	16/18 (89%)	248 *ABCB1, ABL1, ABL2, ADRB1, ADRB2, AKT1, AKT2, AKT3, ALK, ALOX5, APC, APC2, AR, ARID1A, ARID1B, ARID2, ARID3A, ARID3B, ARID4A, ARID4B, ARID5A, ARID5B, ASXL1, ATM, ATR, AURKA, BCL2, BCR,* **BRAF**, *BRCA1, BRCA2, BRD4, CBL, CBLB, CCND1, CCNE1, CDC73, CDH1, CDH6, CDK4, CDK6, CDK8, CDKN1A, CDKN1B, CDKN2A, CDKN2B, CEBPA, CHD5, CHEK1, CHEK2, COBRA1, COMT, CREBBP, CRKL, CSF1R, CTNNB1, CYP2A6, CYP2B6, CYP2C8, CYP2C9, CYP2C19, CYP2D6, CYP3A4, CYP3A5, CYP4F2, DNMT3A, DPYD, DRD2, EGFR, EPHA3, EPHA5, EPHA6, EPHA10, EPHB6, ERBB2, ERBB3, ERBB4, ERCC1, ERG, FAM123B, FBXW7, FGFR1, FGFR2, FGFR3, FGFR4, FHIT, FKBP9, FLT1, FLT3, FLT4, FOLR1, G6PD, GATA3, GNA11, GNAQ, GNAS, GSTM1, GSTP1, GSTT1, GUCY1A2, H3F3A, H3F3B, HECW1, HLA-A, HLA-B, HNF1A, HRAS, HSP90AA1, IDH1, IDH2, IGF1R, IKBKE, IKZF1, IL28B, ITPA, JAK1, JAK2, JAK3, JARID2, KCNH2, KCNJ11, KDM5A, KDM5B, KDM5C, KDM6A, KDR, KEAP1,* **KIT**, *KRAS, MAP2K1, MAP2K2, MAP2K4, MAP3K1, MAP3K8, MCL1, MDM2, MDM4, MEN1, MERTK, MET, MITF, MLH1, MLL, MLL2, MLL3, MPL, MRE11A, MSH2, MSH6, MTF2, MTHFR, MTOR, MTUS2, MYC, MYCL1, MYCN, MYD88, NAT2, NF1, NF2, NFE2L2, NKX2-1, NOTCH1, NOTCH2, NOTCH3, NOTCH4, NPM1, NQO1,* **NRAS**, *NTRK1, NTRK2, NTRK3, PAK7, PAX5, PBRM1, PDGFRA, PDGFRB, PDPK1, PHF6, PHF19, PIK3CA, PIK3CD, PIK3R1, PIM1, PLK1, PRKDC, PTCH1, PTEN, PTK2, PTK2B, PTPN11, PTPRD, RAF1, RB1, REL, RET, RICTOR, ROR2, ROS1, RPTOR, RRM1, RUNX1, RUNX1T1, SCN5A, SETD2, SETDB1, SLCO1B1, SMAD2, SMAD3, SMAD4, SMARCA4, SMARCB1, SMO, SOCS1, SPEN, SRC, STAT3, STK11, SUFU, SULT1A1, SUPT4H1, SUPT5H, TCF3, TCF4, TERT, TET1, TET2, TGFBR2, TMPRSS2, TNFAIP3, TNK2, TOP1, TOP2A, TP53, TPMT, TSC1, TSC2, TSHR, TYK2, TYMS, UGT1A1, UTY, VHL, VKORC1, WHSC2, WT1, ZNF668*	(98)

(Continued)

10.3389/fmed.2023.1218404

TABLE 3 (Continued)

# of samples	Population	Yield	Panel size (genes)	Reference
15	Anorectal melanoma; United States (somatic)	14/15 (93%)	467 *ABL1, AKT1, AKT2, AKT3, ALK, ALOX12B, AMER1, APC, AR, ARAF, ARID1A, ARID1B, ARID2, ARID5B, ASXL1, ASXL2, ATM, ATR, ATRX, AURKA, AURKB, AXIN1, AXIN2, AXL, B2M, BAP1, BARD1, BBC3, BCL2L1, BCL2L11, BCL6, BCL11B, BCOR, BCORL1, BCR, BLM, BMPR1A, BRAF, BRCA1, BRCA2, BRCC3, BRD3, BRD4, BRIP1, BTK, BUB1B, CALR, CARD11, CASP8, CBL, CBLB, CBLC, CCND3, CCNE1, CD58, CD74, CD79A, CD79B, CD274, CD276, CDC6, CDC7, CDC45, CDC73, CDCA5, CDH1, CDK4, CDK6, CDK8, CDK12, CDKN1A, CDKN1B, CDKN2A, CDKN2B, CDKN2C, CDT1, CEBPA, CHEK1, CHEK2, CIC, CIITA, CLTC, CLTCL1, CNOT3, CREBBP, CREBBP, CRKL, CRLF2, CRLF2, CSF1R, CSF3R, CTCF, CTLA4, CTNNB1, CUL3, CYLD, DAXX, DCUN1D1, DDB2, DDR2, DICER1, DIS3, DNM2, DNMT1, DNMT3A, DNMT3B, DOT1L, E2F3, ECT2L, EED, EGFL7, EGFR, EIF1AX, EP300, EPCAM, EPHA3, EPHA5, EPHB1, ERBB2, ERBB3, ERBB4, ERCC2, ERCC3, ERCC4, ERCC5, ERG, ESR1, ETV1, ETV4, ETV5, ETV6, EWSR1, EXT1, EXT2, EZH2, EZR, FAM46C, FAM175A, FANCA, FANCC, FANCD2, FANCE, FANCF, FANCG, FAS, FAT1, FBXO11, FBXW7, FGF3, FGF4, FGF19, FGFR1, FGFR2, FGFR3, FGFR4, FH, FIP1L1, FLCN, FLT1, FLT3, FLT4, FOXA1, FOXL2, FOXO1, FUBP1, FUS, FYN, GATA1, GATA2, GATA3, GMNN, GNA11, GNA13, GNAQ, GNAS, GNB1, GOPC, GPC3, GREM1, GRID1, GRIN2A, GSK3B, H3F3A, H3F3C, HGF, HIST1H1C, HIST1H2BD, HIST1H3B, HMGA2, HNF1A, HRAS, ICOSLG, ID3, IDH1, IDH2, IFNGR1, IGF1, IGF1R, IGF2, IKBKE, IL2, IL6ST, IL7R, IL10, INPP4A, INPP4B, INSR, IRF1, IRF4, IRF8, IRS1, IRS2, ITK, JAK1, JAK2, JAK3, JUN, KAT6A, KCNJ5, KDM5C, KDM6A, KDM6B, KDR, KEAP1, KIAA1549, KIF5B,* **KIT**, *KLF4, KLF6, KLHL6, KMT2A, KMT2C, KMT2D, KRAS, LAMB4, LATS1, LATS2, LMO1, LRIG3, LUC7L2, MAP2K1, MAP2K2, MAP2K4, MAP3K1, MAP3K13, MAPK1, MAX, MCL1, MCM2, MCM3, MCM4, MCM5, MCM6, MCM7, MDC1, MDM2, MDM4, MECOM, MED12, MEF2B, MEN1, MET, MITF, MLH1, MLLT10, MPL, MRE11A, MSH2, MSH6, MTOR, MUTYH, MYC, MYCL, MYCN, MYD88, MYOD1, NBN, NCOR1,* **NF1**, *NF2, NFE2L2, NIPBL, NKX2-1, NKX3-1, NOTCH1, NOTCH2, NOTCH3, NOTCH4, NPM1, NRAS, NT5C2, NTRK1, NTRK2, NTRK3, NUP98, NUP214, NUTM1, PAK1, PAK7, PALB2, PARK2, PARP1, PAX5, PAX8, PBRM1, PDCD1, PDGFRA, PDGFRB, PDPK1, PHF6, PHF8, PHOX2B, PICALM, PIGA, PIK3C2G, PIK3C3, PIK3CA, PIK3CB, PIK3CD, PIK3CG, PIK3R1, PIK3R2, PIK3R3, PLAG1, PLK2, PMAIP1, PML, PMS1, PMS2, PNRC1, POLE, POT1, PPARG, PPP2R1A, PRDM1, PRF1, PRKAR1A, PRPF8, PRPF40B, PTCH1, PTEN, PTPN1, PTPN11, PTPRC, PTPRD, PTPRS, PTPRT, PTTG1, RAC1, RAD21, RAD50, RAD51, RAD51B, RAD51C, RAD51D, RAD52, RAD54L, RAF1, RARA, RASA1, RB1, RBM10, RECQL4, REL, RET, RFWD2, RHOA, RICTOR, RIT1, RNF43, ROS1, RPL5, RPL10, RPS6KA4, RPS6KB2, RPTOR, RUNX1, RYBP, SBDS, SDHA, SDHAF2, SDHB, SDHC, SDHD, SETBP1, SETD2, SF1, SF3A1,* **SF3B1**, *SH2B3, SH2D1A, SHQ1, SLC45A3, SMAD2, SMAD3, SMAD4, SMARCA4, SMARCB1, SMARCD1, SMARCE1, SMC1A, SMC3, SMO, SOCS1, SOX2, SOX9, SOX17, SPEN, SPOP, SRC, SRSF2, SS18, SSX1, SSX2, SSX4, STAG1, STAG2, STAG3, STAT3, STAT5B, STAT6, STK11, STK40, SUFU, SUZ12, SYK, TAF15, TBL1XR1, TBX3, TCF3, TCF12, TERT, TET1, TET2, TET3, TFE3, TGFBR1, TGFBR2, TMEM127, TMPRSS2, TNFAIP3, TNFRSF14, TOPBP1,* **TP53**, *TP53BP1, TP63, TPM3, TRAF7, TSC1, TSC2, TSHR, U2AF1, U2AF2, UBR5, USP6, VHL, VTCN1, WAS, WRN, WT1, XIAP, XPA, XPC, XPO1, YAP1, YES1, ZRSR2*	(99)
451 families	Patients with cutaneous and uveal melanomas who had family history of melanoma, but no *CDKN2A* or *CDK4* mutations; Netherlands (germline)	18/451 (4%)	30 *ACD,* **BAP1**, *BRIP1, CBLB, CDK4, CDKN2A, CENPS, CREB3L1, DOT1L, ERCC3, MC1R,* **MITF**, *MLLT6, NEK10, NEK11, NEK2, NEK4, OCA2, PARP1, POLE, POLH, POT1, PTEN, RAD51B, RASEF, TERF1, TERF2IP, TERF2IP, TERT, TINF2*	(100)

(Continued)

10.3389/fmed.2023.1218404

TABLE 3 (Continued)

# of samples	Population	Yield	Panel size (genes)	Reference
264	High risk melanoma patients with family history, other cancers, multiple primary melanomas, or early onset; Czech Republic (germline analysis of peripheral blood)	43/264 (16%)	217 *ABLIM1, ACD, AGR3, APC, APEX1, ARNT, ASIP, ATM, ATRN, AURKA, BAP1, BARD1, BBC3, BLM, BMPR1A, BRAF, BRCA1, BRCA2, BRIP1, BRMS1, CASP8, CASP10, CBL, CCAR2, CCND1, CCNH, CDH1, CDK4, CDK7, CDK10, CDKN1A, CDKN1B, CDKN1C,* **CDKN2A**, *CDKN2B, CEBPA, CHEK2, CLPTM1L, COX8A, CTLA4, CTNNB1, CYP1A1, CYP1A2, CYP3A5, CYP11A1, CYP17A1, CYP19A1, DAB2IP, DCAF4, DDB1, DDB2, EDNRB, EGF, EGFR, EIF1AX, EPCAM, ERBB2, ERBB4, ERCC1, ERCC2, ERCC3, ERCC4, ERCC5, ERCC6, ERCC8, EXOC2, EZH2, FANCC, FANCL, FANCM, FAS, FASLG, FGFR2, FGFR4, FH, FLCN, FLT1, FOXP3, FTO, GATA2, GATA4, GC, GNA11, GNAQ, GPC3, GSTM1, GSTM3, GSTP1, GSTT1, H2AFY, HERC2, HRAS, IDH1, IDH2, IFIH1, IFNA1, IFNG, IL2RA, IL4, IL6, IL8, IL10, ING4, IRF4, KAT6A, KIAA1967, KIT, KMT2A, KRAS, LRIG1, MAP2K1, MC1R, MDM2, MET, MGMT, MITF, MLH1, MLH3, MMP1, MMP3, MSH2, MSH3, MSH6, MTAP, MUTYH, MX2, MYH7B,* **NBN**, *NCOA6, NF1, NF2, NFKB1, NFKBIE, NOD2, NOTCH3, NRAS, OBFC1,* **OCA2**, *PALB2, PARP1, PAX5, PDGFRA, PIGU, PIK3CA, PIK3R1, PIK3R4, PLA2G6, PMAIP1, PMS1, PMS2, POLD1, POLE, POLH, POMC, POT1, PPM1D, PPP6C, PRF1, PTCH1, PTEN, PTGS2, PTPN11, PTPN22, RAC1, RAD23A, RAD23B, RAD51C, RAD51D, RASEF, RB1, RECQL, RECQL4, RET, RHOBTB2, RUNX1, SBDS, SDHA, SDHB, SDHC, SDHD, SETDB1, SF3B1, SH2B3, SLC24A4, SLC45A2, SLX4, SMAD4, SMARCB1, SNX31, STAG2, STK11, STK19, SUZ12, TACC1, TERC, TERF1, TERF2, TERF2IP, TERT, TINF2, TLR3, TP53, TRPM1, TSC1, TSC2, TYR, TYRP1, VDR, VHL, WRN, WT1, XAB2, XPA, XPC, XRCC1, XRCC3, ZNF365*	(101)
102	Melanoma patients with multiple primary melanomas; Italy (germline analysis of peripheral blood)	76/102 (75%)	29 *ACD, AGR3, ARNT, ASIP,* **ATM**, **BAP1**, *CASP8, CCND1, CDK4, CDKAL1, CDKN2A, FTO, GC, IRF4,* **MC1R**, *MITF, MX2, OBFC1, OCA2, PALB2, PARP1, POT1, RMND2, SLC45A2, TERF21P, TERT, TMEM38B, TYR, TYRP1*	(102)

Bolded: Top three mutated genes.

10.3389/fmed.2023.1218404

mutations allowed enrollment of patients into early phase trials targeted toward mutations identified via sequencing panels.

There is heterogeneity with regards to the number of genes and which melanoma genes are included among gene sequencing panels. One retrospective analysis comparing five separate NGS panels found sizes ranging from 50 to 400 genes, with only 23 overlapping genes between the five panels (104). Among our review of the literature, number of genes varied from as few as 7 to as many as 467 genes between studies (Table 3) (92, 99). Often, larger panels exist as general cancer sequencing panels that are used across multiple cancer types and contain general oncogenes not prevalent in melanoma.

The exact composition of the NGS panels vary between groups and play a role in determining sensitivity of the test, particularly for melanoma at special sites. For example, melanomas from acral, mucosal, and uveal sites have been shown to harbor unique mutations. Mutations in *KIT* are enriched at acral and mucosal sites, while mutations in *GNAQ* and *GNA11* are increased among uveal melanomas (86, 105). This was demonstrated in one study with a large cohort of 699 patients, including acral, mucosal, and uveal melanomas sequenced with a 46 gene pan-cancer NGS panel (91). The authors noted a high rate of acral, mucosal, and uveal melanomas with no detected mutations, 33, 44, and 92% respectively, compared to 15% of cutaneous melanomas. This is thought to be due to omission of subtype-specific genes such as *GNAQ*, *GNA11*, and *BAP1* in the panel, decreasing sensitivity of the test. This particular panel also excluded genes such as *TERT*, *NF1*, and *RAC1*, which were contemporaneously identified, further decreasing sensitivity (85, 87).

The current state of NGS sequencing panels has matured with increasing number of commercial panels, some of which have obtained FDA approval. These panels have been developed to capture many gene targets across different cancer types, so called "pan-cancer" panels. Three panels are FDA approved and have been tested on melanoma specimen: MSK-IMPACT, FoundationOne CDx, and PGDx elio tissue complete. The MSK-IMPACT targeted sequencing panel consisting of 468-gene was approved by the FDA in 2017 for tumor profiling and not as a companion diagnostic to any medication (106). Studies utilizing the MSK-IMPACT panel show melanoma to be among the most actionable among various cancers, with rates of actionable mutations ranging from 58 to 76% of clinical samples (103, 107). Similarly, the FoundationOne panel was initially developed with 287 genes and has undergone changes in the panel leading to 324 gene panel approved by the FDA in 2017 as a companion diagnostic for 15 different targeted therapies including BRAF or BRAF/MEK inhibitor combinations (108). The FoundationOne panel in a study of 30 metastatic melanoma cases showed clinically relevant genomic alterations in all patients (Table 3) (97). Lastly, Personal Genome Diagnostics' PDGx elio tissue complete was approved in 2020 containing 505 genes and an automated bioinformatic analysis platform. The platform was validated using a pan-solid tumor sample including 455 melanomas showing high accuracy and concordance for sequence alterations, structural variants, and tumor mutation burden (109).

Next-generation sequencing panels for detection of germline melanoma susceptibility genes

The application of NGS sequencing panels in melanoma also extends to patients at high-risk of developing multiple melanomas due to the presence of germline mutations in melanoma susceptibility genes. *CDKN2A*, which encodes p16(INK4A) and p14(ARF) cell cycle-related tumor suppressors, was the first familial susceptibility gene and among the most highly penetrant with 30-90% risk of melanoma by age 80 years. Other high-to-moderate risk genes include *CDK4*, *BAP1*, *TERT*, *POT1*, *MITF*, *TERF2IP*, and *ACD* (101).

Several studies have utilized NGS panels to investigate the presence of melanoma susceptibility genes among melanoma patients with risk factors (Table 3). Diagnostic yield among ranged widely from 4 to 75%. In one study of 264 Czech melanoma patient indicated for genetic testing due to presence early melanomas (<25 years old), presence of multiple primary melanomas or other cancers in their personal or family history, 71/254 (27%) of patients had a pathogenic or likely pathogenic germline variant identified, 43/264 (16%) carried a mutation in a gene associated with melanoma or other cancer, 9/264 (3%) carried clinically important high-to-moderate melanoma risk genes (*CDKN2A*, *POT1*, *ACD*), and 22/264 (8%) in other cancer syndrome genes (*NBN*, *BRCA1/2*, *CHEK2*, *ATM*, *WRN*, *RB1*) (101). In a separate study of 451 families with no germline *CDKN2A* or *CDK4* mutations, the diagnostic yield was low with only 18/451 (4%) families having pathogenic variants (100). Lastly, an Italian study reported higher diagnostic yield with 76/102 (75%) of patients having at least one pathogenic mutation in *MC1R*, *ATM*, *BAP1*, *CDKN2A*, *PALB2*, or *TYR* (102). This difference is attributed to inclusion of *MC1R*, a low-risk susceptibility gene responsible for pigmentary regulation, as well as the cohort consisting of patients with multiple primary melanomas rather than with family history. Such targeted panels are available as commercial clinical NGS tests for melanoma that are intended for germline testing of susceptibility genes (Table 4). These panels are anticipated to continue to grow as the compendium of known deleterious variants expands and is better characterized.

Other genetic aberrations in melanoma

Tumor mutational burden is defined as the number of non-synonymous mutations per million bases and correlates with the amount of neoantigens in tumors. Immunotherapy with checkpoint inhibitors is more effective in treating tumors with higher levels of this biomarker (110, 111). Early studies utilized WES, however this has been extended to targeted panels (111). NGS panel-based determination of TMB show high concordance between TMB predicted by NGS panels and that using WES (109). The commercial panel FoundationOne CDx reports TMB and has gained approval in 2020 as the companion diagnostic for pembrolizumab with high TMB (>10 mutations/Mb).

One class of driver mutations arise from gene fusions in tumors. Traditionally, gene fusions have been detected at the protein level by immunohistochemistry (IHC), or at the DNA level by fluorescence *in-situ* hybridization (FISH). Even though some DNA-based NGS assays have been developed for the intronic detection of gene fusions, RNA-based NGS has shown higher sensitivity for the detection of fusion transcripts, by sequencing fused exons from different genes (intergenic fusions) or exon skipping (intragenic fusions) (112). In advanced stage non-small cell lung cancer, testing for clinically relevant gene fusions such as those driven by the *ALK* or *ROS1* genes is recommended by national guidelines, since these fusions can be targeted by small

TABLE 4 Commercial NGS testing companies and clinical tests available in the United States.

Company	Genodermatoses		Melanoma susceptibility
	EB	Ichthyosis	
GeneDx	28 *CD151, CDSN, CHST8, COL17A1, COL7A1, CSTA, DSG1, DSP, DST, EXPH5, FERMT1, FLG2, ITGA3, ITGA6, ITGB4, JUP, KLHL24, KRT1, KRT10, KRT14, KRT5, LAMA3, LAMB3, LAMC2, PKP1, PLEC, SERPINB8, TGM5*	49 *ABCA12, ABHD5, ALDH3A2, ALOX12B, ALOXE3, AP1S1, ARSL (ARSE), CASP14, CDSN, CERS3, CHST8, CLDN1, CSTA, CYP4F22, EBP, ELOVL4, FLG, FLG2, GJB2, GJB3, GJB4, GJB6, KDSR, KRT1, KRT10, KRT2, KRT9, LIPN, LOR, MBTPS2, NIPAL4, NSDHL, PEX7, PHGDH, PHYH, PNPLA1, POMP, PSAT1, SDR9C7, SERPINB8, SLC27A4, SNAP29, SPINK5, ST14, STS, TGM1, TGM5, VPS33B, ZMPSTE24*	9 *BAP1, BRCA2, CDK4, CDKN2A, MITF, POT1, PTEN, RB1, TP53*
Fulgent	13 *CD151, COL17A1, COL7A1, DSP, ITGA3, ITGB4, KRT14, KRT5, LAMA3, LAMB3, LAMC2, MMP1, PLEC*	44 *ABCA12, ABHD5, ALDH3A2, ALOX12B, ALOXE3, AP1S1, ARSE, CASP14, CERS3, CLDN1, CRYL1, CYP4F22, EBP, ELOVL4, ERCC2, ERCC3, FLG, GJA1, GJB2, GJB3, GJB4, GJB6, GTF2H5, KRT1, KRT10, KRT2, KRT9, LIPN, LOR, MPLKIP, NIPAL4, PEX7, PHYH, PNPLA1, POMP, SLC27A4, SNAP29, SPINK5, ST14, STS, SUMF1, TGM1, TGM5, VPS33B*	15 *BAP1, BRCA2, CDK4, CDKN2A, CHEK2, MC1R, MITF, MUTYH, POT1, PTEN, RB1, SLC45A2, TERT, TP53, TYR*
Invitae	46* *AAGAB, AQP5, ATP2C1, CAST, CD151, CDSN, COL17A1, COL7A1, CTSC, DSG1, DSP, DST, ENPP1, EXPH5, FERMT1, GJB6, ITGA3, ITGA6, ITGB4, JUP, KANK2, KLHL24, KRT1, KRT10, KRT14, KRT16, KRT17, KRT5, KRT6A, KRT6B, KRT6C, KRT9, LAMA3, LAMB3, LAMC2, LOR, PKP1, PLEC, POMP, RHBDF2, RSPO1, SERPINB7, SERPINB8, SLURP1, TAT, TRPV3*	46 *ABCA12, ABHD5, ALDH3A2, ALOX12B, ALOXE3, AP1S1, AQP5, CAST, CDSN, CERS3, CLDN1, CYP4F22, EBP, ELOVL1, ELOVL4, GJA1, GJB2, GJB3, GJB4, GJB6, KDSR, KRT1, KRT10, KRT2, KRT9, LIPN, LOR, MBTPS2, NIPAL4, PEX7, PHYH, PNPLA1, POMP, SDR9C7, SERPINB7, SERPINB8, SLC27A4, SNAP29, SPINK5, ST14, STS, SULT2B1, SUMF1, TGM1, VPS33B, ZMPSTE24*	9 *BAP1, BRCA2, CDK4, CDKN2A, MITF, POT1, PTEN, RB1, TP53*
Blueprint	26 *ATP2C1, CDSN, COL17A1, COL7A1, CSTA, DSG1, DSG2, DSG4, DSP, DST, EXPH5, FERMT1, GRIP1, ITGA3, ITGA6, ITGB4, KLHL24, KRT1, KRT14, KRT5, LAMA3, LAMB3, LAMC2, PKP1, PLEC, TGM5*	39 *ABCA12, ABHD5, ALDH3A2, ALOX12B, ALOXE3, CASP14, CDSN, CERS3, CSTA, CYP4F22, EBP, ERCC2, FLG, GJA1, GJB2, GJB3, GJB4, KDSR, KRT1, KRT10, KRT2, KRT9, LIPN, LOR, MBTPS2, MPLKIP, NIPAL4, OSMR, PEX7, PHYH, PNPLA1, SDR9C7, SLC27A4, SPINK5, ST14, STS, SUMF1, TGM1, TGM5*	19 *BAP1, BRCA1, BRCA2, CDK4, CDKN2A, DDB2, ERCC2, ERCC3, ERCC4, ERCC5, MITF, POT1, PTCH1, PTEN, SUFU, TP53, WRN, XPA, XPC*
Prevention Genetics	18 *COL17A1, COL7A1, DSP, DST, FERMT1, ITGA3, ITGA6, ITGB4, JUP, KRT10, KRT14, KRT5, LAMA3, LAMB3, LAMC2, PKP1, PLEC, TGM5*	19 *ABCA12, ABHD5, ALOX12B, ALOXE3, AP1S1, CERS3, CLDN1, CYP4F22, KRT1, KRT10, KRT2, KRT9, LIPN, NIPAL4, PNPLA1, POMP, SLC27A4, ST14, TGM1*	10 *BAP1, BRCA2, CDK4, CDKN2A, CHEK2, MITF, POT1, PTEN, RB1, TP53*
CTGT	24 *CAST, CDSN, CHST8, COL17A1, COL7A1, CSTA, DSP, DST, EXPH5, FERMT1, ITGA3, ITGA6, ITGB4, JUP, KLHL24, KRT14, KRT5, LAMA3, LAMB3, LAMC2, PKP1, PLEC, SERPINB8, TGM5*	32 *ABCA12, ALOX12B, ALOXE3, CASP14, CAST, CDSN, CERS3, CHST8, CSTA, CYP4F22, FLG, FLG2, GJA1, GJB3, GJB4, KDSR, KRT1, KRT10, KRT2, KRT83, LIPN, LOR, MBTPS2, NIPAL4, PNPLA1, POMP, SERPINB8, ST14, STS, SULT2B1, TGM1, TGM5*	

*Combined with palmoplantar keratoderma. Numbers show size of gene panel.

molecule inhibitors, such as crizotinib (113). *ALK* fusions have been detected in Spitz nevi, Spitz tumors, and Spitzoid melanomas, allowing to further characterize these diagnostically challenging tumors (114). Beyond *ALK* and *ROS1*, although of rare occurrence, *NTRK1/2/3* rearranged tumors demonstrates remarkable responsiveness to larotrectinib and entrectnib in a tumor type-agnostic manner (115).

Cutaneous lymphoma

Cutaneous lymphomas (CL) are a heterogeneous group of lymphomas that present in the skin. The two main types of CLs are cutaneous T-cell lymphomas (CTCL) and cutaneous B-cell lymphomas (116). CTCL is much more common than cutaneous B-cell lymphomas, with Mycosis Fungoides (MF) and Sezary

Syndrome (SS) representing the most common subtypes of CTCL (117). This section of our review will discuss how NGS has advanced the understanding of CLs by improving its diagnostic sensitivity, therapy response monitoring and prognosis predictions, and identifying possible pathogenic mechanisms and inspiring potential targeted treatment options.

Diagnosis, therapy monitoring, and prognosis predictions

A principal diagnostic test for MF is the T-cell receptor (TCR) clonality assay (118). Polymerase chain reaction (PCR) coupled with capillary electrophoresis (CE) is the most widely used method. However, this PCR-CE method often produces ambiguous results due to the low abundance of clonal T lymphocytes, which results in clonal peaks that are weak and cannot be size-resolved by CE. NGS, on the other hand, has been found to have increased specificity and sensitivity for T-cell clonality detection over previous techniques (119). For example, a study with 35 MF patients found that 85% were found to have a clonal T-cell rearrangement using NGS, compared to just 44% using CE–based detection (118). Additionally, NGS of TCR in MF and SS patients was found to provide increased specificity and sensitivity when compared to flow cytometry and PCR (120).

NGS has also allowed researchers to monitor the therapeutic response and minimal residual disease in CTCL patients, which can significantly improve patient management during the long period of remission that MF and SS patients often enter after bone marrow transplantation (120). Discoveries using NGS technologies have also enhanced prognosis predictions in CTCL. For example, Park et al. used WGS among other genomic analyzes and found PD1 deletions to sufficiently reverse the exhaustion phenotype of T-cells (observed in PD1 wild-type), enhance the proliferation of lymphoma cells, and result in diminished rates of survival (121). In this way, PD1 deletions may now be considered an indication of worse prognosis for CTCL.

Identification of recurrent mutations and signaling pathways with roles in pathogenesis and targeted treatment

Using NGS, researchers have identified numerous genetic mutations in CTCL that have shed light on possible pathogenic mechanisms and potential options for targeted therapy (Table 5). Park et al. used WGS among other genomic analyzes to identify 86 putative driver genes for CTCL, 19 of which had not yet been implicated in CTCL (121). Targeted therapies against these recently identified driver genes may have the potential to improve clinical outcomes for CTCL patients. Another study used targeted sequencing to sequence 585 genes linked to cancer in 71 skin or blood samples from 61 CTCL patients (117). The study identified recurrent mutations in tumor suppressor genes (*TP53*, *FAT1*, *FAT3*), as well as in genes responsible for chromatin remodeling (*ARID1B*), methylation of DNA (*DNMT1*) and histone (*MLL2*, *MLL3*, *KDM6A*), DNA mismatch repair (*MSH3*) and DNA damage response (*ATM*, *MDC1*) (117). All of which may play a role in CTCL pathogenesis. Additionally, Jones et al. used NGS and found CTCL to express signature 7 (123) – a mutational signature that has characteristics of UV induced mutations and is commonly found in malignant skin cancers such as melanoma and squamous carcinoma (125). Signature 7 was found to contribute to 52 and 23% of the mutational burden in MF and SS, respectively (123). In fact, analysis of data from the British 100,000 WGS project found that CTCL cases were the only non-Hodgkin's lymphoma cases to express Signature 7 (123). These findings suggest that UV radiation may play a role in the lymphomagenesis of CTCL. Furthermore, Chang et al. collected and re-analyzed genomic data of 139 patients with MF or SS from seven separate NGS studies and identified 125 genes to be significantly mutated ($p < 0.05$). Notably, *TP53* was one of the most commonly mutated oncogenes and was detected in 19% of cases (122). Furthermore, NGS can also be used to identify germline variants that may increase cancer risk. For example, Gross et al., used NGS to identify a germline *BRCA2* mutation in a pediatric patient with transformed MF. This signifies how NGS has the potential to identify at-risk family members, particularly in families with familial cancer syndromes and germline mutations, so that necessary cancer screening and other risk-reducing measures can be implemented (126).

NGS has also shed light on the numerous altered signaling pathways of CTCL. Chang et al. showed CTCL patients to have mutations in the nuclear factor-kappaB (NF-κB) pathway (122). Constitutive activation of this pathway has been found to be involved in apoptosis resistance in CTCL tumor cells, therefore targeting this pathway may have therapeutic effects (127). In fact, a phase II clinical trial showed Bortezomib, a NF-κB signaling inhibitor, to be well tolerated with an overall response rate of 67% in individuals with relapsed or refractory CTCL (128). In addition, Chang et al. found TP53 and NF-κB gene pathway mutations to be mutually exclusive, suggesting that tumor variants may originate from distinct genetic backgrounds (122). Furthermore, it was found that gene mutations within NF-kB pathway exhibited mutual exclusivity, which indicates that the pathogenesis of CTCL may be induced by only one pathway. Lastly, the researchers found that patients who did not have p53 or NF-κB pathway gene mutations also did not express any other significant mutations. This suggests that lymphomagenesis may be triggered by other significant alterations in the transcriptome or epigenome. Beyond the NF-κB pathway, NGS studies have identified other recurrently altered signaling pathways in CTCL patients which may play a role in CTCL pathogenesis, such as JAK–STAT, PI3K-serine/threonine protein kinases, fibroblast growth factor receptors, and peroxisome proliferator-activated receptors (124).

The use of NGS has allowed for the identification of diverse genetic mutations and has implicated numerous altered signaling pathways to be involved in CTCL pathogenesis. These new insights have the potential of guiding future targeted therapies to improve CTCL patient outcomes.

Discussion and conclusions

NGS has offered distinct advantages to prior genetic testing techniques in applications where numerous genes require sequencing. Given the inherent heterogeneity of genodermatoses and cutaneous malignancies, NGS DNA sequencing offers an efficient means of testing across a large range of possible mutations. Advantages also exist in the ability for digital sequencing results to be quantitated allowing sensitive analysis of clonal cell populations, such as in CTCL.

TABLE 5 Mutations identified using NGS in CTCL.

Mutation category	Mutation	Reference
Tumor suppressor genes	*ARID1A, DNMT3A, MSH2, PDCD1, TMCC1, NR3C1, ATXN1, HLA-B/C, TNFA/P3, FOXO3, AHR, LATS1, EGR3, CDKN2A, HNPRNK, TGFBR1, ZEB1, AGAP6, FAS/PTEN, MGMT, WT1, ATM, CDKN1B, SOCS2, RB1, ZFPM1, TP53, GRAP, ZBTB7A, SBNO2, MAP4K1, PD1, FUBP1, ANO6, BACH2, NFKB2, CTCF, FAT1, FAT3*	(117, 121)
Oncogenes	*IRF4, CARD11, PTPRN2, JAK2/PD-L1/PD-L2, PRKCQ, TP53, PLCG1, FAS, POT1, DNMT3A, KIT, TNFRSF1B, RHOA*	(121, 122)
Hotspot point mutations	*NFKB1, KLF2, JUNB, TBL1XR1*	(121)
Enrichment of mutational signatures	Signature 1 (related to aging), Signature 7 (related to UV induced mutations), Signature 11 (related to alkylating agents), Signature 17 (possibly related to oxidative damage)	(121, 123)
Chromosome arm-level somatic copy number variants (SCNVs)	17p deletion, 10q deletion, 17q amplification in Leukemic CTCLs	(121)
Signaling pathways	• Receptor Tyrosine Kinase (*IRS2, FOXO3*) • JAK/STAT (*JAK3, STAT5A/B, SOCS1*) • NOTCH (*NOTCH1, NOTCH2*) • NF-kB pathway (*PLCG1, CARD11, TNFRSF1B, KIT*) • TP53 pathway • PI3K-serine/threonine protein kinases (*AKT*) • Fibroblast growth factor receptors (*FGFR*) • Peroxisome proliferator-activated receptors (*PPAR*) • T-cell–specific pathways (*MAP4K1, ANO6, GRAP, NR3C1, SBNO2, SOCS2, BACH2, NFKB1, KLF2, JUNB, AHR, ZFMP1, ZBTB7A*)	(117, 121, 122, 124)
DNA damage repair and epigenetic	*ATM, MDC1, MSH3, ARID1B, MLL2, MLL3, KDM6A, DNMT1*	(117)
Miscellaneous	Androgen Receptor (*AR*) (subclonal level)	(117)

The use of NGS for diagnosis of EB and ichthyosis exemplifies the potential applications of NGS for genodermatoses in general. The diagnostic yield in these two groups of genodermatoses has among the highest diagnostic yields among genetic diseases, attributable to the well-characterized mutational spectrum (28). The ability of NGS to sequence across the entire region of many genes in parallel and at great depth allows accurate diagnosis of clinically heterogeneous diseases. Due to the decreasing costs of sequencing and improved ease of workflows, NGS testing is increasingly being considered as the first-line testing for many genodermatoses.

For melanoma, NGS panels have become a powerful tool for molecular characterization. NGS is increasingly being used in the clinical diagnosis and management of melanomas. Melanomas show among the highest yield of actionable targets, attributable to prevalence of hotspot *BRAF* mutations and other well characterized mutations. Furthermore, TMB has further improved NGS's role in management. NGS has shown superiority to traditional Sanger-based diagnostics particularly in the ability to sequence large number of genes in parallel. This is potentially beneficial in avoiding errors due to missed reflex testing of *NRAS* and *KIT* in *BRAF* WT melanomas (129). Compared to Sanger sequencing, NGS shows comparable cost, with one study showing slightly lower cost at €415 EUR per sample versus €465 with conventional testing (94). This is expected to decrease further with improvements in sequencing technology. As with timing, sequencing results are variable depending on the analytical demands on the backend. One study showed completion of NGS panels in three working days, shorter than conventional methods (94). With automated validated analysis, such as with PGDx's platform, turnaround with commercial panels can be as fast as 4-5 days.

Limitations

NGS has some limitations that need to be addressed before it can be widely adopted, including issues with speed, cost, technical limitations, and availability.

In the case of EB, NGS has not entirely supplanted biopsy-based IFM due to limitations including turnaround time. Compared to IFM, which can provide diagnosis within hours to days, NGS techniques, such as WGS and WES in practice takes weeks, while targeted sequencing may be performed more rapidly on the order of days. Current turnaround time for most commercial tests range from 2 to 4 weeks, precluding first-line use of NGS testing in early and severe cases where prompt management and assessment of prognosis is required. This is illustrated in practice by the more frequent use of IFM early in life with severe cases, while genetic testing is used later. The median age genetic analysis was 24.5 months compared to 1.0 month for IFM (19). Optimization of steps can reduce turnaround time as demonstrated in an EB cohort where authors describe a 72-h procedure as well as availability of rapid commercial WES tests with verbal results available in 7 days (27). One of the key bottlenecks regarding timing is analysis and identification of pathogenic variants. While analysis from published reports is often manually intensive, improvement in databases of known pathogenic variants and automation of analysis pipelines can shorten turnaround time.

In terms of increased turnaround time due to the sequencing step, throughput of sequencing platforms is important given the rarity of these conditions where very few samples will be sequenced at a time. Many of the studies reviewed utilize low throughput devices such as the MiSeq (Illumina) and Ion Torrent (Thermo Fisher). Newer

small-scale platforms are being produced that are ideal for targeted sequencing panels. Alternatively, sequencing individual gene panels or exomes can be run together with other applications on high-throughput platform, allowing decreased costs of testing.

Another often cited limitation of NGS testing is cost. While testing costs on the order of hundreds to one thousand United States dollars, these costs are similar if not lower than conventional testing methods. In early estimates of cost, authors in 2012 commented that the cost of WES was similar to skin biopsy analysis with IFM and TEM (130). Other authors noted that the cost of WES was similar to sequencing the *COL7A1* gene locus alone at approximately £900 GBP (16), and that a targeted sequencing panel was estimated to cost even less at €350 EUR (27). Recent cost analysis of targeted sequencing of EB in Brazil noted that while higher in cost compared to IFM (R$ 800 vs. R$ 500 BRL), the greater diagnostic efficiency supported use as first-line diagnostic (131).

There are also technical limitations of NGS in genome coverage. In many studies, large copy number variations were noted to be missed with NGS techniques. In an early study, a patient with previously characterized whole-exon deletion was not detected by NGS (36). One challenge with NGS in melanoma is the choice between whole exome versus targeted panels. While targeted panels are currently optimized for cancer-related genes, detection of structural variants beyond well-established single nucleotide variants is challenging. Structural variants are much more prevalent in mucosal and acral melanomas as shown through whole genome sequencing studies (86, 132). Due to limitations in the detection of genomic events driving melanomas in these locations, techniques with broader coverage are needed. Newer analysis tools with improved performance in calling copy number variations have become available that may allow improved identification.

Finally, availability of testing has been another limitation to NGS testing. The infrastructure needed for NGS testing requires not only sequencing capabilities, but also bioinformatic support. While most studies referred to in this review utilize in-house custom sequencing panels and analysis pipelines, commercial versions of EB, ichthyosis, and several other disease-focused gene panels are available and have been used in published studies (42). Availability of NGS testing for EB is available in at least six commercial labs (GeneDx, Fulgent, Invitae, Blueprint Genetics, Prevention Genetics, CTGT) and several university labs (Table 4). Tests for diseases are listed and searchable at the NIH Genetic Testing Registry.

Wider adoption has been limited by cost and timing of this technique. With improved scale and technological improvements in sequencing platforms, cost has been decreasing, meeting parity with traditional techniques for many applications. Similarly, with improved characterization of the spectrum of genetic mutations as well as improved algorithms for identifying mutations, the timing will also continue to shorten. In practice, know-how of NGS technology is not necessary as many labs and commercial services offer many tests. Among well characterized genodermatoses, such as EB and ichthyosis, specific panels have been curated to allow for high sensitivity testing. Similarly, for malignancies, cancer gene panels allow testing for the most common genetic mutations.

The possible applications of NGS also go well beyond that covered within the scope of this review. Novel applications not covered within the scope of this review also further underscore the utility of NGS, including pre-implantation genetic testing, liquid biopsies testing cell-free tumor DNA in patient serum, as well as whole exome sequencing for neoantigen identification for use in personalized immunotherapy. Beyond DNA sequencing, other techniques exist including sequencing of RNA, which has many applications including improving detection of variants in genodermatoses and malignancies. Other techniques such as DNA methylation, chromatin modification, chromatin accessibility, and single cell sequencing are used frequently in research and have potential applications in clinical Dermatology.

Author contributions

AK, HD, and PK contributed to writing. AK, HD, and DM contributed in conception. All authors contributed to the article and approved the submitted version.

Conflict of interest

The authors declare that the research was conducted in the absence of any commercial or financial relationships that could be construed as a potential conflict of interest.

Publisher's note

References

1. Lier A, Penzel R, Heining C, Horak P, Fröhlich M, Uhrig S, et al. Validating comprehensive next-generation sequencing results for precision oncology: the NCT/DKTK molecularly aided stratification for tumor eradication research experience. *JCO Precis Oncol.* (2018) 2018:1–13. doi: 10.1200/PO.18.00171

2. Kwon E-KM, Basel D, Siegel D, Martin KL. A review of next-generation genetic testing for the dermatologist. *Pediatr Dermatol.* (2013) 30:401–8. doi: 10.1111/pde.12062

3. Behjati S, Tarpey PS. What is next generation sequencing? *Arch Dis Child Educ Pract Ed.* (2013) 98:236–8. doi: 10.1136/archdischild-2013-304340

4. Almogy G, Pratt M, Oberstrass F, Lee L, Mazur D, Beckett N, et al. Cost-efficient whole genome-sequencing using novel mostly natural sequencing-by-synthesis chemistry and open fluidics platform. *bioRxiv*. (2022) 2022:493900. doi: 10.1101/2022.05.29.493900

5. Grada A, Weinbrecht K. Next-generation sequencing: methodology and application. *J Investig Dermatol.* (2013) 133:1–4. doi: 10.1038/jid.2013.248

6. Nakagawa H, Fujita M. Whole genome sequencing analysis for cancer genomics and precision medicine. *Cancer Sci.* (2018) 109:513–22. doi: 10.1111/cas.13505

7. Ross JP, Dion PA, Rouleau GA. Exome sequencing in genetic disease: recent advances and considerations. *F1000Res.* (2020) 9:336. doi: 10.12688/f1000research.19444.1

8. Amary MF, Damato S, Halai D, Eskandarpour M, Berisha F, Bonar F, et al. Ollier disease and Maffucci syndrome are caused by somatic mosaic mutations of IDH1 and IDH2. *Nat Genet.* (2011) 43:1262–5. doi: 10.1038/ng.994

9. Cabral RM, Kurban M, Wajid M, Shimomura Y, Petukhova L, Christiano AM. Whole-exome sequencing in a single proband reveals a mutation in the CHST8 gene in autosomal recessive peeling skin syndrome. *Genomics.* (2012) 99:202–8. doi: 10.1016/j.ygeno.2012.01.005

10. McGrath JA, Stone KL, Begum R, Simpson MA, Dopping-Hepenstal PJ, Liu L, et al. Germline mutation in EXPH5 implicates the Rab27B effector protein Slac2-b in

inherited skin fragility. *Am J Hum Genet*. (2012) 91:1115–21. doi: 10.1016/j.ajhg.2012.10.012

11. Chiu FPC, Doolan BJ, McGrath JA, Onoufriadis A. A decade of next-generation sequencing in genodermatoses: the impact on gene discovery and clinical diagnostics*. *Br J Dermatol*. (2021) 184:606–16. doi: 10.1111/bjd.19384

12. Yang Y, Muzny DM, Reid JG, Bainbridge MN, Willis A, Ward PA, et al. Clinical whole-exome sequencing for the diagnosis of Mendelian disorders. *N Engl J Med*. (2013) 369:1502–11. doi: 10.1056/NEJMoa1306555

13. Clark MM, Stark Z, Farnaes L, Tan TY, White SM, Dimmock D, et al. Meta-analysis of the diagnostic and clinical utility of genome and exome sequencing and chromosomal microarray in children with suspected genetic diseases. *NPJ Genom Med*. (2018) 3:16. doi: 10.1038/s41525-018-0053-8

14. Has C, Liu L, Bolling MC, Charlesworth AV, El Hachem M, Escámez MJ, et al. Clinical practice guidelines for laboratory diagnosis of epidermolysis bullosa. *Br J Dermatol*. (2020) 182:574–92. doi: 10.1111/bjd.18128

15. McDonagh E, McGrath J, Kelsell D, Foulger R, Daugherty L, Stark Z, et al. *Epidermolysis bullosa and congenital skin fragility (Version 1.51)*. PanelApp. (2022). Available at: https://panelapp.genomicsengland.co.uk/panels/554/ (Accessed May 20, 2022).

16. Takeichi T, Liu L, Fong K, Ozoemena L, McMillan JR, Salam A, et al. Whole-exome sequencing improves mutation detection in a diagnostic epidermolysis bullosa laboratory. *Br J Dermatol*. (2015) 172:94–100. doi: 10.1111/bjd.13190

17. Fine J-D, Bruckner-Tuderman L, Eady RAJ, Bauer EA, Bauer JW, Has C, et al. Inherited epidermolysis bullosa: updated recommendations on diagnosis and classification. *J Am Acad Dermatol*. (2014) 70:1103–26. doi: 10.1016/j.jaad.2014.01.903

18. Has C, Bauer JW, Bodemer C, Bolling MC, Bruckner-Tuderman L, Diem A, et al. Consensus reclassification of inherited epidermolysis bullosa and other disorders with skin fragility. *Br J Dermatol*. (2020) 183:614–27. doi: 10.1111/bjd.18921

19. Phillips GS, Huang A, Augsburger BD, Kaplan L, Peoples K, Bruckner AL, et al. A retrospective analysis of diagnostic testing in a large North American cohort of patients with epidermolysis bullosa. *J Am Acad Dermatol*. (2022) 86:1063–71. doi: 10.1016/j.jaad.2021.09.065

20. Chen F, Huang L, Li C, Zhang J, Yang W, Zhang B, et al. Next-generation sequencing through multigene panel testing for the diagnosis of hereditary epidermolysis bullosa in Chinese population. *Clin Genet*. (2020) 98:179–84. doi: 10.1111/cge.13791

21. Vahidnezhad H, Youssefian L, Saeidian AH, Touati A, Sotoudeh S, Abiri M, et al. Multigene next-generation sequencing panel identifies pathogenic variants in patients with unknown subtype of epidermolysis bullosa: subclassification with prognostic implications. *J Investig Dermatol*. (2017) 137:2649–52. doi: 10.1016/j.jid.2017.07.830

22. Mariath LM, Santin JT, Frantz JA, Doriqui MJR, Kiszewski AE, Schuler-Faccini L. An overview of the genetic basis of epidermolysis bullosa in Brazil: discovery of novel and recurrent disease-causing variants. *Clin Genet*. (2019) 96:189–98. doi: 10.1111/cge.13555

23. Yu Y, Wang Z, Mi Z, Sun L, Fu X, Yu G, et al. Epidermolysis bullosa in Chinese patients: genetic analysis and mutation landscape in 57 pedigrees and sporadic cases. *Acta Dermatol Venereol*. (2021) 101:adv00503. doi: 10.2340/00015555-3843

24. Lucky AW, Dagaonkar N, Lammers K, Husami A, Kissell D, Zhang K. A comprehensive next-generation sequencing assay for the diagnosis of epidermolysis bullosa. *Pediatr Dermatol*. (2018) 35:188–97. doi: 10.1111/pde.13392

25. Has C, Küsel J, Reimer A, Hoffmann J, Schauer F, Zimmer A, et al. The position of targeted next-generation sequencing in epidermolysis bullosa diagnosis. *Acta Dermatol Venereol*. (2018) 98:437–40. doi: 10.2340/00015555-2863

26. Nilay M, Saxena D, Mandal K, Moirangthem A, Phadke SR. Novel pathogenic variants in an Indian cohort with epidermolysis bullosa: expanding the genotypic spectrum. *Eur J Med Genet*. (2021) 64:104345. doi: 10.1016/j.ejmg.2021.104345

27. Tenedini E, Artuso L, Bernardis I, Artusi V, Percesepe A, de Rosa L, et al. Amplicon-based next-generation sequencing: an effective approach for the molecular diagnosis of epidermolysis bullosa. *Br J Dermatol*. (2015) 173:731–8. doi: 10.1111/bjd.13858

28. Hartman P, Beckman K, Silverstein K, Yohe S, Schomaker M, Henzler C, et al. Next generation sequencing for clinical diagnostics: five year experience of an academic laboratory. *Mol Genet Metab Rep*. (2019) 19:100464. doi: 10.1016/j.ymgmr.2019.100464

29. Oji V, Tadini G, Akiyama M, Blanchet Bardon C, Bodemer C, Bourrat E, et al. Revised nomenclature and classification of inherited ichthyoses: results of the first ichthyosis consensus conference in Sorèze 2009. *J Am Acad Dermatol*. (2010) 63:20643494:607–41. doi: 10.1016/j.jaad.2009.11.020

30. Sun Q, Burgren NM, Cheraghlou S, Paller AS, Larralde M, Bercovitch L, et al. The genomic and phenotypic landscape of ichthyosis. *JAMA Dermatol*. (2022) 158:16. doi: 10.1001/jamadermatol.2021.4242

31. Takeichi T, Akiyama M. Inherited ichthyosis: non-syndromic forms. *J Dermatol*. (2016) 43:242–51. doi: 10.1111/1346-8138.13243

32. Uitto J, Youssefian L, Saeidian A, Vahidnezhad H. Molecular genetics of keratinization disorders – What's new about ichthyosis. *Acta Dermatol Venereol*. (2020) 100:adv00095. doi: 10.2340/00015555-3431

33. Diociaiuti A, el Hachem M, Pisaneschi E, Giancristoforo S, Genovese S, Sirleto P, et al. Role of molecular testing in the multidisciplinary diagnostic approach of ichthyosis rare skin diseases. *Orphanet J Rare Dis*. (2016) 11:384. doi: 10.1186/s13023-016-0384-4

34. Sitek JC, Kulseth MA, Rypdal KB, Skodje T, Sheng Y, Retterstøl L. Whole-exome sequencing for diagnosis of hereditary ichthyosis. *J Eur Acad Dermatol Venereol*. (2018) 32:1022–7. doi: 10.1111/jdv.14870

35. Cheng R, Liang J, Li Y, Zhang J, Ni C, Yu H, et al. Next-generation sequencing through multi-gene panel testing for diagnosis of hereditary ichthyosis in Chinese. *Clin Genet*. (2020) 97:770–8. doi: 10.1111/cge.13704

36. Scott CA, Plagnol V, Nitoiu D, Bland PJ, Blaydon DC, Chronnell CM, et al. Targeted sequence capture and high-throughput sequencing in the molecular diagnosis of ichthyosis and other skin diseases. *J Investig Dermatol*. (2013) 133:573–6. doi: 10.1038/jid.2012.332

37. Simpson JK, Martinez-Queipo M, Onoufriadis A, Tso S, Glass E, Liu L, et al. Genotype–phenotype correlation in a large English cohort of patients with autosomal recessive ichthyosis. *Br J Dermatol*. (2020) 182:729–37. doi: 10.1111/bjd.18211

38. Hellström Pigg M, Bygum A, Gånemo A, Virtanen M, Brandrup F, Zimmer AD, et al. Spectrum of autosomal recessive congenital ichthyosis in scandinavia: clinical characteristics and novel and recurrent mutations in 132 patients. *Acta Derm Venereol*. (2016) 96:932–7. doi: 10.2340/00015555-2418

39. Youssefian L, Vahidnezhad H, Saeidian AH, Touati A, Sotoudeh S, Mahmoudi H, et al. Autosomal recessive congenital ichthyosis: genomic landscape and phenotypic spectrum in a cohort of 125 consanguineous families. *Hum Mutat*. (2019) 40:288–98. doi: 10.1002/humu.23695

40. Bučková H, Nosková H, Borská R, Réblová K, Pinková B, Zapletalová E, et al. Autosomal recessive congenital ichthyoses in the Czech Republic. *Br J Dermatol*. (2016) 174:405–7. doi: 10.1111/bjd.13918

41. Chiramel MJ, Mathew L, Athirayath R, Chapla A, Sathishkumar D, Mani T, et al. Genotype of autosomal recessive congenital ichthyosis from a tertiary care center in India. *Pediatr Dermatol*. (2022) 39:420–4. doi: 10.1111/pde.14944

42. Harjama L, Karvonen V, Kettunen K, Elomaa O, Einarsdottir E, Heikkilä H, et al. Hereditary palmoplantar keratoderma – phenotypes and mutations in 64 patients. *J Eur Acad Dermatol Venereol*. (2021) 35:1874–80. doi: 10.1111/jdv.17314

43. Waldman A, Schmults C. Cutaneous Squamous Cell Carcinoma. *Hematol Oncol Clin North Am*. (2019) 33:1–12. doi: 10.1016/j.hoc.2018.08.001

44. Rogers HW, Weinstock MA, Feldman SR, Coldiron BM. Incidence estimate of nonmelanoma skin Cancer (keratinocyte carcinomas) in the US population, 2012. *JAMA Dermatol*. (2015) 151:1081. doi: 10.1001/jamadermatol.2015.1187

45. Brougham NDLS, Dennett ER, Cameron R, Tan ST. The incidence of metastasis from cutaneous squamous cell carcinoma and the impact of its risk factors. *J Surg Oncol*. (2012) 106:811–5. doi: 10.1002/jso.23155

46. Lobl MB, Clarey D, Schmidt C, Wichman C, Wysong A. Analysis of mutations in cutaneous squamous cell carcinoma reveals novel genes and mutations associated with patient-specific characteristics and metastasis: a systematic review. *Arch Dermatol Res*. (2022) 314:711–8. doi: 10.1007/s00403-021-02213-2

47. Stang A, Khil L, Kajüter H, Pandeya N, Schmults CD, Ruiz ES, et al. Incidence and mortality for cutaneous squamous cell carcinoma: comparison across three continents. *J Eur Acad Dermatol Venereol*. (2019) 33:6–10. doi: 10.1111/jdv.15967

48. Lobl MB, Clarey DD, Higgins S, Sutton A, Wysong A. Sequencing of cutaneous squamous cell carcinoma primary tumors and patient-matched metastases reveals ALK as a potential driver in metastases and low mutational concordance in immunocompromised patients. *JID Innov*. (2022) 2:100122. doi: 10.1016/j.xjidi.2022.100122

49. Pickering CR, Zhou JH, Lee JJ, Drummond JA, Peng SA, Saade RE, et al. Mutational landscape of aggressive cutaneous squamous cell carcinoma. *Clin Cancer Res*. (2014) 20:6582–92. doi: 10.1158/1078-0432.CCR-14-1768

50. Durinck S, Ho C, Wang NJ, Liao W, Jakkula LR, Collisson EA, et al. Temporal dissection of tumorigenesis in primary cancers. *Cancer Discov*. (2011) 1:137–43. doi: 10.1158/2159-8290.CD-11-0028

51. Jacob JM, Ferry EK, Gay LM, Elvin JA, Vergilio J-A, Ramkissoon S, et al. Comparative genomic profiling of refractory and metastatic penile and nonpenile cutaneous squamous cell carcinoma: implications for selection of systemic therapy. *J Urol*. (2019) 201:541–8. doi: 10.1016/j.juro.2018.09.056

52. Fizazi K, Greco FA, Pavlidis N, Daugaard G, Oien K, Pentheroudakis G, et al. Cancers of unknown primary site: ESMO clinical practice guidelines for diagnosis, treatment and follow-up. *Ann Oncol*. (2015) 26:v133–8. doi: 10.1093/annonc/mdv305

53. Zheng Q, Capell BC, Parekh V, O'Day C, Atillasoy C, Bashir HM, et al. Whole-exome and transcriptome analysis of UV-exposed epidermis and carcinoma in situ reveals early drivers of carcinogenesis. *J Invest Dermatol*. (2021) 141:295–307.e13. doi: 10.1016/j.jid.2020.05.116

54. Jones J, Wetzel M, Brown T, Jung J. Molecular profile of advanced cutaneous squamous cell carcinoma. *J Clin Aesthet Dermatol*. (2021) 14:32–8.

55. Lee CS, Bhaduri A, Mah A, Johnson WL, Ungewickell A, Aros CJ, et al. Recurrent point mutations in the kinetochore gene KNSTRN in cutaneous squamous cell carcinoma. *Nat Genet*. (2014) 46:1060–2. doi: 10.1038/ng.3091

56. Yilmaz AS, Ozer HG, Gillespie JL, Allain DC, Bernhardt MN, Furlan KC, et al. Differential mutation frequencies in metastatic cutaneous squamous cell carcinomas versus primary tumors. *Cancer*. (2017) 123:1184–93. doi: 10.1002/cncr.30459

57. Schwaederle M, Elkin SK, Tomson BN, Carter JL, Kurzrock R. Squamousness: next-generation sequencing reveals shared molecular features across squamous tumor types. *Cell Cycle*. (2015) 14:2355–61. doi: 10.1080/15384101.2015.1053669

58. Lawrence MS, Stojanov P, Mermel CH, Robinson JT, Garraway LA, Golub TR, et al. Discovery and saturation analysis of cancer genes across 21 tumour types. *Nature*. (2014) 505:495–501. doi: 10.1038/nature12912

59. Luo Y, Rao Y, Gu X, Chai P, Yang Y, Lin J, et al. Novel MSH6 mutation predicted metastasis in eyelid and periocular squamous cell carcinoma. *J Eur Acad Dermatol Venereol*. (2022) 36:2331–42. doi: 10.1111/jdv.18454

60. Chakravarthy A, Reddin I, Henderson S, Dong C, Kirkwood N, Jeyakumar M, et al. Integrated analysis of cervical squamous cell carcinoma cohorts from three continents reveals conserved subtypes of prognostic significance. *Nat Commun*. (2022) 13:5818. doi: 10.1038/s41467-022-33544-x

61. Johnson DE, Burtness B, Leemans CR, Lui VWY, Bauman JE, Grandis JR. Head and neck squamous cell carcinoma. *Nat Rev Dis Primers*. (2020) 6:92. doi: 10.1038/s41572-020-00224-3

62. Tessier-Cloutier B, Pors J, Thompson E, Ho J, Prentice L, McConechy M, et al. Molecular characterization of invasive and in situ squamous neoplasia of the vulva and implications for morphologic diagnosis and outcome. *Mod Pathol*. (2021) 34:508–18. doi: 10.1038/s41379-020-00651-3

63. Lazo de la Vega L, Bick N, Hu K, Rahrig SE, Silva CD, Matayoshi S, et al. Invasive squamous cell carcinomas and precursor lesions on UV-exposed epithelia demonstrate concordant genomic complexity in driver genes. *Mod Pathol*. (2020) 33:2280–94. doi: 10.1038/s41379-020-0571-7

64. Li YY, Hanna GJ, Laga AC, Haddad RI, Lorch JH, Hammerman PS. Genomic analysis of metastatic cutaneous squamous cell carcinoma. *Clin Cancer Res*. (2015) 21:1447–56. doi: 10.1158/1078-0432.CCR-14-1773

65. Kacew AJ, Harris EJ, Lorch JH, Haddad RI, Chau NG, Rabinowits G, et al. Chromosome 3q arm gain linked to immunotherapy response in advanced cutaneous squamous cell carcinoma. *Eur J Cancer*. (2019) 113:1–9. doi: 10.1016/j.ejca.2019.03.004

66. Leong KG, Karsan A. Recent insights into the role of Notch signaling in tumorigenesis. *Blood*. (2006) 107:2223–33. doi: 10.1182/blood-2005-08-3329

67. Close V, Close W, Kugler SJ, Reichenzeller M, Yosifov DY, Bloehdorn J, et al. FBXW7 mutations reduce binding of NOTCH1, leading to cleaved NOTCH1 accumulation and target gene activation in CLL. *Blood*. (2019) 133:830–9. doi: 10.1182/blood-2018-09-874529

68. Weng AP, Ferrando AA, Lee W, Morris JP, Silverman LB, Sanchez-Irizarry C, et al. Activating mutations of NOTCH1 in human T cell acute lymphoblastic leukemia. *Science*. (2004) 306:269–71. doi: 10.1126/science.1102160

69. Lefort K, Mandinova A, Ostano P, Kolev V, Calpini V, Kolfschoten I, et al. Notch1 is a p53 target gene involved in human keratinocyte tumor suppression through negative regulation of ROCK1/2 and MRCKalpha kinases. *Genes Dev*. (2007) 21:562–77. doi: 10.1101/gad.1484707

70. Al-Rohil RN, Tarasen AJ, Carlson JA, Wang K, Johnson A, Yelensky R, et al. Evaluation of 122 advanced-stage cutaneous squamous cell carcinomas by comprehensive genomic profiling opens the door for new routes to targeted therapies. *Cancer*. (2016) 122:249–57. doi: 10.1002/cncr.29738

71. South AP, Purdie KJ, Watt SA, Haldenby S, den Breems N, Dimon M, et al. NOTCH1 mutations occur early during cutaneous squamous cell carcinogenesis. *J Invest Dermatol*. (2014) 134:2630–8. doi: 10.1038/jid.2014.154

72. Zilberg C, Lee MW, Yu B, Ashford B, Kraitsek S, Ranson M, et al. Analysis of clinically relevant somatic mutations in high-risk head and neck cutaneous squamous cell carcinoma. *Mod Pathol*. (2018) 31:275–87. doi: 10.1038/modpathol.2017.128

73. Li L, Li F, Xia Y, Yang X, Lv Q, Fang F, et al. UVB induces cutaneous squamous cell carcinoma progression by de novo ID4 methylation via methylation regulating enzymes. *EBioMedicine*. (2020) 57:102835. doi: 10.1016/j.ebiom.2020.102835

74. Chung CH, Guthrie VB, Masica DL, Tokheim C, Kang H, Richmon J, et al. Genomic alterations in head and neck squamous cell carcinoma determined by cancer gene-targeted sequencing. *Ann Oncol*. (2015) 26:1216–23. doi: 10.1093/annonc/mdv109

75. Gao Y-B, Chen Z-L, Li J-G, Hu X-D, Shi X-J, Sun Z-M, et al. Genetic landscape of esophageal squamous cell carcinoma. *Nat Genet*. (2014) 46:1097–102. doi: 10.1038/ng.3076

76. Kantidakis T, Saponaro M, Mitter R, Horswell S, Kranz A, Boeing S, et al. Mutation of cancer driver MLL2 results in transcription stress and genome instability. *Genes Dev*. (2016) 30:408–20. doi: 10.1101/gad.275453.115

77. Gupta N, Weitzman RE, Murad F, Koyfman SA, Smile TD, Chang MS, et al. Identifying Brigham and Women's hospital stage T2a cutaneous squamous cell carcinomas at risk of poor outcomes. *J Am Acad Dermatol*. (2022) 86:1301–8. doi: 10.1016/j.jaad.2021.11.046

78. Brantsch KD, Meisner C, Schönfisch B, Trilling B, Wehner-Caroli J, Röcken M, et al. Analysis of risk factors determining prognosis of cutaneous squamous-cell carcinoma: a prospective study. *Lancet Oncol*. (2008) 9:713–20. doi: 10.1016/S1470-2045(08)70178-5

79. Li B, Xu WW, Lam AKY, Wang Y, Hu H-F, Guan XY, et al. Significance of PI3K/AKT signaling pathway in metastasis of esophageal squamous cell carcinoma and its potential as a target for anti-metastasis therapy. *Oncotarget*. (2017) 8:38755–66. doi: 10.18632/oncotarget.16333

80. Siegel RL, Miller KD, Fuchs HE, Jemal A. Cancer statistics, 2022. *CA Cancer J Clin*. (2022) 72:7–33. doi: 10.3322/caac.21708

81. Davies H, Bignell GR, Cox C, Stephens P, Edkins S, Clegg S, et al. Mutations of the BRAF gene in human cancer. *Nature*. (2002) 417:949–54. doi: 10.1038/nature00766

82. Gruis NA, van der Velden PA, Sandkuijl LA, Prins DE, Weaver-Feldhaus J, Kamb A, et al. Homozygotes for CDKN2 (p16) germline mutation in Dutch familial melanoma kindreds. *Nat Genet*. (1995) 10:351–3. doi: 10.1038/ng0795-351

83. Whelan AJ, Bartsch D, Goodfellow PJ. A familial syndrome of pancreatic Cancer and melanoma with a mutation in the CDKN2 tumor-suppressor Gene. *N Engl J Med*. (1995) 333:975–7. doi: 10.1056/NEJM199510123331505

84. Gutiérrez-Castañeda LD, Nova JA, Tovar-Parra JD. Frequency of mutations in BRAF, NRAS, and KIT in different populations and histological subtypes of melanoma: a systemic review. *Melanoma Res*. (2020) 30:62–70. doi: 10.1097/CMR.0000000000000628

85. Cancer Genome Atlas Network. Genomic classification of cutaneous melanoma. *Cells*. (2015) 161:1681–96. doi: 10.1016/j.cell.2015.05.044

86. Hayward NK, Wilmott JS, Waddell N, Johansson PA, Field MA, Nones K, et al. Whole-genome landscapes of major melanoma subtypes. *Nature*. (2017) 545:175–80. doi: 10.1038/nature22071

87. Krauthammer M, Kong Y, Bacchiocchi A, Evans P, Pornputtapong N, Wu C, et al. Exome sequencing identifies recurrent mutations in NF1 and RASopathy genes in sun-exposed melanomas. *Nat Genet*. (2015) 47:996–1002. doi: 10.1038/ng.3361

88. Bastian BC. The molecular pathology of melanoma: an integrated taxonomy of melanocytic neoplasia. *Annu Rev Pathol*. (2014) 9:239–71. doi: 10.1146/annurev-pathol-012513-104658

89. Elder DE, Bastian BC, Cree IA, Massi D, Scolyer RA. The 2018 World Health Organization classification of cutaneous, mucosal, and uveal melanoma: detailed analysis of 9 distinct subtypes defined by their evolutionary pathway. *Arch Pathol Lab Med*. (2020) 144:500–22. doi: 10.5858/arpa.2019-0561-RA

90. Chapman PB, Hauschild A, Robert C, Haanen JB, Ascierto P, Larkin J, et al. Improved survival with Vemurafenib in melanoma with BRAF V600E mutation. *N Engl J Med*. (2011) 364:2507–16. doi: 10.1056/NEJMoa1103782

91. Siroy AE, Boland GM, Milton DR, Roszik J, Frankian S, Malke J, et al. Beyond BRAF V600: clinical mutation panel testing by next-generation sequencing in advanced melanoma. *J Investig Dermatol*. (2015) 135:508–15. doi: 10.1038/jid.2014.366

92. Reiman A, Kikuchi H, Scocchia D, Smith P, Tsang YW, Snead D, et al. Validation of an NGS mutation detection panel for melanoma. *BMC Cancer*. (2017) 17:150. doi: 10.1186/s12885-017-3149-0

93. Miraflor AP, de Abreu FB, Peterson JD, Turner SA, Amos CI, Tsongalis GJ, et al. Somatic mutation analysis in melanoma using targeted next generation sequencing. *Exp Mol Pathol*. (2017) 103:172–7. doi: 10.1016/j.yexmp.2017.08.006

94. De Unamuno Bustos B, Murria Estal R, Pérez Simó G, de Juan Jimenez I, Escutia Muñoz B, Rodríguez Serna M, et al. Towards personalized medicine in melanoma: implementation of a clinical next-generation sequencing panel. *Sci Rep*. (2017) 7:495. doi: 10.1038/s41598-017-00606-w

95. Cosgarea I, Ugurel S, Sucker A, Livingstone E, Zimmer L, Ziemer M, et al. Targeted next generation sequencing of mucosal melanomas identifies frequent NF1 and RAS mutations. *Oncotarget*. (2017) 8:40683–92. doi: 10.18632/oncotarget.16542

96. Park C, Kim M, Kim MJ, Kim H, Ock CY, Keam B, et al. Clinical application of next-generation sequencing–based panel to BRAF wild-type advanced melanoma identifies key oncogenic alterations and therapeutic strategies. *Mol Cancer Ther*. (2020) 19:937–44. doi: 10.1158/1535-7163.MCT-19-0457

97. Carlson JA, Caldeira Xavier JC, Tarasen A, Sheehan CE, Otto G, Miller VA, et al. Next-generation sequencing reveals pathway activations and new routes to targeted therapies in cutaneous metastatic melanoma. *Am J Dermatopathol*. (2017) 39:1–13. doi: 10.1097/DAD.0000000000000729

98. Jeck WR, Parker J, Carson CC, Shields JM, Sambade MJ, Peters EC, et al. Targeted next generation sequencing identifies clinically actionable mutations in patients with melanoma. *Pigment Cell Melanoma Res*. (2014) 27:653–63. doi: 10.1111/pcmr.12238

99. Yang HM, Hsiao SJ, Schaeffer DF, Lai C, Remotti HE, Horst D, et al. Identification of recurrent mutational events in anorectal melanoma. *Mod Pathol*. (2017) 30:286–96. doi: 10.1038/modpathol.2016.179

100. Potjer TP, Bollen S, Grimbergen AJEM, van Doorn R, Gruis NA, van Asperen CJ, et al. Multigene panel sequencing of established and candidate melanoma susceptibility genes in a large cohort of Dutch non-CDKN2A/CDK4 melanoma families. *Int J Cancer*. (2019) 144:2453–64. doi: 10.1002/ijc.31984

101. Stolarova L, Jelinkova S, Storchova R, Machackova E, Zemankova P, Vocka M, et al. Identification of germline mutations in melanoma patients with early onset, double primary tumors, or family Cancer history by NGS analysis of 217 genes. *Biomedicine*. (2020) 8:404. doi: 10.3390/biomedicines8100404

102. Casula M, Paliogiannis P, Ayala F, De Giorgi V, Stanganelli I, Mandalà M, et al. Germline and somatic mutations in patients with multiple primary melanomas: a next generation sequencing study. *BMC Cancer*. (2019) 19:772. doi: 10.1186/s12885-019-5984-7

103. Schram AM, Reales D, Galle J, Cambria R, Durany R, Feldman D, et al. Oncologist use and perception of large panel next-generation tumor sequencing. *Ann Oncol*. (2017) 28:2298–304. doi: 10.1093/annonc/mdx294

104. Dimitrova M, Kim MJ, Osman I, Jour G. Impact of molecular testing in advanced melanoma on outcomes in a tertiary cancer center and as reported in a publicly available database. *Cancer Rep*. (2021) 4:1380. doi: 10.1002/cnr2.1380

105. Yeh I, Jorgenson E, Shen L, Xu M, North JP, Shain AH, et al. Targeted genomic profiling of Acral melanoma. *J Natl Cancer Inst*. (2019) 111:1068–77. doi: 10.1093/jnci/djz005

106. Cheng DT, Mitchell TN, Zehir A, Shah RH, Benayed R, Syed A, et al. Memorial Sloan Kettering-integrated mutation profiling of actionable cancer targets (MSK-IMPACT): a hybridization capture-based next-generation sequencing clinical assay for solid tumor molecular oncology. *J Mol Diagn*. (2015) 17:251–64. doi: 10.1016/j.jmoldx.2014.12.006

107. Zehir A, Benayed R, Shah RH, Syed A, Middha S, Kim HR, et al. Mutational landscape of metastatic cancer revealed from prospective clinical sequencing of 10,000 patients. *Nat Med*. (2017) 23:703–13. doi: 10.1038/nm.4333

108. Frampton GM, Fichtenholtz A, Otto GA, Wang K, Downing SR, He J, et al. Development and validation of a clinical cancer genomic profiling test based on massively parallel DNA sequencing. *Nat Biotechnol*. (2013) 31:1023–31. doi: 10.1038/nbt.2696

109. Keefer LA, White JR, Wood DE, Gerding KMR, Valkenburg KC, Riley D, et al. Automated next-generation profiling of genomic alterations in human cancers. *Nat Commun*. (2022) 13:2830. doi: 10.1038/s41467-022-30380-x

110. Johnson DB, Frampton GM, Rioth MJ, Yusko E, Xu Y, Guo X, et al. Targeted next generation sequencing identifies markers of response to PD-1 blockade. *Cancer Immunol Res*. (2016) 4:959–67. doi: 10.1158/2326-6066.CIR-16-0143

111. Snyder A, Makarov V, Merghoub T, Yuan J, Zaretsky JM, Desrichard A, et al. Genetic basis for clinical response to CTLA-4 blockade in melanoma. *N Engl J Med*. (2014) 371:2189–99. doi: 10.1056/NEJMoa1406498

112. Matter MS, Chijioke O, Savic S, Bubendorf L. Narrative review of molecular pathways of kinase fusions and diagnostic approaches for their detection in non-small cell lung carcinomas. *Transl Lung Cancer Res*. (2020) 9:2645–55. doi: 10.21037/tlcr-20-676

113. Lindeman NI, Cagle PT, Aisner DL, Arcila ME, Beasley MB, Bernicker EH, et al. Updated molecular testing guideline for the selection of lung Cancer patients for treatment with targeted tyrosine kinase inhibitors: guideline from the College of American Pathologists, the International Association for the Study of Lung Cancer, and the Association for Molecular Pathology. *Arch Pathol Lab Med*. (2018) 142:321–46. doi: 10.5858/arpa.2017-0388-CP

114. Yeh I, de la Fouchardiere A, Pissaloux D, Mully TW, Garrido MC, Vemula SS, et al. Clinical, histopathologic, and genomic features of Spitz tumors with ALK fusions. *Am J Surg Pathol*. (2015) 39:581–91. doi: 10.1097/PAS.0000000000000387

115. Drilon A, Laetsch TW, Kummar S, DuBois SG, Lassen UN, Demetri GD, et al. Efficacy of Larotrectinib in TRK fusion-positive cancers in adults and children. *N Engl J Med*. (2018) 378:731–9. doi: 10.1056/NEJMoa1714448

116. Kheterpal M, Mehta-Shah N, Virmani P, Myskowski PL, Moskowitz A, Horwitz SM. Managing patients with cutaneous B-cell and T-cell lymphomas other than mycosis Fungoides. *Curr Hematol Malig Rep*. (2016) 11:224–33. doi: 10.1007/s11899-016-0322-5

117. Argyropoulos KV, Horwitz SM, Rapaport F, Velardi E, Myskowski P, Querfeld C, et al. High-depth, targeted, next generation sequencing identifies novel genetic alterations in cutaneous T-cell lymphoma. *Blood*. (2015) 126:1485–5. doi: 10.1182/blood.V126.23.1485.1485

118. Sufficool KE, Lockwood CM, Abel HJ, Hagemann IS, Schumacher JA, Kelley TW, et al. T-cell clonality assessment by next-generation sequencing improves detection sensitivity in mycosis fungoides. *J Am Acad Dermatol*. (2015) 73:228–236.e2. doi: 10.1016/j.jaad.2015.04.030

119. Fujii K, Kanekura T. Next-generation sequencing Technologies for Early-Stage Cutaneous T-cell lymphoma. *Front Med (Lausanne)*. (2019) 6:181. doi: 10.3389/fmed.2019.00181

120. Weng W-K, Armstrong R, Arai S, Desmarais C, Hoppe R, Kim YH. Minimal residual disease monitoring with high-throughput sequencing of T cell receptors in cutaneous T cell lymphoma. *Sci Transl Med*. (2013) 5:7420. doi: 10.1126/scitranslmed.3007420

121. Park J, Daniels J, Wartewig T, Ringbloom KG, Martinez-Escala ME, Choi S, et al. Integrated genomic analyses of cutaneous T-cell lymphomas reveal the molecular bases for disease heterogeneity. *Blood*. (2021) 138:1225–36. doi: 10.1182/blood.2020009655

122. Chang L-W, Patrone CC, Yang W, Rabionet R, Gallardo F, Espinet B, et al. An integrated data resource for genomic analysis of cutaneous T-cell lymphoma. *J Investig Dermatol*. (2018) 138:2681–3. doi: 10.1016/j.jid.2018.06.176

123. Jones CL, Degasperi A, Grandi V, Amarante TD, Ambrose JC, Arumugam P, et al. Spectrum of mutational signatures in T-cell lymphoma reveals a key role for UV radiation in cutaneous T-cell lymphoma. *Sci Rep*. (2021) 11:3962. doi: 10.1038/s41598-021-83352-4

124. Mirza A-S, Horna P, Teer JK, Song J, Akabari R, Hussaini M, et al. New insights into the complex mutational landscape of Sézary syndrome. *Front Oncol*. (2020) 10:514. doi: 10.3389/fonc.2020.00514

125. Alexandrov LB, Nik-Zainal S, Wedge DC, Aparicio SAJR, Behjati S, Biankin AV, et al. Signatures of mutational processes in human cancer. *Nature*. (2013) 500:415–21. doi: 10.1038/nature12477

126. Gross AM, Turner J, Kirkorian AY, Okoye GA, Luca DC, Bornhorst M, et al. A pediatric case of transformed mycosis Fungoides in a BRCA2 positive patient. *J Pediatr Hematol Oncol*. (2020) 42:e361–4. doi: 10.1097/MPH.0000000000001481

127. Sors A, Jean-Louis F, Pellet C, Laroche L, Dubertret L, Courtois G, et al. Down-regulating constitutive activation of the NF-κB canonical pathway overcomes the resistance of cutaneous T-cell lymphoma to apoptosis. *Blood*. (2006) 107:2354–63. doi: 10.1182/blood-2005-06-2536

128. Zinzani PL, Musuraca G, Tani M, Stefoni V, Marchi E, Fina M, et al. Phase II trial of proteasome inhibitor Bortezomib in patients with relapsed or refractory cutaneous T-cell lymphoma. *J Clin Oncol*. (2007) 25:4293–7. doi: 10.1200/JCO.2007.11.4207

129. Fisher KE, Zhang L, Wang J, Smith GH, Newman S, Schneider TM, et al. Clinical validation and implementation of a targeted next-generation sequencing assay to detect somatic variants in non-small cell lung, melanoma, and gastrointestinal malignancies. *J Mol Diagn*. (2016) 18:299–315. doi: 10.1016/j.jmoldx.2015.11.006

130. Cho RJ, Simpson MA, McGrath JA. Next-generation diagnostics for Genodermatoses. *J Investig Dermatol*. (2012) 132:E27–8. doi: 10.1038/skinbio.2012.8

131. Mariath LM, Kiszewski AE, Frantz JA, Siebert M, Matte U, Schuler-Faccini L. Gene panel for the diagnosis of epidermolysis bullosa: proposal for a viable and efficient approach. *An Bras Dermatol*. (2021) 96:155–62. doi: 10.1016/j.abd.2020.05.015

132. Furney SJ, Turajlic S, Stamp G, Nohadani M, Carlisle A, Thomas JM, et al. Genome sequencing of mucosal melanomas reveals that they are driven by distinct mechanisms from cutaneous melanoma. *J. Pathol*. (2013) 230:261–9. doi: 10.1002/path.4204

frontiers | Frontiers in Medicine

TYPE Original Research
PUBLISHED 09 October 2023
DOI 10.3389/fmed.2023.1265827

OPEN ACCESS

EDITED BY
Laura Atzori,
University of Cagliari, Italy

REVIEWED BY
Luca Pilloni,
University of Cagliari, Italy
Giorgio Filosa,
Retired, Jesi, Italy

*CORRESPONDENCE
Darius Mehregan
✉ dmehregan@wayne.edu

RECEIVED 24 July 2023
ACCEPTED 18 September 2023
PUBLISHED 09 October 2023

CITATION
Warbasse E, Mehregan D, Utz S, Stansfield RB and Abrams J (2023) PRAME immunohistochemistry compared to traditional FISH testing in spitzoid neoplasms and other difficult to diagnose melanocytic neoplasms. *Front. Med.* 10:1265827. doi: 10.3389/fmed.2023.1265827

PRAME immunohistochemistry compared to traditional FISH testing in spitzoid neoplasms and other difficult to diagnose melanocytic neoplasms

Elizabeth Warbasse[1], Darius Mehregan[2]*, Sarah Utz[3], R. Brent Stansfield[4] and Judith Abrams[5]

[1]Department of Dermatology and Cutaneous Surgery, University of South Florida Morsani College of Medicine, Tampa, FL, United States, [2]Department of Dermatology, Wayne State University School of Medicine, Detroit, MI, United States, [3]Essentia Health, Duluth, MN, United States, [4]Office of Graduate Medical Education, Wayne State University School of Medicine, Detroit, MI, United States, [5]Wayne State University School of Medicine, Detroit, MI, United States

PRAME (PReferentially expressed Antigen in Melanoma) is a gene first identified in melanoma. It has been proposed as a useful marker to differentiate melanoma from benign melanocytic neoplasms. Recently genomic testing using fluorescence *in situ* hybridization has been used to aid in the diagnosis of difficult melanocytic neoplasms. We have compared PRAME staining to FISH testing results in 83 difficult to classify melanocytic neoplasms which showed spitzoid histologic features. A relatively low sensitivity of 29.6% and high specificity of 76.8% is seen with PRAME staining as compared to genomic testing with fluorescence *in situ* hybridization. This study highlights the limitations of PRAME staining in spitzoid neoplasms.

KEYWORDS

PRAME, immunohistochemistry, dermatopathology, fluorescence *in situ* hybridization, Spitz, melanoma, melanocytic neoplasms

1. Introduction

PRAME (Preferentially expressed Antigen in Melanoma) is a gene that was first identified via analysis of genetic material from a melanoma patient in 1997; it is found in melanoma cells, as well as in the normal tissues of the testes, and to a smaller degree, endometrium, ovaries, and the adrenal glands (1). Squamous cell carcinomas of the lung, some sarcomas, and acute leukemias may also be positive for PRAME, which has led to its use as a potential target for immunotherapy (1, 2). In the field of dermatopathology, PRAME immunohistochemical stain has been proposed as a tool to identify melanoma cells in skin biopsies. This study aims to investigate the utility of PRAME immunohistochemical staining in difficult to diagnose melanocytic neoplasms, particularly spitzoid neoplasms.

Fluorescence *in-situ* hybridization (FISH) genomic testing in spitzoid and other difficult melanocytic neoplasms has been shown to have a sensitivity of up to 97.6% and a specificity of 72.7% (3). However, it is costly and time consuming, thus not always utilized in making the diagnosis of melanoma, which has long relied upon histopathology. FISH testing may be correlated with histopathologic assessment in these difficult to diagnose cases. Prior studies

have demonstrated that the PRAME gene has been shown to be expressed in 13.6% of nonmalignant melanocytic nevi (4). This presents a potential pitfall in the specificity of PRAME diagnostic utility. In addition, the number of studies involving difficult to classify melanocytic neoplasms and PRAME staining is small. Studies to determine whether PRAME expression in malignant and non-malignant melanocytic lesions such as dysplastic nevi, melanoma, and Spitz nevi correlates with the results of genomic testing are also small in number with some conflicting results. Lezcano et al. recently found 90% concordance between PRAME immunohistochemistry and cytogenetic study results in diagnostically difficult melanocytic neoplasms (including atypical Spitz tumor/nevus versus spitzoid melanoma, dysplastic nevus versus melanoma, and traumatized or mitotically active nevus versus melanoma) and concluded that it may be a useful ancillary test in this subset (5). Contrastingly, Raghavan et al. concluded that caution must be exercised when interpreting the results of PRAME immunohistochemistry in spitzoid neoplasms (6). Googe et al. found that while the majority of invasive melanomas in their study were PRAME positive (either focally or diffusely), 16% were entirely PRAME negative, raising further concerns over the reliability of PRAME (7). They also found 73% of Spitz nevi in their sample to be PRAME negative.

An additional area of discrepancy in the literature is the interpretation of PRAME positivity, with multiple approaches documented. The predominant approach seems to be that of Lezcano et al. which utilizes a scale of 0 to 4+ to grade the percentage of PRAME positive melanocytes, with 4+ representing "diffusely positive" with greater than 75% of melanocytes staining for PRAME (8). Googe et al. additionally commented on categorization as focally or diffusely positive PRAME staining, with 1+ to 3+ staining considered focally positive and 4+ considered diffusely positive (7). Umano et al. broke from the precedent of the 0–4+ PRAME positivity scale, and instead utilized a scale of 1+ to 3+, with 1+ considered slightly positive to 3+ considered intense positivity; they also commented on the location of the PRAME positive cells as junctional versus intradermal (9). Meanwhile, Raghavan et al. defined greater than 60% of positively staining melanocytes as PRAME positivity and also commented on intensity of the stain (6).

The purpose of this study is to contribute to the existing scientific literature, which at present demonstrates some caution over the utility and reliability of the use of PRAME as a screening or ancillary test for melanocytic lesions, particularly with regard to difficult spitzoid melanocytic neoplasms.

2. Methods

Samples were collected from the slide archive at Pinkus Dermatopathology Laboratory under an IRB-approved protocol based on a previous diagnosis of atypical spitz nevus, spitz nevus, spitzoid melanoma, or atypical compound melanocytic neoplasm. Exclusion criteria included insufficient tissue sample for study or absence of prior FISH cytogenetic testing. Inclusion criteria were biopsy specimens with a previous diagnosis of spitzoid melanoma, atypical spitzoid neoplasms or Spitz nevus with previous FISH testing. Archived cases which had undergone FISH testing were reviewed. Classical Spitz nevi in children which typically do not require ancillary testing were not included. Cases with a spitzoid morphology including epithelioid melanocytes, epidermal hyperplasia and clefting of the epidermis around the junctional nests but lacking sharp lateral circumscription or maturation with depth which had been sent for ancillary FISH testing were included. All lesions had a dermal component that showed a lack of maturation with depth. Spindle cell nevus of Reed and desmoplastic spitz nevi were not included. The final diagnosis was made by a combination of histologic findings and FISH results. These included Spitz nevi in adults, atypical Spitz nevi/atypical spitz tumors, and spitzoid melanomas.

A total of 83 spitzoid and atypical compound neoplasms were included for study. All had previously had FISH cytogenetic testing for melanoma performed. PRAME immunohistochemistry was performed on all samples, with nodular melanoma used as a control. Four micrometer tissue sections were treated with high pH 8 epitope retrieval for 10 min. The sections were stained with PRAME (Cell Marque clone EP46, Rocklin CA) for 15 minutes and detected using the Leica Bond III system with red chromogen (Deer Park, Ill). p16 staining was also performed in 21 of the cases.

2.1. PRAME immunohistochemistry

The staining pattern for PRAME antibody was investigated in non-malignant and difficult to diagnose melanocytic lesions, predominately those with spitzoid features including nests of epithelioid or spindle cell melanocytes, clefting around nests of melanocytes and epidermal hyperplasia. We correlated and compared PRAME results with previously obtained FISH analyses, as well as with staining in nodular melanoma and normal skin as positive and negative controls, respectively.

Investigators were blinded to the corresponding FISH results of each sample when quantifying the percentage of melanocytes staining positively for PRAME. The number of PRAME positive staining melanocytes in a square millimeter were counted in each sample by two independent researchers and then classified into a five-part scale based on the precedent set by Lezcano et al. (8). Samples with zero positively staining melanocytes were classified as negative (0); samples with staining of greater than zero through 25% of tumor cells are classified as 1+, staining of greater than 25% through 50% of tumor cells is considered 2+, staining of greater than 50% through 75% of tumor cells staining is 3+, and greater than 75% or more melanocytes staining is labeled as 4+ or "diffuse."

Individuals whose PRAME results were 0 or 1+ were classified as PRAME negative, as in Figure 1; those whose results were 2+–4+ were classified as PRAME positive, as in Figures 2–5.

2.2. Fluorescence *in situ* hybridization

The PRAME scale results were then correlated with the genomic testing results for each sample. Each sample had a pre-existing NeoSITE™ Melanoma FISH analysis performed by NeoGenomics, which included the genes RREB1 (6p25), cMYC (8q24), CDKN2A (p16)/CEN9, and CCND1 (11q13). The high stringency cutoff for a positive result with this test is >29% for any probe, whereas the low stringency cutoffs for "borderline positive" results are less than 29% of cells with RREB (6p25) gain but greater than 16%, cMYC (8q24) gain in greater than 10%, CDKN2A (p16)/CEN9 homozygous deletion in

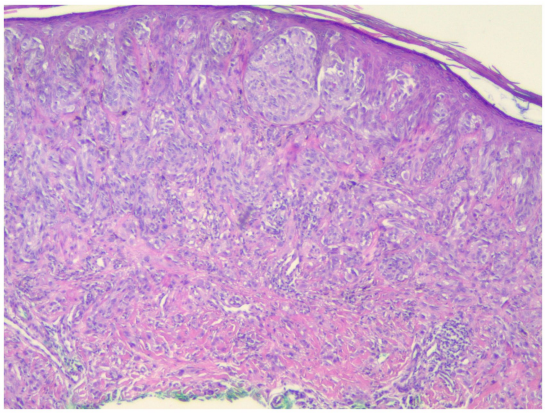

FIGURE 1
This spitzoid melanoma failed to stain with PRAME but was positive by FISH (H&E; 40×).

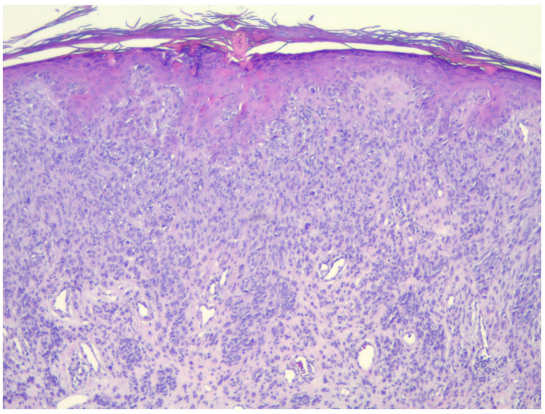

FIGURE 3
This spitz nevus stained positive for PRAME but was negative for FISH (40×).

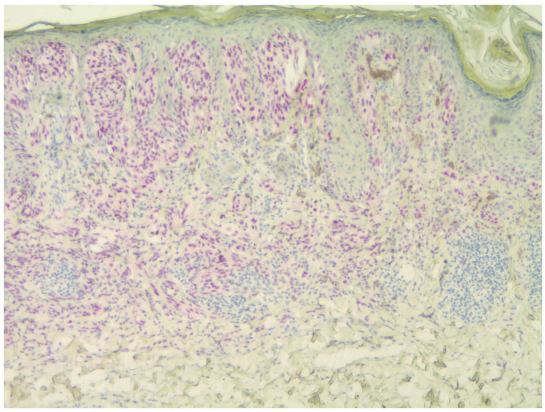

FIGURE 2
Spitzoid melanoma showing 3+ staining by PRAME (PRAME, 40×).

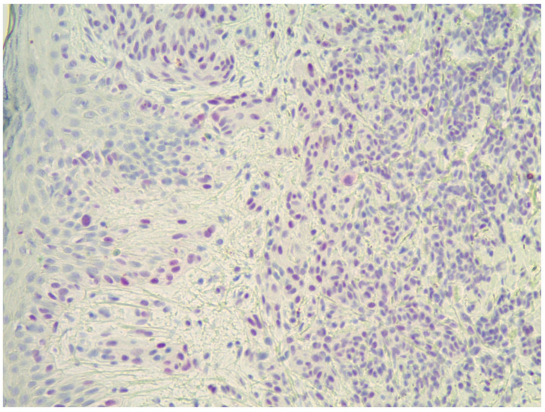

FIGURE 4
Strong positive PRAME staining in a spitz nevus which was negative for all FISH markers (40×).

greater than 10%, and CCND1 (11q13) gain in greater than 19% of cells. Negative results are defined as RREB (6p25) <16%, cMYC (8q24) <10%, CDKN2A (p16)/CEN9 < 10%, and CCND1 (11q13) <19%. Gerami et al. have found the high stringency cutoffs to be 94% sensitive and 98% specific in differentiating between benign and malignant melanocytic neoplasms, but only 70% sensitive in spitzoid neoplasms (10).

Data analysis was conducted in the R statistical programming language (version 4.1.2).

3. Results

Eighty-three spitzoid and atypical compound neoplasms were ultimately included in this study. Twenty-seven were ultimately categorized as malignant by FISH. Patient ages ranged from 2–79 with a mean age of 33.2 and a median age of 30.0.

The body-site distribution of the samples was as follows: 21.7% from the head and face, 22.9% from the trunk, 30.1% from the upper extremity (including shoulder), and 25.3% from the lower extremity.

p16 staining was performed in 21 cases, with loss of p16 observed in two cases which were diagnosed as melanoma. These two cases showed 0 and 1+ PRAME staining but received FISH staining over the high stringency cut off values for malignancy. In the cases in which p16 expression was retained there were 7 melanomas and 12 Spitz or atypical Spitz nevi.

FISH for melanoma had been previously performed in every case, and PRAME IHC was performed on all cases.

Of the 83 samples, 56 were FISH negative, and 27 were FISH positive. The distribution with respect to PRAME is summarized in Tables 1–3. Out of the 83 specimens graded on the PRAME 0–4+ scale, 49 were PRAME 0, 13 stained 1+, five stained 2+, three stained 3+, and 13 stained 4+, as demonstrated in Table 1. If a lower cutoff is utilized for PRAME positivity, defining positivity as staining 2+, 3+, or 4+, 21 out of the 83 samples would be PRAME positive, and 62 would be PRAME negative (defined as PRAME 0 or 1+), as demonstrated in Table 2.

In this dataset, the sensitivity of PRAME for malignant lesions is 29.6%, with a 95% confidence limit of 13.8 to 50.2%, as demonstrated in Table 3. The estimated sensitivity is too low to indicate a useful

marker. In addition, the confidence limit is very wide and includes 50%, indicating an imprecise estimate.

The specificity of PRAME for malignant lesions is 76.8% with a confidence limit of 63.6–87.0%. Estimated specificity is near the level that indicates usefulness, but the confidence limit is wide, again indicating lack of precision.

In our dataset, a subgroup analysis was performed looking at the differences in specificity, sensitivity, positive predictive value (PPV), and negative predictive value (NPV) when the threshold for positivity was adjuste, as in Tables 4, 5. When adjusted for a positivity threshold of 3+ to 4+ PRAME staining, our sensitivity lowered slightly from 29.6 to 25.9% (from 8/27 to 7/27), however the specificity increased from 83.9% (47/56) to 89.3% (50/56), respectively, as shown in Table 5. Similarly, the PPVs and NPVs increased as seen in the tables below, suggesting that by raising the threshold of positivity we were able to eliminate false negatives without sacrificing the capture of true positives.

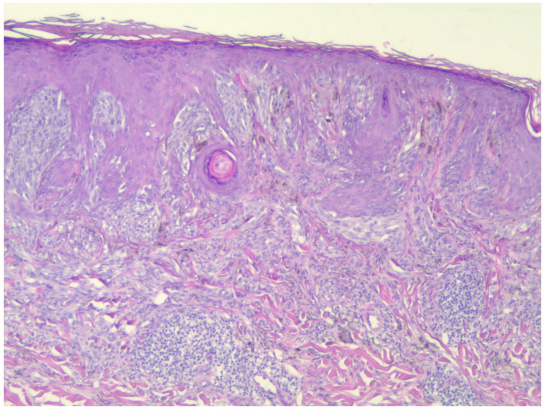

FIGURE 5
This spitzoid melanoma showed positive PRAME staining and was positive by FISH (H&E; 40×).

TABLE 1 Distribution of PRAME staining on the five-point scale established by Lezcano et al. with corresponding FISH results (FISH benign corresponds to negative FISH, FISH malignant corresponds to positive FISH).

PRAME staining results	FISH benign	FISH malignant	Total
0	38	11	49
1+	5	8	13
2+	4	1	5
3+	3	0	3
4+	6	7	13
Total	56	27	83

TABLE 2 Distribution of PRAME staining when categorized as negative (PRAME 0 or 1+) or positive (PRAME 2+, 3+, or 4+) with corresponding FISH results (FISH benign corresponds to negative FISH, FISH malignant corresponds to positive FISH).

PRAME staining	FISH benign	FISH malignant	Total
Negative	43	19	62
Positive	13	8	21
Total	56	27	83

4. Discussion

Immunohistochemical stains including HMB-45, Mart-1, Ki-67, and p16 are commonly utilized in the diagnosis of difficult melanocytic lesions. PRAME (PReferentially expressed antigen in melanoma) is a cancer testis antigen found to be overexpressed in melanoma. In large studies approximately 90% of primary melanomas showed nuclear PRAME staining while 98% of nevi are negative (11). O'Connor et al. reviewed PRAME staining in 101 benign melanocytic nevi and 42 malignant melanomas (12). They showed that using a 75% of cells staining score was associated with a sensitivity of 0.63, a specificity of 0.97 and an accuracy rate of 87% (12). However, due to the relative rarity of spitzoid melanoma, there is less data available for these neoplasms. Smaller studies using PRAME have been reported. Chen et al. reported 5 cases of spitzoid melanomas of which 3 (60%) stained diffusely positive for PRAME. 11 Koh et al. also utilized PRAME staining in spitzoid neoplasms (13). In their study of 35 lesions, 20% of Spitz nevi showed staining of greater than 75% of cells while 82% of spitzoid melanomas were similarly positive (13). However neither of these studies correlated FISH results with PRAME staining. Fluorescence *in-situ* hybridization (FISH) utilizing probes for genes RREB1 (6p25), cMYC (8q24), CDKN2A (p16)/CEN9, and CCND1 (11q13) has been shown to be sensitive and specific for differentiating Spitz nevi from spitzoid appearing melanoma. Our study looked predominately at spitzoid melanocytic neoplasms in young adults which are a common diagnostic dilemma.

The risk of false negatives must be taken into account when determining the threshold for "diffusely positive." As missing the diagnosis of melanoma is a very grave risk, we would recommend erring on the side of caution and utilizing a lower threshold for the percentage of PRAME positive cells considered as a positive test. However, in our study set, even by lowering our positivity threshold

TABLE 3 Sensitivity, specificity, positive predictive value (PPV), and negative predictive value (NPV) of PRAME in our sample, positing PRAME as the experimental test in comparison to FISH.

	n/*N*	Pct	(95% CI)
Sensitivity	8/27	29.6%	(13.8, 50.2%)
Specificity	43/56	76.8%	(63.6%, 87.0%)
PPV	8/21	38.1%	(18.1, 61.6%)
NPV	43/62	69.4%	(56.3, 80.4%)

Key: *n*/*N*, numeric; Pct, percent.

TABLE 4 Subgroup analyses adjusting for different positivity thresholds: positivity defined as anything staining greater than PRAME 1+, PRAME 2+, or 3+ accordingly.

FISH result	>PRAME 1+	>PRAME 2+	>PRAME 3+
FISH Benign	43 Neg/13 Pos	47 Neg/9 Pos	50 Neg/6 Pos
FISH Malignant	19 Neg/8 Pos	20 Neg/7 Pos	20 Neg/7 Pos

TABLE 5 Subgroup analyses adjusting for different positivity thresholds: positivity defined as anything staining greater than PRAME 1+, PRAME 2+, or 3+ accordingly with adjusted sensitivity, specificity, positive predictive value (PPV), and negative predictive value (NPV) of PRAME in our sample at these different cutoffs, positing PRAME as the experimental test in comparison to FISH.

	>PRAME 1+	>PRAME 2+	>PRAME 3+
Statistic	n/N Pct	n/N Pct	n/N Pct
Sensitivity	8/27 29.6%	7/27 25.9%	7/27 25.9%
Specificity	43/56 76.8%	47/56 83.9%	50/56 89.3%
PPV	8/21 38.1%	7/16 43.8%	7/13 53.8%
NPV	43/62 69.4%	47/67 70.1%	50/70 71.4%

Key: *n/N*, numeric; Pct, percent.

to PRAME 2+, we recaptured only 1 of the 20 samples that were identified as false negatives by FISH analysis; 8 of these FISH positive samples were quantified as PRAME 1+ and 11 did not stain for PRAME whatsoever, as in Figure 1. This poses a serious risk of utilizing PRAME alone in the diagnosis of melanoma in atypical spitzoid melanocytic neoplasms.

A screening test should have a higher sensitivity than that which we found in our study; had PRAME been used as a screening test to determine which cases warranted the more costly and time-consuming genetic testing in our study, only 8 out of the 27 or 29.6% of cases ultimately diagnosed as malignant after genetic testing would have been identified.

Despite the relatively small sample size of this study, there were 20 cases which would be classified as negative for PRAME on the 0–4+ scale but which were FISH positive, and ultimately were diagnosed as malignant, raising concern for the safety of utilizing PRAME immunohistochemistry as a screening test.

5. Conclusion

The differential diagnosis of spitzoid melanocytic neoplasms can be difficult. Ancillary testing including immunostaining for p16 and PRAME as well as fluorescence *in situ* hybridization have been utilized as diagnostic aids. In our study we sought to evaluate whether PRAME staining correlated with FISH results. We have concluded that PRAME immunohistochemistry does not show good correlation with FISH results in spitzoid melanocytic neoplasms, and ultimately, our study did not confirm its relevance as a screening tool. We also suggest, in line with Raghavan et al. that a lower threshold percentage of PRAME positive staining melanocytes might be utilized to increase the sensitivity of PRAME as a potential screening test. The lack of consensus in the literature on the appropriate percentage of positively staining melanocytes required for a lesion to be considered "diffusely positive" can also make it difficult to interpret the significance of this test between studies, although the majority follow the precedent set by Lezcano et al. However, the smaller sample size is a limitation of this study.

Although Lezcano et al. concluded that PRAME immunohistochemistry may still have use as an ancillary test as it is largely positive in melanomas and negative in benign lesions, our study showed some lack of concordance with FISH testing. We recommend that PRAME staining be interpreted in combination with other immunohistochemical results. Further study of the use of PRAME immunohistochemistry in these difficult to diagnose melanocytic neoplasms, particularly spitzoid neoplasms, is still warranted, particularly in the setting of larger datasets.

Data availability statement

The raw data supporting the conclusions of this article will be made available by the authors, without undue reservation.

Ethics statement

The studies involving humans were approved by Wayne State University Institutional Review Board. The studies were conducted in accordance with the local legislation and institutional requirements. The human samples used in this study were acquired from a by-product of routine care or industry. Written informed consent for participation was not required from the participants or the participants' legal guardians/next of kin in accordance with the national legislation and institutional requirements.

Author contributions

EW: Data curation, Investigation, Project administration, Writing – original draft, Writing – review & editing. DM: Investigation, Writing – original draft, Writing – review & editing, Conceptualization, Data curation, Methodology, Project administration, Supervision. SU: Investigation, Writing – original draft, Writing – review & editing, Funding acquisition. RS: Data curation, Formal analysis, Methodology, Software, Writing – review & editing. JA: Data curation, Formal analysis, Methodology, Software, Writing – review & editing.

Funding

The author(s) declare financial support was received for the research, authorship, and/or publication of this article. This research was funded by Wayne State University School of Medicine GME Residency Seed Grant.

Conflict of interest

The authors declare that the research was conducted in the absence of any commercial or financial relationships that could be construed as a potential conflict of interest.

Publisher's note

References

1. Ikeda H, Lethé B, Lehmann F, van Baren N, Baurain JF, de Smet C, et al. Characterization of an antigen that is recognized on a melanoma showing partial HLA loss by CTL expressing an NK inhibitory receptor. *Immunity*. (1997) 6:199–208. doi: 10.1016/S1074-7613(00)80426-4

2. Gutzmer R, Rivoltini L, Levchenko E, Testori A, Utikal J, Ascierto PA, et al. Safety and immunogenicity of the PRAME cancer immunotherapeutic in metastatic melanoma: results of a phase I dose escalation study. *ESMO Open*. (2016) 1:e000068. doi: 10.1136/esmoopen-2016-000068

3. Gerami P, Alsobrook JP, Palmer TJ, Robin HS. Development of a novel noninvasive adhesive patch test for the evaluation of pigmented lesions of the skin. *J Am Acad Dermatol*. (2014) 71:237–44. doi: 10.1016/j.jaad.2014.04.042

4. Lezcano C, Jungbluth AA, Nehal KS, Hollmann TJ, Busam KJ. PRAME expression in melanocytic tumors. *Am J Surg Pathol*. (2018) 42:1456–65. doi: 10.1097/PAS.0000000000001134

5. Lezcano C, Jungbluth AA, Busam KJ. Comparison of immunohistochemistry for PRAME with cytogenetic test results in the evaluation of challenging melanocytic tumors. *Am J Surg Pathol*. (2020) 44:893–900. doi: 10.1097/PAS.0000000000001492

6. Raghavan SS, Wang JY, Kwok S, Rieger KE, Novoa RA, Brown RA. PRAME expression in melanocytic proliferations with intermediate histopathologic or spitzoid features. *J Cutan Pathol*. (2020) 47:1123–31. doi: 10.1111/cup.13818

7. Googe PB, Flanigan KL, Miedema JR. Preferentially expressed antigen in melanoma immunostaining in a series of melanocytic neoplasms. *Am J Dermatopathol*. (2021) 43:794–800. doi: 10.1097/DAD.0000000000001885

8. Lezcano C, Pulitzer M, Moy AP, Hollmann TJ, Jungbluth AA, Busam KJ. Immunohistochemistry for PRAME in the distinction of nodal nevi from metastatic melanoma. *Am J Surg Pathol*. (2020) 44:503–8. doi: 10.1097/PAS.0000000000001393

9. Umano GR, Errico ME, D'Onofrio V, Delehaye G, Trotta L, Spinelli C, et al. The challenge of melanocytic lesions in pediatric patients: clinical-pathological findings and the diagnostic value of PRAME. *Front Oncol*. (2021) 11:688410. doi: 10.3389/fonc.2021.688410

10. Gerami P, Li G, Pouryazdanparast P, Blondin B, Beilfuss B, Slenk C, et al. A highly specific and discriminatory FISH assay for distinguishing between benign and malignant melanocytic neoplasms. *Am J Surg Pathol*. (2012) 36:808–17. doi: 10.1097/PAS.0b013e31824b1efd

11. Chen Y-P, Zhang W-w, Qiu Y-t, Ke LF, Chen H, Chen G. Prame is a useful marker for the differential diagnosis of melanocytic tumors and histological mimics. *Histopathology*. (2023) 82:285–95. doi: 10.1111/his.14814

12. O'Connor MK, Dai H, Fraga G. PRAME immunohistochemistry for melanoma diagnosis: ASTARD-compliant diagnostic accuracy study. *J Cutan Pathol*. (2022) 49:780–6. doi: 10.1111/cup.14267

13. Koh S, Lau S, Scapa J, Cassarino DS. PRAME immunohistochemistry of spitzoid neoplasms. *J Cutan Path*. (2022) 49:709–16. doi: 10.1111/cup.14245

frontiers | Frontiers in Medicine

TYPE Review
PUBLISHED 22 November 2023
DOI 10.3389/fmed.2023.1268479

OPEN ACCESS

EDITED BY
Bahar Dasgeb,
The State University of New Jersey,
United States

REVIEWED BY
Gerardo Cazzato,
University of Bari Aldo Moro, Italy
Jisun Cha,
Schweiger Dermatology Group, United States

*CORRESPONDENCE
Jason B. Lee
✉ jason.lee@jefferson.edu

RECEIVED 28 July 2023
ACCEPTED 13 October 2023
PUBLISHED 22 November 2023

CITATION
Waseh S and Lee JB (2023) Advances in melanoma: epidemiology, diagnosis, and prognosis.
Front. Med. 10:1268479.
doi: 10.3389/fmed.2023.1268479

Advances in melanoma: epidemiology, diagnosis, and prognosis

Shayan Waseh[1] and Jason B. Lee[2]*

[1]Department of Dermatology, Temple University Hospital, Philadelphia, PA, United States, [2]Department of Dermatology, Thomas Jefferson University, Philadelphia, PA, United States

Unraveling the multidimensional complexities of melanoma has required concerted efforts by dedicated community of researchers and clinicians battling against this deadly form of skin cancer. Remarkable advances have been made in the realm of epidemiology, classification, diagnosis, and therapy of melanoma. The treatment of advanced melanomas has entered the golden era as targeted personalized therapies have emerged that have significantly altered the mortality rate. A paradigm shift in the approach to melanoma classification, diagnosis, prognosis, and staging is underway, fueled by discoveries of genetic alterations in melanocytic neoplasms. A morphologic clinicopathologic classification of melanoma is expected to be replaced by a more precise molecular based one. As validated, convenient, and cost-effective molecular-based tests emerge, molecular diagnostics will play a greater role in the clinical and histologic diagnosis of melanoma. Artificial intelligence augmented clinical and histologic diagnosis of melanoma is expected to make the process more streamlined and efficient. A more accurate model of prognosis and staging of melanoma is emerging based on molecular understanding melanoma. This contribution summarizes the recent advances in melanoma epidemiology, classification, diagnosis, and prognosis.

KEYWORDS

melanoma, melanoma epidemiology, melanoma genomics, melanoma diagnosis, melanoma classification

Introduction

The word melanoma brings about fear among the public, patients, and clinicians alike. Perceived as the deadliest form of skin cancer, the scientific community of researchers and clinicians has made concerted efforts to bring about meaningful changes in morbidity and mortality associated with the cancer. Early on, the focus has been on screening and early detection of melanoma that have resulted in a rapid rise in the incidence of early thin melanomas in the last 50 years in countries of fair skin individuals. The diagnosis and treatment of melanoma have made significant strides in the past decade, which coincided with the understanding of genomic basis of melanomas. The diagnosis of melanoma is no longer solely relied upon histologic interpretation of skin biopsies, but, rather, more precise molecular based ancillary tests have emerged to aid the pathologists. The treatment of advanced melanoma has entered the golden era as targeted personalized therapies have emerged that have significantly altered the mortality rate. In this contribution, the current advances in melanoma epidemiology, diagnosis, and prognosis are reviewed.

Epidemiology

While the incidence and mortality of most cancers have declined over the past several decades, the incidence of melanoma continues to rise, particularly in the countries of fair-skinned populations of European descent. In 2020, the global burden of melanoma increased to 325,000 cases from 230,000 cases in 2012, a 41% increase (1). The highest incidence of melanoma is observed in Australia and New Zealand (1). In the United States (US), melanoma is the fifth most common cancer diagnosed with an estimated 99,780 new cases and 7,650 deaths in 2022, while 97,920 melanoma *in-situ* new cases are expected, a number that rivals the invasive melanomas (2).

Incidence and mortality

Invasive melanomas account for about 1% of all skin cancer cases, but they account for over 75% of skin cancer deaths (3). Though melanoma is perceived as a deadly cancer, the overall 5-year survival rate is 93.5% (3). The relative high survival rate of melanoma reflects the high proportion of localized disease (78%) that comprise the newly diagnosed invasive melanomas, which has 5-year survival rate of 99.6% (3). Despite the high survival rate, the small fraction of Stage I disease progression accounts for majority of the melanoma deaths (4). Stage III and IV disease have a survival rate of 73.9 and 35.1% respectively, a significant improvement since the introduction of targeted therapies and immunotherapies (3). In 2015, the 5-year survival rate of Stage IV disease was only 15% in comparison.

According to the Surveillance, Epidemiology, End Results (SEER) Program, the median age of melanoma diagnosis in the US is 66 years old (3). The lifetime risk of developing melanoma in White people is 2.6% (1 in 38), 0.6% (1 in 167) in Hispanic people, and 0.1% (1 in 1000) in Black people (5). The incidence rate is higher in men, a rate that is 1.6 times higher than women. While melanoma can develop at any skin site, the arms and legs are the most common site of involvement in women and the head, neck, back, and trunk are more commonly involved in men (6). African-American patients are more likely to develop melanoma on the plantar feet and other sun protected areas (3). Additionally, African-American patients are likely to have more advanced melanoma at the time of diagnosis and generally have a worse prognosis than their White counterparts.

Epidemic of melanoma

Over the past four decades, there has been a dramatic rise in the incidence of melanoma that has reached epidemic proportions. In the US, a threefold increase in the incidence rate has been observed during this period according to the SEER data all the while the mortality rate remained stable for most of the period (Figure 1) (7). Similar incidence and mortality trends have been observed in developed countries in Europe and Australia over the same period. In the US, the sharp rise in the incidence has coincided with promotion of skin cancer screening and public awareness campaigns in the early 80s. Cancer screening, in general, has an intuitive appeal for clinicians and the lay public: detect cancers early when it's more curable and manageable to prevent their expected morbidity and mortality. The late A. B. Ackerman urged clinicians and pathologists to diagnose melanomas early at a stage that is small, flat, and curable (8). The widespread adoption of dermatoscopy, a diagnostic technique promoted to detect incipient and incognito melanomas, further contributed to the detection of even earlier stage melanomas (9, 10).

The sharp rise in the incidence of early-stage melanomas without the concomitant rise in mortality has brought the issue of overdiagnosis in the foreground (7, 11–15). Overdiagnosis is defined as identification of a cancer, if left alone, that would not have caused death (16, 17). It is an epidemiologic phenomenon that is easily discernable at the population level, but not at the patient or slide level.

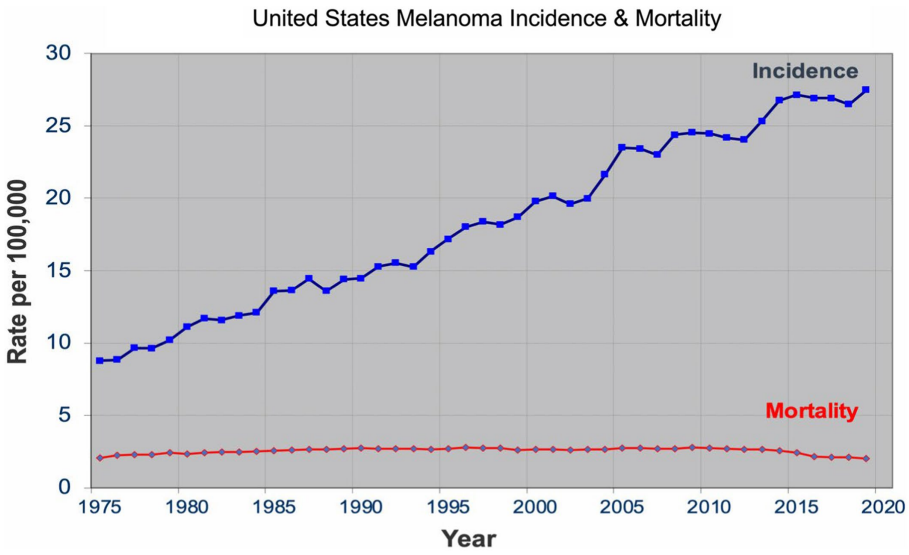

FIGURE 1
United States melanoma incidence and mortality.

The mounting epidemiologic evidence indicates that most of the early melanomas diagnosed represent indolent or biologically benign forms, which are not the obligate precursors to the deadly forms of melanoma, and that the stable mortality reflects the stable incidence of the aggressive melanomas that screening do not capture (7, 18–21). Furthermore, over the past two decades, the incidence of melanoma *in situ* has dramatically increased from 28,600 in 2000 to 101,280 in 2021 in the US (22, 23). Despite the marked increase, no decrease in late disease have been observed. Moreover, they are diagnosed at a later age than the invasive melanomas, further bolstering the argument that they are not obligate precursors of invasive melanomas (24–26).

Effective cancer screening results in a decrease in late-stage disease and mortality. By this metric, cervical and colon cancer screenings qualify as effective cancer screening programs (27). For both cancers, there is a reliable precursor lesion that are screened and removed, human papillomavirus induced cervical intraepithelial neoplasia and colon polyps, respectively. For melanoma, a reliable precursor lesion has been elusive. First described by Wallace Clark in 1978, the dysplastic nevus was promulgated as a precursor lesion to melanoma (28–31), which began an era of close monitoring and their removal that still continues today. The countless biopsies and subsequent excisions of dysplastic nevi, over the past four decades, however, failed to make a difference in the late-stage disease and mortality rate.

The United States Preventive Service Task Force (USPSTF) has consistently given a grade of I for insufficient evidence for or against skin cancer screening, primarily because there are no population-level or randomized controlled trials that demonstrate the benefits of screening (32). There was an initial excitement about the preliminary population data that indicated a decreased melanoma-specific mortality in northern Germany, but the benefit was short-lived and longer follow-up, and the subsequent nationwide population screening had no impact on melanoma-specific mortality (33–35). Accordingly, no major medical societies and organizations in the US have a formal recommendation on skin cancer screening.

According to Welch and coworkers (12), the rapid rise in the incidence is the byproduct of "epidemic of inspection, surveillance, and biopsy of pigmented skin lesions." The authors recommend curtailing self-referral of skin biopsy specimens, increasing the threshold to biopsy, particularly small, pigmented lesions, increasing the histopathological threshold in the diagnosis of melanomas, and ceasing all population-based skin cancer screenings. The dermatology community is unlikely to follow these recommendations as perceived benefits of screening and early detection are entrenched in the community and overdiagnosis cannot be perceived at the patient or slide level. Without any pivot in the detection strategy, however, epidemiologic evidence of overdiagnosis is expected to become more pronounced. Thyroid cancer has similar issues of overdiagnosis and has a nearly identical incidence and mortality rate pattern. In 2017, USPSTF gave a grade of D for thyroid cancer screening, which resulted in a decrease in the incidence with a mortality rate that remained unchanged in the subsequent years (36, 37). Without formal evidence of benefit, population skin cancer screening is at risk of receiving a grade of D for discourage screening as did thyroid cancer screening. Opportunities awaits dermatology community to perform the necessary studies that show the benefits of screening, particularly in populations that are at high risk of developing melanoma (38).

Risk factors

Environmental

Ultraviolet radiation (UVR) from sun exposure has been firmly established as the dominant environmental factor that increases the risk of developing melanoma (39). Intermittent sun exposure, particularly resulting in blistering sunburns, has been hypothesized to increase the risk of melanoma development (40). Meta-analyses have concluded that the relative risk is approximately 2 for sunburn history and 1.3 for tanning bed history (41, 42). In comparison, smoking and lung cancer have a relative risk of 10–20. The relationship between UVR and melanoma risk is a complex one, a relationship that still needs to be further clarified.

Current epidemiologic data suggest the existence of three heterogeneous forms of melanomas: (1) slow-growing melanomas associated with intermittent sun exposure and melanocytic nevi, (2) slow-growing indolent melanomas associated with chronic sun exposure occurring on the head and neck (Figures 2, 3), (3) fast-growing aggressive melanomas minimally associated with sun exposure and melanocytic nevi (Figure 4) (43–45). The fast-growing melanomas are not amenable to screening due to their rapid growth rate. They also elude detection because they do not harbor predictable clinical features, often simulating a benign and malignant non-melanocytic lesions and even inflammatory diseases (46). Nodular melanomas, particularly amelanotic ones, present as rapid growers (46). The current epidemic of melanoma consists of mostly slow growing thin melanomas because of screening efforts, which identify melanomas with early stages that are stretched out much

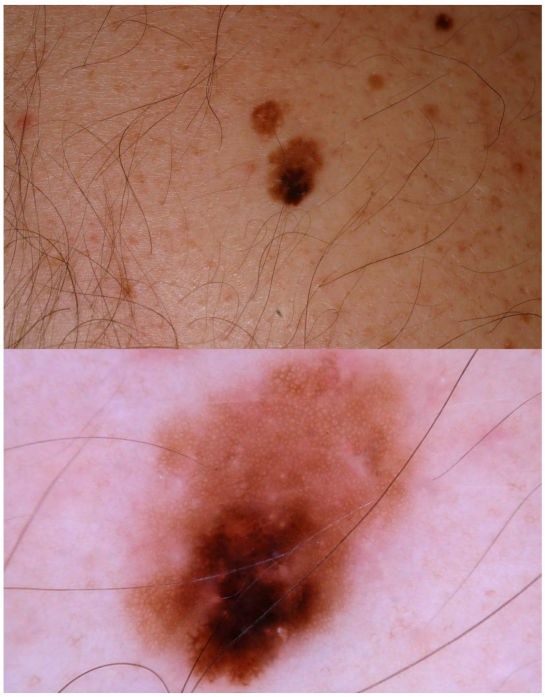

FIGURE 2
A patient multiple nevi presents with a changing mole. Dermatoscopic image shows an asymmetric melanocytic lesion with regular network and black blotch.

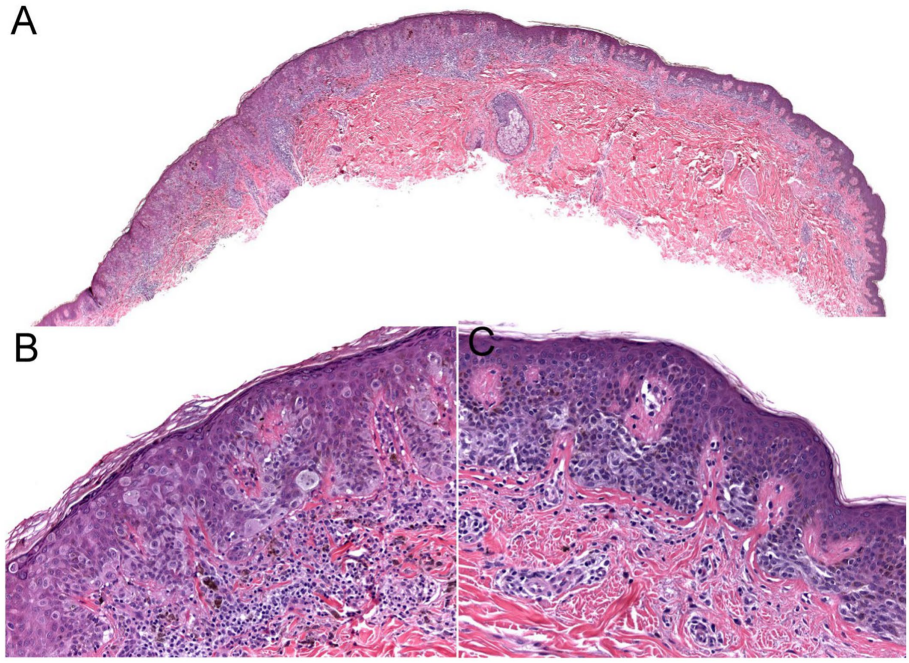

FIGURE 3
The biopsy of the Figure 2 lesion showing a thin (Stage 1A) superficial spreading melanoma arising in a dysplastic nevus. **(A)** A shave biopsy showing a melanocytic lesion with an asymmetric architecture (20× magnification). **(B)** The left side of the lesion shows the melanoma *in situ* component: large atypical pagetoid melanocytes in pagetoid spread within the epidermis (200× magnification). **(C)** The right side of the lesion shows the nevus component: nested monomorphous melanocytes at the dermoepidermal junction (200× magnification).

longer in time. Lentigo maligna and superficial spreading type of melanoma fall into this category of melanoma.

Phenotype risk factors

Phenotype risk factors for developing melanoma includes Caucasian race with fair skin, high nevus count, giant congenital nevus, particularly garment or bathing trunk nevus, and Clark/dyplastic nevus (47, 48). Caucasians have 20 times the risk of developing melanoma compared to Black people (3). Immunosuppression and prior history of melanoma also confer a higher risk.

Giant congenital nevus (>20 cm), particularly garment or bathing trunk nevi, has a significant life-time risk of developing melanoma, ranging from 2.3 to 14% (49). Though some giant congenital nevi may be amenable for prophylactic removal, the garment or bathing trunk nevi are usually too large to remove. Lifetime monitoring for development of melanoma and symptoms due to neurocutaneous melanocytosis is required for these patients.

Precursor lesion: the dysplastic nevus

In the paradigm of multistep progression of cancer, identification of a reliable precursor lesion is crucial for early detection and reducing the morbidity and mortality associated with the cancer.

In an attempt to follow the successful cervical and colon cancer model and assuming the linear multistep progression paradigm, identification of a precursor lesion for melanoma was sought by clinicians and researchers fighting the battle against melanoma. In 1978, Clark and colleagues described six melanoma prone families where they observed flat melanocytic nevi with irregular border and color variegation in majority of the family members who developed melanoma (28). The authors proposed that these nevi, referred to as B-K moles at the time, have a higher risk of transforming into melanoma. Shortly thereafter, without any formal evidence, these nevi, renamed as dysplastic nevi, received a stamp of approval in a NIH consensus conference of being a marker and precursor to melanoma (30). Over 40 years of practice of close scrutiny and their removal has not resulted in any convincing evidence of their association with melanoma (50, 51). Many authors have concluded that the nevus may serve as a phenotype marker but not a precursor lesion to melanoma (50–54). Some have argued against their precursor status from the outset (55).

Genetics risk factors

Exciting advances have been made in the discoveries of the genetic underpinnings of cutaneous melanocytic neoplasms, benign and malignant. Germline mutations that significantly increases the life-time risk of developing melanoma include CDKN2A, CDK4, BAP1, TERT, MITF, MC1R, and POT1 (Table 1) (56). These germline mutations underlie the familial or hereditary melanoma *dominant* syndromes, in which melanoma is the predominant cancer of the syndrome. Germline mutations that underlie melanoma *subordinate* or *mixed cancer* syndromes include PTEN, TP53, BRCA1, BRCA2, and XP A-G (57). In these syndromes, other cancers have a higher penetrance rate than melanoma.

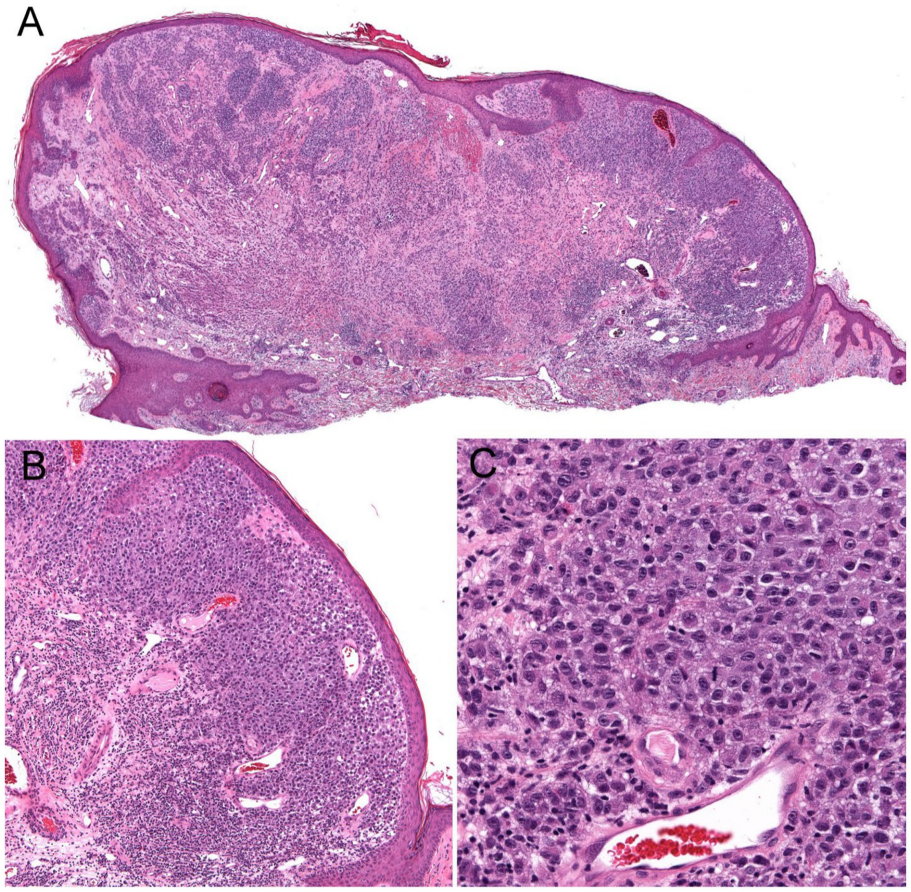

FIGURE 4
Unsuspected nodular melanoma (Stage 2B) clinically diagnosed as an inflamed skin tag. **(A)** Polypoid asymmetrical melanocytic lesion with irregular distribution of melanocytes (40× magnification). **(B)** Melanocytes arranged in sheets in the superficial dermis (100× magnification). **(C)** Large atypical melanocytes that vary in size and shape with occasional mitotic figures (400× magnification).

While only 5–12% of melanomas are thought to be hereditary, approximately 40% of hereditary melanomas are attributable to CDKN2A mutations, making CDKN2A the most commonly mutated gene responsible for an autosomal dominant pattern of hereditary melanoma (58). Coding for tumor suppressors p16 and p14 (ARF) which regulate the cell cycle, patients with germline mutation in the CDKN2A gene have a high risk of developing melanoma, glioblastoma, and pancreatic carcinoma (57). Compared to the 2.6% lifetime risk of developing melanoma in the US White population, patients with germline CDKN2A mutation increases that risk to 28 to 76% depending on the presence of other factors. In one study, the risk of melanoma in CDKN2A mutation carriers was approximately 14% by age 50 years, 24% by age 70 years, and 28% by age 80 years (59). In comparison, as one of the mutations for the hereditary pancreatic syndromes, CDKN2A carriers confers a 17% lifetime risk of developing pancreatic cancer (60). Furthermore, while CDKN2A is common somatically mutated in sporadic melanoma, somatic biallelic inactivation of CDKN2A occurs exclusively within invasive melanoma (56). Therefore, the gene continues to represent an important mutational contributor to melanoma development both familial and sporadic.

First discovered in uveal melanoma, mutations in the BAP1 gene interfere with its function as a deubiquitinating enzyme and tumor suppressor (61). Malignancies associated with germline mutations in BAP1 include cutaneous melanoma, ocular melanoma, mesothelioma, renal cell carcinoma, and basal cell carcinoma (61–64). They also may develop small dome-shaped nevi with a spitzoid melanocytes that show loss of BAP1, referred to as BAP1 deficient nevus or Wiesner nevus (65). The vast majority of Wiesner nevus occurs sporadically, and, thus, genetic testing should be based on detailed patient's history.

TERT, which encodes the telomerase reverse transcriptase subunit of the telomerase enzyme is another important predisposing mutation for the development of melanoma (66). Mutations in the TERT gene allow for the escape of premalignant cells from senesce and apoptosis, contributing to the development of malignancy. First identified in melanoma, TERT mutations have become increasingly identified as one of the most common noncoding mutations in all cancers. Importantly, somatic TERT promoter mutations portend poor prognostic factors, including a higher likelihood of increased tumor thickness and the presence of ulceration, high mitotic rate, and lymph node metastasis (56, 66).

Gene testing for melanoma

Except for the CDKN2A gene, formal guidelines for genetic testing for mutations responsible for the hereditary melanomas

TABLE 1 Germline mutations associated with increased melanoma risk.

Gene	Function	Histopathologic subtype	Additional associations
Cyclin dependent kinase inhibitor 2A (CDKN2A)	Tumor suppressor via: (1) p16-mediated inhibition of CDK4 inhibition and phosphorylation of RB (2) p14ARK-mediated inhibition of HDM2 and ubiquitination of p53	Superficial spreading melanoma	Pancreatic, upper GI, and pulmonary cancer Astrocytomas, neurofibromas, schwannomas
Cyclin dependent kinase 4 (CDK4)	Oncogene responsible for downstream inhibition of RB phosphorylation	Superficial spreading melanoma	Pancreatic cancer
Telomerase reverse transcriptase (TERT)	Telomerase component	Nodular melanoma Superficial spreading melanoma	Numerous visceral malignancies
Production of telomeres 1 (POT1)	Component of shelterin complex responsible for telomere regulation	Superficial spreading melanoma	Numerous visceral malignancies
ACD shelterin complex subunit and telomerase recruitment factor (ACD)	Component of shelterin complex responsible for telomere regulation	Superficial spreading melanoma Lentigo maligna melanoma	Numerous visceral malignancies
TERF2 interacting protein (TERF2IP)	Component of shelterin complex responsible for telomere regulation	Superficial spreading melanoma Lentigo maligna melanoma	Numerous visceral malignancies
Melanocyte inducing transcription factor (MITF)	Transcription factor	Amelanotic melanoma Nodular melanoma	Renal cell carcinoma Phenotype of darker hair, fair skin, and non-blue eye color
Melanocortin-1 receptor (MC1R)	G protein coupled receptor for melanocyte-stimulating hormone	Melanoma in specific anatomic sites (e.g., arms)	Phenotype of red hair, freckling, light skin, and UV sensitivity
BRCA1 associated protein 1 (BAP1)	Deubiquinating enzyme and BRCA1 binding partner involved in trascriptional regulation and DNA repair	BAP1-inactivated nevi	Numerous visceral malignancies

Adapted from Toussi et al. (56).

do not exist (57). The "rules of two or three" apply to testing for CDKN2A mutation and not for others (67). Genetic test should be considered for history of three or more primary melanomas and/or pancreatic cancer in geographic areas of high melanoma prevalence and two or more primary melanomas or *in situ* melanomas in areas of low prevalence. History of invasive melanomas in multiple family members at ages earlier than 40 should raise the suspicion of hereditary melanoma syndrome. Leachman and coworkers have outlined more detailed suggestions of screening for germline mutations other than CDKN2A (67). Though technological advances in genomic analysis have enabled discovery of new mutations associated with melanoma and the ease of testing for gene mutations, the actual benefits of the testing and surveillance, in terms of outcomes, are not available.

One of the commonly tested genes is BRCA1 and BRCA2 mutations for evaluation of genetic basis of breast cancers. They both play a role in contributing to the repair of damaged DNA and the destruction of cells with irreparable DNA damage. Although BRCA1 mutations have failed to demonstrate an increased risk of melanoma, BRCA2 mutations have been linked to an increase incidence of melanoma in large breast and ovarian cancer families. An in-depth analysis of published data, however, showed insufficient evidence to warrant increased skin cancer surveillance in these patients without other risk factors (68).

Melanoma diagnosis

The current clinicopathologic classification of melanoma has been widely adopted and employed in clinical practice for its simplicity and ease of implementation. The classification consists of four major distinct clinicopathologic subtypes with its own corresponding *in situ* lesions: lentigo maligna, superficial spreading, acral lentiginous, and nodular (69, 70). The classification relies heavily on the interpretation of the histopathologic findings, a highly subjective discipline with issues of interobserver reliability (71–74). Though there are melanomas that clearly match the clinical and pathological criteria of a given subtype, many have overlapping histopathologic patterns in the same lesion, making subtyping arbitrary (75, 76). For example, acral lentiginous melanomas have a wide spectrum of histopathologic patterns that encompasses histopathologic patterns observed in the other three subtypes of melanomas. In addition, the classification does not intrinsically incorporate prognostic information. Instead, known extrinsic prognostic factors are added to the pathology report, primarily Breslow depth and ulceration that dictate management. The classification assumes a linear model of progression for all melanomas where melanoma *in situ* lesions are assumed to be the obligate early lesion that becomes invasive and subsequently metastasizes. Though progression of melanomas varies widely, all subtypes of melanomas

are treated the same, driven primarily by the thickness of the melanoma.

Recently, the World Health Organization introduced a new classification of melanoma that includes epidemiologic and genomic information in addition to the clinicopathologic criteria. The classification has been expanded to 9 different subtypes that account for the very rare and mucosal melanomas (Table 2) (77). This classification also assumes a linear model of progression in which the melanocytic nevus with the same driver mutation as the melanoma is proposed as the precursor lesion for each subtype. Except for the rare giant or garment congenital nevi where there is a known higher risk of developing melanoma within the nevus, evidence is lacking for the precursor model of progression. The rate at which the precursor nevus acquires the requisite mutations to transform into melanoma is unknown and the rare occurrences of these nevi make it hard to verify their precursor status. The long experience with Clark/dysplastic nevus has not supported the precursor model of melanoma progression (50, 51).

Melanocytic pathology assessment tool and hierarchy for diagnosis (MPATH-Dx)

While guidelines have been established for melanomas, a standardized management guidelines have not been established for a large group of melanocytic neoplasms for reasons that have plagued the gold standard in diagnosing melanocytic neoplasms—interobserver reliability. In addition, the lack of standardized diagnostic terms for melanocytic neoplasms and disagreements about the fundamental nature of various melanocytic neoplasms have contributed to the confusion among clinicians and patients and the lack of standard management. The local and regional variation on the diagnostic term for the "B-K mole" first described by Clark and colleagues, which includes dysplastic nevus, atypical nevus, nevus with architectural disorder, and Clark nevus, exemplifies the issue of standardization of diagnostic terminology. In 2014, MPATH-Dx schema was introduced to simplify and standardize reporting of melanocytic neoplasms by bring about clarity to classification and management of melanocytic neoplasms, regardless of the different diagnostic terms used (78). The initial version MPATH-Dx consisted of 5 classes with benign and malignant diagnoses with minimal disagreement at the two ends of the classification hierarchy. In early 2023, a new version of MPATH-Dx was published after years of feedback that also accounts for the schema of 2018 WHO classification of melanocytic neoplasms (Table 3) (79). The previous 5 class hierarchy has been simplified into four, essentially removing the original Class II by eliminating the moderately atypical nevus following the WHO classification and moving Spitz nevus into the new Class II group. The new Class I group, referred to as low grade, requires no further treatment while Class II group, referred to as high grade, requires further treatment, which includes a diverse spectrum of melanocytic lesions—high grade dysplastic or atypical nevus, cellular blue nevus, and melanoma *in situ*. As acknowledged by the authors, the MPATH-Dx schema does not escape the issues of inherent subjectivity of pathologic diagnosis of melanocytic neoplasms. While the concordance rates for the two ends of the

TABLE 2 World Health Organization classification of melanoma.

Relationship with sun exposure	No.	Subtype	Genetic hallmarks
Melanomas arising in sun exposed skin	1	Low-CSD melanoma/superficial spreading melanoma	High frequency of *BRAF* p. V600 mutations
	2	High-CSD melanoma (including lentigo maligna melanoma and high-CSD nodular melanoma)	Predominating mutually exclusive *NF1*, *NRAS*, other *BRAF* (non-p. V600E), and perhaps *KIT* mutations
	3	Desmoplastic melanoma	Recurrent inactivating *NF1* mutations, *NFKBIE* promoter mutations, and several different activating mutations in the MAPK pathway (e.g., *MAP2K1*)
Melanomas arising at sun-shielded sites or without known etiological associations with UV radiation exposure	4	Malignant Spitz tumor (Spitz melanoma)	Mutations in *HRAS* and kinase fusions in *ROS1*, *NTRK1*, *NTRK3*, *ALK*, *BRAF*, *MET*, and *RET*; *CDKN2A* homozygous deletions, *TERT* promoter mutations, and *MAP3K8* fusions / truncating mutations only in aggressive or lethal variants
	5	Acral melanoma (including nodular melanoma in acral skin)	Multiple amplifications of *CCND1*, *KIT*, and *TERT*; mutations of *BRAF*, *NRAS*, and *KIT*; kinase fusions of *ALK* or *RET* in a few cases
	6	Mucosal melanoma	Numerous copy number and structural variations; uncommonly, *KIT* and *NRAS* mutations
	7	Melanoma arising in congenital nevus	In large to giant congenital nevi: *NRAS* mutation; in small to medium-sized congenital nevi, *BRAF* mutations
	8	Melanoma arising in blue nevus	Initiating mutations in the Gaq signaling pathway (*GNAQ*, *GNA11*, *CYSLTR2*, *PLCB4*); monosomy 3 (associated with loss of *BAP1*) and chromosome 89 gains in aggressive cases; additional secondary copy number aberrations in *SF3B1* and *EIF1AX*
	9	Uveal melanoma	Mutually exclusive mutations in the Gaq pathway (*GNAQ*, *GNA11*, *PLCB4*, *CYSLTR2*); *BAP1*, *SF3B1*, and *EIF1AX* mutations during progression

Adapted from Elder et al. (77).

TABLE 3 Melanocytic pathology assessment tool and hierarchy for diagnosis (MPATH-Dx).

Class	Risk of tumor progression	Probability of progression, No. per population	Treatment recommendation	Examples
0	NA	NA	Consider repeat biopsy	Nondiagnostic or unsatisfactory
I: low grade	Very low risk for continued proliferation and progression to invasive melanoma	1 in 10,000 to 1 in 100,000	No further treatment	1. Common acquired nevi, no atypia 2. Congenital nevi, no atypia 3. Atypical and dysplastic nevi, low-grade atypia 4. Common blue nevi
II: high grade	Low risk for progression to invasive melanoma	1 in 100 to 1 in 1000	Re-excision with margins < 1 cm	1. Atypical and dysplastic nevi, high grade atypia 2. Spitz nevi, tumors, or melanocytomas, and atypical variants 3. Cellular blue nevi or melanocytomas and atypical variants 4. Plexiform or deep penetrating nevi or melanocytomas 5. Lentigo maligna 6. Melanoma *in situ*
III: melanoma pT1a	Relatively low risk for local and regional metastasis	1 in 10 to 1 in 100	Follow national guidelines (e.g., wide excision with 1 cm margins)	1. Melanoma AJCC stage pT1a, <0.8 mm Breslow thickness 2. Melanoma pT1a lr (low risk) 3. Melanoma pT1a
IV: melanoma ≥ pT1b	Moderate to increased risk for regional or distant metastasis	1 in 2 to 1 in 10	Follow national guidelines (eg, wide excision with 1–2 cm margins and consideration of sentinel lymph node staging and other therapies)	Melanoma AJCC stage pT1b or greater, ≥0.8 mm Breslow thickness

Adapted from Barnhill et al. (79).

diagnostic spectrum is good, the concordance rate is poor for thin melanomas, Spitz nevi, and grading of melanocytic lesions (74). In addition, many clinicians will find the margin recommendation of up to 1 cm for melanocytic lesions in Class II vague and arbitrary. Clinicians will look for more precise margin recommendations as 2-, 5-, and 10-millimeter margins make for significant differences in surgery and impact for patients depending on the site and patient's age. Furthermore, there will be clinicians who will object to the recommendation of removal of routine Spitz, cellular blue, deep penetrating nevi that are included in Class II. Despite these limitations of the scheme, MPATH-Dx is working toward more precise classification, clarity in management, and standardization of reporting that are needed in the diagnostic pathway.

Clinical diagnosis

The ABCD mnemonic has been a diagnostic aid in the early detection of melanoma since the 1980s, and the recent inclusion of "evolution" as an "E" criterion has been reported to increase its sensitivity. The ABCDE criteria refers to the presence of asymmetry, border irregularity, color variability, a diameter of 6 mm or greater, and evolution or recent change. With the incorporation of ABCDE criteria, diagnostic accuracy of naked-eye examination for melanoma has been estimated to be approximately 65% overall (80–82). The introduction of dermatoscopy has been a major change in the clinical diagnosis of melanocytic neoplasms at the bedside. While the diagnostic technique is not new, the availability of small handheld version of the device coincided with the widespread adoption of dermatoscopy in the modern era. The modern dermatoscope provides a light source, usually a 10× magnification and, more importantly, polarization, which renders the cornified layer translucent, allowing the visualization of subsurface structures (83). Whole new diagnostic criteria of subsurface structures have emerged in diagnosing a variety of inflammatory, infectious, and neoplastic disease of the skin, particularly early melanomas, one of the major objectives of dermatoscopy. Various dermatoscopic criteria have been developed for benign and malignant melanocytic neoplasms. The presence of an atypical pigment network, blue-white veil, atypical vascular patterns, and irregular streaks, pigmentation, globules, or regression structures on dermatoscopy have a higher association with melanoma (84). Diagnostic algorithms that have been developed include the 7-point checklist, Menzies method, and the CASH criteria (84). Each of these algorithms has been shown to increase sensitivity and specificity in melanoma identification. Meta-analyses of large studies have suggest up to 18 and 10% increase in the sensitivity and specificity in the diagnosis of melanoma, respectively (85–87). Major limitations of the studies were that most were retrospective in design evaluated by a group of experts in the field involving images of already managed melanocytic lesions with no impact on management. Accordingly, the more recent Cochrane review (88) concluded that the evidence base of dermatoscopy is limited and "when used by *specialists*, dermoscopy

is better at diagnosing melanoma compared to inspection of a suspicious skin lesion using the naked eye alone." Conclusive evidence was lacking to "explicitly estimate the sensitivity and specificity of dermoscopy, either with or without visual inspection." Furthermore, despite the enthusiasm and widespread adoption of the diagnostic technique, evidence of desired impact in terms of decreased biopsy rates, cost savings, and improved outcomes of patients are not available. The words of late Carli from 2007 hold true today: "Dermoscopy not yet shown to increase sensitivity of melanoma diagnosis in real practice." (89) Further studies are needed to validate the widespread use for the diagnosis of melanomas, particularly in the general dermatology and primary care settings.

Recently, a tape-strip test, Pigmented Lesion Assay (DermTech, La Jolla, CA), has been introduced that analyzes the RNA from the stratum corneum for expression levels of RNA Linc00518 (Linc) and PRAME, which are overexpressed in melanomas. The assay also provides the status of TERT, a frequent somatic driver mutation in melanoma. In limited number of studies, the test boasts a greater than 99% negative predictive value, greater than 91% sensitivity, and 70% specificity in the diagnosis of melanoma (90–92). The test has not been widely in use and its role has not been studied extensively. In theory the high negative predictive value should provide reassurance to monitor the pigmented lesion with a negative test. The test also has been promoted to be useful in cosmetically sensitive or difficult to biopsy areas of the skin. Further independent studies and experience are needed to determine whether the promising results are reproducible and the exact role of the test.

Artificial intelligence

Artificial intelligence (AI) is expected have a profound impact on practice of medicine in the coming years, particularly perceptual specialties such as radiology, pathology, and dermatology as significant advances have been made in image recognition AI algorithms. Jaffe et al. evaluated an AI algorithm that was able to sift through 1,550 images of suspicious and benign skin lesions and identify melanoma with a sensitivity of 100% (93). Importantly, the specificity of the algorithm was found to be 64.8% which was only slightly less than the 69.9% specificity of clinicians. Other studies have shown that artificial intelligence is able to perform similarly to dermatoscopic evaluation in the identification of melanoma (94).

Currently there are no Food and Drug Administration (FDA) approved or cleared AI products in the US for the diagnosis or for the triage purposes of pigmented lesions. The number of commercially available smartphone applications, however, is rapidly growing. Because the diagnostic accuracy of the applications has been inconsistent and unreliable, several reviews have recommended against their use (95–97).

DermAssist, developed by Google, has been CE-marked as a Class 1 Medical Device in Europe with potential for worldwide expansion. The deep learning system within DermAssist was found to be non-inferior compared to 6 dermatologists and superior to 12 primary care physicians and nurse practitioners in providing a diagnosis for a set of 26 common skin conditions (98). When allowed to provide a three-diagnosis differential, the deep learning system was able to achieve a sensitivity of 90% compared to 89% in the dermatologist group and 69 and 72% in the primary care physician and nurse practitioner groups, respectively (98).

As the databases of clinical, dermatoscopic, and histologic images for melanocytic lesions grow, validated training data sets that are more generalizable are expected to emerge, setting the stage for AI augmented practice of dermatology. It is important to note that 90% of the databases used to create the DermAssist software extracted images from patients with lighter skin types; therefore, concerns regarding bias and equal access to the benefits of AI remain to be addressed, particularly in regard to skin of color (99).

Histopathological diagnosis

Despite the emergence of sophisticated molecular based tests, histopathological diagnosis of melanoma still remains the gold standard. The inherent subjective nature of histologic diagnosis of melanocytic neoplasms has resulted in high rate of discordance among pathologists (71–74). While thick bulky melanomas usually pose no issues, biopsies of ever smaller and thin lesions have further highlighted the problem of interobserver reliability. In the largest iteration of concordance study of melanocytic neoplasms among pathologists, only 25% concordance rate was observed for Spitz and atypical nevi and 45% concordance rate was observed for atypical spitz tumor, severely atypical nevi, and melanoma *in situ*, rates that are unacceptably low to be a valid diagnostic test (74). The low concordance rate among pathologists indicates markedly different thresholds are being applied to a large group of melanocytic neoplasms that have a significant impact on management. With the advances in molecular diagnostics, pathologists are turning to more precise molecular based ancillary diagnostic tests.

Historically, immunohistochemical stains had minimal diagnostic role, having only the confirmatory role of classifying the neoplasm as melanocytic. With insights on molecular signatures of melanomas, several immunohistochemical stains with a more diagnostic role have become available that include PReferentially expressed Antigen in Melanoma (PRAME) and p16. PRAME is overexpressed in melanomas and other cancers. Reflective of its discriminator power, it is included in several gene expression profiling tests for the prognostication of uveal melanoma (Decision Dx-UM), diagnosis of melanoma (myPath Melanoma), and guidance on the decision to biopsy (DermTech). Sensitivity ranging from 67–94% has been reported using PRAME IHC for the diagnosis of melanoma (100–104). For spindle cell desmoplastic melanomas, S100 and SOX10 continues to play a key role in their diagnosis as lower sensitivity ranging from 20 to 35% was observed (104, 105). Other useful IHC stains in the diagnosis of melanoma include p16. The loss of p16 expression, the product of CDKN2A gene, strongly correlates with the diagnosis of melanoma that can be demonstrated with the available IHC stain (106). Differentiating Spitz nevus from spitzoid melanoma, however, is not always helpful (107). Immunohistochemical stains have emerged for detecting the status of BRAF, BAP1, and cKit for the guidance role in targeted therapies.

Molecular diagnostic tests

Current molecular diagnostic tests for melanoma available to pathologists include comparative genomic hybridization (CGH), fluorescence *in situ* hybridization (FISH), gene expression profiling (GEP). CGH identifies chromosomal copy number variations,

including the deletion or multiplications of chromosomal segments (108). The technique involves DNA labeling with fluorochromes that subsequently allow for comparison with reference DNA to highlight genomic areas with gains or losses of DNA material. Advent of single-nucleotide polymorphism arrays allows for targeting genetic loci to the resolution of specific point mutations within the genome of melanocytes, allowing for the identification of loss of heterozygosity, even in chromosomal copy-neutral mutations which are missed with traditional CGH (109). Early CGH studies demonstrated that over 95% of melanomas demonstrated chromosomal number abnormalities in contrast to only 13% of benign nevi (109, 110). More recent studies have demonstrated the utility of CGH in differentiating melanoma from traditionally diagnostically challenging melanocytic entities, such as cellular blue nevi and Spitz nevi. Spitz nevi have been shown to demonstrate only isolated chromosomal number abnormalities at limited loci, while spitzoid melanomas demonstrate multiple copy number abnormalities in various segments (110).

In contrast to CGH that analyzes the whole genome, FISH allows for visualization of gains and losses of specific genomic segments. As normal somatic cells are expected to have two copies of any specific chromosome or chromosomal segment, the presence of more or less than two fluorescent signals indicates the presence of a chromosomal number abnormality. FISH has shown promising results in the differentiation of unequivocal lesions, including conjunctival nevi, epithelioid blue nevi, and, in particular Spitz nevi, and their respective melanoma counterparts with reported sensitivity of 83% and specificity of 94% (111).

While the original FISH assay utilized four probes targeting 6p25 (RREB1), 6q23 (MYB), 11q13 (cyclin D1), and Cep6, two additional probes targeting CDKN2A (9p21) and MYC (8q24) were added, which has increased sensitivity and specificity to 94 and 98%, respectively (112). Although FISH offers a greater ease-of-use and less tissue and labor requirements, CGH has been found to be more sensitive and specific given its ability to assay the entire genome. The high cost and false-positives are additional shortcomings of FISH assays, particularly in lesions that demonstrate polyploidy, such as Spitz nevi which can demonstrate tetraploidy, thus triggering a false positive result (110).

Leveraging real-time reverse transcription-polymerase chain reaction (qRT-PCR) technology, myPath (Castle Biosciences, Friendswood, Texas), a GEP test, has become available for pathologists to aid in the diagnosis of ambiguous melanocytic neoplasms. The assay analyzes the expression of 23 genes that includes PRAME and S100. The assay returns a numerical score that corresponds to likely *benign*, *likely malignant* or likely *indeterminate*. Retrospective validation studies have yielded sensitivity and specificity as high as 94 and 96%, respectively, in unambiguous melanocytic lesions (113–115). A significantly lower sensitivity in the 50% range was observed in studies in which ambiguous melanocytic lesions were evaluated (116, 117). Larger prospective studies on ambiguous melanocytic neoplasms are needed to demonstrate the utility and reliability of the ambiguous lesions for which the test was intended.

Artificial intelligence

Artificial intelligence augmented practice of dermatopathology is in its nascent stage. Several studies suggesting that performance AI is equal to or better than experienced pathologists have been published in the diagnosis of melanoma in artificial study settings (118–123). To harness the potential of AI in dermatopathology, some barriers need to be solved. Application of AI requires digitalization of slides, cost of which have prevented most laboratories adopting digitalization of the laboratory workflow. Generalizability of results requires large, validated data training sets. Most published studies use proprietary small data training sets that may not be generalizable. Lastly, AI cannot solve the issue of diagnostic discordance issue among dermatopathologists for melanocytic lesions, which will continue to be a barrier in the training and application of AI models (124).

Prognosis and staging

Clinician have long relied on American Joint Committee (AJCC) on Cancer staging guidelines. The 8th edition of the AJCC melanoma staging system was implemented in 2018. The primary determinant of the localized stage is the Breslow depth of the melanoma and ulceration. Breslow depth is measured from the granular layer of the epidermis down to the greatest depth of the melanoma. One of the biggest changes from the 7th edition is the change in the definition of T1a and T1b. While the cutoff for T1a and T1b stage was ″ 1 mm in the 7th edition, it was lowered to < 0.8 mm in the 8th edition (125). The result of the change directed more patients to a sentinel biopsy. The full impact of directing more patients for a sentinel biopsy in not known, but the rate of sentinel node positivity appears unchanged in one population-based study (126). A more individualized approach was suggested that accounted for clinicopathologic and molecular features.

Based on qRT-PCR technology that can be performed on paraffin embedded sections, several prognostic gene expression profiling assay tests have become available (127). In the US, 31-gene profiling assay (DecisionDx-Melanoma by Castle Biosciences) has been developed to provide prognostic risk stratification independent of the AJCC staging system. The assay predicts the risk of recurrence or metastasis in stage I, II, and III melanoma. The risk stratification scores consist of 1A (low risk), 1B/2A (intermediate risk) and 2A (high risk) (128). Multiple studies have consistently reported that the assay results independently predict metastatic risk, highlighting the utility of the GEP test (128–131).

While clinicians believe that GEP testing may have clinical benefit for patients with stage II and IIIA disease, the controversy has been for testing patients with stage I disease, a group with a very low risk of recurrence and metastasis (128). As stage I disease make up over 70% of new cases melanoma each year in the US, the test has the potential for high utilization for this stage of the disease, which has raised concerns about the high cost of the test ($7,193 per test) with unknown clinical benefit at this time (132). Meta-analysis by Marchetti and coworkers have concluded the performance of GEP tests for stage I disease was poor and highlighted the potential harm for patients in this group (127, 133). More recently, Kangas-Dick et al. reported that the GEP test did not perform better than traditional clinicopathologic prognostic features in predicting melanoma recurrence risk (134). Proponents and opponents of the GEP test all have criticized the methodologies of the studies that oppose their stance. Consensus statements for and against the test have been published (128, 133, 135). Currently, the American Academy of Dermatology (AAD) and National Comprehensive Cancer Network (NCCN) do not endorse the routine use of GEP. To settle the issue of validity and clinical applicability, authors have recommended

prospective randomized clinical trial with predetermined end points free of industry sponsorship bias (128, 132, 133, 136).

Conclusion

The remarkable advances in understanding the genomic underpinning of melanoma are paving the road for a paradigm shift in the approach to melanoma classification, diagnosis, staging, and therapy. The more precise, objective-based classification and diagnosis of melanoma are expected to replace the clinicopathologic one that is currently widely in use. Molecular diagnostics will play a greater role in the clinical and histologic diagnosis of melanoma as validated, convenient, and cost-effective molecular-based tests are expected to emerge. AI augmented clinical and histopathologic diagnosis of melanoma is expected to make the process more streamlined, precise, and efficient. The next iteration of AJCC staging will better reflect the rapid advances molecular basis of prognostication that is expected to be incorporated. The one issue that needs more immediate attention from the dermatology community is overdiagnosis. Though there is no debate on whether the overdiagnosis of melanoma exists, there is debate as to the degree. Epidemiologic evidence all but indicates a significant degree of overdiagnosis, providing a compelling reason for a shift in strategy from the current approach to melanoma detection. The immediate need is to identify the small fraction of aggressive melanomas within the sea of indolent early melanomas that are being detected today. The resolution of this knowledge gap requires appropriate attention both in terms of funding and research.

Author contributions

SW: Writing – original draft, Writing – review & editing, Data curation, Formal analysis. JL: Conceptualization, Supervision, Writing – original draft, Writing – review & editing.

Funding

The author(s) declare that no financial support was received for the research, authorship, and/or publication of this article.

Conflict of interest

The authors declare that the research was conducted in the absence of any commercial or financial relationships that could be construed as a potential conflict of interest.

Publisher's note

References

1. Arnold M, Singh D, Laversanne M, Vignat J, Vaccarella S, Meheus F, et al. Global burden of cutaneous melanoma in 2020 and projections to 2040. *JAMA Dermatol.* (2022) 158:495–503. doi: 10.1001/jamadermatol.2022.0160

2. Siegel RL, Miller KD, Fuchs HE, Jemal A. Cancer statistics, 2022. *CA Cancer J Clin.* (2022) 72:7–33. doi: 10.3322/caac.21708

3. SEER. (n.d.) Melanoma of the Skin – Cancer stat facts. SEER web site. Available at: https://seer.cancer.gov/statfacts/html/melan.html (Accessed July 9, 2023)

4. Landow SM, Gjelsvik A, Weinstock MA. Mortality burden and prognosis of thin melanomas overall and by subcategory of thickness, SEER registry data, 1992-2013. *J Am Acad Dermatol.* (2017) 76:258–63. doi: 10.1016/j.jaad.2016.10.018

5. American Cancer Society. (2023) Melanoma skin Cancer statistics. Available at: https://www.cancer.org/cancer/types/melanoma-skin-cancer/about/key-statistics.html (Accessed July 9, 2023)

6. Olsen CM, Thompson JF, Pandeya N, Whiteman DC. Evaluation of sex-specific incidence of melanoma. *JAMA Dermatol.* (2020) 156:553–60. doi: 10.1001/jamadermatol.2020.0470

7. Kurtansky NR, Dusza SW, Halpern AC, Hartman RI, Geller AC, Marghoob AA, et al. An epidemiologic analysis of melanoma Overdiagnosis in the United States, 1975-2017. *J Invest Dermatol.* (2022) 142:1804–1811.e6. doi: 10.1016/j.jid.2021.12.003

8. Ackerman AB. Macular and patch lesions of malignant melanoma: malignant melanoma *in situ*. *J Dermatol Surg Oncol.* (1983) 9:615–8. doi: 10.1111/j.1524-4725.1983.tb00868.x

9. Menzies SW, Zalaudek I. Why perform dermoscopy? The evidence for its role in the routine management of pigmented skin lesions. *Arch Dermatol.* (2006) 142:1211–2. doi: 10.1001/archderm.142.9.1211

10. Ring C, Cox N, Lee JB. Dermatoscopy. *Clin Dermatol.* (2021) 39:635–42. doi: 10.1016/j.clindermatol.2021.03.009

11. Burton RC, Armstrong BK. Recent incidence trends imply a nonmetastasizing form of invasive melanoma. *Melanoma Res.* (1994) 4:107–13. doi: 10.1097/00008390-199404000-00005

12. Welch HG, Mazer BL, Adamson AS. The rapid rise in cutaneous melanoma diagnoses. *N Engl J Med.* (2021) 384:72–9. doi: 10.1056/NEJMsb2019760

13. Glasziou PP, Jones MA, Pathirana T, Barratt AL, Bell KJ. Estimating the magnitude of cancer overdiagnosis in Australia. *Med J Aust.* (2020) 212:163–8. doi: 10.5694/mja2.50455

14. Whiteman DC, Olsen CM, MacGregor S, Law MH, Thompson B, Dusingize JC, et al. The effect of screening on melanoma incidence and biopsy rates. *Br J Dermatol.* (2022) 187:515–22. doi: 10.1111/bjd.21649

15. Adamson AS, Suarez EA, Welch HG. Estimating Overdiagnosis of melanoma using trends among black and white patients in the US. *JAMA Dermatol.* (2022) 158:426–31. doi: 10.1001/jamadermatol.2022.0139

16. Carter SM, Degeling C, Doust J, Barratt A. A definition and ethical evaluation of overdiagnosis. *J Med Ethics.* (2016) 42:705–14. doi: 10.1136/medethics-2015-102928

17. Brodersen J, Schwartz LM, Heneghan C, O'Sullivan JW, Aronson JK, Woloshin S. Overdiagnosis: what it is and what it isn't. *BMJ Evid Based Med.* (2018) 23:1–3. doi: 10.1136/ebmed-2017-110886

18. Lipsker DM, Hedelin G, Heid E, Grosshans EM, Cribier BJ. Striking increase of thin melanomas contrasts with stable incidence of thick melanomas. *Arch Dermatol.* (1999) 135:1451–6. doi: 10.1001/archderm.135.12.1451

19. Croswell JM, Ransohoff DF, Kramer BS. Principles of cancer screening: lessons from history and study design issues. *Semin Oncol.* (2010) 37:202–15. doi: 10.1053/j.seminoncol.2010.05.006

20. Vecchiato A, Zonta E, Campana L, Dal Bello G, Rastrelli M, Rossi CR, et al. Long-term survival of patients with invasive ultra-thin cutaneous melanoma: a single-center retrospective analysis. *Medicine (Baltimore).* (2016) 95:e2452. doi: 10.1097/MD.0000000000002452

21. Eguchi MM, Elder DE, Barnhill RL, Piepkorn MW, Knezevich SR, Elmore JG, et al. Prognostic modeling of cutaneous melanoma stage I patients using cancer registry data identifies subsets with very-low melanoma mortality. *Cancer.* (2023) 129:89–97. doi: 10.1002/cncr.34490

22. Greenlee RT, Murray T, Bolden S, Wingo PA. Cancer statistics, 2000. *CA Cancer J Clin.* (2000) 50:7–33. doi: 10.3322/canjclin.50.1.7

23. Siegel RL, Miller KD, Fuchs HE, Jemal A. Cancer statistics, 2021. *CA Cancer J Clin*. (2021) 71:7–33. doi: 10.3322/caac.21654

24. Olsen CM, Pandeya N, Rosenberg PS, Whiteman DC. Incidence of in situ vs invasive melanoma: testing the "obligate precursor" hypothesis. *J Natl Cancer Inst*. (2022) 114:1364–70. doi: 10.1093/jnci/djac138

25. Elder DE. Obligate and potential precursors of melanoma. *J Natl Cancer Inst*. (2022) 114:1320–2. doi: 10.1093/jnci/djac139

26. Patel VR, Roberson ML, Pignone MP, Adamson AS. Risk of mortality after a diagnosis of melanoma in situ. *JAMA Dermatol*. (2023) 159:e231494:703–10. doi: 10.1001/jamadermatol.2023.1494

27. Esserman LJ, Thompson IM, Reid B. Overdiagnosis and overtreatment in cancer: an opportunity for improvement. *JAMA*. (2013) 310:797–8. doi: 10.1001/jama.2013.108415

28. Clark WH, Reimer RR, Greene M, Ainsworth AM, Mastrangelo MJ. Origin of familial malignant melanomas from heritable melanocytic lesions. 'The B-K mole syndrome'. *Arch Dermatol*. (1978) 114:732–8.

29. Consensus conference: precursors to malignant melanoma. *JAMA*. (1984) 251:1864–6. doi: 10.1001/jama.1984.03340380046022

30. NIH Consensus conference. Diagnosis and treatment of early melanoma. *JAMA*. (1992) 268:1314–9. doi: 10.1001/jama.1992.03490100112037

31. Kanzler MH, Mraz-Gernhard S. Primary cutaneous malignant melanoma and its precursor lesions: diagnostic and therapeutic overview. *J Am Acad Dermatol*. (2001) 45:260–76. doi: 10.1067/mjd.2001.116239

32. Mangione CM, Barry MJ, Nicholson WK, Chelmow D, Coker TR, Davis EM, et al. Screening for skin Cancer: US preventive services task force recommendation statement. *JAMA*. (2023) 329:1290–5. doi: 10.1001/jama.2023.4342

33. Breitbart EW, Waldmann A, Nolte S, Capellaro M, Greinert R, Volkmer B, et al. Systematic skin cancer screening in northern Germany. *J Am Acad Dermatol*. (2012) 66:201–11. doi: 10.1016/j.jaad.2010.11.016

34. Boniol M, Autier P, Gandini S. Melanoma mortality following skin cancer screening in Germany. *BMJ Open*. (2015) 5:e008158. doi: 10.1136/bmjopen-2015-008158

35. Stang A, Jöckel K. Does skin cancer screening save lives? A detailed analysis of mortality time trends in Schleswig-Holstein and Germany. *Cancer*. (2016) 122:432–7. doi: 10.1002/cncr.29755

36. Bibbins-Domingo K, Grossman DC, Curry SJ, Barry MJ, Davidson KW, Doubeni CA, et al. Screening for thyroid Cancer: US preventive services task force recommendation statement. *JAMA*. (2017) 317:1882–7. doi: 10.1001/jama.2017.4011

37. SEER. (n.d.) Cancer of the Thyroid – Cancer stat facts. SEER web site. Available at: https://seer.cancer.gov/statfacts/html/thyro.html (Accessed July 9, 2023).

38. Adamson AS. The USPSTF I statement on skin Cancer screening-not a disappointment but an opportunity. *JAMA Dermatol*. (2023) 159:579–81. doi: 10.1001/jamadermatol.2023.0706

39. Fears TR, Scotto J, Schneiderman MA. Mathematical models of age and ultraviolet effects on the incidence of skin cancer among whites in the United States. *Am J Epidemiol*. (1977) 105:420–7. doi: 10.1093/oxfordjournals.aje.a112400

40. Holman CD, Armstrong BK, Heenan PJ. Relationship of cutaneous malignant melanoma to individual sunlight-exposure habits. *J Natl Cancer Inst*. (1986) 76:403–14.

41. An S, Kim K, Moon S, Ko K-P, Kim I, Lee JE, et al. Indoor tanning and the risk of overall and early-onset melanoma and non-melanoma skin Cancer: systematic review and Meta-analysis. *Cancers (Basel)*. (2021) 13:5940. doi: 10.3390/cancers13235940

42. Gandini S, Sera F, Cattaruzza MS, Pasquini P, Picconi O, Boyle P, et al. Meta-analysis of risk factors for cutaneous melanoma: II Sun exposure. *Eur J Cancer*. (2005) 41:45–60. doi: 10.1016/j.ejca.2004.10.016

43. Lipsker D, Engel F, Cribier B, Velten M, Hedelin G. Trends in melanoma epidemiology suggest three different types of melanoma. *Br J Dermatol*. (2007) 157:338–43. doi: 10.1111/j.1365-2133.2007.08029.x

44. Martorell-Calatayud A, Nagore E, Botella-Estrada R, Scherer D, Requena C, Serra-Guillén C, et al. Defining fast-growing melanomas: reappraisal of epidemiological, clinical, and histological features. *Melanoma Res*. (2011) 21:131–8. doi: 10.1097/CMR.0b013e328342f312

45. Argenziano G, Kittler H, Ferrara G, Rubegni P, Malvehy J, Puig S, et al. Slow-growing melanoma: a dermoscopy follow-up study. *Br J Dermatol*. (2010) 162:267–73. doi: 10.1111/j.1365-2133.2009.09416.x

46. Hermes HM, Sahu J, Schwartz LR, Lee JB. Clinical and histologic characteristics of clinically unsuspected melanomas. *Clin Dermatol*. (2014) 32:324–30. doi: 10.1016/j.clindermatol.2013.10.003

47. Rhodes AR, Weinstock MA, Fitzpatrick TB, Mihm MC, Sober AJ. Risk factors for cutaneous melanoma. A practical method of recognizing predisposed individuals. *JAMA*. (1987) 258:3146–54. doi: 10.1001/jama.1987.03400210088032

48. Holly EA, Kelly JW, Shpall SN, Chiu SH. Number of melanocytic nevi as a major risk factor for malignant melanoma. *J Am Acad Dermatol*. (1987) 17:459–68. doi: 10.1016/s0190-9622(87)70230-8

49. Krengel S, Hauschild A, Schäfer T. Melanoma risk in congenital melanocytic naevi: a systematic review. *Br J Dermatol*. (2006) 155:1–8. doi: 10.1111/j.1365-2133.2006.07218.x

50. Duffy K, Grossman D. The dysplastic nevus: from historical perspective to management in the modern era: part II. Molecular aspects and clinical management. *J Am Acad Dermatol*. (2012) 67:19.e1–19.e32. doi: 10.1016/j.jaad.2012.03.013

51. Spaccarelli N, Drozdowski R, Peters MS, Grant-Kels JM. Dysplastic nevus part II: dysplastic nevi: molecular/genetic profiles and management. *J Am Acad Dermatol*. (2023) 88:13–20. doi: 10.1016/j.jaad.2022.05.071

52. Kittler H, Tschandl P. Dysplastic nevus: why this term should be abandoned in dermatoscopy. *Dermatol Clin*. (2013) 31:579–88, viii. doi: 10.1016/j.det.2013.06.009

53. Rosendahl CO, Grant-Kels JM, Que SKT. Dysplastic nevus: fact and fiction. *J Am Acad Dermatol*. (2015) 73:507–12. doi: 10.1016/j.jaad.2015.04.029

54. Lozeau DF, Farber MJ, Lee JB. A nongrading histologic approach to Clark (dysplastic) nevi: a potential to decrease the excision rate. *J Am Acad Dermatol*. (2016) 74:68–74. doi: 10.1016/j.jaad.2015.09.030

55. Ackerman AB. What naevus is dysplastic, a syndrome and the commonest precursor of malignant melanoma? A riddle and an answer. *Histopathology*. (1988) 13:241–56. doi: 10.1111/j.1365-2559.1988.tb02036.x

56. Toussi A, Mans N, Welborn J, Kiuru M. Germline mutations predisposing to melanoma. *J Cutan Pathol*. (2020) 47:606–16. doi: 10.1111/cup.13689

57. Leachman SA, Lucero OM, Sampson JE, Cassidy P, Bruno W, Queirolo P, et al. Identification, genetic testing, and management of hereditary melanoma. *Cancer Metastasis Rev*. (2017) 36:77–90. doi: 10.1007/s10555-017-9661-5

58. Ransohoff KJ, Jaju PD, Tang JY, Carbone M, Leachman S, Sarin KY. Familial skin cancer syndromes: increased melanoma risk. *J Am Acad Dermatol*. (2016) 74:423–36. doi: 10.1016/j.jaad.2015.09.070

59. Begg CB, Orlow I, Hummer AJ, Armstrong BK, Kricker A, Marrett LD, et al. Lifetime risk of melanoma in CDKN2A mutation carriers in a population-based sample. *J Natl Cancer Inst*. (2005) 97:1507–15. doi: 10.1093/jnci/dji312

60. Vasen HF, Gruis NA, Frants RR, van Der Velden PA, Hille ET, Bergman W. Risk of developing pancreatic cancer in families with familial atypical multiple mole melanoma associated with a specific 19 deletion of p16 (p16-Leiden). *Int J Cancer*. (2000) 87:809–11.

61. Wiesner T, Obenauf AC, Murali R, Fried I, Griewank KG, Ulz P, et al. Germline mutations in BAP1 predispose to melanocytic tumors. *Nat Genet*. (2011) 43:1018–21. doi: 10.1038/ng.910

62. Farley MN, Schmidt LS, Mester JL, Peña-Llopis S, Pavia-Jimenez A, Christie A, et al. A novel germline mutation in BAP1 predisposes to familial clear-cell renal cell carcinoma. *Mol Cancer Res*. (2013) 11:1061–71. doi: 10.1158/1541-7786.MCR-13-0111

63. Abdel-Rahman MH, Pilarski R, Cebulla CM, Massengill JB, Christopher BN, Boru G, et al. Germline BAP1 mutation predisposes to uveal melanoma, lung adenocarcinoma, meningioma, and other cancers. *J Med Genet*. (2011) 48:856–9. doi: 10.1136/jmedgenet-2011-100156

64. de la Fouchardière A, Cabaret O, Savin L, Combemale P, Schvartz H, Penet C, et al. Germline BAP1 mutations predispose also to multiple basal cell carcinomas. *Clin Genet*. (2015) 88:273–7. doi: 10.1111/cge.12472

65. Llamas-Velasco M, Pérez-Gónzalez YC, Requena L, Kutzner H. Histopathologic clues for the diagnosis of Wiesner nevus. *J Am Acad Dermatol*. (2014) 70:549–54. doi: 10.1016/j.jaad.2013.10.032

66. Motaparthi K, Kim J, Andea AA, Missall TA, Novoa RA, Vidal CI, et al. TERT and TERT promoter in melanocytic neoplasms: current concepts in pathogenesis, diagnosis, and prognosis. *J Cutan Pathol*. (2020) 47:710–9. doi: 10.1111/cup.13691

67. Leachman SA, Carucci J, Kohlmann W, Banks KC, Asgari MM, Bergman W, et al. Selection criteria for genetic assessment of patients with familial melanoma. *J Am Acad Dermatol*. (2009) 61:677.e1–677.e14. doi: 10.1016/j.jaad.2009.03.016

68. Gumaste PV, Penn LA, Cymerman RM, Kirchhoff T, Polsky D, McLellan B. Skin cancer risk in BRCA1/2 mutation carriers. *Br J Dermatol*. (2015) 172:1498–506. doi: 10.1111/bjd.13626

69. McGovern VJ, Mihm MC, Bailly C, Booth JC, Clark WH Jr, Cochran AJ, et al. The classification of malignant melanoma and its histologic reporting. *Cancer*. (1973) 32:1446–57. doi: 10.1002/1097-0142(197312)32:63.0.co;2-8

70. *Human malignant melanoma/edited by Wallace H. Clark, Jr., Leonard I. Goldman, Michael J. Mastrangelo*. New York: Grune & Stratton (1979).

71. Farmer ER, Gonin R, Hanna MP. Discordance in the histopathologic diagnosis of melanoma and melanocytic nevi between expert pathologists. *Hum Pathol*. (1996) 27:528–31. doi: 10.1016/s0046-8177(96)90157-4

72. Corona R, Mele A, Amini M, de Rosa G, Coppola G, Piccardi P, et al. Interobserver variability on the histopathologic diagnosis of cutaneous melanoma and other pigmented skin lesions. *J Clin Oncol*. (1996) 14:1218–23. doi: 10.1200/JCO.1996.14.4.1218

73. Shoo BA, Sagebiel RW, Kashani-Sabet M. Discordance in the histopathologic diagnosis of melanoma at a melanoma referral center. *J Am Acad Dermatol*. (2010) 62:751–6. doi: 10.1016/j.jaad.2009.09.043

74. Elmore JG, Barnhill RL, Elder DE, Longton GM, Pepe MS, Reisch LM, et al. Pathologists' diagnosis of invasive melanoma and melanocytic proliferations: observer accuracy and reproducibility study. *BMJ*. (2017) 357:j2813. doi: 10.1136/bmj.j2813

75. Weyers W, Euler M, Diaz-Cascajo C, Schill WB, Bonczkowitz M. Classification of cutaneous malignant melanoma: a reassessment of histopathologic criteria for the distinction of different types. *Cancer*. (1999) 86:288–99. doi: 10.1002/(sici)1097-0142(19990715)86:23.0.co;2-s

76. Hurt MA. Types of melanoma? *J Am Acad Dermatol*. (2008) 58:1059–60. doi: 10.1016/j.jaad.2007.12.009

77. Elder DE, Bastian BC, Cree IA, Massi D, Scolyer RA. The 2018 World Health Organization classification of cutaneous, mucosal, and uveal melanoma: detailed analysis of 9 distinct subtypes defined by their evolutionary pathway. *Arch Pathol Lab Med*. (2020) 144:500–22. doi: 10.5858/arpa.2019-0561-RA

78. Piepkorn MW, Barnhill RL, Elder DE, Knezevich SR, Carney PA, Reisch LM, et al. The MPATH-dx reporting schema for melanocytic proliferations and melanoma. *J Am Acad Dermatol*. (2014) 70:131–41. doi: 10.1016/j.jaad.2013.07.027

79. Barnhill RL, Elder DE, Piepkorn MW, Knezevich SR, Reisch LM, Eguchi MM, et al. Revision of the melanocytic pathology assessment tool and hierarchy for diagnosis classification Schema for melanocytic lesions: a consensus statement. *JAMA Netw Open*. (2023) 6:e2250613. doi: 10.1001/jamanetworkopen.2022.50613

80. Lindelöf B, Hedblad MA. Accuracy in the clinical diagnosis and pattern of malignant melanoma at a dermatological clinic. *J Dermatol*. (1994) 21:461–4. doi: 10.1111/j.1346-8138.1994.tb01775.x

81. Grin CM, Kopf AW, Welkovich B, Bart RS, Levenstein MJ. Accuracy in the clinical diagnosis of malignant melanoma. *Arch Dermatol*. (1990) 126:763–6. doi: 10.1001/archderm.1990.01670300063008

82. Morton CA, Mackie RM. Clinical accuracy of the diagnosis of cutaneous malignant melanoma. *Br J Dermatol*. (1998) 138:283–7. doi: 10.1046/j.1365-2133.1998.02075.x

83. Braun RP, Rabinovitz HS, Oliviero M, Kopf AW, Saurat J. Dermoscopy of pigmented skin lesions. *J Am Acad Dermatol*. (2005) 52:109–21. doi: 10.1016/j.jaad.2001.11.001

84. Argenziano G, Soyer HP, Chimenti S, Talamini R, Corona R, Sera F, et al. Dermoscopy of pigmented skin lesions: results of a consensus meeting via the internet. *J Am Acad Dermatol*. (2003) 48:679–93. doi: 10.1067/mjd.2003.281

85. Mayer J. Systematic review of the diagnostic accuracy of dermatoscopy in detecting malignant melanoma. *Med J Aust*. (1997) 167:206–10. doi: 10.5694/j.1326-5377.1997.tb138847.x

86. Bafounta ML, Beauchet A, Aegerter P, Saiag P. Is dermoscopy (epiluminescence microscopy) useful for the diagnosis of melanoma? Results of a meta-analysis using techniques adapted to the evaluation of diagnostic tests. *Arch Dermatol*. (2001) 137:1343–50. doi: 10.1001/archderm.137.10.1343

87. Vestergaard ME, Macaskill P, Holt PE, Menzies SW. Dermoscopy compared with naked eye examination for the diagnosis of primary melanoma: a meta-analysis of studies performed in a clinical setting. *Br J Dermatol*. (2008) 159:669–76. doi: 10.1111/j.1365-2133.2008.08713.x

88. Dinnes J, Deeks JJ, Chuchu N, Ferrante di Ruffano L, Matin RN, Thomson DR, et al. Dermoscopy, with and without visual inspection, for diagnosing melanoma in adults. *Cochrane Database Syst Rev*. (2018) 2018:CD011902. doi: 10.1002/14651858.CD011902.pub2

89. Carli P. Dermoscopy not yet shown to increase sensitivity of melanoma diagnosis in real practice. *Arch Dermatol*. (2007) 143:659–66. doi: 10.1001/archderm.143.5.664-b

90. Ferris LK, Gerami P, Skelsey MK, Peck G, Hren C, Gorman C, et al. Real-world performance and utility of a noninvasive gene expression assay to evaluate melanoma risk in pigmented lesions. *Melanoma Res*. (2018) 28:478–82. doi: 10.1097/CMR.0000000000000478

91. Gerami P, Yao Z, Polsky D, Jansen B, Busam K, Ho J, et al. Development and validation of a noninvasive 2-gene molecular assay for cutaneous melanoma. *J Am Acad Dermatol*. (2017) 76:114–120.e2. doi: 10.1016/j.jaad.2016.07.038

92. Ferris LK, Jansen B, Ho J, Busam KJ, Gross K, Hansen DD, et al. Utility of a noninvasive 2-gene molecular assay for cutaneous melanoma and effect on the decision to biopsy. *JAMA Dermatol*. (2017) 153:675–80. doi: 10.1001/jamadermatol.2017.0473

93. Phillips M, Marsden H, Jaffe W, Matin RN, Wali GN, Greenhalgh J, et al. Assessment of accuracy of an artificial intelligence algorithm to detect melanoma in images of skin lesions. *JAMA Netw Open*. (2019) 2:e1913436. doi: 10.1001/jamanetworkopen.2019.13436

94. Rajpara SM, Botello AP, Townend J, Ormerod AD. Systematic review of dermoscopy and digital dermoscopy/ artificial intelligence for the diagnosis of melanoma. *Br J Dermatol*. (2009) 161:591–604. doi: 10.1111/j.1365-2133.2009.09093.x

95. Sun MD, Kentley J, Mehta P, Dusza S, Halpern AC, Rotemberg V. Accuracy of commercially available smartphone applications for the detection of melanoma. *Br J Dermatol*. (2022) 186:744–6. doi: 10.1111/bjd.20903

96. Algorithm based smartphone apps to assess risk of skin cancer in adults: systematic review of diagnostic accuracy studies. *BMJ*. (2020) 368:m645. doi: 10.1136/bmj.m645

97. Chuchu N, Takwoingi Y, Dinnes J, Matin RN, Bassett O, Moreau JF, et al. Smartphone applications for triaging adults with skin lesions that are suspicious for melanoma. *Cochrane Database Syst Rev*. (2018) 12:CD013192. doi: 10.1002/14651858.CD013192

98. Liu Y, Jain A, Eng C, Way DH, Lee K, Bui P, et al. A deep learning system for differential diagnosis of skin diseases. *Nat Med*. (2020) 26:900–8. doi: 10.1038/s41591-020-0842-3

99. Dave P, Nambudiri V, Grant-Kels JM. The introduction of "Dr AI": what dermatologists should consider. *J Am Acad Dermatol*. (2023) 88:1401–2. doi: 10.1016/j.jaad.2022.01.014

100. O'Connor MK, Dai H, Fraga GR. PRAME immunohistochemistry for melanoma diagnosis: a STARD-compliant diagnostic accuracy study. *J Cutan Pathol*. (2022) 49:780–6. doi: 10.1111/cup.14267

101. Raghavan SS, Wang JY, Kwok S, Rieger KE, Novoa RA, Brown RA. PRAME expression in melanocytic proliferations with intermediate histopathologic or spitzoid features. *J Cutan Pathol*. (2020) 47:1123–31. doi: 10.1111/cup.13818

102. Olds H, Utz S, Abrams J, Terrano D, Mehregan D. Use of PRAME immunostaining to distinguish early melanoma in situ from benign pigmented conditions. *J Cutan Pathol*. (2022) 49:510–4. doi: 10.1111/cup.14212

103. Alomari AK, Tharp AW, Umphress B, Kowal RP. The utility of PRAME immunohistochemistry in the evaluation of challenging melanocytic tumors. *J Cutan Pathol*. (2021) 48:1115–23. doi: 10.1111/cup.14000

104. Lezcano C, Jungbluth AA, Nehal KS, Hollmann TJ, Busam KJ. PRAME expression in melanocytic tumors. *Am J Surg Pathol*. (2018) 42:1456–65. doi: 10.1097/PAS.0000000000001134

105. Plotzke JM, Zoumberos NA, Hrycaj SM, Harms PW, Bresler SC, Chan MP. PRAME expression is similar in scar and desmoplastic melanoma. *J Cutan Pathol*. (2022) 49:829–32. doi: 10.1111/cup.14286

106. Pavey SJ, Cummings MC, Whiteman DC, Castellano M, Walsh MD, Gabrielli BG, et al. Loss of p16 expression is associated with histological features of melanoma invasion. *Melanoma Res*. (2002) 12:539–47. doi: 10.1097/00008390-200212000-00003

107. Mason A, Wititsuwannakul J, Klump VR, Lott J, Lazova R. Expression of p16 alone does not differentiate between Spitz nevi and Spitzoid melanoma. *J Cutan Pathol*. (2012) 39:1062–74. doi: 10.1111/cup.12014

108. Bauer J, Bastian BC. Distinguishing melanocytic nevi from melanoma by DNA copy number changes: comparative genomic hybridization as a research and diagnostic tool. *Dermatol Ther*. (2006) 19:40–9. doi: 10.1111/j.1529-8019.2005.00055.x

109. Figl A, Scherer D, Nagore E, Bermejo JL, Botella-Estrada R, Gast A, et al. Single-nucleotide polymorphisms in DNA-repair genes and cutaneous melanoma. *Mutat Res*. (2010) 702:8–16. doi: 10.1016/j.mrgentox.2010.06.011

110. Miedema J, Andea AA. Through the looking glass and what you find there: making sense of comparative genomic hybridization and fluorescence in situ hybridization for melanoma diagnosis. *Mod Pathol*. (2020) 33:1318–30. doi: 10.1038/s41379-020-0490-7

111. Gerami P, Mafee M, Lurtsbarapa T, Guitart J, Haghighat Z, Newman M. Sensitivity of fluorescence in situ hybridization for melanoma diagnosis using RREB1, MYB, Cep6, and 11q13 probes in melanoma subtypes. *Arch Dermatol*. (2010) 146:273–8. doi: 10.1001/archdermatol.2009.386

112. Gerami P, Li G, Pouryazdanparast P, Blondin B, Beilfuss B, Slenk C, et al. A highly specific and discriminatory FISH assay for distinguishing between benign and malignant melanocytic neoplasms. *Am J Surg Pathol*. (2012) 36:808–17. doi: 10.1097/PAS.0b013e31824b1efd

113. Ko JS, Matharoo-Ball B, Billings SD, Thomson BJ, Tang JY, Sarin KY, et al. Diagnostic distinction of malignant melanoma and benign nevi by a gene expression signature and correlation to clinical outcomes. *Cancer Epidemiol Biomark Prev*. (2017) 26:1107–13. doi: 10.1158/1055-9965.EPI-16-0958

114. Clarke LE, Flake DD, Busam K, Cockerell C, Helm K, McNiff J, et al. An independent validation of a gene expression signature to differentiate malignant melanoma from benign melanocytic nevi. *Cancer*. (2017) 123:617–28. doi: 10.1002/cncr.30385

115. Clarke LE, Warf MB, Flake DD, Hartman A-R, Tahan S, Shea CR, et al. Clinical validation of a gene expression signature that differentiates benign nevi from malignant melanoma. *J Cutan Pathol*. (2015) 42:244–52. doi: 10.1111/cup.12475

116. Reimann JDR, Salim S, Velazquez EF, Wang L, Williams KM, Flejter WL, et al. Comparison of melanoma gene expression score with histopathology, fluorescence in situ hybridization, and SNP array for the classification of melanocytic neoplasms. *Mod Pathol*. (2018) 31:1733–43. doi: 10.1038/s41379-018-0087-6

117. Minca EC, Al-Rohil RN, Wang M, Harms PW, Ko JS, Collie AM, et al. Comparison between melanoma gene expression score and fluorescence in situ hybridization for the classification of melanocytic lesions. *Mod Pathol*. (2016) 29:832–43. doi: 10.1038/modpathol.2016.84

118. Hart SN, Flotte W, Norgan AP, Shah KK, Buchan ZR, Mounajjed T, et al. Classification of melanocytic lesions in selected and whole-slide images via convolutional neural networks. *J Pathol Inform*. (2019) 10:5. doi: 10.4103/jpi.jpi_32_18

119. Hekler A, Utikal JS, Enk AH, Berking C, Klode J, Schadendorf D, et al. Pathologist-level classification of histopathological melanoma images with deep neural networks. *Eur J Cancer*. (2019) 115:79–83. doi: 10.1016/j.ejca.2019.04.021

120. Hekler A, Utikal JS, Enk AH, Solass W, Schmitt M, Klode J, et al. Deep learning outperformed 11 pathologists in the classification of histopathological melanoma images. *Eur J Cancer*. (2019) 118:91–6. doi: 10.1016/j.ejca.2019.06.012

121. Stiff KM, Franklin MJ, Zhou Y, Madabhushi A, Knackstedt TJ. Artificial intelligence and melanoma: a comprehensive review of clinical, dermoscopic, and histologic applications. *Pigment Cell Melanoma Res*. (2022) 35:203–11. doi: 10.1111/pcmr.13027

122. Brinker TJ, Schmitt M, Krieghoff-Henning EI, Barnhill R, Beltraminelli H, Braun SA, et al. Diagnostic performance of artificial intelligence for histologic melanoma recognition compared to 18 international expert pathologists. *J Am Acad Dermatol*. (2022) 86:640–2. doi: 10.1016/j.jaad.2021.02.009

123. Ianni JD, Soans RE, Sankarapandian S, Chamarthi RV, Ayyagari D, Olsen TG, et al. Tailored for real-world: a whole slide image classification system validated on Uncurated multi-site data emulating the prospective pathology workload. *Sci Rep*. (2020) 10:3217. doi: 10.1038/s41598-020-59985-2

124. Wells A, Patel S, Lee JB, Motaparthi K. Artificial intelligence in dermatopathology: diagnosis, education, and research. *J Cutan Pathol*. (2021) 48:1061–8. doi: 10.1111/cup.13954

125. Keung EZ, Gershenwald JE. The eighth edition American joint committee on Cancer (AJCC) melanoma staging system: implications for melanoma treatment and care. *Expert Rev Anticancer Ther*. (2018) 18:775–84. doi: 10.1080/14737140.2018.1489246

126. Weitemeyer MB, Helvind NM, Brinck AM, Hölmich LR, Chakera AH. More sentinel lymph node biopsies for thin melanomas after transition to AJCC 8th edition do not increase positivity rate: a Danish population-based study of 7148 patients. *J Surg Oncol*. (2022) 125:498–508. doi: 10.1002/jso.26723

127. Marchetti MA, Coit DG, Dusza SW, Yu A, McLean LT, Hu Y, et al. Performance of gene expression profile tests for prognosis in patients with localized cutaneous melanoma: a systematic review and Meta-analysis. *JAMA Dermatol*. (2020) 156:953–62. doi: 10.1001/jamadermatol.2020.1731

128. Grossman D, Okwundu N, Bartlett EK, Marchetti MA, Othus M, Coit DG, et al. Prognostic gene expression profiling in cutaneous melanoma: identifying the knowledge gaps and assessing the clinical benefit. *JAMA Dermatol*. (2020) 156:1004–11. doi: 10.1001/jamadermatol.2020.1729

129. Hsueh EC, DeBloom JR, Lee J, Sussman JJ, Covington KR, Middlebrook B, et al. Interim analysis of survival in a prospective, multi-center registry cohort of cutaneous melanoma tested with a prognostic 31-gene expression profile test. *J Hematol Oncol*. (2017) 10:152. doi: 10.1186/s13045-017-0520-1

130. Keller J, Schwartz TL, Lizalek JM, Chang E-S, Patel AD, Hurley MY, et al. Prospective validation of the prognostic 31-gene expression profiling test in primary cutaneous melanoma. *Cancer Med*. (2019) 8:2205–12. doi: 10.1002/cam4.2128

131. Greenhaw BN, Covington KR, Kurley SJ, Yeniay Y, Cao NA, Plasseraud KM, et al. Molecular risk prediction in cutaneous melanoma: a meta-analysis of the 31-gene expression profile prognostic test in 1,479 patients. *J Am Acad Dermatol*. (2020) 83:745–53. doi: 10.1016/j.jaad.2020.03.053

132. Kovarik CL, Chu EY, Adamson AS. Gene expression profile testing for thin melanoma: evidence to support clinical use remains thin. *JAMA Dermatol*. (2020) 156:837–8. doi: 10.1001/jamadermatol.2020.0894

133. Marchetti MA, Bartlett EK, Dusza SW, Bichakjian CK. Use of a prognostic gene expression profile test for T1 cutaneous melanoma: will it help or harm patients? *J Am Acad Dermatol*. (2019) 80:e161–2. doi: 10.1016/j.jaad.2018.11.063

134. Kangas-Dick AW, Greenbaum A, Gall V, Groisberg R, Mehnert J, Chen C, et al. Evaluation of a gene expression profiling assay in primary cutaneous melanoma. *Ann Surg Oncol*. (2021) 28:4582–9. doi: 10.1245/s10434-020-09563-7

135. Farberg AS, Marson JW, Glazer A, Litchman GH, Svoboda R, Winkelmann RR, et al. Expert consensus on the use of prognostic gene expression profiling tests for the Management of Cutaneous Melanoma: consensus from the skin Cancer prevention working group. *Dermatol Ther (Heidelb)*. (2022) 12:807–23. doi: 10.1007/s13555-022-00709-x

136. Sabel MS. Genomic expression profiling in melanoma and the road to clinical practice. *Ann Surg Oncol*. (2022) 29:764–6. doi: 10.1245/s10434-021-110993

frontiers | Frontiers in Medicine

TYPE Case Report
PUBLISHED 15 December 2023
DOI 10.3389/fmed.2023.1243459

OPEN ACCESS

EDITED BY
Bahar Dasgeb,
Rutgers, The State University of New Jersey, United States

REVIEWED BY
Nicola Pimpinelli,
University of Florence, Italy
Shabnam Momtahen,
Dartmouth College, United States
Jaroslaw Jedrych,
Johns Hopkins Medicine, United States

*CORRESPONDENCE
Neda Nikbakht
✉ neda.nikbakht@jefferson.edu

RECEIVED 20 June 2023
ACCEPTED 19 October 2023
PUBLISHED 15 December 2023

CITATION
Bhatti S, Joffe D, Banner L, Talasila S, Mandel J, Lee J, Porcu P and Nikbakht N (2023) Utility of T-cell immunosequencing in distinguishing mycosis fungoides progression from treatment related cutaneous adverse events.
Front. Med. 10:1243459.
doi: 10.3389/fmed.2023.1243459

Utility of T-cell immunosequencing in distinguishing mycosis fungoides progression from treatment related cutaneous adverse events

Safiyyah Bhatti[1,2], Daniel Joffe[1], Lauren Banner[1], Sahithi Talasila[1], Jenna Mandel[1], Jason Lee[1], Pierluigi Porcu[2] and Neda Nikbakht[1]*

[1]Department of Dermatology and Cutaneous Biology, Thomas Jefferson University, Philadelphia, PA, United States, [2]Department of Hematology and Oncology, Thomas Jefferson University, Philadelphia, PA, United States

Cutaneous adverse events of both topical and systemic drugs in patients with mycosis fungoides (MF) present a diagnostic challenge as it is often difficult to distinguish drug associated rash from disease progression in the skin. Mogamulizumab and mechlorethamine gel are approved treatments for MF, both of which can cause treatment related cutaneous adverse events. It can often be challenging to distinguish mogamulizumab associated rash (MAR) and mechlorethamine gel associated hypersensitivity dermatitis from MF progression both clinically and histologically. High-throughput sequencing (HTS) of the T-cell receptor (TCR), also known as immunosequencing, can be used to assess T-cell clonality to support a diagnosis of MF. After identification of the malignant TCR clone at baseline, immunosequencing can track the established malignant TCR sequence and its frequency over time with high sensitivity. As a result, immunosequencing clone tracking can aid in distinguishing disease progression from treatment side effects. Here, we present a case series to demonstrate how monitoring of the malignant T-cell frequency by immunosequencing can aid in diagnosis of mogamulizumab and mechlorethamine gel cutaneous adverse events.

KEYWORDS

T-cell immunosequencing, mogamulizumab, mogamulizumab associated rash, mycosis fungoides, mechlorethamine gel

Introduction

Mycosis fungoides (MF) presents a diagnostic challenge to clinicians as it can be difficult to distinguish MF from its clinical and histopathological mimickers, particularly in early stages. Additionally, in patients with MF it can be difficult to distinguish cutaneous eruptions that result from MF treatment from progression of disease. Therefore, an accurate diagnosis of such skin eruptions is crucial in guiding management (1, 2). Two common therapies used in the treatment of MF that are frequently associated with cutaneous side effects include mogamulizumab and mechlorethamine gel. Mogamulizumab is an anti-C-C chemokine receptor 4 monoclonal antibody used in the treatment of refractory MF and Sézary Syndrome (SS) (3). Mechlorethamine gel is a topical nitrogen mustard approved for the treatment of early-stage MF in the United States (4). Both treatments can cause cutaneous side effects in up to 60% of patients that mimic MF clinically and histologically making it challenging to differentiate from MF progression (1, 2).

To make a diagnosis of MF, many factors need to be considered including clinical presentation, histopathological features, immunophenotype, and T-cell clonality (5). Clonality has historically been assessed by polymerase chain reaction-based assays (PCR-electrophoresis). PCR-electrophoresis detects T-cell receptor (TCR)β or TCRγ gene rearrangements in tissue samples. This method is unable to identify the exact nucleotide sequences and associated frequencies of the identified TCRs. Instead, it relies on amplicon base-pair length as a proxy for identification of the malignant clone. A normal distribution of amplicons' base-pair length implies polyclonality; whereas, single peaks suggest monoclonality (6–8).

Immunosequencing, or high-throughput sequencing (HTS) of the TCR has recently emerged as a new and more precise method for assessing T-cell clonality in MF (9, 10). Immunosequencing can identify the precise TCR nucleotide sequences and their frequencies at 100-fold greater sensitivity than PCR-electrophoresis, and can be used in both blood and skin specimens (9–11). Establishment of malignant TCR sequence and frequency using immunosequencing can offer a more robust approach to make an accurate diagnosis when the clinical presentation and histopathology are unclear. Furthermore, after the malignant TCR identity is established at baseline, immunosequencing can aid in distinguishing disease progression from treatment side effect by tracking the established malignant sequence. We present three cases demonstrating how to utilize immunosequencing to distinguish persistent disease from treatment related cutaneous side effects of mogamulizumab and mechlorethamine gel. All patients were consented for participation in this study.

Case description 1

A 44-year-old male with a history of hairy cell leukemia and pediatric gangliocytoma presented with a rash of ten months duration. Physical examination findings are shown in Figure 1A. He underwent biopsy that showed superficial dermal and intraepidermal infiltrates of atypical CD3 expressing lymphocytes with decreased expression of CD7 and slight predominance of CD4 over CD8 (Figures 1B–F). Immunosequencing assay (ClonoSEQ-Adaptive Biotechnologies) identified one dominant TCRβ sequence present in two separate skin biopsies (Figure 2F). Blood immunosequencing also identified a dominant TCRβ sequence identical to the dominant clone detected in skin (Figure 2F). Flow cytometry analysis revealed 600 CD4+/CD26- cells in 1 uL blood indicating B1 status. With 40% body surface area (BSA) involvement and B1 blood status, the patient was diagnosed with stage IB MF. He was initially treated with topical steroids and narrowband ultraviolet B, followed by total skin electron beam therapy and mechlorethamine gel. One year later, blood and skin evaluation revealed the persistence of the dominant clone with sustained frequencies and unchanged B1 status by flow cytometry (Figure 2F). As a result, we began treatment with mogamulizumab infusions.

Four months after starting mogamulizumab therapy, the patient developed a new, worsening rash that clinically resembled his MF (Figure 2A). Biopsy findings demonstrated a psoriasiform spongiotic dermatitis with a dermal infiltrate of CD3+ cells, predominance of CD8 over CD4, and no epidermotropism (Figures 2B–E). Immunosequencing did not detect the previously identified malignant clone or any other dominant clones in either blood or skin biopsies (Figure 2F). Overall findings were consistent with mogamulizumab-associated rash (MAR). He was treated with topical corticosteroids with improvement of the rash and continued mogamulizumab infusions for an additional three months. He achieved complete remission of mycosis fungoides in skin and blood.

Case description 2

An 88-year-old female presented with a pruritic rash on her back, chest, buttocks, and upper and lower extremities (Figures 3A,B). Her BSA was 65% and biopsy of the rash revealed superficial dense lymphocytic infiltrate associated with fibroplasia and epidermotropism. The lymphocytes stained positively for CD3 with decreased expression of CD7, and a predominance of CD4 compared to CD8 especially in the epidermotropic lymphocytes. Immunosequencing identified a dominant TCRβ sequence shared both in the blood and skin (Figure 3G). Peripheral blood flow cytometry analysis revealed 1900 CD4+/CD26- cells in 1 uL blood indicating B2 status. Positron emission tomography/computed tomography (PET/CT) scan showed no metabolically active lymph nodes. Based on skin biopsy results and B2 blood status, the patient was diagnosed with Stage IVA MF. Given a lower level of blood involvement, she was initially treated with extracorporeal photopheresis (ECP), leading to improvement of rash and pruritis. Six months later, restaging of blood revealed B1 status by flow cytometry analysis. In contrast, blood immunosequencing showed unchanged frequencies of the previously identified malignant clone (Figure 3G). Due to the sustained frequencies of the malignant clone in blood, ECP was discontinued, and the patient was treated with mogamulizumab.

Five months after beginning mogamulizumab, the patient developed a new rash on the neck and flank resembling her MF (Figures 3C,D). Biopsy of the flank demonstrated spongiotic dermatitis with a dense superficial infiltrate of mostly lymphocytes. The majority of lymphocytes expressed CD3 and CD8, and a minority expressed CD4 (Figures 3E,F). Peripheral blood flow cytometry analysis detected no evidence of blood involvement (B0 blood status). Immunosequencing did not identify a dominant clone in skin or blood (Figure 3G), excluding MF from the differential and confirming the diagnosis of MAR. She was treated with systemic and topical corticosteroids leading to significant improvement. Subsequently, MAR completely resolved with reduced mogamulizumab infusion frequency (once every 4 weeks). In addition, she achieved complete remission of her mycosis fungoides in both blood and skin.

Case description 3

A 90-year-old female presented with a year-long history of eczematous patches on the trunk and extremities (Figure 4A). Biopsy of an abdominal lesion demonstrated fibroplasia with dermal and epidermal infiltration of atypical CD3+, CD4+ lymphocytes with diminished CD7 expression that formed Pautrier's microabscesses

Abbreviations: MF, Mycosis Fungoides; MAR, Mogamulizumab-Associated Rash; HTS, High-throughput sequencing; TCR, T-cell receptor; SS, Sezary Syndrome; BSA, Body Surface Area; PCR, Polymerase Chain Reaction.

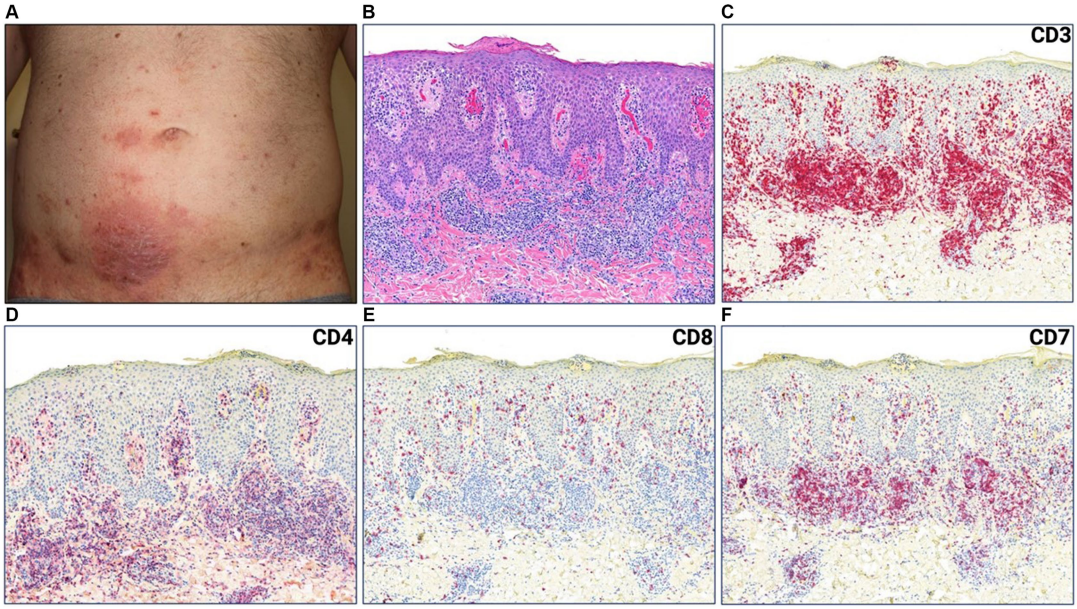

FIGURE 1
(A) Erythematous plaque with scale crust on lower abdomen. **(B)** Punch biopsy demonstrating superficial dermal and intraepidermal infiltrates of atypical lymphocytes with fibroplasia and parakeratosis (H&E 50x). **(C)** CD3, **(D)** CD4, **(E)** CD8, **(F)** CD7 immunostains (H&E 50x).

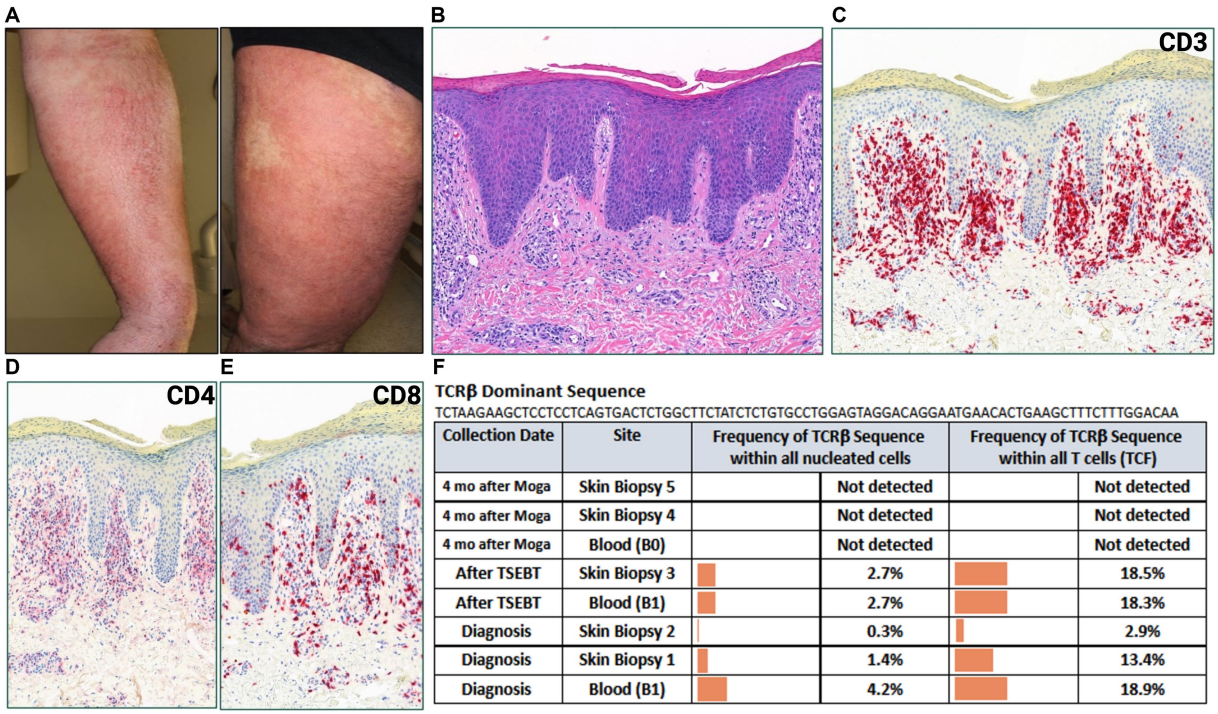

TCRβ Dominant Sequence
TCTAAGAAGCTCCTCCTCAGTGACTCTGGCTTCTATCTCTGTGCCTGGAGTAGGACAGGAATGAACACTGAAGCTTTCTTTGGACAA

Collection Date	Site	Frequency of TCRβ Sequence within all nucleated cells		Frequency of TCRβ Sequence within all T cells (TCF)	
4 mo after Moga	Skin Biopsy 5		Not detected		Not detected
4 mo after Moga	Skin Biopsy 4		Not detected		Not detected
4 mo after Moga	Blood (B0)		Not detected		Not detected
After TSEBT	Skin Biopsy 3		2.7%		18.5%
After TSEBT	Blood (B1)		2.7%		18.3%
Diagnosis	Skin Biopsy 2		0.3%		2.9%
Diagnosis	Skin Biopsy 1		1.4%		13.4%
Diagnosis	Blood (B1)		4.2%		18.9%

FIGURE 2
(A) Erythematous, lichenified and excoriated plaques with serum seepage on forearm and leg. **(B)** Punch biopsy demonstrating psoriasiform dermatitis with dermal lymphocytic infiltrate (H&E 50x). **(C)** CD3, **(D)** CD4, **(E)** CD8 immunostains (H&E 50x). **(F)** Immunosequencing data demonstrating the TCRβ sequence of the dominant (malignant) clone and its frequency among all cells for each indicated blood or skin biopsy specimen. T-cell Receptor (TCR), Tumor Clone Frequency (TCF), Total Skin Electron Beam Therapy (TSEBT), Moga (Mogamulizumab).

(Figure 4C). These immunohistological findings confirmed a diagnosis of MF. Immunosequencing of skin biopsy demonstrated one dominant TCRβ sequence (Figure 4E). Peripheral blood flow cytometry analysis did not detect blood involvement by MF and immunosequencing of the blood did not identify a dominant T-cell clone (Figure 4E).

Mechlorethamine gel treatment was initiated for Stage IA MF. Three months later, she presented to the clinic for an exuberant progressive

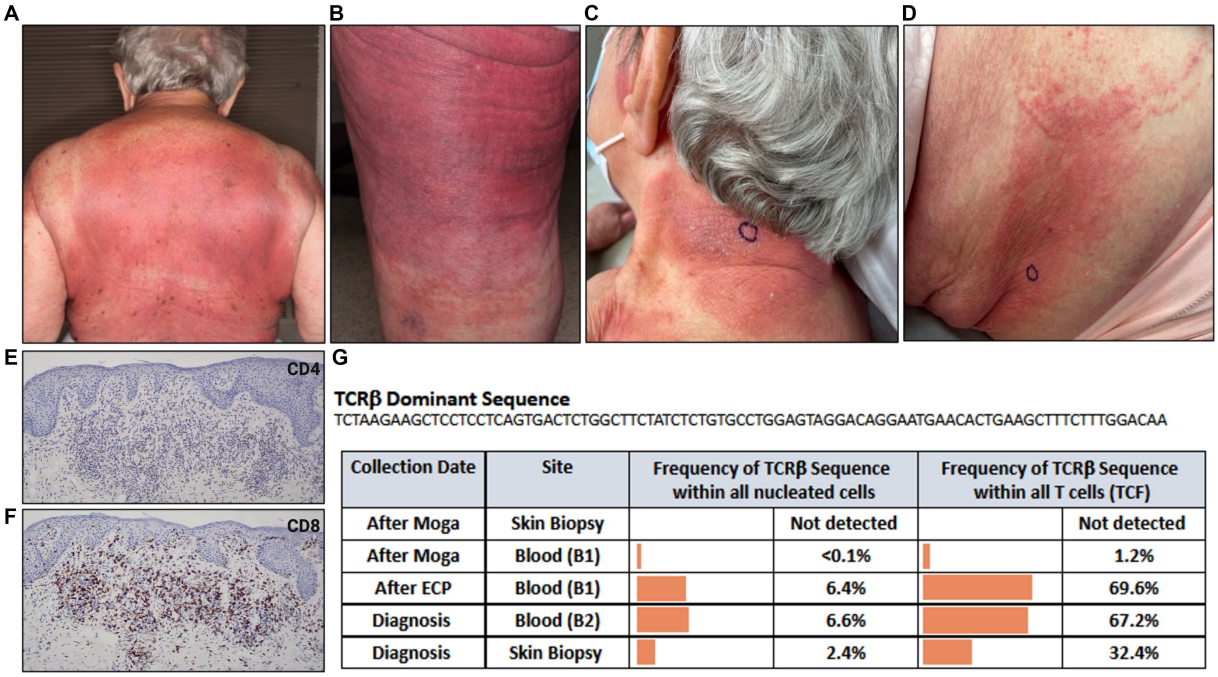

Collection Date	Site	Frequency of TCRβ Sequence within all nucleated cells		Frequency of TCRβ Sequence within all T cells (TCF)	
After Moga	Skin Biopsy		Not detected		Not detected
After Moga	Blood (B1)		<0.1%		1.2%
After ECP	Blood (B1)		6.4%		69.6%
Diagnosis	Blood (B2)		6.6%		67.2%
Diagnosis	Skin Biopsy		2.4%		32.4%

FIGURE 3
Erythematous patches and thin purple-red plaques involving most skin surface areas on **(A)** back and **(B)** posterior thigh. **(C)** Indurated, lichenified plaque with well-defined border on posterior neck. **(D)** Erythematous papules and ill-defined erythematous patch on flank. **(E)** CD4, **(F)** CD8 immunostains. **(G)** Immunosequencing data demonstrating the TCRβ sequence of the dominant (malignant) clone and its frequency among all cells for each indicated blood or skin biopsy specimen. Extracorporeal Photopheresis (ECP), Moga (Mogamulizumab), T-cell Receptor (TCR), Tumor Clone Frequency (TCF).

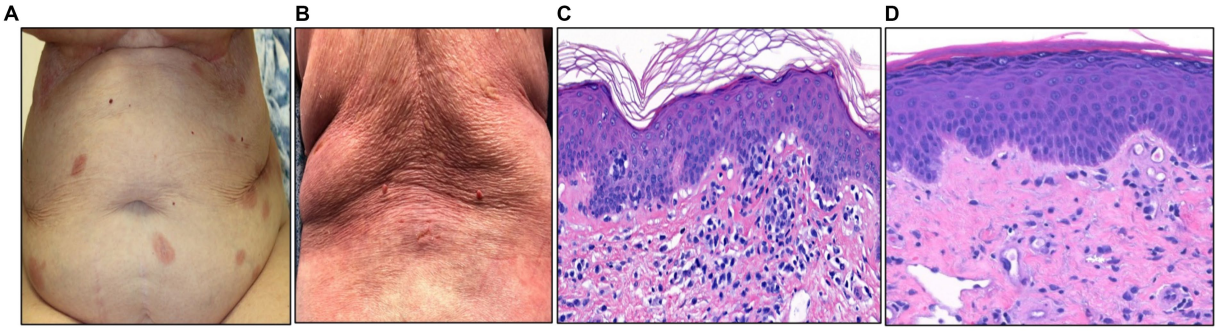

Collection Date	Site	Frequency of TCRβ Sequence within all nucleated cells		Frequency of TCRβ Sequence within all T cells (TCF)	
After mechlorethamine	Skin Biopsy		Not detected		Not detected
Diagnosis	Blood (B0)		Not detected		Not detected
Diagnosis	Skin Biopsy		4.6%		49%

FIGURE 4
(A) Erythematous patches on the abdomen. **(B)** Diffuse erythema on the back. **(C)** Punch biopsy demonstrating superficial dermal fibroplasia with atypical epidermotropic lymphocytes seen in the epidermis as microabscesses (H&E 100x). **(D)** Punch biopsy demonstrating superficial perivascular dermatitis with telangiectasis within the papillary dermis (H&E 100x). **(E)** Immunosequencing data demonstrating the TCRβ sequence of the dominant (malignant) clone and its frequency among all cells for each indicated blood or skin biopsy specimen. T-cell Receptor (TCR), Tumor Clone Frequency (TCF).

rash along with a burning sensation across her body with increased pruritus and pain. Physical exam revealed diffuse erythema accompanied by fissuring and oozing in abdominal folds and back (Figure 4B). Given the clinical presentation of extensive skin involvement, there was concern for progression to erythrodermic MF. A biopsy was obtained to distinguish MF progression from

mechlorethamine gel associated hypersensitivity dermatitis. The biopsy showed superficial perivascular dermatitis with telangiectasis within the papillary dermis (Figure 4D). Immunosequencing did not reveal a clonal population (Figure 4E). These findings confirmed the diagnosis of cutaneous hypersensitivity reaction secondary to mechlorethamine gel. As a result, mechlorethamine gel was discontinued and the patient received systemic and topical corticosteroid therapy leading to resolution of her rash. Additionally, the patient achieved complete remission of her MF.

Discussion

In all three cases described, patients developed new rashes after treatment with mogamulizumab or mechlorethamine gel that were clinically similar to their MF presentations. We utilized immunosequencing to monitor response to treatment and to distinguish disease progression from treatment related cutaneous reactions. Immunosequencing initially identified the dominant, presumably malignant, T-cell clone in each case and monitored the frequency of these clones over time. The malignant T-cell clones were not identified by immunosequencing in biopsies obtained from the new skin rashes. This finding along with other histopathological features confirmed the diagnoses of MAR or mechlorethamine gel associated hypersensitivity dermatitis in our cases.

MAR and mechlorethamine gel associated hypersensitivity dermatitis have some distinct histopathological features. MAR may show spongiotic, psoriasiform, interface or granulomatous dermatitis, along with large histiocytes in dermal infiltrate and lack of significant lymphoid atypia (12). Immunohistopathologic findings to help further identify MAR include a decreased or normal CD4:CD8 ratio and retained CD5 and CD7 expression (2). A superficial perivascular dermatitis is the main histopathological finding in mechlorethamine gel associated hypersensitivity dermatitis. Ultimately, TCR sequencing utilizing HTS can also help distinguish MAR and mechlorethamine gel associated hypersensitivity dermatitis from disease progression. In biopsies of MAR or mechlorethamine gel associated hypersensitivity dermatitis, immunosequencing is likely to either not detect the malignant clone or detect its frequency at lower levels that may not reach the cut off for dominancy. If a dominant clone is detected by immunosequencing in such biopsies, it is likely to be distinct from the original malignant clone, presumably representing a new reactive clone.

Although all three patients described in these cases had only one dominant clone, it can be challenging when multiple dominant sequences are identified in one patient (13). Theoretically, one malignant T cell can have up to two rearranged TCRβ sequences. When three or more dominant TCRβ sequences are detected, multiple dominant clones are present in the samples. In such instances, each dominant clone identified needs to be tracked over time, especially the clone that is most prevalent. Future incorporation of clinical-grade RNA-based sequencing assays may improve our understanding of which dominant sequences are relevant to the patient's disease. Regardless, it is best to track all dominant clones identified by immunosequencing to monitor disease.

In our experience, immunosequencing presents a unique tool to aid in diagnosing difficult cases, differentiating disease progression from cutaneous adverse effects, and monitoring response to treatment. The advantage immunosequencing has over PCR-electrophoresis includes a higher sensitivity to detect malignant clones, track their frequencies over time, and to determine the relationship of the new dominant clone(s) to the original malignant clone (9, 10). We propose to utilize immunosequencing for distinguishing cutaneous adverse events from disease progression in patients with MF treated with mogamulizumab or mechlorethamine gel. Limitations of this study include our small sample size at a single center. We recognize that larger studies are needed to further evaluate the utility of immunosequencing and clone tracking in MF.

Data availability statement

The original contributions presented in the study are included in the article/supplementary material, further inquiries can be directed to the corresponding author.

Ethics statement

Ethics approval was obtained for the study involving humans in accordance with the local legislation and institutional requirements. Written informed consent was obtained from the participants or the participants' legal guardians/next of kin in accordance with the national legislation and the institutional requirements. Written informed consent was obtained from the individual(s) for the publication of any potentially identifiable images or data included in this article.

Author contributions

SB and DJ wrote and prepared the manuscript for publication. ST contributed to editing and preparing the final manuscript. LB, PP, JM, and JL contributed to editing the manuscript. NN contributed to conceptualization, editing, and writing of the manuscript. All authors contributed to the article and approved the submitted version.

Funding

NN is supported via a grant from the National Cancer Institute R03CA252818.

Acknowledgments

The authors would like to acknowledge ClonoSEQ-Adaptive Biotechnologies.

Conflict of interest

The authors declare that the research was conducted in the absence of any commercial or financial relationships that could be construed as a potential conflict of interest.

Publisher's note

References

1. Garcia-Saleem TJ, Stonesifer CJ, Khaleel AE, Geskin LJ. Management of Mycosis Fungoides with topical Chlormethine/Mechlorethamine gel: a Columbia University cutaneous lymphoma center experience. *Acta Derm Venereol*. (2021) 101:adv00544. doi: 10.2340/00015555-3911

2. Hirotsu KE, Neal TM, Khodadoust MS, Wang JY, Rieger KE, Strelo J, et al. Clinical characterization of Mogamulizumab-associated rash during treatment of mycosis Fungoides or Sézary syndrome. *JAMA Dermatol*. (2021) 157:700–7. doi: 10.1001/jamadermatol.2021.0877

3. Kim YH, Bagot M, Pinter-Brown L, Rook AH, Porcu P, Horwitz SM, et al. Mogamulizumab versus vorinostat in previously treated cutaneous T-cell lymphoma (MAVORIC): an international, open-label, randomised, controlled phase 3 trial. *Lancet Oncol*. (2018) 19:1192–204. doi: 10.1016/S1470-2045(18)30379-6

4. Denis D, Beneton N, Laribi K, Maillard H. Management of mycosis fungoides-type cutaneous T-cell lymphoma (MF-CTCL): focus on chlormethine gel. *Cancer Manag Res*. (2019) 11:2241–51. doi: 10.2147/CMAR.S138661

5. Krishnasamy S, Correia E, Kartan S, Wang X, Porcu P, Cha J, et al. Application of the current diagnostic algorithm for early mycosis fungoides to a single center cohort: identification of challenges and suggestions for modification. *J Cutan Pathol*. (2022) 49:772–9. doi: 10.1111/cup.14243

6. Mahe E, Pugh T, Kamel-Reid S. T cell clonality assessment: past, present and future. *J Clin Pathol*. (2018) 71:195–200. doi: 10.1136/jclinpath-2017-204761

7. van Dongen JJ, Langerak AW, Bruggemann M, Evans PA, Hummel M, Lavender FL, et al. Design and standardization of PCR primers and protocols for detection of clonal immunoglobulin and T-cell receptor gene recombinations in suspect lymphoproliferations: report of the BIOMED-2 concerted action BMH4-CT98-3936. *Leukemia*. (2003) 17:2257–317. doi: 10.1038/sj.leu.2403202

8. Walia R, Yeung CCS. An update on molecular biology of cutaneous T cell lymphoma. *Front Oncol*. (2019) 9:1558. doi: 10.3389/fonc.2019.01558

9. de Masson A, O'Malley JT, Elco CP, Garcia SS, Divito SJ, Lowry EL, et al. High-throughput sequencing of the T cell receptor beta gene identifies aggressive early-stage mycosis fungoides. *Sci Transl Med*. (2018) 10:eaar5894. doi: 10.1126/scitranslmed.aar5894

10. Kirsch IR, Watanabe R, O'Malley JT, Williamson DW, Scott LL, Elco CP, et al. TCR sequencing facilitates diagnosis and identifies mature T cells as the cell of origin in CTCL. *Sci Transl Med*. (2015) 7:308ra158. doi: 10.1126/scitranslmed.aaa9122

11. Weng WK, Armstrong R, Arai S, Desmarais C, Hoppe R, Kim YH. Minimal residual disease monitoring with high-throughput sequencing of T cell receptors in cutaneous T cell lymphoma. *Sci Transl Med*. (2013) 5:214ra171. doi: 10.1126/scitranslmed.3007420

12. Musiek ACM, Rieger KE, Bagot M, Choi JN, Fisher DC, Guitart J, et al. Dermatologic events associated with the anti-CCR4 antibody Mogamulizumab: characterization and management. *Dermatol Ther (Heidelb)*. (2022) 12:29–40. doi: 10.1007/s13555-021-00624-7

13. Gleason L, Cohen A, South AP, Porcu P, Nikbakht N. Emergence of Malignant T-Cell Intraclonal CDR3 Variants in Mycosis Fungoides. *JAMA Dermatol*. (2023).

frontiers | Frontiers in Medicine

TYPE Original Research
PUBLISHED 05 January 2024
DOI 10.3389/fmed.2023.1249796

OPEN ACCESS

EDITED BY
Bahar Dasgeb,
The State University of New Jersey,
United States

REVIEWED BY
Montserrat Fernández Guarino,
Ramón y Cajal University Hospital, Spain
Ada Girnita,
Karolinska Institutet (KI), Sweden

*CORRESPONDENCE
Je-Ho Mun
✉ jehomun@gmail.com

RECEIVED 29 June 2023
ACCEPTED 07 December 2023
PUBLISHED 05 January 2024

CITATION
Park C, Kim DH, Hur K and Mun J-H (2024) Clinical and histopathological features of lentigo maligna and lentigo maligna melanoma: a retrospective analysis in Korea. *Front. Med.* 10:1249796.
doi: 10.3389/fmed.2023.1249796

Clinical and histopathological features of lentigo maligna and lentigo maligna melanoma: a retrospective analysis in Korea

Chanyong Park[1], Dong Hyo Kim[2,3], Keunyoung Hur[2,3] and Je-Ho Mun[1,2,3]*

[1]Seoul National University College of Medicine, Seoul, Republic of Korea, [2]Department of Dermatology, Seoul National University College of Medicine, Seoul, Republic of Korea, [3]Department of Dermatology, Seoul National University Hospital, Seoul, Republic of Korea

Introduction: Lentigo maligna (LM) and lentigo maligna melanoma (LMM) are rare in Asian countries. The histopathological diagnosis of LM is often challenging, and misdiagnosis is common. Although histopathologic features of LM/LMM are known, statistical analysis of them were scarcely reported. In this study, we aimed to investigate the histopathological characteristics of LM/LMM in Korean patients and identify key histopathological clues distinguishing LM from benign lentigo.

Methods: We performed a retrospective study of the clinical and histopathological features of patients diagnosed with LM/LMM at our center between 2011 and 2022. We assessed the histopathological features in each case based on 16 pathological criteria according to previous literature. Pathologically confirmed cases of benign lentigo were analyzed for comparison.

Results: Twenty-one patients (10 with LM and 11 with LMM) were analyzed. Several statistically significant difference existed between the features of LM and benign lentigo ($N = 10$), including asymmetry of overall structure ($p < 0.001$), cytologic atypia ($p < 0.001$), predominant single-cell proliferation ($p < 0.001$), melanocytic nests ($p = 0.033$), melanocytes forming rows ($p = 0.003$), pagetoid spread of melanocytes ($p < 0.001$), and hair follicle invasion by atypical melanocytes ($p < 0.001$). Degree of solar elastosis was more severe in group "Age ≥ 60" ($p = 0.015$), and group "Diameter ≥ 20 mm" ($p = 0.043$). Presence of elongated rete ridges were less common in the older than 60 age group ($p = 0.015$) and group "Diameter ≥ 20 mm." Invasion was associated with mitosis ($p = 0.001$, OR 49.285), multinucleated cells ($p = 0.035$, OR 17.769), and degree of lymphocyte infiltration ($p = 0.004$).

Conclusion: This study investigated the clinical and histopathologic characteristics of LM and LMM in Koreans. Although histopathological diagnosis is challenging, especially in the early stages of LM, our data showed essential histopathological changes in architectural, cytological, and dermal patterns. Considering the potential aggressiveness of LM/LMM, it is essential to recognize its histopathological features and provide timely management.

KEYWORDS

Hutchinson's melanoma, freckle, lentigo maligna, lentigo maligna melanoma, melanoma, pathology, pigmented skin lesions

1 Introduction

Lentigo maligna/lentigo maligna melanoma (LM/LMM) is the most common facial melanoma subtype (1). There are significant racial differences in incidence of LM/LMM. According to one study reporting racial differences of epidemiology of melanoma subtypes, age-adjusted incidence of LMM in non-Hispanic white population was 1.87 (1.83–1.90) per 100,000 person-years, while that of Asians/pacific islanders was 0.06 (0.05–0.08) per 100,000 person-years (2).

To the best of our knowledge, there have been few reports on the histopathological features of LM/LMM in Asian patients. In this study, we investigated the clinical and histopathological characteristics of LM and LMM in Korean patients at our center. In addition, we explored the key histopathological clues for the differential diagnosis of LM/LMM in the early stages by comparing LM and benign lentigo.

2 Materials and methods

We retrospectively analyzed the clinical and histopathological features of patients diagnosed with LM/LMM at Seoul National University Hospital between 2011 and 2022. Patients with facial and scalp LM/LMM and available histopathological findings were included. The assessed demographic and clinical factors included sex, age at onset, disease duration, lesion location, lesion multiplicity, diameter, depth, presence or absence of metastasis, sentinel lymph node biopsy, clinical impression, presence or absence of symptoms, presence or absence of previous biopsy/laser therapy, previous history of skin cancer, underlying diseases, operation date, and last follow-up date.

We assessed the histopathological features in each case based on 16 pathological criteria according to previous literature (Table 1) (3–5). They consist of one structural change (asymmetry of overall architecture), three cytologic changes (atypical melanocytes, multinucleated melanocytes, and mitosis), seven epidermal patterns (predominant single melanocyte proliferation, melanocytic nests, melanocyte-forming rows, pagetoid spread of melanocytes, hair follicle invasion of atypical melanocytes, sub-epidermal cleft, and the presence of elongated rete ridges), and five dermal changes (dermal lymphocyte infiltration, dermal invasion of atypical melanocytes, solar elastosis, dermal melanophages, and vascular proliferation). We graded the dermal invasion of atypical melanocytes and solar elastosis into three levels (grades 1–3). All the specimens were evaluated by two authors (CP and JHM). Disagreements were resolved by a consensus meeting involving other evaluators (DHK and KH) based on the above definitions in Table 1. Cases of histopathologically confirmed benign lentigo on the face acquired from our database were included as a control group to compare the histological features with those of LM. This study was approved by the Institutional Review Board of the Seoul National University Hospital.

Continuous variables are presented as means ± standard deviation, and categorical variables are presented as frequencies with percentages. Statistical analyzes were conducted using SPSS Statistics 26 software

TABLE 1 Definitions of histopathologic variables included in the investigation.

Histopathologic variables	Definition
Structure	
Asymmetry of overall architecture	Defined as present when a central line divided the lesion into two parts that looked different in shape, in thickness, or in number and position of dermal cells, absent only when the lesion appeared perfectly symmetrical
Cytologic change	
Atypical melanocytes	Atypia defined as melanocytic nuclei enlarged (more than keratinocytic ones), variable in size and in shape, hyperchromatic, with eosinophilic or amphophilic nucleoli
Multinucleated melanocytes Mitosis of melanocytes(≥1/10HPF)	Presence of melanocytes that containing more than 1 nuclei (2–3 or more) Presence of melanocytes cell division – considered present when observed more than 1 in 10 HPF
Epidermal change	
Predominant single melanocytes proliferation	Epidermal melanocytes disposed as solitary units predominating over melanocytic nests in some high power fields
Melanocytic nests	Intraepidermal melanocytes were defined as arranged in nests when they formed clusters of five or more cells no matter where they were located (within the basal epidermis or in higher layers of the epidermis)
Pagetoid spread of melanocytes	Melanocytes scattered in the epidermis and in the follicular epithelium in a pattern similar to that of Paget disease
Hair follicle invasion of atypical melanocytes Presence of bulb-like elongated rete ridges	Presence of hair follicle involvement by atypical melanocytes Presence of bulb-like shaped, downward thickening of rete ridges
Dermal change	
Dermal lymphocyte infiltration Degree of lymphocyte infiltration	Defined as present when dermal lymphocytic infiltrate was evident underlying and/or in the context of the lesion Degree of lymphocyte infiltration in dermis. 0 = absent, 1 = mild, 2 = moderate, 3 = severe
Dermal invasion of atypical melanocytes	Invasion of dermis by atypical melanocytes
Presence of solar elastosis Degree of solar elastosis	Presence of elastotic fibers in the normal skin surrounding the melanoma Degree of solar elastosis. 0 = absent, 1 = mild, 2 = moderate, 3 = severe
Dermal Melanophages	Presence of histiocytes with phagocytosed melanin
Vascular proliferation	Presence of (significant) proliferation of vessels

(IBM Corp., Armonk, NY, United States). Fisher's exact test and the Mann–Whitney U test were used to determine statistically meaningful correlations between demographic and histopathological variables. Statistical significance was set at $p < 0.05$. Odds ratios were calculated using 2 × 2 tables and Haldane's correction was applied for cells with zero (6).

3 Results

3.1 Demographics and clinical characteristics of patients with LM/LMM

A total of 21 patients (12 women [57.1%]) with LM/LMM were included in this study (Table 2). Mean age at diagnosis was 68.1 ± 10.63 (range, 49–84). Mean duration of the disease was 8.1 ± 5.26 years (range, 1–20). The most frequent location of the lesions was the cheek in 13 patients (61.9%). Twenty (95.2%) patients had a single lesion, whereas one patient with xeroderma pigmentosum presented with multiple lesions. One patient (4.7%) experienced recurrence after surgery and 20 patients were diagnosed first.

Mean lesion diameter was 24.95 ± 13.69 mm (range, 5–60). Ten (47.6%) patients had *in situ* melanoma (LM), and 11 (52.4%) had invasive melanoma (LMM). Mean Breslow thickness of the invasive cases was 4.23 ± 5.02 mm (range, 0.3–16). The majority of patients were asymptomatic, while three (14.2%) patients had symptoms such as itching, bleeding, or pain. Notably, eight (38%) patients had a history of misdiagnosis as a benign lesion. Among them, six (75.0%) had undergone skin biopsy at local dermatology clinics but were diagnosed with benign lesions, including junctional nevi or lentigo. The patient had no history of skin cancer. Twenty (95.2%) patients were treated with surgical excision, and one patient (4.8%) was successfully treated with topical imiquimod. Among the patients who underwent surgical treatment, one (5.0%) experienced recurrence. Metastasis was found in two (9.5%) cases. Mean follow-up period was 33.88 ± 21.48 months (range, 2.13 ~ 71.86).

TABLE 2 Patient demographics ($N = 21$).

Characteristic	Value
Age at onset (years, SD)	60, 12.23
Sex, *n* (%)	
Female	12 (57.1%)
Male	9 (42.9%)
Disease duration (years, SD)	8.1, 5.26
Locations, *n*(%)	
Forehead and temple	5 (23.8%)
Nose	1 (4.7%)
Cheek	13 (61.9%)
Lower cutaneous lip	1 (4.7%)
Mucosal lip	2 (9.5%)
Eyebrow	1 (4.7%)
Ear	1 (4.7%)
Lesion number, *n* (%)	
Single	20 (95.2%)
Multiple	1 (4.7%)
Diameter (mm, SD)	24.95, 13.69
Presence/absence of invasion	
In situ	10 (47.6%)
Invasive	11 (52.3%)
Depth (mm, SD)	4.23, 5.02
Metastasis, *n* (%)	
No metastasis	19 (90.4%)
Metastasis present	2 (9.5%)
Misdiagnosed as benign lesion a previous biopsy	8 (38%)
Yes	6
No	2
Symptoms, *n* (%)	
Present	3 (14.2%)
None	17 (80.9%)
SLN biopsy, *n* (%)	
Yes	5 (23.8%)
No	16 (76.1%)
Previous Laser therapy, *n* (%)	
Yes	8 (38%)
No	13 (61.9%)
Previous skin cancer, *n* (%)	
Yes	0 (0%)
No	21 (100%)
Underlying diseases, *n* (%)	
Yes	12 (57.1%)
No	9 (42.9%)

SD, standard deviation; SLN, sentinel lymph node.

3.2 Histopathology features of LM/LMM

Asymmetry of the overall architecture was observed in all the cases (100%). Atypical melanocytes, multinucleated melanocytes, and mitosis were observed in 21 (100%), five (23.8%), and 14 (66.7%) cases, respectively. For epidermal changes, all specimens had a predominant single melanocyte proliferation pattern, while hair follicle invasion of atypical melanocytes, pagetoid spread of melanocytes, melanocyte-forming rows, melanocytic nests, presence of bulb-like elongated rete ridges, and subepidermal clefts were found in 20 (95.2%), 20 (95.2%), 14 (66.7%), 13 (61.9%), 11 (52.3%), and 11 cases (52.3%), respectively. Lymphocyte infiltration was observed in all the cases. When the density of lymphocyte infiltration was graded from 1 to 3 (1 = mild, 2 = moderate, and 3 = severe), grades 1, 2, and 3 were observed in nine (42.8%), ten (47.6%), and two (9.5%) cases, respectively. Dermal invasion of atypical melanocytes was observed in 11 specimens (52.3%). All specimens exhibited solar elastosis, which was graded from 1 to 3 (1 = mild, 2 = moderate, and 3 = severe). Among the 21 specimens, nine were grade 1, eight were grade 2, and four were grade 3. Nineteen (90.4%) patients had dermal melanophages and nine (42.8%) showed vascular proliferation (Table 3).

To identify key histopathologically distinguishing points in the early stages of LMM, we further compared the clinical and

TABLE 3 Histopathologic data, *n* (%) (*N* = 21).

Histopathologic features	LM (*N* = 10)	LMM (*N* = 11)	*p* value	Odds ratio
Structure				
Asymmetry of overall architecture	10 (100%)	11 (100%)	–	1.095
Cytologic change				
Atypical melanocytes	10 (100%)	11 (100%)	–	1.095
Multinucleated melanocytes	0	5 (45.5%)	0.035	17.769
Mitosis (≥1/10HPF)	3 (30%)	11 (100%)	0.001	49.285
Epidermal change				
Predominant single melanocyte proliferation	10 (100%)	11 (100%)	–	1.095
Melanocytic nests	5 (50%)	8 (72.7%)	0.387	2.667
Melanocytes forming rows	7 (70%)	7 (63.6%)	1.000	0.75
Pagetoid spread of melanocytes	9 (90%)	11 (100%)	0.476	3.631
Hair follicle invasion of atypical melanocytes	9 (90%)	11(100%)	0.476	3.631
Subepidermal cleft	3 (30%)	8(72.7%)	0.086	6.222
Presence of bulb-like elongated rete ridges	5 (50%)	7(63.6%)	0.670	1.75
Dermal change				
Dermal lymphocytes infiltration	10 (100%)	11 (100%)	–	1.095
Lymphocyte density (1, 2, 3)			0.004	
1	8 (80%)	1 (9%)		
2	2 (20%)	8 (72.7%)		
3	0	2 (18.1%)		
Presence of solar elastosis	10 (100%)	11 (100%)	–	1.095
Degree of solar elastosis (1,2,3)			0.376	
1	3 (30%)	6 (54.5%)		
2	4 (40%)	4 (36.3%)		
3	3 (30%)	1 (9%)		
Dermal melanophages	8 (80%)	11 (100%)	0.214	6.764
Vascular proliferation	2 (20%)	7 (63.6%)	0.080	7

LM, lentigo maligna; LMM, lentigo maligna melanoma.

histopathological features of benign lentigo (*N* = 10) with those of LM (N = 10; Tables 4, 5). Several histopathological features were statistically relevant, including asymmetry of the overall structure ($p < 0.001$, odds ratio [OR] 133), cytologic atypia ($p < 0.001$, OR 441), predominant single-cell proliferation ($p < 0.001$, OR 441), melanocytic nests ($p = 0.033$, OR 21), melanocyte-forming rows ($p = 0.003$, OR 45), pagetoid spread of melanocytes ($p < 0.001$, OR 133), and hair follicle invasion by atypical melanocytes ($p < 0.001$, OR 133).

Additional analyzes were performed to evaluate the association between the histopathological findings and clinical features, including age, sex, tumor diameter, and presence of invasion. The degree of solar elastosis was more severe in patients aged >60 years ($p = 0.015$), and elongated rete ridges were more common in patients aged <60 years (p = 0.015). In large lesions (diameter > 20 mm), the degree of solar elastosis was more severe ($p = 0.043$), and elongated rete ridges were less common ($p = 0.005$). Mitosis ($p = 0.001$, OR 49.285) and multinucleated cells ($p = 0.035$, OR 17.769) were significantly more common in invasive cases than in *in-situ* melanoma. The degree of lymphocyte infiltration was higher in the invasive disease group than in the noninvasive disease group ($p = 0.004$).

TABLE 4 Demographics and clinical features between patients with lentigo and LM (*N* = 10, each).

Characteristic	Lentigo (*N* = 10)	LM (*N* = 10)
Age at diagnosis(years, SD)	69.5, 9.99	66.77, 12.46
Sex, *n* (%)		
Female	7 (70%)	7 (70%)
Male	3 (30%)	3 (30%)
Disease duration (years, SD)	4.59, 6.77	8, 4.92
Locations, *n* (%)		
Forehead/Temple	3 (30%)	1 (10%)
Nose	3 (30%)	1 (10%)
Cheek	3 (30%)	7 (70%)
Lip	0	1 (10%)
Eyebrow	1 (10%)	0
Diameter (mm, SD)	12.6, 6.41	22.8, 15.71

SD, standard deviation; LM, lentigo maligna.

TABLE 5 Comparison of histopathologic features of lentigo and LM patients, *n* (%) (*N* = 20).

Histopathologic features	Lentigo (*N* = 10)	LM (*N* = 10)	*p* value	Odd ratio
Structure				
Asymmetry of overall architecture	1 (10%)	10 (100%)	<0.001	133
Cytologic change				
Atypical melanocytes	0	10 (100%)	<0.001	441
Multinucleated melanocytes	0	0	–	
Mitosis (≥1/10HPF)	0	3 (30%)	0.211	9.8
Epidermal change				
Predominant single melanocyte proliferation	0	10 (100%)	<0.001	441
Melanocytic nests	0	5 (50%)	0.033	21
Melanocytes forming rows	0	7 (70%)	0.003	45
Pagetoid spread of melanocytes	0	9 (90%)	<0.001	133
Hair follicle invasion of atypical melanocytes	0	9 (90%)	<0.001	133
Subepidermal cleft	0	3 (30%)	0.211	9.8
Presence of bulb-like elongated rete ridges	9 (90%)	5 (50%)	0.141	0.111
Dermal change				
Dermal lymphocytes infiltration	6 (60%)	10 (100%)	0.087	14.538
Lymphocyte density (1, 2, 3)			1.000	
1	5 (50%)	8 (80%)		
2	1 (10%)	2 (20%)		
3	0	0		
Presence of solar elastosis	10 (100%)	10 (100%)		1
Degree of solar elastosis (1,2,3)			0.148	
1	3 (30%)	3 (30%)		
2	7 (70%)	4 (40%)		
3	0	3 (30%)		

LM, lentigo maligna.

4 Discussion

LM refers to melanoma *in situ* arising on chronically sun-damaged skin (7), and the term "LMM" is used to describe the invasive form of LM (8). LM has the potential to progress to LMM, an invasive tumor with aggressive behavior (9). Therefore, recognizing lesions at an early stage is crucial to minimize the risk of metastasis. The accurate diagnosis of LM/LMM is often challenging, particularly in countries where the incidence of LM/LMM is low. In this study, 38% of the patients were initially misdiagnosed with benign lesions, such as junctional nevi or lentigines, despite previous histopathological examination by skin biopsy. This suggests that it is difficult for pathologists to accurately diagnose LM in its early stages. The lack of experience among pathologists in diagnosing LM and unclear pathologic criteria may contribute to diagnostic delay.

Although several histopathological features of LM/LMM are known (10), essential features for differentiation from benign lentigo have rarely been explored. In this study, the comparison between LM and benign lentigo revealed several statistically significant features, including asymmetry of overall structure, cytologic atypia, predominant single-cell proliferation, melanocytic nests, melanocyte-forming rows, pagetoid spread of melanocytes, and hair follicle invasion by atypical melanocytes. The presence of bulb-like, elongated rete ridges is a characteristic feature of solar lentigo. Although it was observed in the majority of lentigo cases (90% [9/10]), 5 LM (50%) and 6 LMM (54.6%) cases had this pattern. This indicates that the presence of bulb-like elongated rete ridges does not exclude a diagnosis of LM or LMM.

Moreno et al. (3) reported a study of 96 patients with LM/LMM and analyzed the relationship between various histological features and the presence of invasive lesions. In their study, the presence of melanocyte rows ($p = 0.02$, OR 11.5), subepidermal cleft ($p = 0.049$, OR 2.8), melanocytic nests ($p = 0.04$, OR 3.0), and a lower degree of solar elastosis ($p = 0.07$, OR 0.4) were associated with invasive lesions. However, in our study, mitosis ($p = 0.001$, OR 49.285), multinucleated cells ($p = 0.035$, OR 17.769), and a severe degree of lymphocyte infiltration ($p = 0.004$) were associated with invasion. However, the presence of melanocyte rows ($p = 1.000$, OR 0.75), subepidermal cleft ($p = 0.086$, OR 6.222), melanocytic nests ($p = 0.387$, OR 2.667), and the degree of solar elastosis were not significantly associated with invasion. This difference between the two studies may have originated from different sample sizes or ethnicities of the patient groups. This suggests the necessity for further studies regarding the differences in LM/LMM between Western and Asian patients.

The presentation of LM or LMM has several differences between Asian and Western patients. Invasive lesions were more common in Korean patients. In addition, they had larger lesions compared to

Western patients. In a study that analyzed patients in the United States with histologically confirmed LM (Navarrete-Dechent, Cristian et al.) (11), the mean overall LM clinical diameter was 11.4 mm (SD, 8.3; range, 2–56 mm). In our study, it was 24.95 mm (standard deviation [SD], 13.69; range: 5–60 mm). The ratio of *in situ* lesions (LM) to invasive lesions (LMM) in the Western study was 2.70, while that in our study was 0.91. Our results were consistent with a previous study of clinical and histologic features of 19 Korean patients (12), in which the majority of cases were invasive, as the ratio of LM/LMM was 0.35 (5 *in situ*, 14 invasive). Compared to that study (12), our data showed a shorter mean disease duration, suggesting some improvement in early diagnosis of LM/LMM. Melanoma overdiagnosis has become a significant global concern, including in the United States (13–15). Data indicate that the incidence of melanoma *in situ* is currently 50 times higher than in 1975 (25 vs. 0.5 per 100,000 population), and the incidence of invasive melanoma has also increased from 7.9 to 25.4 per 100,000 population over the same period (13). However, in South Korea, the incidence of melanoma did not show an exponential increase, and the number of invasive melanoma cases appears to be higher than *in situ* cases. According to data from the Korea Central Cancer Registry, the age-standardized incidence rate of cutaneous melanoma has only mildly increased from 0.51 in 1999–2002 to 0.67 in 2011–2014 among men (average annual percentage change [AAPC], 3.0 [95% CI, 0.8 to 5.3]), and from 0.43 in 1999–2002 to 0.60 in 2011–2014 among women (AAPC, 3.5 [95% CI, 2.4 to 4.6]) (16). Considering previous reports and our data, we believe that the diagnosis of LM/LMM is underreported in South Korea. Given the aggressiveness of melanoma and the management challenges, along with the scarring tendency, primarily when it manifests on the face, that often follows surgical treatment, we believe early diagnosis remains an essential component for effective treatment.

The limitations of our study include its retrospective design and small sample size. However, considering the rarity of LM/LMM in Asians, our study analyzed the clinical and histopathological features of the largest number of Korean patients with LM/LMM. As our patient group consisted only of East Asian patients, further studies are necessary to determine whether there are differences between Western and Asian patients with LM and LM/LMM.

In summary, this study analyzed the clinical and histopathologic characteristics of LM in Korean patients. Compared to Western data, the lesion size was larger, and the ratio of the *in situ* stage (LM) to the invasive stage (LMM) was lower in our study. Although histopathological diagnosis is challenging, especially in the early stages of LM, our data showed essential histopathological changes in architectural, cytological, and dermal patterns. Considering the aggressiveness of LM/LMM, it is important to recognize its histopathological features and provide timely management.

Data availability statement

The original contributions presented in the study are included in the article/supplementary material, further inquiries can be directed to the corresponding author.

Ethics statement

The studies involving humans were approved by the Institutional Review Board of the Seoul National University Hospital. The studies were conducted in accordance with the local legislation and institutional requirements. The ethics committee/institutional review board waived the requirement of written informed consent for participation from the participants or the participants' legal guardians/next of kin because retrospective study design, minimal risks to subjects, anonymous data.

Author contributions

CP, DK, and J-HM conceived and designed the study. CP performed the statistical analyzes. CP and J-HM wrote the first draft of the manuscript. All authors contributed to the article and approved the submitted version.

Acknowledgments

We wish to thank all the patients included in this study.

Conflict of interest

The authors declare that the research was conducted in the absence of any commercial or financial relationships that could be construed as a potential conflict of interest.

Publisher's note

References

1. Pralong P, Bathelier E, Dalle S, Poulalhon N, Debarbieux S, Thomas L. Dermoscopy of lentigo maligna melanoma: report of 125 cases. *Br J Dermatol.* (2012) 167:280–7. doi: 10.1111/j.1365-2133.2012.10932.x

2. Wang Y, Zhao Y, Ma S. Racial differences in six major subtypes of melanoma: descriptive epidemiology. *BMC Cancer.* (2016) 16:691. doi: 10.1186/s12885-016-2747-6

3. Moreno A, Manrique-Silva E, Virós A, Requena C, Sanmartín O, Traves V, et al. Histologic features associated with an invasive component in lentigo maligna lesions. *JAMA Dermatol.* (2019) 155:782–8. doi: 10.1001/jamadermatol.2019.0467

4. Gonzalez ML, Young ED, Bush J, McKenzie K, Hunt E, Tonkovic-Capin V, et al. Histopathologic features of melanoma in difficult-to-diagnose lesions: a case-control study. *J Am Acad Dermatol.* (2017) 77:543–548.e1. doi: 10.1016/j.jaad.2017.03.017

5. Urso C, Rongioletti F, Innocenzi D, Batolo D, Chimenti S, Fanti PL, et al. Histological features used in the diagnosis of melanoma are frequently found in benign melanocytic naevi. *J Clin Pathol.* (2005) 58:409–12. doi: 10.1136/jcp.2004.020933

6. Valenzuela C. 2 solutions for estimating odds ratios with zeros. *Rev Med Chil.* (1993) 121:1441–4.

7. Tiodorovic-Zivkovic D, Argenziano G, Lallas A, Thomas L, Ignjatovic A, Rabinovitz H, et al. Age, gender, and topography influence the clinical and dermoscopic appearance of lentigo maligna. *J Am Acad Dermatol*. (2015) 72:801–8. doi: 10.1016/j.jaad.2015.01.030

8. Martínez-Leboráns L, Garcías-Ladaria J, Oliver-Martínez V, Alegre de Miquel V. Extrafacial lentigo maligna: a report on 14 cases and a review of the literature. *Actas Dermosifiliogr*. (2016) 107:e57–63. doi: 10.1016/j.ad.2015.10.018

9. Iznardo H, Garcia-Melendo C, Yélamos O. Lentigo maligna: Clinical presentation and appropriate management. *Clin Cosmet Investig Dermatol*. (2020) 13:837–55. doi: 10.2147/CCID.S224738

10. Juhász ML, Marmur ES. Reviewing challenges in the diagnosis and treatment of lentigo maligna and lentigo-maligna melanoma. *Rare Cancers Ther*. (2015) 3:133–45. doi: 10.1007/s40487-015-0012-9

11. Navarrete-Dechent C, Aleissa S, Connolly K, Hibler BP, Dusza SW, Rossi AM, et al. Clinical size is a poor predictor of invasion in melanoma of the lentigo maligna type. *J Am Acad Dermatol*. (2021) 84:1295–301. (in English). doi: 10.1016/j.jaad.2020.10.023

12. Hong WJ, Jang HS, Lee SH, Lee SE, Chung KY, Roh MR. Retrospective review of 19 patients with Lentigo Maligna melanoma. *Korean J Dermatol*. (2016) 54:769–75. doi: 10.1159/000499689

13. Welch HG, Mazer BL, Adamson AS. The rapid rise in cutaneous melanoma diagnoses. *N Engl J Med*. (2021) 384:72–9. doi: 10.1056/NEJMsb2019760

14. Bjørch MF, Gram EG, Brodersen JB. Overdiagnosis in malignant melanoma: a scoping review. *BMJ Evid Based Med*. (2023) 4:bmjebm-2023-112341. doi: 10.1136/bmjebm-2023-112341

15. Kittler H. How to combat over, diagnosis of melanoma. *Dermatol Pract Concept*. (2023) 13:e2023248. doi: 10.5826/dpc.1304a248

16. Oh CM, Cho H, Won YJ, Kong HJ, Roh YH, Jeong KH, et al. Nationwide trends in the incidence of melanoma and non-melanoma skin cancers from 1999 to 2014 in South Korea. *Cancer Res Treat*. (2018) 50:729–37. doi: 10.4143/crt.2017.166

frontiers | Frontiers in Medicine

TYPE Brief Research Report
PUBLISHED 08 January 2024
DOI 10.3389/fmed.2023.1288844

OPEN ACCESS

EDITED BY
Andreas Recke,
University of Lübeck, Germany

REVIEWED BY
Xuming Mao,
University of Pennsylvania, United States
Christoffer Gebhardt,
University Medical Center
Hamburg-Eppendorf, Germany

*CORRESPONDENCE
Bahar Dasgeb
✉ bahardasgeb@gmail.com

RECEIVED 05 September 2023
ACCEPTED 11 December 2023
PUBLISHED 08 January 2024

CITATION
Gandarillas S, Newland ES, Toppmeyer D, Stephenson R, Denzin L and Dasgeb B (2024) HLA inherence as a potential parameter in checkpoint inhibitor-associated autoimmune adverse event assessment.
Front. Med. 10:1288844.
doi: 10.3389/fmed.2023.1288844

HLA inherence as a potential parameter in checkpoint inhibitor-associated autoimmune adverse event assessment

Sophia Gandarillas[1], Elizabeth Schoenberg Newland[2], Deborah Toppmeyer[3], Ryan Stephenson[3], Lisa Denzin[4] and Bahar Dasgeb[5]*

[1]Department of Dermatology, Wayne State University, Detroit, MI, United States, [2]Department of Dermatology, Johns Hopkins School of Medicine, Baltimore, MD, United States, [3]Department of Medical Oncology, Rutgers Cancer Institute of New Jersey, New Brunswick, NJ, United States, [4]Department of Pediatrics, Child Health Institute of New Jersey, Rutgers Medical School, New Brunswick, NJ, United States, [5]Department of Surgical Oncology, Rutgers Cancer Institute of New Jersey, New Brunswick, NJ, United States

Background: The success of immunotherapy has made it a lifesaving treatment, but not without side effects. Currently, the risk factors for developing immune-related adverse events (irAEs) in patients who receive immunotherapy are poorly understood, and there is no risk-stratifying mechanism for potentially fatal irAEs. It is postulated that oncology patients with preexisting autoimmune diseases are likely to have flares on immunotherapy. However, some patients develop *de novo* autoimmune conditions on immunotherapy without a prior history. Literature reports have postulated that human leukocyte antigen (HLA) inherence may play a role in irAEs. However, this potential remains underexplored.

Methods: The oncology patients who developed autoimmune adverse events on immunotherapy for whom the continuation of treatment was prudent or lifesaving were selected. Of note, all nine patients received checkpoint inhibitors (CIs). Of the nine selected patients, only one had a prior history of an autoimmune condition. None of the nine selected patients had an active autoimmune condition at the time of CI initiation. Their HLA was typed, and the results were cross-referenced with the literature reports in PubMed and Google search with the corresponding autoimmune condition of each patient.

Results: Herein, we report nine patients with irAEs for whom retrospective HLA typing revealed the inherence of multiple related HLA alleles that may correspond to the autoimmune condition that they had developed on immunotherapy. It is to be mentioned that the inherence of enriched disease-related HLA alleles was shared among patients with the same irAEs. These patients developed a range of irAEs including bullous pemphigoid, pemphigus foliaceus/vulgaris, thyroiditis, vitiligo, and hepatitis on immunotherapy. Although some combinations of disease-related HLA were well reported in otherwise idiopathic autoimmune diseases, a frequently repeated HLA allele combination in our patient population was found to be rarely seen in the general population.

Conclusion: The authors suggest that an enriched inherence of disease-related HLA alleles may play a role in the genetic propensity for the development of irAEs in oncology patients, who receive immunotherapy, including CIs. Inherence of more than one or a cluster of particular autoimmune disease-related HLA alleles in patients who receive immunotherapy may unmask the corresponding autoimmune disease as the genotype inherence presents with the

phenotype of the corresponding condition. It is suggested that enriched linked HLA genotypes, which are otherwise rare in the general population, may present as the corresponding phenotype of the autoimmune condition. Such clinical presentation, enhanced by immunotherapy, such as CIs, can play a role in risk stratifying patients for precision medicine and improve the outcome.

KEYWORDS

irAE, oncology, checkpoint inhibitors, HLA, HLA inherence

What is already known on this topic

Immunotherapies are known to trigger immune-relatedadverse events (irAEs), though currently there is no way to predict who will and will not develop these serious reactions. Certain HLA types have been associated with autoimmune diseases. This study proposes that HLA typing may be a way to predict who and who will not develop these adverse events.

What this study adds

This pilot study is a proof-of-concept study for the possible use of HLA biomarkers as a predictive tool for adverse events related to immunotherapy. We have found that indeed HLA types do correlate with patients' propensity for developing potentially fatal irAEs.

How this study might affect research, practice, or policy

We hope this study is the beginning of a collective effort to study HLA biomarkers on a population-wide basis. Population-based studies may allow us to narrow down a few HLA subtypes that predispose to the most dangerous irAEs. HLA subtyping prior to starting immunotherapy may allow quicker diagnosis and treatment of any irAEs that arise.

Background

Immunotherapy has significantly improved the prognosis of oncology patients. It saves and extends life, but not without side effects. Almost 60% of patients on immunotherapy experience immune-related adverse events (irAEs) (1). The risk factors for developing irAEs are poorly understood, although it is postulated that patients with preexisting autoimmune diseases are more likely to have flares on immunotherapy rather than developing a *de novo* autoimmune condition (2). However, some patients on immunotherapy develop an autoimmune condition without a prior history. The incidence of irAEs is increasing as the success of immunotherapy has made it one of the most frequently used and a pillar of oncologic treatment. Although studies have suggested that HLA inherence may play a role in irAEs, this area remains under investigation with the latest data showing that certain types of HLA alleles may be associated with organ or tissue-specific irAEs (3–7). Herein, we report nine patients with irAEs for whom retrospective HLA typing revealed inherence of enriched disease-related-HLA alleles, and only one of the nine patients had a prior history of a related autoimmune condition.

Methods

Nine oncology patients who developed autoimmune adverse events on CI, for whom the continuation of treatment was lifesaving, were HLA typed with high resolution by blood test as part of the diagnosis and assessment workup for the corresponding presented autoimmune AE. Simultaneously, their blood samples were also tested for the presence of serologic autoantibodies related to the corresponding irAE. In cases of cutaneous irAE, skin biopsies were also done for histologic as well as direct immunofluorescent (DIF) evaluation. Of the nine patients, only one had a prior history of an autoimmune condition. None of the nine patients had an active autoimmune condition at the time of CI initiation. The results of their high-resolution HLA type and serologic auto-antibody were cross-referenced with the literature reports in PubMed and Google search with the corresponding autoimmune condition of each patient for diagnostic assessment. Additionally, for those who had skin biopsy, their histopathologic and DIF reports were concluded in the diagnostic assessment and evaluation process.

Results

Patient A is a middle-aged woman with lymphatic metastatic melanoma who received monthly nivolumab for a year with a favorable response. After nine infusions, the patient developed an itchy rash with tense blisters on her upper and mid chest (Figure 1A). The patient's skin biopsy showed bullous pemphigoid (BP) and her blood workup was positive for BP-180 antibodies

Abbreviations: HLA, human leukocyte antigen; irAEs, immune-related adverse events; BP, bullous pemphigoid; PV, pemphigus vulgaris; TSH, thyroid-stimulating hormone; T3, triiodothyronine; T4, thyroxine; TPO, thyroid peroxidase; PET/CT, positron emission tomography/computed tomography; AITD, autoimmune thyroid disease; CTLA4, cytotoxic t-lymphocyte associated protein; PD1/PDL1, programmed cell death-1, programmed cell death ligand-1; IMH, immune-mediated hepatitis; LFTs, liver function tests.

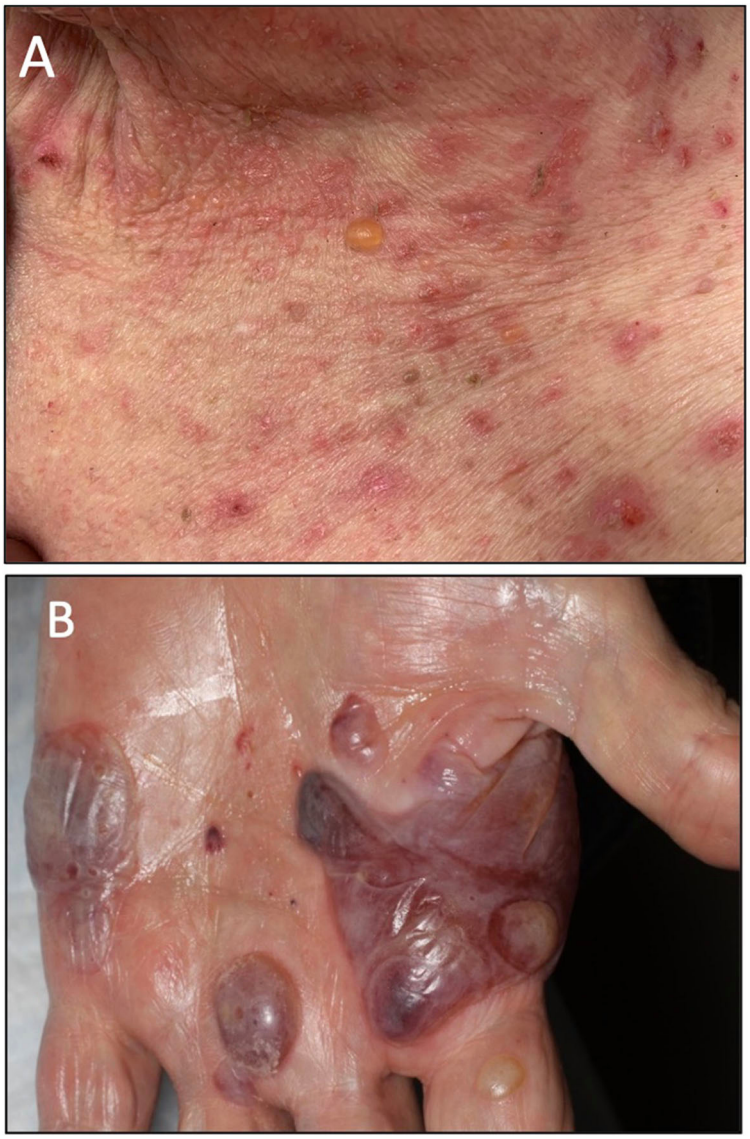

FIGURE 1
(A) Clinical presentation of patient A showing an intense BP blister on her chest. **(B)** Clinical presentation of patient B showing several tense hemorrhagic BP bullae on the left palm.

(Tables 1, 2). She was treated with a course of rapidly tapering prednisone, followed by daily topical triamcinolone ointment. Since the patient had a favorable response to Nivolumab and the irAE was well controlled and limited to her chest, Nivolumab was continued until there was no evidence of detectable melanoma on her restaging workup, when nivolumab was stopped. Thereafter, the BP-180 antibody became undetectable, and the blisters on her chest resolved. The high-resolution HLA typing revealed inherence of well-reported BP-associated HLA allele; DQA1 01:03 (Table 1) (8, 9). Additionally, a further enriched cluster of other BP-associated HLA alleles was also present (Table 2).

Patient B is an elderly patient with distant metastatic melanoma on nivolumab. After the third infusion, the patient developed painful, pruritic, blood-filled bullae confined to the patient's palms and feet (Figure 1B). The fourth infusion was withheld, a skin biopsy and serologic antibodies showed BP, and the patient was treated with clobetasol under occlusion given the confined distribution of the disease involving only palms and soles (Figures 2A–C). Given patient B's significant metastatic tumor burden and prior failure of other treatment options, nivolumab was continued as a lifesaving measure in light of localized non-progressing BP. Patient B eventually passed away after a year due to tumor burden. HLA typing revealed DRB1 11:04, DQA1 05:05, and DQB1*03:01 (Table 1) all of which are well reported to be associated with BP (10). Once again, an enriched cluster of other BP-associated HLA alleles was also present.

Patients C and D with a diagnosis of lymphatic and distant metastatic melanoma, respectively, developed BP on immunotherapy. Patient C presented with mild urticarial BP

10.3389/fmed.2023.1288844

TABLE 1 The outline of patients' demographics, and their corresponding therapeutic agents, full high-resolution HLA report, and the primary tumor type.

Patient	Age	Sex	Fits	Rx	Time to IrAE	IrAE	HLA	Tumor
A	66	F	IV	Nivolumab	Ninth infusion	BP	HLA A 02:01 HLA A 33:01 HLA B 15:01 HLA B 53:01 HLA C 03:03 HLA C 04:01 HLA DRB3 02:02 HLA DRB1 08:04 **HLA DRB1 13**:01 **HLA DQA1 01:03** **HLA DQA1 04:01** **HLA DQB1 03**:19* HLA DQB1 06:03 HLA DPA1 01:03 HLA DPA1 02:02 HLA DPB1 01:01P HLA DPB1 02:01P	Melanoma
B	75	M	III	Nivolumab	Third infusion	BP	HLA A 02:05 HLA A 03:02 HLA B 49:01 HLA B 51:01 HLA C 07:01 HLA C 15:02 **HLA DQA1 01**:04 **HLA DQA1 05:05** **HLA DQB1 03:01*** **HLA DQB1 05**:02 **HLA DRB1 11:04** HLA DRB1 14:01 HLA DRB3 02:01 HLA DRB3 02:24 HLA DPA1 01:03 HLA DPB1 04:01 HLA DPB1 104:01	Melanoma
C	79	M	II	Nivolumab	Fifth infusion	BP	HLA A 25:01 HLA A 32:01 HLA B 18:01 HLA B 40:02 HLA Bw 6 HLA C 02:02 HLA C 12:03 HLA DRB1 11:01	Melanoma

(Continued)

10.3389/fmed.2023.1288844

TABLE 1 (Continued)

Patient	Age	Sex	Fits	Rx	Time to IrAE	IrAE	HLA	Tumor
							HLA DRB1 14:07 HLA DRB3 02:02 **HLA DQB1 03:01*** **HLA DQB1 05**:03 HLA DPB1 02:01 HLA DPB1 04:02	
D	71	M	II	Ipilimumab Nivolumab	First infusion	BP	HLA A 01:01 HLA A 03:01 HLA B 07:02 **HLA B 37: 01** HLA Bw 6 HLA Bw 4 HLA C 06:02 HLA C 07:02 HLA DRB1 11:03 HLA DRB1 11:04 HLA DRB3 02:02 **HLA DQB1 03*** HLA DPB1 15:01 HLA DPB1 104:01	Melanoma
E	88	F	II	Pembrolizumab	Third infusion	BP	HLA A 01:01 **HLA A 11:01** HLA B 35:01 **HLA B 37:01** HLA C 04:01 HLA C 06:02 HLA DRB1 01:01 HLA DRB1 11:03 HLA DRB3 02:02 **HLA DQB1 05:01** **HLA DQB1 03:01*** HLA DPB1 04:01 HLA DPB1 04:02	Squamous cell carcinoma
F	56	F	II	Ipilimumab	Third infusion	PV	HLA A 03:01 HLA A 25:01 HLA C 03:04 HLA C 07:02 **HLA DRB1 04:01** **HLA DRB1 13:01** **HLA DQA1 01:03** **HLA DQA1 03:01** **HLA DQB1 03:02***	Melanoma

(Continued)

TABLE 1 (Continued)

Patient	Age	Sex	Fits	Rx	Time to IrAE	IrAE	HLA	Tumor
							HLA DQB1 06:03 HLA DPA1 02:01 HLA DPB1 01:01P HLA DPB1 17:01P	
G	44	F	III	Pembrolizumab	First infusion	Thyroiditis	HLA-A 03:01 HLA-A 30:01 HLA B 13:02 HLA B 35:03 HLA Bw 4 HLA Bw 6 HLA C 04:01 HLA C 06: 02 **HLA DRB1 09:01** HLA DRB1 11:01 HLA DRB3 02:02 H**LA DQB1 03:01*** **HLA DQB1 03:02*** **HLA DRB4 01:03 **** HLA DPB1 04:02	Breast carcinoma
H	61	F	VI	Nivolumab	Fourth infusion	Thyroiditis Vitiligo	**HLA A 02:179 (T,V)** HLA A 03:01 HLA B 49:01 HLA B 53:01 **HLA Bw 4 (V)** HLA C 07:01 HLA C 07: 02 **HLA DRB1 07:01 (V)** **HLA DRB1 08:04 (T)** **HLA DRB4 01:03 (T)**** **HLA DQB1 02:02 (V)** **HLA DQB1 03:19 (V)*** HLA DPB1 01:01	Melanoma
I	69	F	II	Nivolumab	First infusion	Thyroiditis Hepatitis	HLA A 02:01 HLA A 11:01 HLA B 40:01 HLA B 55:01 HLA Bw 6 HLA C 03:03 HLA C 03: 04 HLA DRB1 07:01 **HLA DRB1 04:01 (Hep)** HLA DRB3 02:02 **HLA DRB4 01:03 (T)****	Melanoma

(Continued)

TABLE 1 (Continued)

Patient	Age	Sex	Fits	Rx	Time to IrAE	IrAE	HLA	Tumor
							HLA DQB1 03 (Hep)* HLA DPB1 04:01 HLA DPB1 10:01	

Although a full high-resolution HLA report is provided, the HLA alleles that are found to be related to the patients' irAEs are shown in bold. For those patients who have more than one irAE, the related HLA is noted with a letter in front as follows: T, thyroiditis; V, vitiligo; Hep, hepatitis.

*All 9 patients with irAEs had the HLA DQB1 03 allele, reported with an enriched presence in patients with BP and other autoimmune diseases.

**All patients with thyroiditis had DRB4 01:03 allele.

Seven of nine patients had combined HLA DRB3 02 and DPB1alleles (highlighted in red) which are well reported in various idiopathic autoimmune diseases. All seven patients with HLA DRB3 02 and DPB1alleles showed concurrent inherence HLA DRB allele, which is a rare and uncommon finding in the general population.

involving <30% body surface area which was well controlled with topical Triamcinolone. Nivolumab continued until restaging showed no detectable disease, at which point BP resolved once the immunotherapy stopped (Tables 1, 2). Patient D with distant metastatic melanoma was on combination Ipilimumab/Nivolumab (Ipi/Nivo) therapy and developed a blistering BP involving more than 30% of body surface area after the first infusion. The Ipi/Nivo was discontinued in favor of systemic targeted therapy based on the patient's tumor mutation, and the blisters resolved. Both patients C and D had skin biopsy and serology autoantibody levels consistent with the diagnosis of BP. Additionally, both patients had more than one inherent HLA allele reported to be associated with BP. It is worth mentioning that of all four aforementioned patients with pemphigoid irAE, patient D had the least number of enriched clusters of inherent BP-associated HLA alleles of only two, and just one was strongly associated with the disease, HLA DQB1*03:01 (10). This information became useful when patient D was considered for restarting immunotherapy when systemic targeted therapy failed and mono-immunotherapy with Nivolumab was cautiously reintroduced. New small blisters re-appeared on his chest but remained limited, and itching was well tolerated with topical Clobetasol. Of note is that all four BP patients exhibited HLA DQB1*03.

Patient E is an elderly patient with non-operable advanced ulcerating squamous cell carcinomas involving bilateral lower legs on pembrolizumab. After the three infusions, a pruritic bullous eruption appeared on her trunk and extremities and got worse after every infusion. A skin biopsy confirmed bullous pemphigoid and was consistent with positive serology autoantibody results. Pembrolizumab was stopped, the blisters resolved, and the patient was switched to cetuximab with favorable response. HLA typing was done, which revealed HLA A 11:01, B 37:01, DQB1 05:01, and DQB *03 all reported in association with BP (8) (Table 1).

Patient F is a middle-aged adult in remission from stage III melanoma on adjuvant ipilimumab, who presented with pruritic chest lesions, which worsened with each infusion. The patient's serology and skin biopsy results (Table 2) showed pemphigus vulgaris. The lesions resolved with discontinuation of adjuvant ipilimumab followed by a decline of desmoglein antibodies to an undetectable level (Table 2). HLA typing revealed DQB1*0302, DQA1 0301, and DRB1 04 (Table 1), all of which have been reported in association with pemphigus (11).

Patient G is a middle-aged patient with a history of breast ductal adenocarcinoma, who developed a thyroid storm requiring hospitalization 10 days after the first pembrolizumab infusion. Patient D's TSH level dropped to 0.02 and free T4 rose to 7.72 from a normal baseline. After the pembrolizumab was discontinued, the patient's TSH and T4 eventually normalized to 3.57 and 1.67, respectively. Patient D was not investigated for thyroid autoimmunity at the time of thyroiditis. Thyroid autoantibodies (anti-TPO, anti-TSH receptor, and anti-thyroglobulin) were investigated 3.5 years later, rendering negative results (Table 1). However, HLA typing was done to risk stratify the patient for other potentially life-threatening irAEs in order to prepare for re-challenging the patient with immunotherapy due to disease recurrence. The high-resolution HLA revealed inherence of DRB 109:01, DQB1*03:01, DQB1*03:02, and DRB4, all reported to be associated with thyroid autoimmunity and diabetes (12–14). Notably, the patient has a strong family history of type I diabetes and became pre-diabetic during the treatment course.

Patient H with metastatic acral melanoma was started on nivolumab and thyroiditis presented after the patient's fourth infusion. Serology showed a TSH of 126, a free T4 of 0.3, and a T3 of 36. Nivolumab was discontinued and the patient's laboratory values improved to a TSH of 15.2 and a free T4 of 1.7. The patient's thyroid autoantibodies were tested positive at the time of thyroiditis with a TPO antibody of >900 and a thyroglobulin antibody of 1:20. HLA typing revealed DRB1 08:04, DRB4, and A 02:179 alleles, all of which have been linked to autoimmune thyroid disease (AITD) (15, 16). The patient also developed vitiligo at the same time; the high-resolution HLA typing also revealed vitiligo-associated alleles, such as HLA Bw 4, DRB1 07:01, and HLA A 02:179 among others (Table 1) (17–21).

Patient I with stage IIIB melanoma of the nose was on adjuvant nivolumab. After the first nivolumab infusion, the patient showed serologic thyroid abnormalities with a low TSH (0.006), elevated free T4 (3.09), and elevated free T3 (6.6) while remaining clinically asymptomatic. After cycle 9, thyroid serology became more abnormal with elevated TSH (16.4), low free T3 (1.4), and low free T4 (0.38) in addition to elevated ALT (166 IU/L), AST (94 IU/L), and alkaline phosphatase (291 IU/L) accompanied with abdominal pain, vomiting, and mild diarrhea, which resulted in discontinuation of Nivolumab followed by tapering of oral prednisone. Hepatitis resolved, and thyroid hormone therapy was initiated. Restating PET/CT showed no evidence of detectable melanoma. Similar to patients F and G, patient H also showed HLA DRB4, which is a well-reported allele linked with autoimmune thyroiditis. This patient also had HLA type DRB1 04:01, which

TABLE 2 The outline shows the patients' serologic test results, as well as the reports of the skin histopathology and DIF if relevant.

Patient	irAE	Histology	DIF	Serology and antibody
A	BP	**Eosinophilic subepidermal blister**	**4+ strong linear patterns at basement membrane** **C3: Positive** IgG: Negative IgM: Negative IgA: Negative	**BP180: Positive** BP230: Negative Desmoglein-1:Negative Desmoglein- 3: Negative D/C Nivolumab: BP 180: Negative
B	BP	**Eosinophilic subepidermal blister**	**Strong linear pattern at basement membrane** **C3: Positive** **IgG: Positive** IgM: negative	**BP180: Positive** BP230: Negative Desmoglein-1: Negative Desmoglein- 3: Negative Nivolumab was continued due to: limited disease lack of alternative treatment
C	BP	**Eosinophilic subepidermal blister**	Not done	**BP180: Positive** BP230: Negative Desmoglein-1:Negative Desmoglein- 3: Negative Adjuvant Nivolumab was continued due to: - mildly symptomatic clinical disease - life-extending advantage of adjuvant therapy
D	BP	**Eosinophilic subepidermal blister**	Not done	**BP180: Positive** BP230: Negative Desmoglein-1:Negative Desmoglein- 3: Negative D/C Ipi/Nivo BP180: Negative Switched to targeted therapy. The disease progressed, and Nivolumab re-started. Mild BP recurred **BP180: Positive**
E	BP	**Eosinophilic subepidermal blister**	Not done	**BP180: Positive** BP230: Negative Desmoglein-1:Negative Desmoglein- 3: Negative
F	PV	**Intraepidermal blister and acantholysis.**	**Intercellular pattern** **G C3: Positive** **IgG: Positive**	**Desmoglein-1: Positive** **Desmoglein-3: Intermediate** BP180: Negative BP 230: Negative D/C Ipilimumab: Desmoglein-1: Negative Desmoglein-3: Negative
G	Thyroiditis	No biopsy	Not done	Not done
H	Thyroiditis Vitiligo	No biopsy	Not done	Not done
I	Thyroiditis Hepatitis	No biopsy	Not done	Not done

Bolded items are items of particular note that demonstrate the diagnosis.

is reported in association with autoimmune hepatitis (Table 1) (22, 23).

Discussion

Checkpoint inhibitors enhance CD8 T-cell cytotoxic function by downregulating the inhibitory brakes, which can cause irAEs (24). The mechanism of irAEs is complex and occasionally life-threatening. These adverse events can occur in any organ; most commonly the skin (46–62%) and colon (22–48%) (6, 25). It is prudent to better understand such irAEs, and when possible, risk stratify patients accordingly to achieve a more precise decision at the point of care when continuation of immunotherapy is considered lifesaving (26). Though there is no current standard to predict toxicities, HLA typing has been proposed as a potential risk-stratifying parameter for irAE (26, 27). We propose that the presented patients who developed bullous pemphigoid, pemphigus vulgaris, thyroiditis, vitiligo, and hepatitis may be associated with their genetic propensity

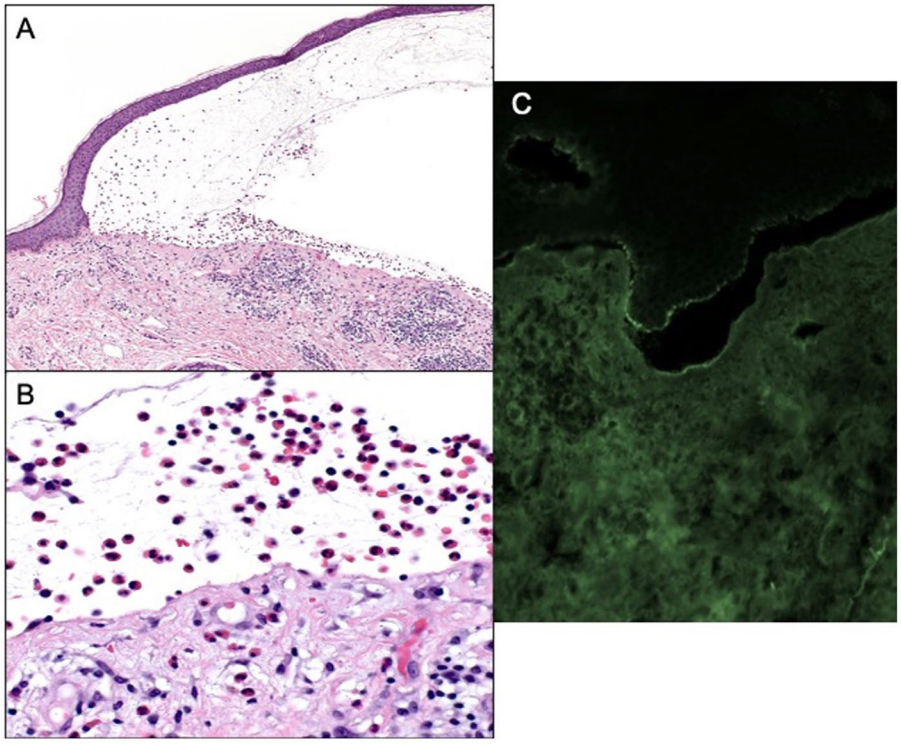

FIGURE 2
(A) Subepidermal blistering with an abundance of eosinophils 100× magnification and hematoxylin and eosin. **(B)** Eosinophils within blister cavity, 400× magnification. **(C)** Positive DIF, linear staining for IgG and C3 along the epidermal-dermal basement membrane.

toward such autoimmune conditions, which became unmasked by immunotherapy (Table 1).

Bullous pemphigoid has been reported with almost all immunotherapies (1, 27). There are HLA associations with BP among certain populations including DQB1*03:01 in Caucasians and Iranians, and DQB1*03:02, DRB1*11:01, and DRB1 04:03 in the Japanese (12). In Brazilian populations, DQB1* 03:01, DQA1 01:03, and DQA1 05:05 alleles have been associated with BP (9). In the northern Chinese, HLA-DQA1 05:05, DQB1 05:01, and DRB1 11:04 were found in association with BP (10). In the Han Chinese population HLA-A 11:01 and HLA-B 37:01 and in the Iranian population DQB1 05:01 have been shown to be associated with BP (8, 28). All five patients who presented with immunotherapy-associated BP had an enriched cluster of multiple HLA alleles, which at times formed a haplotype linked with BP in various population study reports. Of these alleles, the HLA DQB1*03 is widely reported in association with BP, in addition to other autoimmune conditions, such as alopecia areata, thyroiditis, celiac disease, colitis, and type 2 autoimmune hepatitis (28–34). It is of note that all nine patients presented here with irAEs exhibited HLA DQB1 *03 allele in their HLA inherence. This is in light of the HLA DQB1*03 frequency of <20% in the US with the HLA DQB1*03:01 frequency of 17.7% specifically. The enriched presence of alleles, such as HLA DQB1 *03:01 in presented patients, in light of the low prevalence in the general population, suggests that HLA typing had the potential to be considered a biomarker to stratify irAEs in high-risk patients (35, 36).

A clinically meaningful HLA association with the development of melanoma is well reported in the literature. Additionally, some of these melanoma-linked HLA alleles are reported to overlap with those associated with immunotherapy-triggered irAEs in oncology patients. Of such linked HLAs, overlap between melanoma and CI-associated BP adverse events only includes HLA-DPB1∗ 01 and HLADPB1∗10 which were found in patients A and I who had CI-associated BP adverse events and melanoma. Of note, neither of these alleles have been found to be associated with poor outcomes in melanoma (37). It may warrant further investigation and larger data to determine if melanoma patients with the aforementioned HLA may have a clinically meaningful risk of developing BP adverse events on immunotherapy, including CI.

Notably, all nine presented patients had HLA DQB1*03 allele. This allele is not only well reported with an enriched presence in BP patients, but also has been found to be linked to many other autoimmune conditions, including alopecia areata, celiac disease, and type 2 autoimmune hepatitis (29–34). Additionally, the HLA DRB4 01:03 allele, well known to be linked with autoimmune thyroiditis, was present in all 3 thyroiditis patients presented here.

Immunotherapy-associated PV is well reported in the literature with recent studies reporting the first case of PV triggered by ipilimumab (11, 25, 38). The HLA typing of patient F revealed multiple PV-associated HLA alleles, including but not limited to the DQB1*03:02 and DQA1 03:01 (12–14, 39–41). Such an enriched inheritance of a multiple disease-associated genotype lead to the suggestion that the enhancement of the immune system by

immunotherapy may unmask an otherwise underlying dormant disease to clinical presentation via HLA (42–44).

Thyroid toxicity has also been well reported with immunotherapy (45). The incidence of thyroid irAE due to pembrolizumab is reported in ∼17% and usually presents within a few weeks after the first dose. Progression from thyrotoxicosis to hypothyroidism post-immunotherapy is almost universal (46).

Patients G and H had multiple thyroiditis-associated HLA alleles including DRB1 09:01, reported in the Japanese with Hashimoto's thyroiditis, DQB1*03:01 reported in the Caucasians, and DQB1*03:02 in the Greek population with autoimmune thyroiditis (13, 14). Interestingly, DQB1*03:01 and *03:02, detected in patient G, are known to present a shared genetic predisposition for type 1 diabetes and autoimmune thyroid disease (41), shedding light in part on the strong family history of diabetes in patient G (41, 47). Patient H possessed multiple predisposing autoimmune thyroiditis HLA alleles including HLA A2 and DRB1 08:04, which have been linked with Hashimoto's thyroiditis and Graves' disease, with the latter being reported with early onset of the disease. The HLA DRB4 seen in patient I is also well reported with Hashimoto's thyroiditis and other autoimmune thyroid conditions (48). In oncology patients, it is reported that time to thyrotoxicosis occurs within 6 weeks of the first immunotherapy infusion (15, 16).

Vitiligo is also well reported as an irAE of immunotherapy, especially in melanoma patients treated with PD-1 inhibitors with an incidence ranging from 7.5 to 11% (1). The mechanism of vitiligo seen in patients treated with CIs is thought to be a cross-reaction between the shared antigens in melanoma and normal melanocytes, such as MART1, GP100, or tyrosinase (1). Usually, vitiligo presents progressively, bilaterally, and symmetrically after a few months of immunotherapy and persists beyond the duration of treatment. The development of vitiligo has been proposed to be associated with favorable survival and prognosis (1). Expression of some HLA genes, such as DRB and DQB, is reported to contribute to 30% of vitiligo patients (19). Patient H with vitiligo irAE has predisposing HLA DRB1 07:01, DQB1 02:02, and DQB1 03:19, the transcription of which to cytoplasmic mRNA has been shown to increase the expression of HLA-DQ protein on the surface of antigen-presenting cells known to promote the autoreactive T cell activation with a known role in vitiligo pathophysiology (18). In otherwise healthy individuals, the onset of vitiligo is presumably due to an environmental insult and in our patient, we suggest that immunotherapy is the possible culprit. Moreover, our patient has additional vitiligo-linked HLAs, including DRB1 07:01 and A 02:179, according to the reported meta-analysis (20).

The overall incidence of hepatitis induced by immunotherapies has been reportedly low ∼2–15%, and CTLA4 inhibitors have been reported to be associated with more cases of immune-mediated hepatitis (IH) than PD1/PDL1 inhibitors (49). Generally, IH leads to a hepatocellular injury with abnormal findings in liver function test (LFT). Patient I with hepatitis had HLA DRB1*04:01 with a well-reported association with IH, specifically in the Caucasian population, in the literature (22, 23).

Understanding HLA inherence in immunotherapy-associated irAEs is an important first step in the risk stratification of patients who may indeed benefit from HLA-specific modulating immune response treatments to provide the full benefit of a completed course of treatment in the relevant patient population. Although such intervention may be on the horizon and is promising, the current level of understanding warrants further research beyond the presented pilot study to further explore the role of HLA-specific TCR targeting molecules to modulate immune response. The HLA-specific TCR targeting molecules have entered clinical use for the treatments of solid malignancies, including uveal melanoma. The consideration to extend the application of such treatment strategies to the irAEs in patients with HLA-specific solid tumors would warrant risk stratification and biomarker selection. An example is tebentafusp, which is an approved treatment for uveal melanoma by targeting HLA A*02:01 to trigger T cell immune response. In the future, it may be possible to consider a similar approach in patients with HLA-specific solid tumors presenting with CI-associated irAE to treat the underlying disease while ameliorating or evading irAE. However, targeting HLA-specific TCR molecules has only been used clinically in solid tumors and chronic viral infections thus far (50–52).

Although the presented work is limited by the number of patients, it is to be mentioned that all the patients had DQB1 03. This enriched presence of the DQB1 03 allele, in light of its strong link with autoimmune diseases including BP, can present an opportunity for follow-up studies with a larger number of patients to further investigate HLA as a biomarker to stratify the risk of irAEs in patients on immunotherapy. Additionally, the co-inherence of HLA DRB3 and DPB1, which data show to be frequently found in patients with autoimmune conditions, is seen in seven of nine presented patients. It is noted that the limited number of patients in the presented work would not allow such interpretation of our patients. However, the seven aforementioned patients also exhibited an otherwise rare HLA allele; HLA DRB, which is reported in 17% of the general population. Finally, all of our nine patients were found to share the same HLA haplotype region; HLA DRB1, DQA1, and DQB, which encode proteins that are found to play a key role in presenting antigens to CD4+ T cells in the autoimmune disease processes (53). Once again, the pattern of an enriched presence of HLA allele or haplotype in our patients, although limited in number, can be observed as a potential role that HLA typing can play in irAR risk stratification in patients in whom immunotherapy is lifesaving. That being said, further studies with a larger number of patients are warranted to investigate the significance and analyze the benefit of HLA typing as a risk-stratifying tool at the point of care (Table 1).

The authors acknowledge that the presented work is one step along the collective endeavor toward what precision medicine may 1 day provide.

Conclusion

These nine patients highlight a spectrum of irAEs with various severities in oncology patients on immunotherapy, for whom such treatment was considered lifesaving. Therefore, risk stratifying these patients to continue immunotherapy in the face of such irAEs became a challenge in clinical decision-making at the point of care. While clinical information and related serologic tests were used in this process, we also applied the HLA typing to

assess risk. In the process, we learned that our patients had (a) more than one HLA allele linked to their related irAEs and (b) an enriched presence of certain HLA alleles or haplotype regions competed with the general population. Although we present a limited number of patients here, the data suggest in favor of HLA typing as a risk-stratifying tool in addition to the clinical information and related serologic test to assess irAEs of immunotherapy in oncology patients, for whom this treatment is considered to be lifesaving. Currently, there is no standard method to risk stratify patients for potentially fatal toxicities or early detection of irAEs. The authors acknowledge that follow-up studies with larger data are warranted to fulfill the criteria; however, the presented data are a step toward what precision medicine may 1 day offer.

Data availability statement

The original contributions presented in the study are included in the article/supplementary material, further inquiries can be directed to the corresponding author.

Ethics statement

Ethical approval was not required for the study involving humans in accordance with the local legislation and institutional requirements. Written informed consent to participate in this study was not required from the participants or the participants' legal guardians/next of kin in accordance with the national legislation and the institutional requirements. Written informed consent was obtained from the individual(s) for the publication of any potentially identifiable images or data included in this article.

Author contributions

BD: Conceptualization, Data curation, Formal analysis, Investigation, Methodology, Project administration, Writing – original draft, Writing – review & editing. SG: Writing – original draft, Writing – review & editing. EN: Writing – original draft, Writing – review & editing. DT: Formal analysis, Investigation, Writing – review & editing. RS: Formal Analysis, Investigation, Writing – review & editing. LD: Formal analysis, Supervision, Writing – review & editing.

Funding

The author(s) declare that no financial support was received for the research, authorship, and/or publication of this article.

Conflict of interest

The authors declare that the research was conducted in the absence of any commercial or financial relationships that could be construed as a potential conflict of interest.

The author(s) declared that they were an editorial board member of Frontiers, at the time of submission. This had no impact on the peer review process and the final decision.

Publisher's note

References

1. Sibaud V. Dermatologic reactions to immune checkpoint inhibitors: skin toxicities and immunotherapy. *Am J Clin Dermatol.* (2018) 19:345–61. doi: 10.1007/s40257-017-0336-3

2. Myers G. Immune-related adverse events of immune checkpoint inhibitors: a brief review. *Curr Oncol.* (2018) 25:342–7. doi: 10.3747/co.25.4235

3. Chang H, Shin YW, Keam B, Kim M, Im SA, Lee ST. HLA-B27 association of autoimmune encephalitis induced by PD-L1 inhibitor. *Ann Clin Transl Neurol.* (2020) 7:2243–50. doi: 10.1002/acn3.51213

4. Schoenberg E, Mehregan D, Colombe B, Hazan E, Dasgeb B. The potential role of HLA typing to risk stratify melanoma patients on immunotherapy with associated SJS: pitfalls and opportunities. *Int J Dermatol.* (2021) 61:e335–7. doi: 10.1111/ijd.15794

5. Ali OH, Berner F, Bomze D, Fässler M, Diem S, Cozzio A, et al. Human leukocyte antigen variation is associated with adverse events of checkpoint inhibitors. *Eur J Cancer.* (2019) 107:8–14. doi: 10.1016/j.ejca.2018.11.009

6. Jiang N, Yu Y, Zhang M, Tang Y, Wu D, Wang S, et al. Association between germ-line HLA and immune-related adverse events. *Front Immunol.* (2022) 13:952099. doi: 10.3389/fimmu.2022.952099

7. Conroy M, Naidoo J. Immune-related adverse events and the balancing act of immunotherapy. *Nat Commun.* (2022) 13:392. doi: 10.1038/s41467-022-27960-2

8. Fang H, Shen S, Zheng X, Dang E, Zhang J, Shao S, et al. Association of HLA class I and class II alleles with bullous pemphigoid in Chinese Hans. *J Dermatol Sci.* (2018) 89:258–62. doi: 10.1016/j.jdermsci.2017.11.014

9. Chagury AA, Sennes LU, Gil JM, Kalil J, Rodrigues H, Rosales CB, et al. HLA-C*17, DQB1*03:01, DQA1*01:03 and DQA1*05:05 alleles associated to bullous pemphigoid in Brazilian population. *Ann Dermatol.* (2018) 30:8–12. doi: 10.5021/ad.2018.30.1.8

10. Fang H, Zheng X, Sun L, Wang G. The associations of human leukocyte antigen class I and class II alleles in bullous pemphigoid. *EMJ Dermatol.* (2017) 5:53–4.

11. Schoenberg E, Colombe B, Cha J, Orloff M, Shalabi D, Ross NA, et al. Pemphigus associated with ipilimumab therapy. *Int J Dermatol.* (2021) 60, e331–3. doi: 10.1111/ijd.15405

12. Sun Y, Liu H, Wang Z, Fu X, Wang C, Mi Z, et al. The HLA-DQB1*03:01 Is associated with bullous pemphigoid in the Han Chinese population. *J Invest Dermatol.* (2018) 138:1874–7. doi: 10.1016/j.jid.2018.02.021

13. Katahira M, Ogata H, Takashima H, Ito T, Hodai Y, Miwata T, et al. Critical amino acid variants in HLA-DRB1 allotypes in the development of Graves' disease and Hashimoto's thyroiditis in the Japanese population. *Hum Immunol.* (2021) 82:226–31. doi: 10.1016/j.humimm.2020.12.007

14. Kokaraki G, Daniilidis M, Yiangou M, Arsenakis M, Karyotis N, Tsilipakou M, et al. Major histocompatibility complex class II (DRB1*, DQA1*, and DQB1*) and

DRB1*04 subtypes' associations of Hashimoto's thyroiditis in a Greek population. *Tissue Antigens.* (2009) 73:199–205. doi: 10.1111/j.1399-0039.2008.01182.x

15. Shin D-H, Baek I-C, Kim HJ, Choi E-J, Ahn M, Jung MH, et al. HLA alleles, especially amino-acid signatures of HLA-DPB1, might contribute to the molecular pathogenesis of early-onset autoimmune thyroid disease. *PLoS ONE.* (2019) 14:e0216941. doi: 10.1371/journal.pone.0216941

16. Zeitlin AA, Heward JM, Newby PR, Carr-Smith JD, Franklyn JA, Gough SCL, et al. Analysis of HLA class II genes in Hashimoto's thyroiditis reveals differences compared to Graves' disease. *Genes Immun.* (2008) 9:358–63. doi: 10.1038/gene.2008.26

17. Li Z, Ren J, Niu X, Xu Q, Wang X, Liu Y, et al. Meta-analysis of the association between vitiligo and human leukocyte antigen-A. *Biomed Res Int.* (2016) 2016:5412806. doi: 10.1155/2016/5412806

18. Jin Y, Roberts GHL, Ferrara TM, Ben S, van Geel N, Wolkerstorfer A, et al. Early-onset autoimmune vitiligo associated with an enhancer variant haplotype that upregulates class II HLA expression. *Nat Commun.* (2019) 10:391. doi: 10.1038/s41467-019-08337-4

19. Ghaffarnia R, Saffarian Z, Shahbazi M, Zamani M. Contribution of HLA class II genes, DRB4*01:01, DRB1*07:01, and DQB1*03:03:2 to clinical features of Vitiligo disease in Iranian population. *Mol Biol Rep.* (2022) 49:171–8. doi: 10.1007/s11033-021-06855-3

20. Singh A, Sharma P, Kar HK, Sharma VK, Tembhre MK, Gupta S, et al. HLA alleles and amino-acid signatures of the peptide-binding pockets of HLA molecules in vitiligo. *J Invest Dermatol.* (2012) 132:124–34. doi: 10.1038/jid.2011.240

21. Kader Toama MA, Khattab F, Marei A. Association of human leukocyte antigen-DRB1 with the response in patients with vitiligo. *Egyp J Dermatol Venerol.* (2019) 39:71–7. doi: 10.4103/ejdv.ejdv_3_18

22. Oliveira LC, Porta G, Marin ML, Bittencourt PL, Kalil J, Goldberg AC. Autoimmune hepatitis, HLA and extended haplotypes. *Autoimmun Rev.* (2011) 10:189–93. doi: 10.1016/j.autrev.2010.09.024

23. Higuchi T, Oka S, Furukawa H, Tohma S, Yatsuhashi H, Migita K. Genetic risk factors for autoimmune hepatitis: implications for phenotypic heterogeneity and biomarkers for drug response. *Hum Genomics.* (2021) 15:6. doi: 10.1186/s40246-020-00301-4

24. Liudahl SM, Coussens LM. B cells as biomarkers: predicting immune checkpoint therapy adverse events. *J Clin Invest.* (2018) 128:577–9. doi: 10.1172/JCI99036

25. Krammer S, Krammer C, Salzer S, Bagci IS, French LE, Hartmann D. Recurrence of pemphigus vulgaris under nivolumab therapy. *Front Med.* (2019) 6:262. doi: 10.3389/fmed.2019.00262

26. Akturk HK, Couts KL, Baschal EE, Karakus KE, Van Gulick RJ, Turner JA, et al. Analysis of human leukocyte antigen DR alleles, immune-related adverse events, and survival associated with immune checkpoint inhibitor use among patients with advanced malignant melanoma. *JAMA Network Open*. (2022) 5:e2246400. doi: 10.1001/jamanetworkopen.2022.46400

27. Lopez AT, Khanna T, Antonov N, Audrey-Bayan C, Geskin L. A review of bullous pemphigoid associated with PD-1 and PD-L1 inhibitors. *Int J Dermatol.* (2018) 57:664–9. doi: 10.1111/ijd.13984

28. Zhang J, Wang G. Genetic predisposition to bullous pemphigoid. *J Dermatol Sci.* (2020) 100:86–91. doi: 10.1016/j.jdermsci.2020.05.010

29. Megiorni F, Pizzuti A. *HLA-DQA1* and *HLA-DQB1* in Celiac disease predisposition: practical implications of the HLA molecular typing. *J Biomed Sci.* (2012) 19:88. doi: 10.1186/1423-0127-19-88

30. Hiraga N, Imamura M, Kawakami Y, Aikata H, Takahashi S, Akuta N, et al. HLA-DQB1*03 confers susceptibility to chronic hepatitis C in Japanese: a genome-wide association study. *PLoS ONE.* (2013) 8:e84226. doi: 10.1371/journal.pone.0084226

31. Stahl E, Roda G, Dobbyn A, Hu J, Zhang Z, Westerlind H, et al. Collagenous colitis is associated with HLA signature and shares genetic risks with other immune-mediated diseases. *Gastroenterology*. (2020) 159:549–61.e8. doi: 10.1053/j.gastro.2020.04.063

32. Schubert MS, Hutcheson PS, Graff RJ, Santiago L, Slavin RG. HLA-DQB1 *03 in allergic fungal sinusitis and other chronic hypertrophic rhinosinusitis disorders. *J Aller Clin Immunol.* (2004) 114:1376–83. doi: 10.1016/j.jaci.2004.08.029

33. Ujiie H, Muramatsu K, Mushiroda T, Ozeki T, Miyoshi H, Iwata H, et al. HLA-DQB1*03:01 as a biomarker for genetic susceptibility to bullous pemphigoid induced by DPP-4 inhibitors. *J Investig Dermatol.* (2018) 138:1201–4. doi: 10.1016/j.jid.2017.11.023

34. Lapierre P, Alvarez F. Type 2 autoimmune hepatitis: genetic susceptibility. *Front Immunol.* (2022) 13:1025343. doi: 10.3389/fimmu.2022.1025343

35. Chen N, Wang W, Wang F, Dong L, Zhao S, Zhang W, et al. The distributions of HLA-A, HLA-B, HLA-C, HLA-DRB1 and HLA-DQB1 allele and haplotype at high-resolution level in Zhejiang Han population of China. *Int J Immunogen.* (2019) 46:7–16. doi: 10.1111/iji.12411

36. Hernández-Mejía DG, Páez-Gutiérrez IA, Dorsant Ardón V, Camacho Ramírez N, Mosquera M, Cendales PA, et al. Distributions of the HLA-A, HLA-B, HLA-C, HLA-DRB1, and HLA-DQB1 alleles and haplotype frequencies of 1763 stem cell donors in the Colombian Bone Marrow Registry typed by next-generation sequencing. *Front Immunol.* (2023) 13:1057657. doi: 10.3389/fimmu.2022.1057657

37. Dhall A, Patiyal S, Kaur H, Bhalla S, Arora C, Raghava GPS. Computing skin cutaneous melanoma outcome from the HLA-alleles and clinical characteristics. *Front Genet*. (2020) 11:e00221. doi: 10.3389/fgene.2020.00221

38. Ito M, Hoashi T, Endo Y, Kimura G, Kondo Y, Ishii N, et al. Atypical pemphigus developed in a patient with urothelial carcinoma treated with nivolumab. *J Dermatol.* (2019) 46:e90–2. doi: 10.1111/1346-8138.14601

39. Vodo D, Sarig O, Sprecher E. The genetics of pemphigus vulgaris. *Front Med.* (2018) 5:226. doi: 10.3389/fmed.2018.00226

40. Olbrich M, Kunstner A, Witte M, Busch H, Fahnrich A. Genetics and omics analysis of autoimmune skin blistering diseases. *Front Immunol.* (2019) 10:2327. doi: 10.3389/fimmu.2019.02327

41. Kahles H, Fain PR, Baker P, Eisenbarth G, Badenhoop K. Genetics of autoimmune thyroiditis in type 1 diabetes reveals a novel association with DPB1*0201: data from the type 1 diabetes genetics consortium. *Diabetes Care.* (2015) 38(Suppl. 2):S21–28. doi: 10.2337/dcs15-2005

42. Petzl-Erler ML. Beyond the HLA polymorphism: a complex pattern of genetic susceptibility to pemphigus. *Genet Mol Biol.* (2020) 43:e20190369. doi: 10.1590/1678-4685-gmb-2019-0369

43. Wolf R, Tamir A, Brenner S. Drug-induced versus drug-triggered pemphigus. *Dermatologica.* (1991) 182:207–10. doi: 10.1159/000247795

44. Tarhini A, Lo E, Minor DR. Releasing the brake on the immune system: ipilimumab in melanoma and other tumors. *Cancer Biother Radiopharm.* (2010) 25:601–13. doi: 10.1089/cbr.2010.0865

45. Imblum BA, Baloch ZW, Fraker D, LiVolsi VA. Pembrolizumab-Induced Thyroiditis. *Endocr Pathol.* (2019) 30:163–7. doi: 10.1007/s12022-019-9579-2

46. de Filette J, Jansen Y, Schreuer M, Everaert H, Velkeniers B, Neyns B, et al. Incidence of thyroid-related adverse events in melanoma patients treated with pembrolizumab. *J Clin Endocrinol Metab.* (2016) 101:4431–9. doi: 10.1210/jc.2016-2300

47. Frommer L, Kahaly GJ. Type 1 diabetes and autoimmune thyroid disease-the genetic link. *Front Endocrinol.* (2021) 12:618213. doi: 10.3389/fendo.2021.618213

48. Cho WK, Jung MH, Choi EJ, Choi HB, Kim TG, Suh BK. Association of HLA alleles with autoimmune thyroid disease in Korean children. *Horm Res Paediatr.* (2011) 76:328–34. doi: 10.1159/000331134

49. Jennings JJ, Mandaliya R, Nakshabandi A, Lewis JH. Hepatotoxicity induced by immune checkpoint inhibitors: a comprehensive review including current and alternative management strategies. *Expert Opin Drug Metab Toxicol.* (2019) 15:231–44. doi: 10.1080/17425255.2019.1574744

50. Dolgin E. First soluble TCR therapy opens "new universe" of cancer targets. *Nat Biotechnol.* (2022) 40:441–4. doi: 10.1038/s41587-022-01282-6

51. Chen LN, Carvajal RD. Tebentafusp for the treatment of HLA-A*02:01-positive adult patients with unresectable or metastatic uveal melanoma. *Exp Rev Antican Ther.* (2022) 22:1017–27. doi: 10.1080/14737140.2022.2124971

52. Hazini A, Fisher K, Seymour L. Deregulation of HLA-I in cancer and its central importance for immunotherapy. *J Immunother Cancer.* (2021) 9:e002899. doi: 10.1136/jitc-2021-002899

53. Gough SC, Simmonds MJ. The HLA region and autoimmune disease: associations and mechanisms of action. *Curr Genom.* (2007) 8:453–65. doi: 10.2174/138920207783591690

frontiers | Frontiers in Medicine

TYPE Case Report
PUBLISHED 11 March 2024
DOI 10.3389/fmed.2024.1322210

OPEN ACCESS

EDITED BY
Marco Ardigo,
IRCCS San Gallicano Dermatological Institute, Italy

REVIEWED BY
Elisabetta Palazzo,
University of Modena and Reggio Emilia, Italy
Marika Quadri,
University of Modena and Reggio Emilia, Italy

*CORRESPONDENCE
Bahar Dasgeb
✉ bahardasgeb@gmail.com

RECEIVED 16 October 2023
ACCEPTED 28 February 2024
PUBLISHED 11 March 2024

CITATION
Gandarillas S, Tang H and Dasgeb B (2024) Case Report: Dostarlimab for treatment of aggressive cutaneous squamous cell carcinoma.
Front. Med. 11:1322210.
doi: 10.3389/fmed.2024.1322210

Case Report: Dostarlimab for treatment of aggressive cutaneous squamous cell carcinoma

Sophia Gandarillas[1], Horace Tang[2] and Bahar Dasgeb[3]*

[1]Department of Dermatology, Wayne State University, Detroit, MI, United States, [2]Department of Hematology, Community Medical Center, Toms River, NJ, United States, [3]Department of Surgical Oncology, Rutgers Cancer Institute of New Jersey, New Brunswick, NJ, United States

Cutaneous squamous cell carcinoma (cSCC) is the second most common malignancy with the aggressive cSCC subtype being especially worrisome due to its higher metastatic and mortality rate. An 80-year-old immunocompetent Caucasian man presented with a locally advanced and recurrent cSCC for which he underwent six Mohs surgeries, radiation therapy, and standard immunotherapy treatments. Throughout treatment, the patient's cancer continued to progress across different regions of the face. Biopsy and analysis were performed and showed that the cSCCs had a high mutational burden and oncogenes known to be present in tumors with aggressive nature. After the algorithmically applied standard of care failed to cure or control the progressing disease, the genetic analysis favored dostarlimab as a suitable option. With only three doses of 500 mg dostarlimab q3 weeks, the patient showed a fast response with macroscopic resolution of clinically discernible disease of, the previously noted, locally advanced cSCC on his right forehead, as well as other primary keratinocyte carcinomas on his left contralateral face, nose, left leg, and neck. This remarkable case can present an option for complex patients with locally advanced and recurrent cSCC who failed the current standard of care. Moreover, it warrants a proper clinical trial to assess efficacy and potential indication of dostarlimab in such patients. Of note is the presence of a KMT2D mutation and its well-identified correlation with mismatch repair deficiency (dMMR) and poor prognosis, which can play an informative role in clinical decision making and precision therapeutic choice at the point of care.

KEYWORDS

cutaneous squamous cell carcinoma (cSCC), dostarlimab, treatment, cemiplimab, standard of care, KMT2D, keratinocyte carcinoma, recurrent squamous cell carcinoma head and neck

Case presentation

An 80-year-old immunocompetent Caucasian man presented with a locally advanced cutaneous squamous cell carcinoma of the left forehead extending into the left frontal scalp. He was initially treated with six Mohs surgeries which all led to local recurrence. After the last Mohs surgery, he underwent radiation therapy, which also failed, followed by local recurrence within a year. Initial staging with PET/CT scan did not show head and

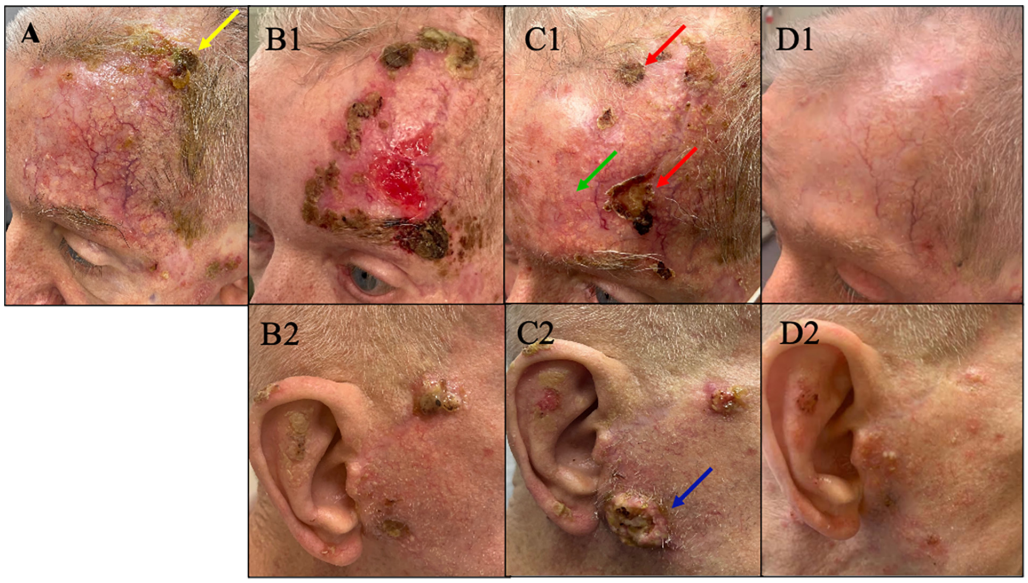

FIGURE 1
(A) Plateau of response with presence of residual cSCC (yellow arrow) on his left forehead after 3 months on cemiplimab. At this point treatment was switched to cetuximab. **(B1,B2)** On cetuximab, the disease progressed on his left forehead and new tumors developed on the contralateral (right) face/ear. At this point pembrolizumab – immunotherapy – was added to his current cetuximab to proceed with combination therapy. **(C1,C2)** After 5 months, despite the initial improvement of the tumor on his left forehead with combination therapy showing a favorable decrease in tumor volume on his left forehead (green arrow), the response plateaued with persisting non-resolving tumors on his left forehand seen in panel **C1** (red arrow). Meanwhile, the disease on contralateral (right) face/ear continued to progress on combination therapy of cetuximab and pembrolizumab (blue arrow). At this point he was switched to dostarlimab. **(D1,D2)** Remarkable response with no discernible clinical cSCC on left forehead and minimally discernible residual disease on contralateral face/ear after just three infusions of dostarlimab. Today after 1 year, this patient continues to tolerate dostarlimab infusion with no limiting adverse events with no clinically detectable disease.

neck lymphadenopathy or distant metastasis. However, additional primary keratinocyte carcinomas, which had developed in the interim, were detected on PET/CT as discernible FDG avid foci on his nose, ipsilateral (left) cheek, as well as left leg. Histopathology showed that except the tumor on his nose, which was BCC, the remainder of the lesions on his left forehead were primary cSCCs. Therefore, he was started on systemic immunotherapy to treat the above clinical presentation with locally advanced numerous tumors as detailed below.

Results

Accordingly, cemiplimab was started as the first-line of systemic treatment to cover the locally advanced cSCCs as well as the BCC on his nose. He initially showed favorable response to cemiplimab and the tumor volume on his left forehead decreased. However, after 3 months, he showed plateaued response to cemiplimab monotherapy with persisting residual disease on his left forehead (yellow arrow in Figure 1A). Therefore, he was switched to cetuximab monotherapy. After 3 months, not only did he show continued progression of the disease on his left forehead, but he also developed new primary cSCCs on his contralateral (right) face/ear (Figures 1B1, B2).

Consequently, he was started on combination therapy with continued cetuximab and addition of immunotherapy – pembrolizumab based on the patient's high mutation rate of 39 muts/mb. Despite an initial favorable response in the first 5 months (green arrow in Figure 1C1), the response plateaued on combination therapy with persisting non resolving tumors on his left forehead (red arrows in Figure 1C1). Moreover, the disease on his contralateral (right) face/ear progressed with new tumors. One of the new primary tumors on his right pre-auricular region (blue arrow in Figure 1C2) was biopsied to confirmed that the progressing disease at multiple sites remains to be cSCC as depicted in the photomicrograph of the histopathology of the biopsied lesion seen in Figure 2. With histologic confirmation of the progressing

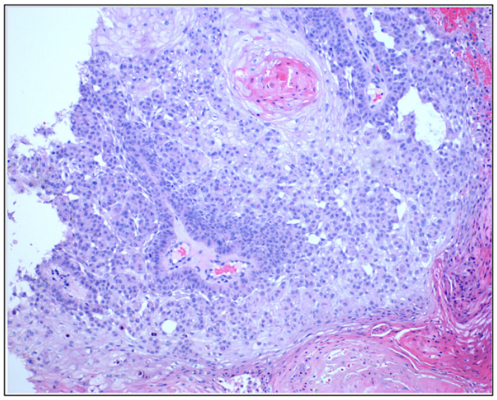

FIGURE 2
Photomicrograph of the presented patients form the preauricular lesions seen in Figure 1C2 (blue arrow) to confirm that the progressing skin lesion while on combination of cetuximab and pembrolizumab is indeed cutaneous SCC.

TABLE 1 Genetic profile of the patient's aggressive cutaneous squamous cell carcinoma with a high mutation burden of 39 muts/mb.

	Gene						
	BRCA2	CDKN2A/B	KMT2D (MLL2)	fNOTCH1 splice site	NOTCH2 splice site	TERT promotor	TP53 splice site
Mutation	F1870fs*4	p16INK4a E61* p14ARF G75V	R2922Q	1100-1G>A	31383+1G>A	-139_-138CC>TT	375+1G>A P71fs*52

FIGURE 3
(A) One BCC on right nose which continued to grow on cemiplimab and combination of cetuximab/pembrolizumab. **(B)** Noticeable improvement after the first dostarlimab infusion. **(C)** No macroscopic disease that is clinically discernible after two infusions of dostarlimab.

disease while on combined cetuximab and pembrolizumab, this combination therapy was discontinued. Genetic analysis was done by Foundation One on the above-mentioned biopsied tumor (Figure 2). According to the Foundation One report, dostarlimab was started (Table 1). To our astonishment, all locally advanced cSCC on his left forehead and right face/ear as well as one solitary biopsy proven BCC his nose, all showed a remarkably fast favorable response with no clinically discernible disease on his forehead and minimal residual tumors on his right face/ear with no interim development of new tumors after three infusions of dostarlimab 500 mg q3 weeks (Figures 1D1, D2). Today, after 1 year, this patient continues to tolerate dostarlimab infusion with no evidence of disease progression.

Discussion

Cutaneous squamous cell carcinoma (cSCC) is the second most common malignancy in humans, after basal cell carcinoma, presenting with an annual incidence of 1.8 million in the US (1, 2). The reported metastatic and mortality rate of cSCC varies at 2%–5% and 1%–2%, respectively (1–3). Aggressive cSCC is a worrisome subtype with higher metastatic and mortality rate affecting the elderly men, immunosuppressed, and patients with underlying genetic diseases such as epidermolysis bullosa compared to general population. Additionally, aggressive SCCs follow a distinct disease course, and distinct histologic and clinical characteristics. Such characteristics include poor differentiation, desmoplastic features, vascular and neural invasion, and depth of >6 mm represent aggressive nature of cSCC. Clinically, aggressive cSCC tumors are ulcerated, >2 cm, and often occur on the sun damaged skin of the head and neck of elderly Caucasian men. These tumors have a higher risk for metastasis, unfavorable response to standard treatments, and eventually end in mortality (2, 3).

It has been shown that aggressive cSCC are driven by mutational variants that are distinct from non-aggressive cSCC. In addition to displaying a high mutation rate, which would favor immunotherapy as the primary treatment, aggressive cSCC been reported to be associated with many tumor suppressor gene mutations. Of those tumor suppressors, TP53, BRCA2, CDKN2A, NOTCH1, HRAS, CASP8, and NOTCH are well reported and overlap with head and neck mucosal SCC (mSCC). Additionally, more novel tumor suppressors genes, including KMT2C, were also frequently found in aggressive cSCC. While TP53 and BRCA2 are the most frequently found tumor suppressor gene mutations in aggressive cSCC, KMT2C is often associated with invasiveness and poor outcome. Of note, TP53 is detected in almost 100% of aggressive cSCCs based on multiple reports. The aforementioned spectrum of oncogenes seen in aggressive cSCC shows striking similarity to head and neck mucosal SCC favoring immunotherapy as the first line treatment of choice. Moreover, a precise understanding of individual patients' driving mutations is prudent to execute an effective targeted treatment should immunotherapy fail in complex patients, which are characterized by recurrent, numerous, and aggressive disease (4, 5).

Of key interest is KMT2D, a tumor suppressing methyltransferase. KMT2D has been found to be mutated in 62% of all cutaneous squamous cell carcinomas and associated with more aggressive and highly metastatic phenotypes (5–7). KMT2D was found to be a key driving mutation in endometrial cancer which responds well to dostarlimab (8, 9). Dostarlimab is an anti-PD-1 monoclonal antibody, which was first recognized for its remarkable favorable response in all 12 of the study's patients with locally advanced colorectal carcinoma with DNA mismatch repair deficiencies (10). Thereafter, dostarlimab has shown favorable outcome as an effective treatment for a wide range of carcinomas such as endometrial, breast, ovarian, adrenocortical, and mucosal head-neck carcinoma, as well as melanoma (10, 11). Once again, studies indicate a meaningful correlation between KMT2D mutations and immune check point-related or mismatch repair genes (12).

The well-reported efficacy of dostarlimab in treatment of malignancies with mismatch repair deficiency (dMMR) led to its FDA approval for advanced solid tumors with dMMR (13). Given the identified correlation between KMT2D and mismatch repair genes, it is prudent to investigate gene mutations in advanced and recurrent keratinocyte carcinomas. KMT2D is not only a reliable prognosticator but can also be an informative biomarker for therapeutic decision making at the point of care.

The presented patient had undergone an algorithmically applied standard of care including Mohs surgery, radiation, and targeted systemic therapy with cetuximab combined with immunotherapy. It was not until dostarlimab was begun that the patient's multiple keratinocyte tumors began to respond. It is worth mentioning that the only non-squamous carcinoma, BCC, on his right nose continued to progress on cemiplimab and pembrolizumab until it responded to dostarlimab (**Figure 3**). To the authors knowledge, there is evidence in the literature to suggest favorable response of cutaneous keratinocytes carcinomas, SCC and BCC, especially those resistant to the standard of care. This remarkable case warrants a proper investigation and clinical trial to assess efficacy of dostarlimab in treatment of complex keratinocyte carcinomas defined by their locally advanced, numerous, and recurrent nature.

Data availability statement

The original contributions presented in this study are included in this article/supplementary material, further inquiries can be directed to the corresponding author.

Ethics statement

Written informed consent was obtained from the individual(s) for the publication of any potentially identifiable images or data included in this article.

Author contributions

SG: Writing – original draft, Writing – review & editing. HT: Data curation, Writing – review & editing. BD: Conceptualization, Data curation, Formal Analysis, Investigation, Methodology, Project administration, Supervision, Writing – original draft, Writing – review & editing.

Funding

The author(s) declare financial support was received for the research, authorship, and/or publication of this article. This work was supported by the Rutgers's Cancer Institute of New Jersey (CINJ), New Brunswick, NJ.

Conflict of interest

The authors declare that the research was conducted in the absence of any commercial or financial relationships that could be construed as a potential conflict of interest.

Publisher's note

All claims expressed in this article are solely those of the authors and do not necessarily represent those of their affiliated organizations, or those of the publisher, the editors and the reviewers. Any product that may be evaluated in this article, or claim that may be made by its manufacturer, is not guaranteed or endorsed by the publisher.

References

1. Ciuciulete A-R, Stepan AE, Andreiana BC, Simionescu CE. Non-melanoma skin cancer: Statistical associations between clinical parameters. *Curr Health Sci J.* (2022) 48:110–5. doi: 10.12865/CHSJ.48.01.16

2. Desai N, Divatia MK, Jadhav A, Wagh A. Aggressive cutaneous squamous cell carcinoma of the head and neck: A review. *Curr Oncol.* (2023) 30:7. doi: 10.3390/curroncol30070487

3. Caudill J, Thomas JE, Burkhart CG. The risk of metastases from squamous cell carcinoma of the skin. *Int J Dermatol.* (2023) 62:483–6. doi: 10.1111/ijd.16164

4. Jones J, Wetzel M, Brown T, Jung J. Molecular profile of advanced cutaneous squamous cell carcinoma. *J Clin Aesthet Dermatol.* (2021) 14:32–8.

5. Fania L, Didona D, Di Pietro FR, Verkhovskaia S, Morese R, Paolino G, et al. Cutaneous squamous cell carcinoma: From pathophysiology to novel therapeutic approaches. *Biomedicines.* (2021) 9:2. doi: 10.3390/biomedicines9020171

6. Dauch C, Shim S, Cole MW, Pollock NC, Beer AJ, Ramroop J, et al. KMT2D loss drives aggressive tumor phenotypes in cutaneous squamous cell carcinoma. *Am J Cancer Res.* (2022) 12:1309–22.

7. Chang D, Shain AH. The landscape of driver mutations in cutaneous squamous cell carcinoma. *NPJ Genom Med.* (2021) 6:1. doi: 10.1038/s41525-021-00226-4

8. Liu C, Zhang Y, Hang C. Identification of molecular subtypes premised on the characteristics of immune infiltration of endometrial cancer. *Ann Transl Med.* (2022) 10:337. doi: 10.21037/atm-22-301

9. Rubio-Pérez J, Hernández R, Hernández T, Doger B, Casado V, Moreno V. Dostarlimab for the treatment of endometrium cancer and other solid tumors. *Drugs Today.* (2021) 57:187–97. doi: 10.1358/dot.2021.57.3.3233363

10. Cercek A, Lumish M, Sinopoli J, Weiss J, Shia J, Lamendola-Essel M, et al. PD-1 blockade in mismatch repair–deficient, locally advanced rectal cancer. *N Engl J Med.* (2022) 386:2363–76. doi: 10.1056/NEJMoa2201445

11. Singh V, Sheikh A, Abourehab MAS, Kesharwani P. Dostarlimab as a miracle drug: Rising hope against cancer treatment. *Biosensors.* (2022) 12:617. doi: 10.3390/bios12080617

12. Chen G, Chen P, Zhou J, Luo G. Pan-cancer analysis of histone methyltransferase KMT2D with potential implications for prognosis and immunotherapy in human cancer. *Comb Chem High Throughput Screen.* (2023) 26:83–92. doi: 10.2174/1386207325666220221092318

13. U.S. Food and Drug Aministration. *FDA grants accelerated approval to dostarlimab-gxly for dMMR advanced solid tumors*. Silver Spring, MD: FDA (2023).

frontiers | Frontiers in Medicine

TYPE Mini Review
PUBLISHED 22 April 2024
DOI 10.3389/fmed.2024.1243659

OPEN ACCESS

EDITED BY
Bahar Dasgeb,
The State University of New Jersey, United States

REVIEWED BY
Roozbeh Sadeghian,
Harrisburg University of Science and Technology, United States

*CORRESPONDENCE
Larisa J. Geskin
✉ ljg2145@cumc.columbia.edu

RECEIVED 21 June 2023
ACCEPTED 22 February 2024
PUBLISHED 22 April 2024

CITATION
Schreidah CM, Gordon ER, Adeuyan O, Chen C, Lapolla BA, Kent JA, Reynolds GB, Fahmy LM, Weng C, Tatonetti NP, Chase HS, Pe'er I and Geskin LJ (2024) Current status of artificial intelligence methods for skin cancer survival analysis: a scoping review.
Front. Med. 11:1243659.
doi: 10.3389/fmed.2024.1243659

Current status of artificial intelligence methods for skin cancer survival analysis: a scoping review

Celine M. Schreidah[1], Emily R. Gordon[1], Oluwaseyi Adeuyan[1], Caroline Chen[1], Brigit A. Lapolla[2], Joshua A. Kent[3], George Bingham Reynolds[4], Lauren M. Fahmy[1], Chunhua Weng[4,5], Nicholas P. Tatonetti[4,5,6,7], Herbert S. Chase[5], Itsik Pe'er[4,8,9] and Larisa J. Geskin[2]*

[1]Vagelos College of Physicians and Surgeons, Columbia University, New York, NY, United States, [2]Department of Dermatology, Columbia University Irving Medical Center, New York, NY, United States, [3]Jacobs School of Medicine and Biomedical Sciences, University at Buffalo, Buffalo, NY, United States, [4]The Data Science Institute, Columbia University, New York, NY, United States, [5]Department of Biomedical Informatics, Columbia University, New York, NY, United States, [6]Department of Computational Biomedicine, Cedars-Sinai Medical Center, Los Angeles, CA, United States, [7]Cedars-Sinai Cancer, Cedars-Sinai Medical Center, Los Angeles, CA, United States, [8]Department of Systems Biology, Columbia University, New York, NY, United States, [9]Department of Computer Science, Columbia University, New York, NY, United States

Skin cancer mortality rates continue to rise, and survival analysis is increasingly needed to understand who is at risk and what interventions improve outcomes. However, current statistical methods are limited by inability to synthesize multiple data types, such as patient genetics, clinical history, demographics, and pathology and reveal significant multimodal relationships through predictive algorithms. Advances in computing power and data science enabled the rise of artificial intelligence (AI), which synthesizes vast amounts of data and applies algorithms that enable personalized diagnostic approaches. Here, we analyze AI methods used in skin cancer survival analysis, focusing on supervised learning, unsupervised learning, deep learning, and natural language processing. We illustrate strengths and weaknesses of these approaches with examples. Our PubMed search yielded 14 publications meeting inclusion criteria for this scoping review. Most publications focused on melanoma, particularly histopathologic interpretation with deep learning. Such concentration on a single type of skin cancer amid increasing focus on deep learning highlight growing areas for innovation; however, it also demonstrates opportunity for additional analysis that addresses other types of cutaneous malignancies and expands the scope of prognostication to combine both genetic, histopathologic, and clinical data. Moreover, researchers may leverage multiple AI methods for enhanced benefit in analyses. Expanding AI to this arena may enable improved survival analysis, targeted treatments, and outcomes.

KEYWORDS

artificial intelligence, skin cancer, oncology, machine learning, deep learning, supervised learning, unsupervised learning, natural language processing

Introduction

Skin cancer is the most common cancer among patients in the United States (1). Over 9,500 people are diagnosed daily, and two people die hourly (2–4). Melanoma, the deadliest skin cancer, (3) accounts for most patient mortality. Epidemiological and clinical investigations improved documentation of skin cancer incidence and prevalence, increasing discussion on prevention and detection. Literature has recognized the paramount importance of early detection and management for skin cancer and the potential for assistance by artificial intelligence (AI) tools at this stage (5). However, monitoring with survival analysis, along with discovery of survival markers are greatly needed for clinical prognostication.

Survival analysis assesses the outcome of time prior to an event of interest (e.g., death, treatment response, disease recurrence, or relapse) and may identify survival markers. Survival analysis in skin cancer research has leveraged univariate and multivariate analyses of national survey databases (6–8). While these analyses elucidated clinical and demographic associations, they are limited by patient reporting and cannot feasibly include multimodal (genetic, histopathologic, and clinical) data. Despite the benefits of focused multimodal cohort survival analyses, significant methodological barriers exist to revealing new insights beyond those via standard statistical methods. For example, innovative multimodal survival analysis time frames pose significant logistical barriers. Leveraging branches of AI may facilitate such research on survival. AI systems possess potential to assist in all stages of research to clinical care: from genomic alteration identification to even clinician-focused workflow tools (9).

Supervised and unsupervised machine learning (ML), deep learning, and natural language processing are AI methods transforming survival analysis. ML automates and scales statistical processes to discover relationships that humans alone cannot find. Four major areas within ML are discussed in this review. Supervised ML makes use of labeled data (i.e., cases where an outcome of interest is known) to find patterns that predict outcomes. Unsupervised ML is used for unlabeled data (i.e., no known outcome of interest) to find structure within data (e.g., to find similar groups or clusters) and previously unknown associations (10). Deep learning is comparatively newer and finds its own data representations, removing much of the need for feature engineering (11). Lastly, natural language processing (NLP) may operate as a form of deep learning built on text data by using neural networks (e.g., human ways of thinking) to find representations of text that form basic, quantifiable understandings of it.

Introduction of AI methods in oncologic research may transform the field, possibly enhancing mechanistic underpinnings of disease, therapeutic target discovery, synergistic treatment regimens, and guidance for clinical decision-making (12–14). With skin cancer rates rising, innovative research leveraging AI is essential (1). Use of AI within cutaneous oncology research has flourished, with studies investigating classification, detection, medical record extraction, risk identification, prediction, and prognosis (12). Applications include tools diagnosing skin cancer using clinical photographs and patient phone applications to track and manage their cancer care (15, 16). AI may augment existing understanding of cutaneous oncology pathogenesis, clinical classification, and prognostication.

In this scoping review, we present publications exemplifying possibilities for AI to innovate skin cancer research, particularly in survival analysis. An advanced search of PubMed was conducted to survey the primary literature from inception to June 11, 2023, using terms related to survival analysis, skin cancer, and AI (Supplemental material), yielding 16 publications. Publications were screened with inclusion and exclusion criteria by multiple investigators (CS, EG, GR), resolving conflicts by discussion and following the guidelines set by the Preferred Reporting Items for Systematic reviews and Meta-Analyses extension for Scoping Reviews (PRISMA-ScR). Criteria for inclusion involved articles incorporating AI in survival analysis for skin cancer patients; original investigations (not reviews); English articles; accessible articles online; no repeated articles. Criteria for exclusion encompassed articles not being original AI investigations on the topic of skin cancer survival analysis; review articles; articles not in English; non-accessible articles online; repeated articles. Two publications were excluded for not utilizing AI methods. Publications were then subject to critical review, with results contextualized within the AI method matrix for skin cancer survival analysis (Table 1). We discuss various types of AI, examples of their application within the field of oncology, and highlight methodology from each publication.

Supervised machine learning

Supervised ML is a subfield of AI that utilizes existing data for future dataset predictions. Following training with known independent variables (i.e., gene expression level) "labeled" with outcomes of interest (e.g., survival time), supervised models can identify patterns and predict outcomes. Ramsdale et al. applied supervised modeling to assess fall risk in older adults with advanced cancer starting chemotherapy (31). After assessing 73 initial features, including number of prior falls and cognitive impairment, the model effectively classified patients as "non-faller" or "faller." Our search yielded skin cancer publications using similar approaches with RNA-level and tumor architecture data.

A 2016 study by Trincado et al. applied supervised ML to predict clinical outcomes across 12 solid tumor types (17). The study assessed relative abundance of transcripts and applied a multivariate feature selection method on isoforms to generate logistic models for each tumor type and stage, with mean classification performance area under the curve (AUC) of 0.783. The authors applied their model to predict patient survival, analyzing significance with Cox proportional hazards model– a regression assessing effect of several quantitative and categorical risk factors on survival time. Wang et al. similarly used Cox proportional hazards in 2019 to investigate pathogenesis of metastatic melanoma (18). Using bioinformatics data from TCGA (The Cancer Genome Atlas) and other databases, the authors identified differential expression of seven mRNAs, five microRNAs (miRNAs), and six long noncoding RNAs (lncRNAs) correlated with survival in metastatic melanoma patients.

In 2021, Su et al. similarly stratified melanoma patients, though according to expression levels of the serine/threonine kinase PLK1 and transmembrane protein NOTCH1 (19). Cox regression analysis found high expression of both PLK1 and NOTCH1 associated with worse overall survival. They suggested that dual targeting may provide novel means for melanoma treatment. They identified downregulation of multiple melanoma-related pathways and found their top five downregulated genes associated with cancer metastasis.

TABLE 1 Summary of included literature on artificial intelligence applied to skin cancer survival analysis.

Article short citation (Author, Year, Journal)	Form of AI	Type of skin cancer(s) Studied	Type of AI data inputs	Source of data	Primary survival outcome(s) investigated	Name of performance metric	Final reported performance metric (numerical)	Limitations discussed
Trincado et al. 2016 (17), Genome Medicine	Supervised learning	Melanoma	RNA sequencing and clinical data; breast tumors according to estrogen receptor (ER) status and melanoma tumors with proliferative and invasive phenotypes	The Cancer Genome Atlas	Tumor staging and clinical outcome	AUC	Logistic model trees (LMT) for each tumor type and stage class – the mean accuracy of the models in terms of AUC is 0.783	Lack of validation on independent cohorts
Wang et al. 2019 (18), Medical Science Monitor	Supervised learning	Melanoma	Long noncoding RNA (lncRNA), microRNA (miRNA) and mRNA	The Cancer Genome Atlas, Gene Ontology database, Kyoto Encyclopedia of Genes and Genomes pathway	Survival	Cox Regression	–	Not discussed
Su et al. 2021 (19), Molecular Cancer Therapeutics	Supervised learning	Melanoma	mRNA expression	The Cancer Genome Atlas	Overall and disease-free survival	Median mRNA expression	Higher expressions of PLK1 and NOTCH1 correlated with worse survival ($p < 0.001$)	Lack of validation in *in vivo* models
Failmezger et al. 2020 (20), Cancer Research	Supervised learning	Melanoma	Topological tumor graphs (TTG)	The Cancer Genome Atlas	Degree of lymphocytic infiltration and overall survival	Cox Regression	–	Lack of access to independent clinical cohorts
Wilson et al. 2021 (21), Artificial Intelligence Medicine	Supervised learning	Melanoma	Gene expression and miRNA expression	University of California at Santa Cruz (UCSC) Xena	Survival status (Dead or Alive)	C-index	MKCox = 0.640	Not discussed
Yang et al. 2018 (22), International Journal of Oncology	Unsupervised learning	Melanoma	Long-coding RNAs (lncRNAs)	The Cancer Genome Atlas	Kaplan-Meiei survival analysis	AUROC	AUROC = 0.816	Limited sample size; sample heterogeneity
Jonckheere and Van Seuningen 2018 (23), Journal of Translational Medicine	Unsupervised learning	Skin cancer (and other cancers)	*MUC4* expression	The Cancer Genome Atlas, Cancer Cell Line Encyclopedia	Overall survival and hazard ratio	AUROC	AUROC MUC4/16/20 = 0.8272	Inadequate statistical power
Yang et al. 2021 (24), PLOS One	Unsupervised learning	Melanoma	Primary tumor (T), regional lymph nodes (N), distant metastasis (M), age (A), and sex (S)	Surveillance, Epidemiology, and End Results Program (SEER) of the National Cancer Institute	Survival time (in months), SEER cause-specific death classification variable, compared to AJCC staging	C-index	C-index = 0.7865	Bias secondary to death certificate errors; the need for a large dataset to obtain robust estimates of survival

(Continued)

10.3389/fmed.2024.1243659

TABLE 1 (Continued)

Article short citation (Author, Year, Journal)	Form of AI	Type of skin cancer(s) Studied	Type of AI data inputs	Source of data	Primary survival outcome(s) investigated	Name of performance metric	Final reported performance metric (numerical)	Limitations discussed
Comes et al. 2022 (25), Scientific Reports	Deep learning	Melanoma	Whole-slide histological images (WSIs)	Clinical Proteomic Tumor Analysis Consortium Cutaneous Melanoma (CPTAC-CM) public database then validated on Istituto Tumori "Giovanni Paolo II" in Bari, Italy	1-year disease free survival	AUC	Best predictive classification performances were obtained in terms of median AUC and accuracy with values of 0.695 and 0.727%, respectively	Relatively small size of the analyzed datasets
Johannet et al. 2021 (26), Clinical Cancer Research	Deep learning	Melanoma	Whole slide image (WSI) analysis of metastatic melanoma tissue	Interdisciplinary Melanoma Cooperative Group (IMCG) database at NYU Langone Health; Vanderbilt University Ingram Cancer Center	Progression free survival	AUC	AUC 0.800 on images from the Aperio AT2 and AUC 0.805 on images from the Leica SCN400	Small sample size
Moore et al. 2021 (27), Scientific Reports	Deep learning	Melanoma	H&E whole slide images	The Cancer Genome Atlas	Disease-specific survival	Automated Digital Tumor-infiltrating lymphocyte Analysis (ADTA) score	ADTA contributed to disease-specific survival prediction ($p = 0.006$)	Reliance of model on pathologists; lack of sentinel lymph node biopsies performed in the cohorts
Chou et al. 2021 (28), Modern Pathology	Deep learning	Melanoma	Whole slide images, % TIF	NYU melanoma database	Recurrence-free survival (RFS) and overall survival (OS)	C-index	% TIL was associated with significantly longer RFS (adjusted HR = 0.92 [0.84–1.00] per 10% increase in % TIL) and OS (adjusted HR = 0.90 [0.83–0.99] per 10% increase in % TIL)	Use of a singular data set
Chiu et al. 2021 (29), Annual International Conference of the IEEE Engineering in Medicine and Biology Society (EMBC)	Deep learning	NMSC (SCC and BCC)	Incidence rate of SCC and BCC	Database from the United Network for Organ Sharing (UNOS)	Risk factors highly associated with skin cancer events	AUC, compared CoxTime, DeepSurv, and Cox proportional hazards models	DeepSurv, CoxTime, and Cox proportional hazards model AUCs are 0.772 ± 0.0084, 0.775 ± 0.0105, and 0.756 ± 0.0092	Not discussed
Liestøl et al. 1994 (30), Statistics in Medicine	Deep learning	Melanoma	Surgically-resected samples	University Hospital of Odense, Denmark during 1962–1977	Survival time following radical surgical resection of tumor	Cox Proportional Hazards Model	–	Inclusion of too many parameters

This table summarizes the publications included from our PubMed Advanced search query following critical review with inclusion/exclusion criteria. Publications are summarized, featuring specific details on skin cancer investigated and performance.

10.3389/fmed.2024.1243659

Beyond RNA expression and protein analysis, supervised ML has also shown promise in mapping the tumor microenvironment architecture. In 2020, Failmezger et al. investigated properties of the tumor microenvironment that may affect melanoma cancer cell targeting (20). Using a novel graph-based algorithm to understand the stromal network, the authors utilized a quantitative morphologic classifier with supervised ML to identify melanoma cancer cells, lymphocytes, and stromal cells. After representing spatial relationships of the three cell types, Cox regression analysis found high stromal clustering and barriers to cancer-infiltrating lymphocytes significantly associated with poor survival.

Supervised ML expands upon previous statistical methods. Wilson et al. (21) exemplified this through application of an alternative Cox loss function for melanoma survival prediction (21). The authors preprocessed gene and miRNA expression data, then training models on training datasets and assessing performance with test sets. Their novel supervised ML approach outperformed other models, highlighting efficiency and flexibility of different supervised algorithms for survival prediction–particularly when integration of various high-throughput data sources is needed.

Overall, these studies show promise for supervised ML in uncovering the genetic basis of melanoma pathogenesis, risk-classifying patients, and predicting tumor behavior based on structure and composition. Current limitations are scarcity of sufficiently populated RNA-sequencing databases and need for validating *in vivo* models. Moreover, a supervised approach requires selection of data and targets with known associations, such that classifying big data can pose a challenge in supervised learning (particularly when compared to unsupervised learning). However, progress in the field shows its value for improved medical decision-making and precision medicine.

Unsupervised machine learning

Unsupervised ML uses algorithms to cluster and analyze unlabeled datasets, relying on the machine to find previously unknown associations. An unsupervised approach may generate multiple clusters and risk-stratify accordingly. Eckardt and colleagues recently developed a large-scale model with unsupervised ML to isolate four patient clusters using clinical and genetic acute myeloid leukemia data; statistical analysis demonstrated significant differences across various clusters (32). Review of the literature reveals various applications of unsupervised ML to cutaneous oncology survival analysis. These studies identified genetic clusters or introduced patient survival-stratifying attributes.

Several studies applied unsupervised ML to genomic signatures. Yang et al. (22) leveraged a TCGA dataset to identify lncRNAs from samples with melanoma stages I-IV, then using hierarchical clustering and support vector machine analyses to classify the lncRNAs (22). Survival methods included standard Kaplan–Meier analysis (33) yielding a predictive signature of six lncRNAs tested with a validation set. This signature encompassed 720 target genes, corresponding to numerous pathways that may affect melanoma prognosis. The method's accuracy in risk-stratification of melanoma samples was >80%. This prognostic marker for melanoma risk-classification set the groundwork for further studies to assess the signature's predictive potential.

Jonckheere and Van Seuningen (23) used unsupervised ML to correlate gene expression with derived prognostic information of *MUC4*, a membrane-bound mucin implicated in multiple cancers (23). This study leveraged online tools to extract *MUC4* Z-score expressions and use hazard ratios and other statistics to generate a list of 187 genes correlated with *MUC4* expression. Two were associated with worse survival in combination with *MUC4*. The large-scale genomic approach enabled authors to overcome prior study limitations of inadequate statistical power, offering potential new biomarkers for targeted treatment. These studies' prognostic signatures offer promising potential for future applications.

Yang et al. (24) utilized an unsupervised ML approach beyond genetic signatures, leveraging the Ensemble Algorithm for Clustering Cancer Data (EACCD) to integrate additional factors into the traditional TNM (tumor, nodes, metastases) staging system for improved melanoma prognostication (24). Prior studies attempted to augment TNM with Cox regression and tree modeling, but these methods had not clearly risk-stratified patients or led to low prediction accuracy. The authors investigated the clinical meaningfulness of their new clusters via supervised learning, finding that using them as input variables increased prognostic prediction accuracy.

These studies show unsupervised ML's many applications to skin cancer and survival analysis. Importantly, there are limitations to these analyses, especially related to clinical interpretability of found groups. For instance, there is a possibility that structure may not be found when leveraging unsupervised learning. Still, unsupervised learning has revealed important structures and key associations that aid in understanding of survival and prognostic outcomes. Figure 1 delineates differences between supervised and unsupervised learning.

Deep learning

Deep learning is a class of multi-layered ML algorithms inspired by the human brain's structure and function to improve accuracy. Early models were explored by Liestøl et al. (30), who applied neural network– a set of algorithms based on interconnected nodes, or artificial neurons in a layered structure–to commonly used regression models to strengthen survival prediction in melanoma patients (30). The authors found these models moderately improved predictions on survival time for melanoma patients following radical surgical resection, providing the groundwork for modern deep learning and survival methods.

Subsequently, deep learning has been used to better prognosticate and identify genomic alterations in melanoma. Comes et al. (25) aimed to predict 1-year disease-free survival (DFS) in melanoma patients using deep learning applied to hematoxylin and eosin-stained whole slide images (WSIs). The study was limited by a cohort of 43 patients from a public database, though annotations provided by expert pathologists. Still, the authors' proposed deep learning model extracted quantitative

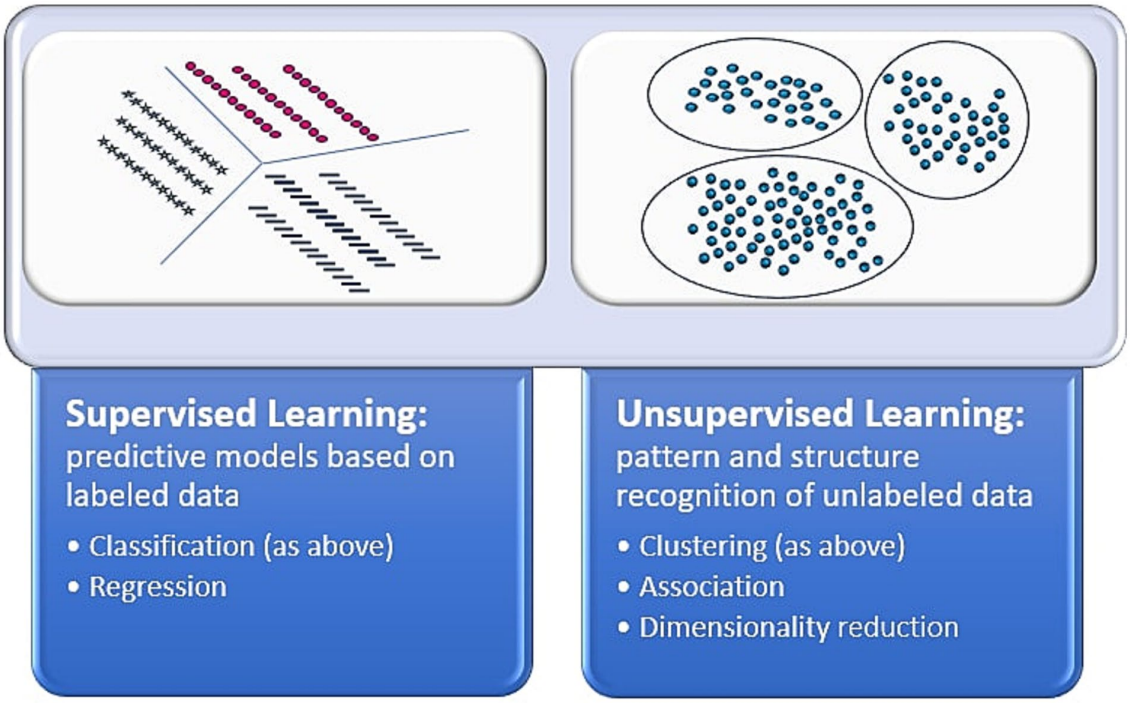

FIGURE 1
Supervised vs. unsupervised learning. This figure depicts the differences between the artificial intelligence methods of supervised and unsupervised learning (39, 40).

imaging biomarkers from WSIs and demonstrated prognostic power in predicting 1-year DFS, contributing to the investigation of deep learning for prognostication in melanoma patients.

A recent study by Johannet et al. also explored deep learning's role, correlating melanoma tissue histology with immune checkpoint inhibitor (ICI) response (26). This study investigated whether neural networks could combine important features of melanoma tissue with clinical and demographic data to predict immunotherapy response. A multivariable classifier demonstrated success in separating high and low-risk patients and predicting treatment response, displaying promise for future integration of deep learning tissue digital pathology analysis and clinical/demographic data.

Moore et al. (27) used a different approach of automated digital analysis (ADTA) to study tumor-infiltrating lymphocytes, or TILs, to augment current staging of primary early-stage (i.e., stage II-III) melanomas (27). The authors utilized previously developed deep learning algorithms to tile WSIs and estimate likelihood of TILs in each tile. ADTA score was calculated as the median of "positive" tiles: the likelihood of at least 77.5% TILs in that tile, over the total number of tiles, of all the patient's images. The authors found that ADTA score correlated with disease-specific survival (DSS) in melanoma and that this approach strengthened predictive value of standard pathology characteristics such as depth and ulceration. Although susceptible to user and cohort variability, this strongly suggests ADTA may exceed performance of standard qualitative TIL assessment for melanoma risk evaluation.

Similarly, a recent study by Chou et al. explored percent of TILs as a predictive measure for melanoma prognosis while offering deep learning as a method to standardize clinician approaches (28). In this retrospective analysis, a neural networks classifier used WSIs to calculate the percentage of TILs in melanoma tissue, which was compared to the manually derived Clark's grading. This study confirmed the previously established percent TIL threshold of 16.6% and the use of TILs as a prognostic marker, as higher percentages of TILs were associated with both longer recurrence-free survival (RFS) and overall survival. These results demonstrate the value of deep learning in improving TIL counting for melanoma prognosis.

Deep learning methods have been instrumental in predicting risk for other skin cancers. Chiu and colleagues in 2021 utilized two deep neural network-based models (DeepSurv and CoxTime) to predict basal and squamous cell carcinoma risk in heart transplant recipients, comparing their performance to Cox proportional hazards models (29). The authors assessed prediction performance post-heart transplantation, finding DeepSurv and CoxTime models significantly exceeded performance comparatively at every time point. They demonstrated superiority of neural networks in providing improved risk predictions in this patient population.

Overall, these deep learning studies illustrate how ML may solve complex problems, from interpreting images with TILs to integrating various data types into a single model. Deep learning models can be criticized for limitations such as requirement for vast amounts of data and lack of applicability to new data. However,

they provide promise in rapidly analyzing various data types and greatly improving current survival methods.

Natural language processing

Natural language processing (NLP) encompasses computer-based algorithms that transform natural language, such as blocks of text, into usable information for research (34). For example, it may integrate contextual nuances, or word clues, to define necessary words to extract for analysis. GPT-4 is a large language model (LLM) that performs tasks from solving advanced mathematical problems to writing personal essays. NLP may utilize a "rules" approach: user instructing the computer on information to extract; another approach is with machine learning: inputting training data, letting the computer practice/learn, and identifying or extracting learned words or phrases of interest. Amidst an increase in availability of accessible biological and medical population databases, NLP holds promise in potentially eliminating the need for manual review among clinicians and researchers (34).

NLP has been utilized in dermatology and oncology, from synthesis of biopsy reports to extraction of symptoms from patient histories to survival analysis. Yuan in 2021 used NLP to find key cancer characteristics from a cohort >40,000 patients with lung cancer (35). They used NLP to compile structured data (i.e., diagnoses) and unstructured data (narrative notes) to develop a prognostic model to estimate lung cancer survival (AUC = 0.82).

Our cutaneous oncology survival analysis search did not yield NLP publications. However, upon manual search for "natural language processing" and "survival analysis," we encountered one melanoma NLP study. Yang in 2021 investigated if TILs were an independent prognostic factor for overall survival in primary cutaneous melanoma (36). NLP combed through notes and identified clinical and histopathologic data, performing regression analyses demonstrating brisk TILs significantly associated with improved survival.

The identified lack of NLP survival analysis publications might be due to limitations in searching or NLP-oriented tasks. Many studies use NLP as a data extraction tool for word frequency or isolation. Thus, it is less predominantly featured in survival analysis, though has potential to uncover prognostic indicators.

Discussion

We reviewed AI's application to survival analysis for cutaneous malignancies. While AI has expanded its reach within oncology, applications to survival analysis and cutaneous oncology remain limited. Secondly, types of skin cancer and data analyzed were similar. Lastly, several publications leveraged multiple AI branches, with increasing focus on deep learning and less on NLP.

Only 16 publications resulted from our query, with several excluded for lack of relevance. Survival analysis remains a ripe area for multimodal AI application, enabling extraction of pathology and clinico-demographic data to generate predictive models. Few publications may have resulted due to our search's limitations; we expect an increase as data extraction advances.

Nearly every publication studied melanoma, despite greater prevalence of non-melanoma skin cancers, likely due to melanoma's mortality burden. Non-melanoma skin cancers are areas for future analysis to elucidate prognostic indicators.

Many publications investigated integrating genetics, clinical data, and/or histology. They used data from similar sources (e.g., TCGA) and similarly reported AUC or C-index. These similarities speak to reliance on large databases and statistical standardization. Additionally, several publications analyzed images with a deep learning approach deconstructing to components, identifying patterns, and mapping results onto current disease understanding. Predictive modeling with images has made significant progress, owing to ease of machine training on thousands of images versus far fewer attributes.

The division between the discussed AI branches is not rigid; researchers might utilize "deep learning" methods but also integrate supervised learning. A multifaceted approach enables researchers to develop more complex algorithms and synthesize disparate data. For example, researchers may use NLP to extract unstructured data from clinical notes, deep learning for histology, and supervised learning for regression toward survival analysis and prognostication. Each approach has benefits and limitations, but together they may enhance modeling potential.

Several investigations illustrate limitations of AI in healthcare (37). LLMs are error-prone, sometimes inconsistently pulling information from records and relying on false generalizations. Other limitations include smaller datasets (potentially over-weighing certain features) or even incomplete and biased datasets, highlighting a need for quality of data inputs to develop algorithms. Disparities in inclusion of skin of color images in datasets poses negative implications for model generation and subsequent performance, biasing models and yielding inequitable results and representation (38). Thus, issues like loss-to-follow-up, note errors, or hospital transfers provide incomplete clinical scenarios; many models had non-excellent performances (AUCs <90%). Relying on new models that incompletely capture clinical situations may have devastating consequences: patients receiving inappropriate treatments or inaccurate prognostication. Thus, critical analysis and data synthesis is essential to AI.

Future investigations may engage with a diversity of cutaneous malignancies, using multiple AI methodologies to leverage benefits and compensate for any weaknesses. Finally, studies may expand beyond survival to integrate quality-of-life analyses.

Overall, this review is an important contribution to increasing literature on AI applications to survival analysis for patients with skin cancer. Innovative applications may reveal unique insights in clinical settings to enable physicians to better assess patient survival and develop targeted treatment.

Author contributions

CS, EG, and LJG: conception and design of study. CS, EG, OA, CC, BL, JK, GR, and LG: acquisition of data and drafting the

manuscript. CS, EG, OA, CC, BL, JK, GR, LF, CW, NT, HC, IP, and LJG: revising the manuscript for important intellectual content. All authors contributed to the article and approved the content for publication.

Funding

This work was supported by the Columbia University Herbert Irving Comprehensive Cancer Center Inter/Intra-Programmatic Pilot Program.

Conflict of interest

LJG has served as an investigator for and/or received research support from Helsinn Group, J&J, Mallinckrodt, Kyowa Kirin, Soligenix, Innate, Incyte, Trillium, Merck, BMS, and Stratpharma; on the speakers' bureau for Mallinckrodt and Recordati; and on the scientific advisory board for SciTech and Celsyntec.

The remaining authors declare that the research was conducted in the absence of any commercial or financial relationships that could be construed as a potential conflict of interest.

Publisher's note

All claims expressed in this article are solely those of the authors and do not necessarily represent those of their affiliated organizations, or those of the publisher, the editors and the reviewers. Any product that may be evaluated in this article, or claim that may be made by its manufacturer, is not guaranteed or endorsed by the publisher.

Supplementary material

The Supplementary material for this article can be found online at: https://www.frontiersin.org/articles/10.3389/fmed.2024.1243659/full#supplementary-material

References

1. Guy GP, Thomas CC, Thompson T, Watson M, Massetti GM, Richardson LC. Vital signs: melanoma incidence and mortality trends and projections — United States, 1982–2030. *Morb Mortal Wkly Rep*. (2015) 64:591–6.

2. Rogers HW, Weinstock MA, Feldman SR, Coldiron BM. Incidence estimate of nonmelanoma skin Cancer (keratinocyte carcinomas) in the U.S. population, 2012. *JAMA Dermatol*. (2015) 151:1081–6. doi: 10.1001/jamadermatol.2015.1187

3. Cancer Facts & Figures 2023|American Cancer Society. (2023). Available at: https://www.cancer.org/research/cancer-facts-statistics/all-cancer-facts-figures/2023-cancer-facts-figures.html (Accessed June 15, 2023).

4. Mansouri B, Housewright CD. The treatment of actinic Keratoses-the rule rather than the exception. *JAMA Dermatol*. (2017) 153:1200. doi: 10.1001/jamadermatol.2017.3395

5. Melarkode N, Srinivasan K, Qaisar SM, Plawiak P. AI-powered diagnosis of skin Cancer: a contemporary review, open challenges and future research directions. *Cancers*. (2023) 15:1183. doi: 10.3390/cancers15041183

6. Zhu S, Sun C, Zhang L, Du X, Tan X, Peng S. Incidence trends and survival prediction of malignant skin Cancer: a SEER-based study. *Int J Gen Med*. (2022) 15:2945–56. doi: 10.2147/IJGM.S340620

7. Smith AJ, Lambert PC, Rutherford MJ. Understanding the impact of sex and stage differences on melanoma cancer patient survival: a SEER-based study. *Br J Cancer*. (2021) 124:671–7. doi: 10.1038/s41416-020-01144-5

8. Yang GB, Barnholtz-Sloan JS, Chen Y, Bordeaux JS. Risk and survival of cutaneous melanoma diagnosed subsequent to a previous Cancer. *Arch Dermatol*. (2011) 147:1395–02. doi: 10.1001/archdermatol.2011.1133

9. Shastry KA, Sanjay HA. Cancer diagnosis using artificial intelligence: a review. *Artif Intell Rev*. (2022) 55:2641–73. doi: 10.1007/s10462-021-10074-4

10. Jiang T, Gradus JL, Rosellini AJ. Supervised machine learning: a brief primer. *Behav Ther*. (2020) 51:675–87. doi: 10.1016/j.beth.2020.05.002

11. LeCun Y, Bengio Y, Hinton G. Deep learning. *Nature*. (2015) 521:436–44. doi: 10.1038/nature14539

12. Elkhader J, Elemento O. Artificial intelligence in oncology: from bench to clinic. *Semin Cancer Biol*. (2022) 84:113–28. doi: 10.1016/j.semcancer.2021.04.013

13. Zhao XM, Iskar M, Zeller G, Kuhn M, van Noort V, Bork P. Prediction of drug combinations by integrating molecular and pharmacological data. *PLoS Comput Biol*. (2011) 7:e1002323. doi: 10.1371/journal.pcbi.1002323

14. Pate A, Emsley R, Ashcroft DM, Brown B, van Staa T. The uncertainty with using risk prediction models for individual decision making: an exemplar cohort study examining the prediction of cardiovascular disease in English primary care. *BMC Med*. (2019) 17:134. doi: 10.1186/s12916-019-1368-8

15. Smak Gregoor AM, Sangers TE, Bakker LJ, Hollestein L, Uyl – de Groot CA, Nijsten T, et al. An artificial intelligence based app for skin cancer detection evaluated in a population based setting. *NPJ Digit Med*. (2023) 6:90. doi: 10.1038/s41746-023-00831-w

16. Alwakid G, Gouda W, Humayun M, Jhanjhi NZ. Diagnosing melanomas in Dermoscopy images using deep learning. *Diagnostics*. (2023) 13:1815. doi: 10.3390/diagnostics13101815

17. Trincado JL, Sebestyén E, Pagés A, Eyras E. The prognostic potential of alternative transcript isoforms across human tumors. *Genome Med*. (2016) 8:85. doi: 10.1186/s13073-016-0339-3

18. Wang LX, Wan C, Dong ZB, Wang BH, Liu HY, Li Y. Integrative analysis of long noncoding RNA (lncRNA), microRNA (miRNA) and mRNA expression and construction of a competing endogenous RNA (ceRNA) network in metastatic melanoma. *Med Sci Monit Int Med J Exp Clin Res*. (2019) 25:2896–07. doi: 10.12659/MSM.913881

19. Su S, Chhabra G, Ndiaye MA, Singh CK, Ye T, Huang W, et al. PLK1 and NOTCH positively correlate in melanoma and their combined inhibition results in synergistic modulations of key melanoma pathways. *Mol Cancer Ther*. (2021) 20:161–72. doi: 10.1158/1535-7163.MCT-20-0654

20. Failmezger H, Muralidhar S, Rullan A, de Andrea CE, Sahai E, Yuan Y. Topological tumor graphs: a graph-based spatial model to infer stromal recruitment for immunosuppression in melanoma histology. *Cancer Res*. (2020) 80:1199–09. doi: 10.1158/0008-5472.CAN-19-2268

21. Wilson CM, Li K, Sun Q, Kuan PF, Wang X. Fenchel duality of cox partial likelihood with an application in survival kernel learning. *Artif Intell Med*. (2021) 116:102077. doi: 10.1016/j.artmed.2021.102077

22. Yang S, Xu J, Zeng X. A six-long non-coding RNA signature predicts prognosis in melanoma patients. *Int J Oncol*. (2018) 52:1178–88. doi: 10.3892/ijo.2018.4268

23. Jonckheere N, Van Seuningen I. Integrative analysis of the cancer genome atlas and cancer cell lines encyclopedia large-scale genomic databases: MUC4/MUC16/MUC20 signature is associated with poor survival in human carcinomas. *J Transl Med*. (2018) 16:259. doi: 10.1186/s12967-018-1632-2

24. Yang CQ, Wang H, Liu Z, Hueman MT, Bhaskaran A, Henson DE, et al. Integrating additional factors into the TNM staging for cutaneous melanoma by machine learning. *PLoS One*. (2021) 16:e0257949. doi: 10.1371/journal.pone.0257949

25. Comes MC, Fucci L, Mele F, Bove S, Cristofaro C, De Risi I, et al. A deep learning model based on whole slide images to predict disease-free survival in cutaneous melanoma patients. *Sci Rep*. (2022) 12:20366. doi: 10.1038/s41598-022-24315-1

26. Johannet P, Coudray N, Donnelly DM, Jour G, Illa-Bochaca I, Xia Y, et al. Using machine learning algorithms to predict immunotherapy response in patients with advanced melanoma. *Clin Cancer Res Off J Am Assoc Cancer Res*. (2021) 27:131–40. doi: 10.1158/1078-0432.CCR-20-2415

27. Moore MR, Friesner ID, Rizk EM, Fullerton BT, Mondal M, Trager MH, et al. Automated digital TIL analysis (ADTA) adds prognostic value to standard assessment of depth and ulceration in primary melanoma. *Sci Rep*. (2021) 11:2809. doi: 10.1038/s41598-021-82305-1

28. Chou M, Illa-Bochaca I, Minxi B, Darvishian F, Johannet P, Moran U, et al. Optimization of an automated tumor-infiltrating lymphocyte algorithm for improved prognostication in primary melanoma. *Mod Pathol Off J U S Can Acad Pathol Inc*. (2021) 34:562–71. doi: 10.1038/s41379-020-00686-6

29. Chiu KC, Du D, Nair N, Du Y. Deep neural network-based survival analysis for skin Cancer prediction in heart transplant recipients. *Annu Int Conf IEEE Eng Med Biol Soc IEEE Eng Med Biol Soc Annu Int Conf*. (2021) 2021:2144–7. doi: 10.1109/EMBC46164.2021.9630234

30. Liestøl K, Andersen PK, Andersen U. Survival analysis and neural nets. *Stat Med*. (1994) 13:1189–00. doi: 10.1002/sim.4780131202

31. Ramsdale E, Kunduru M, Smith L, Culakova E, Shen J, Meng S, et al. Supervised learning applied to classifying fallers versus non-fallers among older adults with cancer. *J Geriatr Oncol*. (2023) 14:101498. doi: 10.1016/j.jgo.2023.101498

32. Eckardt JN, Röllig C, Metzeler K, Heisig P, Stasik S, Georgi JA, et al. Unsupervised meta-clustering identifies risk clusters in acute myeloid leukemia based on clinical and genetic profiles. *Commun Med*. (2023) 3:68. doi: 10.1038/s43856-023-00298-6

33. Goel MK, Khanna P, Kishore J. Understanding survival analysis: Kaplan-Meier estimate. *Int J Ayurveda Res*. (2010) 1:274–8. doi: 10.4103/0974-7788.76794

34. Yim W, Yetisgen M, Harris WP, Kwan SW. Natural language processing in oncology: a review. JAMA. *JAMA Oncol*. (2016) 2:797–04. doi: 10.1001/jamaoncol.2016.0213

35. Yuan Q, Cai T, Hong C, du M, Johnson BE, Lanuti M, et al. Performance of a machine learning algorithm using electronic health record data to identify and estimate survival in a longitudinal cohort of patients with lung Cancer. *JAMA Netw Open*. (2021) 4:e2114723. doi: 10.1001/jamanetworkopen.2021.14723

36. Yang J, Lian JW, Chin YPH, Wang L, Lian A, Murphy GF, et al. Assessing the prognostic significance of tumor-infiltrating lymphocytes in patients with melanoma using pathologic features identified by natural language processing. *JAMA Netw Open*. (2021) 4:e2126337. doi: 10.1001/jamanetworkopen.2021.26337

37. Peng Y, Rousseau JF, Shortliffe EH, Weng C. AI-generated text may have a role in evidence-based medicine. *Nat Med*. (2023) 29:1593–4. doi: 10.1038/s41591-023-02366-9

38. Kleinberg G, Diaz MJ, Batchu S, Lucke-Wold B. Racial underrepresentation in dermatological datasets leads to biased machine learning models and inequitable healthcare. *J Biomed Res*. (2022) 3:42–7.

39. Supervised vs. unsupervised learning. (2021). What's the difference? Available at: https://www.linkedin.com/pulse/supervised-vs-unsupervised-learning-whats-difference-smriti-saini (Accessed December 22, 2023).

40. Mastering of Supervised and Unsupervised Learning. (2023). Know the differences. Labeler. Published February 8, 2023. Available at: https://www.labellerr.com/blog/supervised-vs-unsupervised-learning-whats-the-difference/ (Accessed December 22, 2023).

Frontiers in Medicine

Translating medical research and innovation into improved patient care

A multidisciplinary journal which advances our medical knowledge. It supports the translation of scientific advances into new therapies and diagnostic tools that will improve patient care.

Discover the latest Research Topics

See more →

Frontiers

Avenue du Tribunal-Fédéral 34
1005 Lausanne, Switzerland
frontiersin.org

Contact us

+41 (0)21 510 17 00
frontiersin.org/about/contact